

**SYNTHESIS, CHARACTERIZATION AND
COORDINATION CHEMISTRY OF
BENZIPORPHODIMETHENE**

A THESIS

**Submitted to the Delhi Technological University
for the award of the degree of**

**DOCTOR OF PHILOSOPHY
in
APPLIED CHEMISTRY**

by

RAVI KUMAR SHARMA



**DEPARTMENT OF APPLIED CHEMISTRY
DELHI TECHNOLOGICAL UNIVERSITY
DELHI- 110042 (INDIA)**

AUGUST 2016

**SYNTHESIS, CHARACTERIZATION AND
COORDINATION CHEMISTRY OF
BENZIPORPHODIMETHENE**

by

RAVI KUMAR SHARMA

DEPARTMENT OF APPLIED CHEMISTRY

Submitted

in fulfilment of the requirements for the degree of

DOCTOR OF PHILOSOPHY

to the



DELHI TECHNOLOGICAL UNIVERSITY

DELHI - 110042 (INDIA)

AUGUST 2016

©DELHI TECHNOLOGICAL UNIVERSITY-2016

ALL RIGHTS RESERVED

DEDICATED
TO
MY PARENTS

DECLARATION

I declare that the research work reported in this thesis entitled “**SYNTHESIS, CHARACTERIZATION AND COORDINATION CHEMISTRY OF BENZIPORPHODIMETHENE**” for the award of the degree of *Doctor of Philosophy* in Chemistry has been carried out by me under the supervision of *Dr. Anil Kumar, Department of Applied Chemistry, Delhi Technological University, India.*

The research work embodied in this thesis, except where otherwise indicate, is my original research. This thesis has not been submitted by me earlier in part or full to any other University or Institute for the award of any degree or diploma. This thesis does not contain other person’s data, graphs or other information, unless specifically acknowledged.

Dr. Anil Kumar

Supervisor

Ravi Kumar Sharma

Candidate

Prof. R. C. Sharma

Head of the Department

Applied Chemistry

Delhi Technological University



DELHI TECHNOLOGICAL UNIVERSITY

CERTIFICATE

This is to certify that the Ph.D. thesis entitled "**SYNTHESIS CHARACTERIZATION AND COORDINATION CHEMISTRY OF BENZIPORPHODIMETHENE**" submitted to the Delhi Technological University, Delhi for the award of Doctor of Philosophy is based on the original research work carried out by me under supervision of Dr. Anil Kumar, Department of Applied Chemistry, Delhi Technological University, Delhi, India. It is further certified that the work embodied in this thesis has neither partially nor fully submitted to any other university or institution for the award of any degree or diploma.

Ravi Kumar Sharma

Candidate

(Enrolment No: 2K11/Ph.D/AC/01)

This is to certify that the above statement made by the candidate is correct to the best of our knowledge.

Dr. Anil Kumar

(Supervisor)

Asst. Professor, Applied Chemistry

Delhi Technological University

Prof. R. C. Sharma

Head of the Department, Applied Chemistry

Delhi Technological University

ACKNOWLEDGEMENTS

This thesis is the result of five years of work whereby I have been accompanied and supported by many people. It is a pleasant moment that I have now the opportunity to express my gratitude for all of them.

First of all, I would like to acknowledge my supervisor, my mentor Dr. Anil Kumar for his proficient guidance and continued encouragement that led to the fulfillment of this research work. With great pleasure, I express my heartfelt indebtedness for his advice, fruitful discussions, numerous suggestions, constructive criticism, and constant support throughout the period of my research. The encouragement, patience and the degree of freedom that he gave, made me explore and learn a plethora of new things.

I wish to thank Prof. R. C. Sharma, Dr. D. Kumar, Dr. Ram Singh and Dr. Richa Srivastava for their important contributions during my tenure in the department.

I am obliged to acknowledge Dr. Jay Singh for his continuous encouragement, suggestions and support for my research work. Not only as a teacher but also as a friend he helped me in various aspects to achieve my goals.

I would like to thank Dr. Mohan Singh Mehata, Department of Applied Physics, DTU, for supporting my work and helping me to record photoluminescence spectra and to find quantum yield of my compounds. Without his help, it would not have been an easy task for me.

I am thankful to Dr. Paulraj Rajamani and Dr. Anurag Maurya, Department of Environmental Science, JNU for providing facilities to carry out *in vitro* and cell imaging experiments in their laboratory.

I wish to thank Dr. Firasat Hussain, Department of Chemistry, Delhi University for helping me to solve single crystal XRD data reported in this thesis.

Here it's a great opportunity for me to thank the administrative staff and other members of Chemistry Department, I am extremely thankful to Chauhan ji, Ishwar Yadav ji, Jeevan ji, Ankesh, Deepak, Sanjay, and Raju.

I gratefully acknowledge the financial assistance provided by Delhi Technological University in the form of Junior Research Fellowship and Senior

Research Fellowship during the period of my research. I would like to thank DST for funding and DTU to provide entire infrastructure and facilities.

I would like to specially thank Dr. Ritika Nagpal, my sister-like friend, for helping with the characterization of my samples and for recording NMR and C-NMR data. Thanks Di, I feel extremely lucky to be associated with a person like you who stood behind me at every time of need! I will never have words to express gratitude to you.

I am fortunate to have friends like Gaurav Rastogi and Pankaj with whom I spent a lot of time during my Ph.D. I enjoyed their company.

I would like to take this moment as an opportunity to thank my friends Dr. Richa Pahuja, Dr. Sweta Mishra, Dr. Meenakshi Gusain, Dr. Poonam Singh, Smriti Arora, and Balram Rathi for their encouragement, care, and affection. I am fortunate to have friends like them who make me smile at tough times of my life.

I also thank my school friend Prateek Gupta, my graduation friends Ajay, Sumit, Harleen and Dr. Prashant Chauhan for their concerns and timely help.

I pay sincere gratitude to my primary school teacher Mrs. Manju Sharma, my secondary school teachers Mr. N. P. S Malik, Mr. V. K. Sharma, Mr. Phool Singh, Mr. R. P. Shukla, my chemistry teacher Late Dr. Maha Singh, and my mathematics teacher Mr. R. P. S. Chaudhary, my graduation teachers Dr. Sumanjeet Kaur, Dr. Gurmeet Kaur, Dr. Gurvinder Kaur, Dr. G. S. Sodhi, Dr. Vandana and my post-graduation teacher Dr. Akhilesh Verma, for making me who I am today. As a student, I can never pay back to my loving teachers who always help me to learn and progress. A teacher is like a shadow who always remains with his student by making imprints in his mind. I am glad to have such wonderful persons as my Guru. I am delighted and want to thank the Almighty for giving me such wonderful teachers who enlighten the path of my life.

Lastly but the most important of all, I wish to thank my family; my parents, brother and sisters, who have always been my strength, who have always been by my side through all the thick and thin. Every child's existence is because of his parents, they sacrifice everything for their child. A child can never pay back to his parents. I love you mom and dad for what you did and are doing for me. I cannot imagine myself without you. It's because of your care, love, affection and sacrifices that I am in the

present position of my life. It's your blessings that make me who I am, and what I will be tomorrow. Words are too less to express my feelings for both of you.

Finally, I thank all those who helped and supported me. Thank you so much!

Date:

(Ravi Kumar Sharma)

Place: Delhi

LIST OF CONTENTS

Page No.

Declaration

Certificate

Acknowledgements

List of Contents

List of Tables

List of Figures

Abstract

CHAPTER 1: INTRODUCTION	1- 32
1.1. GENERAL INTRODUCTION	1
1.2. STRUCTURE OF PORPHYRIN	2
1.3. CARBAPORPHYRINOIDS: THE BEGINNING	5
1.4. NOMENCLATURE OF CARBAPORPHYRINOIDS SYSTEM	6
1.5. CRITERIA FOR THE AROMATICITY OF PORPHYRINS	7
1.6. GENERAL SYNTHETIC PROCEDURES FOR PORPHYRINS AND THEIR ANALOGUES	9
1.7. PHOTO-PHYSICAL PROPERTIES OF PORPHYRINS	11
1.8. THE GOUTERMAN FOUR ORBITAL MODEL	12
1.9. BENZIPORPHYRIN: A CLASS OF CARBAPORPHYRINOIDS	14
1.10. OXY-BENZIPORPHYRIN AND <i>para</i> -BENZIPORPHYRIN	15
1.11. BENZIPHORINS & SUBSTITUTED BENZIPORPHODIMETHENES	18
1.12. <i>meta</i> -BENZIPORPHODIMETHENES	19
1.13. NMR SHIFTS IN <i>meta</i> -BENZIPORPHODIMETHENE	22
1.14. METAL COMPLEXES OF <i>meta</i> -BENZIPORPHODIMETHENES	23

1.15.	SOME IMPORTANT PROPERTIES OF METALLATED- <i>meta</i> BENZIPORPHODIMETHENE COMPLEXES	23
1.16.	FLUORESCENCE PHENOMENA: STRUCTURE CORRELATION	25
1.17.	APPLICATIONS	25
	References	27
CHAPTER 2: SCOPE OF THE RESEARCH		33
CHAPTER 3: EXPERIMENTAL SECTION		35
3.1.	MATERIALS	35
3.2.	CHARACTERIZATION AND MEASUREMENTS	35
3.3.	GENERAL REACTION SCHEME	36
3.4.	SYNTHESIS OF COMPOUNDS 1-8 AND Zn ²⁺ 1-8	37
3.5.	PHOTOLUMINESCENCE OF ZINC COMPLEXES OF BPDM COMPOUNDS	46
3.6.	TIME RESOLVED PHOTOLUMINESCENCE OF ZINC COMPLEXES OF <i>meta</i> -BPDM COMPOUNDS	46
3.7.	CELL IMAGING WITH <i>meta</i> -BPDM COMPOUNDS IN BREAST CARCINOMA CELLS	47
3.8.	DENSITY FUNCTIONAL THEORY CALCULATION	48
	References	49
CHAPTER 4: RESULTS AND DISCUSSIONS		50
4.1.	SPECTROSCOPIC RESULTS	50
	4.1.1.ELECTRONIC SPECTROSCOPY	50
	4.1.2.NUCLEAR MAGNETIC RESONANCE (NMR) SPECTROSCOPY	61
	4.1.3.FTIR SPECTRAL ANALYSIS	75
	4.1.4.ESI MASS SPECTROSCOPY	86

4.2.	SINGLE CRYSTAL XRD ANALYSIS	90
4.2.1.	11, 16-Bis(3, 4, 5-trimethoxy-phenyl)-6, 6, 21, 21-tetramethyl- <i>meta</i> -benzporphodimethene (8)	91
4.3.	DENSITY FUNCTIONAL THEORY (DFT) CALCULATION STUDY	99
4.3.1.	COMPUTATIONAL DETAILS	99
4.3.2.	DFT CALCULATION RESULTS	99
4.4.	FLUORESCENCE STUDY	103
4.4.1.	PHOTOLUMINESCENCE (PL) AND TIME RESOLVED PHOTOLUMINESCENCE (TRPL) SPECTRAL ANALYSIS	103
4.4.2.	QUANTUM YIELD ANALYSIS	112
4.5.	CELL IMAGING STUDIES	115
4.5.1.	CELL IMAGING STUDIES FOR ZINC: COMPARATIVE ANALYSIS	115
4.5.2.	CELL IMAGING EXPERIMENT AND CYTOTOXICITY STUDIES	117
4.5.3.	CELL IMAGING RESULTS	118
	References	122
	CHAPTER 5: CONCLUSION AND FUTURE SCOPE	127
	LIST OF PUBLICATIONS	
	ABOUT AUTHOR	

LIST OF TABLES

Table No.		Pg.No.
4.1	Absorption spectra of <i>meta</i> -benziporphodimethenes and their zinc complexes obtained in degassed acetonitrile.	51
4.2	¹ H NMR spectral data for compounds 1-8	62
4.3	¹³ C NMR spectral data for compounds 1-8	63
4.4	FTIR data for free base <i>meta</i> -BPDM Compounds.	76
4.5	FTIR data for zinc complexes of <i>meta</i> -BPDM Compounds.	77
4.6	ESI-mass value for <i>meta</i> -benziporphodimethenes and zinc complex	86
4.7	Atomic co-ordinates and equivalent isotropic displacements parameters for Compound 8 . U(eq) is defined as one third of the trace of the orthogonolized Uij tensor.	92
4.8	Bond distance (Å) and bond angles (°) for compound 8	95
4.9	Summary of X-ray crystallographic data for compound 8	98
4.10	Comparison of Selected bond lengths [Å] and angles [°] of R and Zn ²⁺ . R with receptor, 4 and its Zn ²⁺ . 4 . (R = unsubstituted <i>meta</i> -benziporphodimethenes)	101
4.11	Fluorescence quantum yields of zinc complexes of <i>meta</i> -benziporphodimethenes obtained in degassed toluene calculated using Strickler-Berg relation. (where R= unsubstituted <i>meta</i> -benziporphodimethene)	114

LIST OF FIGURES

Fig.		Pg.No.
1.1	Structure of porphyrin and the sites of modifications	2
1.2	Modified porphyrin after incorporating hetero atoms	3
1.3	Representation of modifications in the central core and the types of porphyrin analogues	4
1.4	Macrocycles with CNNN Core	5
1.5	Fisher and IUPAC Systems of nomenclature	6
1.6	Possible pathways for the delocalisation of π electrons in porphyrins	7
1.7	Representation of delocalisation pathway and Δ 's value for porphyrin (18 π electrons), N-confused Porphyrin (18 π electrons) and in <i>meta</i> -benziporphyrin (6 π electrons)	8
1.8	General Condensation procedure for Porphyrin	9
1.9	Some of the possible approaches for the synthesis of carbocyclic ring moieties	10
1.10	The inner 16 membered ring (A) responsible for maintaining the conjugation for 18- π electrons pathways (B) that generate the porphyrin optical spectrum	11
1.11	Electronic absorption spectra of TPP and Zn-TPP	12
1.12	Gouterman four orbital model	13
1.13	Orbital diagram showing possible transitions for porphyrin macrocycle	13
1.14	Representation of pathway from porphyrin to carbaporphyrinoids	14
1.15	Synthesis of <i>meta</i> -benziporphyrin by Berlin and Breitmaier in 1994	15
1.16	Synthesis of meso substituted <i>meta</i> -benziporphyrins	15
1.17	Synthesis of Oxybenziporphyrins	16
1.18	Hetero Oxybenziporphyrins	16
1.19	Synthesis scheme for para benziporphyrins	17
1.20	Rotation of <i>para</i> benzene in <i>para</i> -benziporphyrin moiety	18
1.21	Phlorin	18
1.22	Synthesis of <i>meta</i> -benziphlorins from <i>meta</i> -benziporphyrin	19
1.23	<i>meta</i> -benziporphodimethene	20
1.24	Synthesis of <i>meta</i> -benziporphodimethenes	20
1.25	UV Spectra of <i>meta</i> -benziporphodimethene	21
1.26	The O' Up and O Down γ lactam embedded N-confused isomers	21
4.1	Electronic spectra of compound 1	52
4.2	Electronic spectra of compound Zn ²⁺ . 1	52
4.3	Electronic spectra of compound 2	53
4.4	Electronic spectra of compound Zn ²⁺ . 2	53
4.5	Electronic spectra of compound 3	54
4.6	Electronic spectra of compound Zn ²⁺ . 3	54
4.7	Electronic spectra of compound 4	55
4.8	Electronic spectra of compound Zn ²⁺ . 4	55
4.9	Electronic spectra of compound 5	56
4.10	Electronic spectra of compound Zn ²⁺ . 5	56
4.11	Electronic spectra of compound 6	57
4.12	Electronic spectra of compound Zn ²⁺ . 6	57
4.13	Electronic spectra of compound 7	58
4.14	Electronic spectra of compound Zn ²⁺ . 7	58

4.15	Electronic spectra of compound 8	59
4.16	Electronic spectra of compound Zn ²⁺ . 8	59
4.17	Combined electronic spectra for compounds 1-8	60
4.18	Combined electronic spectra for complexes Zn ²⁺ . 1-8	60
4.19	¹ H-NMR spectra of compound 1	64
4.20	¹ H-NMR spectra of compound 2	65
4.21	¹ H-NMR spectra of compound 3	66
4.22	¹ H-NMR spectra of compound 4	67
4.23	¹ H-NMR spectra of compound 5	68
4.24	¹ H-NMR spectra of compound 6	69
4.25	¹ H-NMR spectra of compound 7	70
4.26	¹ H-NMR spectra of compound 8	71
4.27	¹³ C-NMR spectra of compound 1	72
4.28	¹³ C-NMR spectra of compound 2	72
4.29	¹³ C-NMR spectra of compound 3	73
4.30	¹³ C-NMR spectra of compound 4	73
4.31	¹³ C-NMR spectra of compound 5	74
4.32	¹³ C-NMR spectra of compound 6	74
4.33	¹³ C-NMR spectra of compound 8	75
4.34	FTIR spectra of compound 1	78
4.35	FTIR spectra of Compound Zn ²⁺ . 1	78
4.36	FTIR spectra of compound 2	79
4.37	FTIR spectra of Compound Zn ²⁺ . 2	79
4.38	FTIR spectra of compound 3	80
4.39	FTIR spectra of Compound Zn ²⁺ . 3	80
4.40	FTIR spectra of compound 4	81
4.41	FTIR spectra of Compound Zn ²⁺ . 4	81
4.42	FTIR spectra of compound 5	82
4.43	FTIR spectra of Compound Zn ²⁺ . 5	82
4.44	FTIR spectra of compound 6	83
4.45	FTIR spectra of Compound Zn ²⁺ . 6	83
4.46	FTIR spectra of compound 7	84
4.47	FTIR spectra of Compound Zn ²⁺ . 7	84
4.48	FTIR spectra of compound 8	85
4.49	FTIR spectra of Compound Zn ²⁺ . 8	85
4.50	ESI mass spectra of compound 1	87
4.51	ESI mass spectra of compound 2	87
4.52	ESI mass spectra of compound 3	88
4.53	ESI mass spectra of compound 4	88
4.54	ESI mass spectra of compound 5	89
4.55	ESI mass spectra of compound 6	89
4.56	ESI mass spectra of compound Zn ²⁺ . 4	90
4.57	X-ray structure of free base <i>meta</i> -benzporphodimethene, 8 .	91
4.58	B3LYP/6-31g** DFT optimized structure of receptor 4 and Zn ²⁺ . 4 .	100
4.59	Molecular orbital diagram of receptor, 4 and its zinc complex. (a) HOMO of receptor, 4 . (b) LUMO of receptor, 4 . (c) HOMO of Zn ²⁺ . 4 . (d) LUMO of Zn ²⁺ . 4 . (e) HOMO-1 of Zn ²⁺ . 4 . (f) LUMO-1 of Zn ²⁺ . 4 .	102
4.60	Photoluminescence of complex Zn ²⁺ . 1	104
4.61	Time resolved photoluminescence of complex Zn ²⁺ . 1	104
4.62	Photoluminescence of complex Zn ²⁺ . 2	105

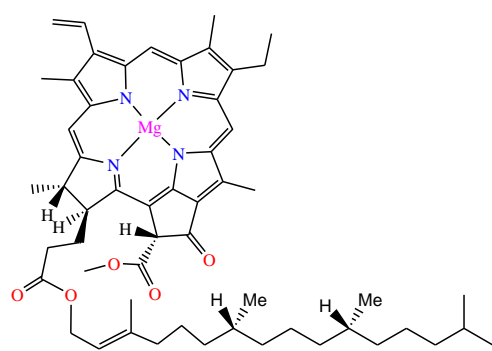
4.63	Time resolved photoluminescence of complex Zn ²⁺ . 2	105
4.64	Photoluminescence of complex Zn ²⁺ . 3	106
4.65	Time resolved photoluminescence of complex Zn ²⁺ . 3	106
4.66	Photoluminescence of complex Zn ²⁺ . 4	107
4.67	Time resolved photoluminescence of complex Zn ²⁺ . 4	107
4.68	Photoluminescence of complex Zn ²⁺ . 5	108
4.69	Time resolved photoluminescence of complex Zn ²⁺ . 5	108
4.70	Photoluminescence of complex Zn ²⁺ . 6	109
4.71	Time resolved photoluminescence of complex Zn ²⁺ . 6	109
4.72	Photoluminescence of complex Zn ²⁺ . 7	110
4.73	Time resolved photoluminescence of complex Zn ²⁺ . 7	110
4.74	Photoluminescence of complex Zn ²⁺ . 8	111
4.75	Time resolved photoluminescence of complex Zn ²⁺ . 8	111
4.76	Combined photoluminescence for complexes Zn ²⁺ . 1-8	112
4.77(a)	MDA-MB-468 cells incubated with compounds 1, 4, 7, 8 and Zn ²⁺ ions for 30 min and respective bright field marked with A-D as well as fluorescence images (just down to its respective bright field image) were captured at 10× objective lens magnification. (A = 1 , B = 4 , C = 7 , D = 8).	119
4.77(b)	MDA-MB-231 cells incubated with Zn ²⁺ ions followed by different concentration (control, 10, 20, 30 and 50 μM) of 4 for 30 min and respective bright field (a, b, c, d, e) as well as fluorescence (f, g, h, i, j) images were captured at 40× objective lens magnification.	120
4.78(a)	MDA-MB-231 cells were incubated with different concentration (control, 10, 20, 30, 50, 75 and 100 μM) of 4 . MTT assay was performed for cytotoxicity. Only 100 μM concentration of 4 was significantly (p < 0.05) toxic for the cell.	120
4.78(b)	MDA-MB-468 cells were incubated with different concentration (control, 10, 50, 100 and 150 μM) of 1, 4, 7 and 8 respectively. MTT assay was performed for cytotoxicity. Only 100 μM and 150 μM concentration of 7 were found significantly (p < 0.05) toxic for the cell.	121

ABSTRACT

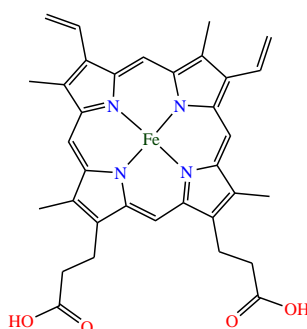
In the present thesis, synthesis characterization and application of newly synthesized *meta*-benzporphodimethene derivatives and their zinc complexes in cell imaging of zinc ions in breast carcinoma cells have been described systematically. The synthesis of *meta*-benzporphodimethenes derivatives have been carried out based on the reported procedures. The modifications on meso phenyl group have been performed based on the choice of electron withdrawing and electron releasing groups. The effect of electron releasing and electron withdrawing groups on absorption spectra, emission spectra, and fluorescence quantum yields have been studied extensively. The cell imaging study of these complexes have been performed to sense cellular zinc ions in breast carcinoma MD-AMB-231 and MD-AMB-468 cells. In view of the cytotoxicity, the MTT assay have been performed. The results shows the internalization of these derivatives into the cells. DFT calculations confirms the symmetrical geometry of zinc complex.

INTRODUCTION**1.1 GENERAL INTRODUCTION**

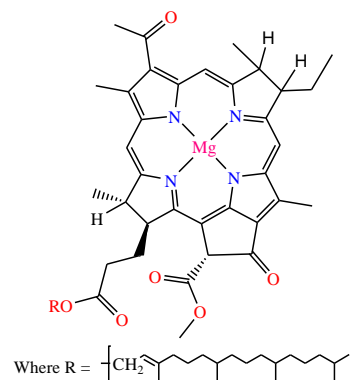
A vast research has been executed on porphyrinoid macrocyclic ring system, and still many aspects are under investigation. The important and well-known molecule is porphyrin. Porphyrin is a tetra-pyrrolic moiety, very stable, aromatic and is one of the most important molecules in the biological system. Porphyrins are important because of its multiple biological functions and its ability to bind a number of transition metal ions. Porphyrin metal complexes play crucial role in the artificial photosynthesis [1], molecular sensing [2], electro-optics [3] and medicine [4]. Porphyrin macrocycles also help in assisting various biological process, including oxygen transport, light harvesting, energy and electron transfer, etc. [5]. Thus porphyrins are often referred as “pigments of life” [6]. They have also been proved as promising candidates to be used in the development of new molecular materials with improved electro- and photochemical properties. These chromophores display interesting photo physical, photochemical and electrochemical properties due to their unusual electronic structure. They also play vital roles in photosynthesis, cellular respiration, and act as a component of metalloenzymes [7]. The basic porphyrin like moieties are found universally in natural pigments in heme, chlorophyll, bacteriochlorophyll, vitamin B₁₂ and cytochromes [5].



Chlorophyll a



Heme



Bacteriochlorophyll- a

In recent years various investigations has been done towards the synthesis of various synthetic analogous and their applications in the research and development [8]. The major objectives of these investigation is to find the applications parallel to natural porphyrins so to mimic the natural phenomena in-vitro. The electronic structure of porphyrins play a significant role to decide the fate of the porphyrin system. The vast varieties of conjugated and non-conjugated porphyrinoid system gives us a choice for selecting moiety for different applications and investigations.

1.2 STRUCTURE OF PORPHYRIN

Porphine is the parent tetra-pyrrolic moiety and is shown in Fig. 1.1. Porphyrin molecule can be modified in a number of ways for various purposes. The central region of porphyrin molecule is NNNN core that is surrounded by four pyrrolic nitrogen atoms as shown in Fig 1.1. The inner core can be modified by substituting a number of hetero atoms like O, S, Se, Te, and P etc. and constitute the core modified porphyrins [9-10]. The core modified porphyrins (also called heteroporphyrins) have the XNNN type of the inner core as shown in Fig 1.2.

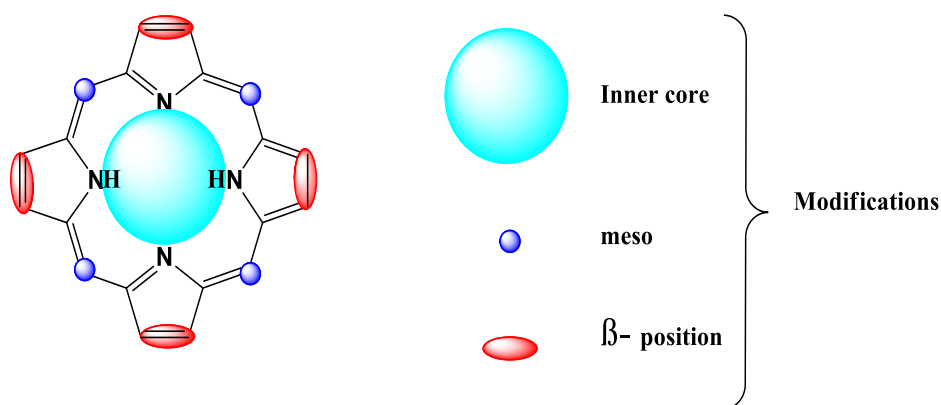
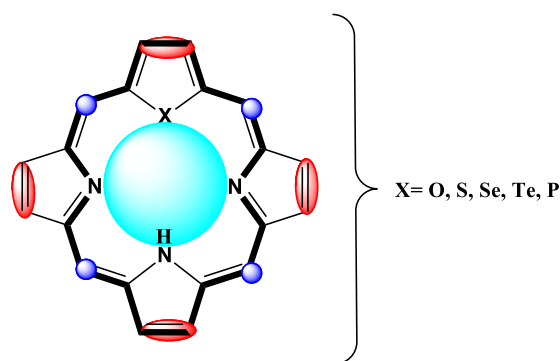


Fig. 1.1 Structure of porphyrin and the sites of modifications



Heteroporphyrins

Fig 1.2 Modified porphyrin after incorporating hetero atoms

The introduction of heteroatoms other than nitrogen in the inner core modifies the inner core arrangement of macrocycle and hence changes its properties in terms of binding ability with transition metal ions and also the electronic spectral properties, as a result shifts in the absorption pattern has been observed generally [10-11]. Macrocycles containing oxygen [12-13], sulphur [14-15], tellurium [16-17], selenium [18-19], and very recently phosphorus [20-22] constitute a large family of porphyrin-like ligands which are able to bind transition metals revealing unusual oxidation states, because of decreased charge of the coordination centre combined with modified donor properties [10,11,23].

These new synthetic analogues are classified according to their structure and the electronic current they possess, and are generally called modified class of porphyrins. Generalization of these modified porphyrin are as follow:

- a) Periphery modified porphyrins: which includes the modifications in the periphery of tetra-pyrrolic moiety and includes beta ' β ' and meso positions [24]. e.g. N confused Porphyrins.
- b) Core modified porphyrins [10]: where inner nitrogen atoms of the tetra-pyrrolic moiety are replaced by other elements (generally chalcogens), also called heteroporphyrins.
- c) Contracted porphyrins [25]: obtained by removing one of the meso carbons resulting in the formation of corroles.
- d) Isomeric porphyrins [26]: structures which have same molecular formula $C_{20}H_{14}N_4$ obtained by scrambling the four pyrrolic subunits and the four bridging carbon atoms.

- e) Inverted porphyrins [10]: which can also be considered porphyrin isomers which have one or more of the core nitrogens pointing out of the ring and hence and called ‘N-confused porphyrins’ or ‘mutant porphyrins’ and are treated as a different class.
- f) Expanded porphyrins [27]: These are the synthetic analogue of porphyrin macrocycles with enlarge core comparative to the other members of the porphyrin family with a minimum of 17 atoms in the inner central core while retaining the extended conjugation of the system [28]. The inner core atoms are generally greater than which result from the expansion of the π -electron conjugation by increasing the number of heterocyclic rings. The resulting chromophores show strong absorptions in the red region compared to those of normal 18π electrons porphyrins. Sapphyrins [29a], smaragdyrins [29b], isosmaragdyrins [29c], pentaphyrins [29d], hexaphyrins [29e], orangarins [29f], amethyrins [29f], octaphyrins [29g,h,i], rosarins [29j], rubyrins [29k], ozaphyrins [29l], bronzaphyrins [29m,n], heptaphyrins [29o], turcasarins [29p], dodecaphyrins [29q], and hexadecaphyrins [29q] are the examples of expanded porphyrins.

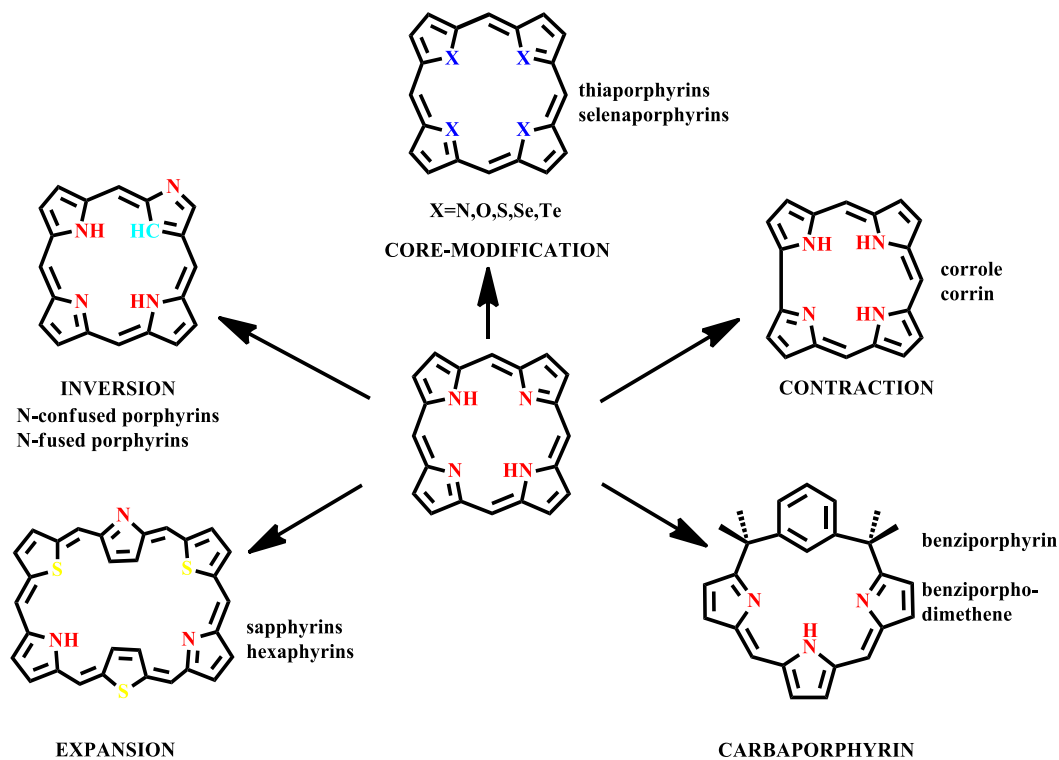


Fig. 1.3 Representation of modifications in the central core and the types of porphyrin analogues

1.3 CARBAPORPHYRINOIDS: THE BEGINNING

The first carbaporphyrins, N-confused porphyrin, was reported in 1994 independently by Furuta [30] and Latos-Grażyński [31]. A careful search through the literature reveals that the structures of N-confused porphyrins were originally suggested in 1943 by Aronoff and Calvin during their re-examination of Rothemund's synthesis of tetraphenylporphyrin [32]. Formally, **1** was obtained by a permutation of a pyrrolic nitrogen and a β -methine pyrrolic carbon of 5,10,15,20-tetraarylporphyrin, resulting in creation of the porphyrin-like skeleton of 2-aza-21-carba-5,10,15,20-tetraarylporphyrin. Macrocycle **1** in Fig. 1.4 introduces a new CNNN cavity which clearly belongs to the general XNNN group which is typical for heteroporphyrins. The newly created coordinating sphere which contains a carbon donor accompanied by three nitrogen atoms can potentially force the system to create a direct metal-carbon bond yielding organometallic compounds in the porphyrin-like environment [33].

A different and rational approach, but affording a similar coordination core (CNNN) was originally introduced by Breitmaier and co-workers [8a]. In 1994, synthesis of the macrocycle **2** (Fig. 1.4) with an *meta*-benzene subunit built into the porphyrin carbon skeleton was reported [8a]. Since then the carbaporphyrin family has been markedly broadened and the number of macrocycles containing the CNNN donor set now includes a variety of hetero- and/or carbocycles built into the porphyrin skeleton.

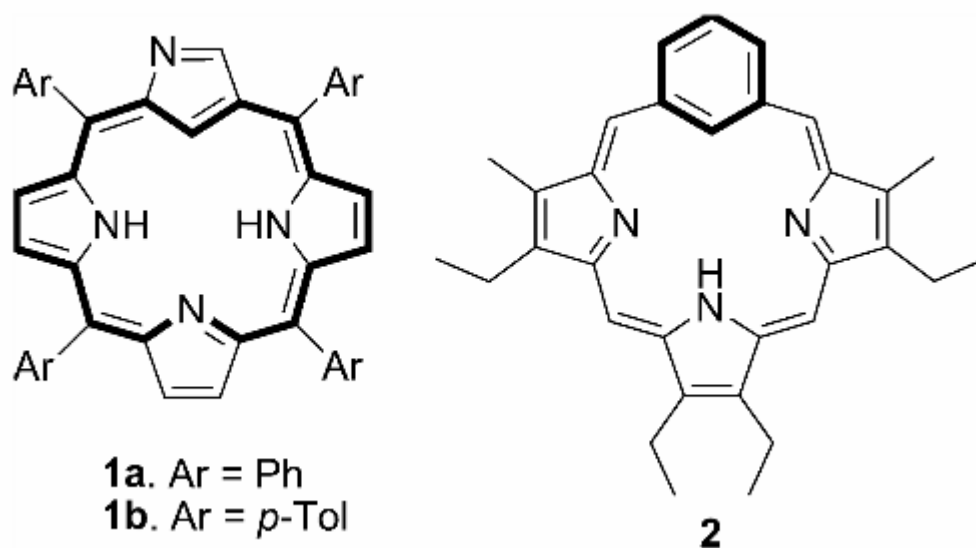


Fig 1.4 Macrocycles with CNNN Core [8a]

1.4 NOMENCLATURE OF CARBAPORPHYRINOIDS SYSTEM

Two nomenclature system are available for naming the porphyrin ring system, namely “Fisher System” and the “IUPAC system”. The fisher system is the oldest system and used the Greek letters to define the positions on the porphyrin macrocycle. The alphabets are used to define the pyrrole units in the macrocycle. In the IUPAC system of nomenclature the carbon skeleton is numbered in ascending order starting from one assigned to a very specific α -position. If the carbon skeleton contains the extra exocyclic rings then the common names are used in order to avoid complexity, e.g. in case of benzocarbaporphyrins. Some of the examples are listed in the Fig. 1.5 for both Fisher and IUPAC nomenclature [34].

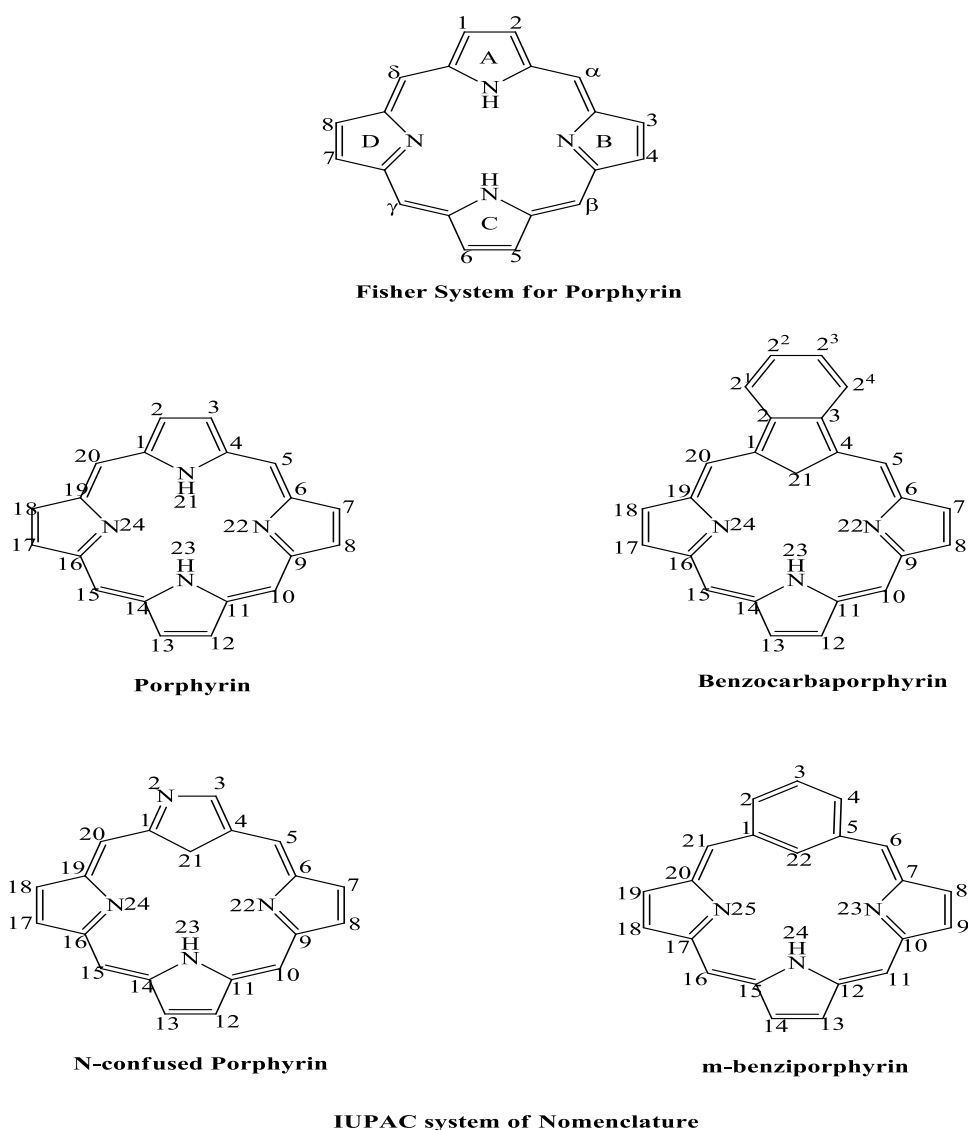


Fig. 1.5 Fisher and IUPAC Systems of nomenclature

1.5 CRITERIA FOR THE AROMATICITY OF PORPHYRINS

Aromaticity plays very important role in the chemistry of porphyrinoid systems. Simple porphyrin molecule is highly aromatic in nature. There are 22π electrons in the simple porphyrin molecule however only 18π electrons take part in complete conjugation in several possible delocalization pathways as shown in Fig 1.6.

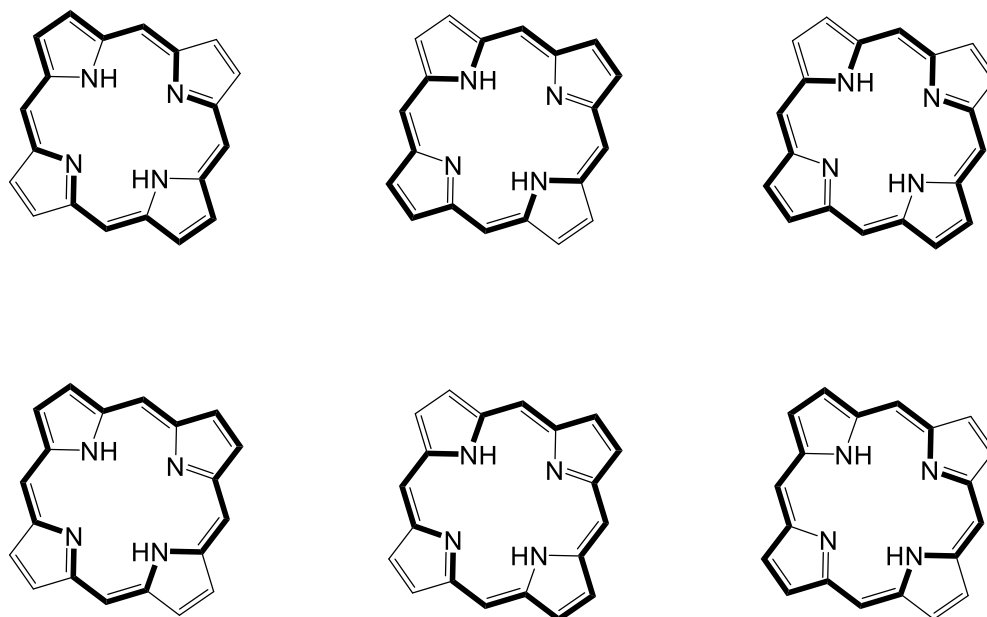


Fig. 1.6 Possible pathways for the delocalisation of π electrons in porphyrins

Porphyrins are deep coloured compounds clearly indicates the extensive delocalisation of π electrons in the carbon skeleton and show absorbance in UV-Visible region [35]. Porphyrin also follow Huckel's rule of aromaticity, $(4n+2)$ π electrons where $n=4$ like other small organic molecules (benzene, naphthalene, anthracene etc.). Usually the flat small molecules are aromatic in nature but flat is not the only criteria for aromaticity. This fact is clearly indicated by the larger macrocycles (Sapphyrins, pentaphyrins, hexaphyrins, etc.) where extended structures, because of their conformational flexibility, frequently present features of aromatic compounds [36]. One of the easiest way to analyse the aromatic character of porphyrin molecules is the NMR analysis. If the molecules is said to be aromatic and is fully conjugated through $4n+2$ π electrons pathway then the periphery protons of the macrocycle will come downfield whereas the inner protons will go up field strongly. The difference between the shift of inner and outer protons is

generally used to identify the aromatic, nonaromatic and antiaromatic character of the macrocycle [37].

The difference of δ_{out} and δ_{in} can be used to determine the aromatic character in the molecule; $\Delta = \delta_{\text{out}} - \delta_{\text{in}}$ Where δ_{out} and δ_{in} are the chemical shifts of the periphery and inner protons respectively. If we take porphyrin molecule as a standard than the factor Δ is found to be ~ 12 ppm. Considering it standard and reference we can compare the aromaticity of other moieties easily and can conclude about their aromatic nature. The N-confused porphyrin like porphyrin possess a similar pathway of 18π electrons and have a factor (Δ) value of ~ 14 ppm and thus is considered aromatic. On the other hand the *meta*-benzporphyrin molecule have the (Δ) value of -1 and is said to be non-aromatic. Actually in the *meta*-benzporphyrin, the benzene ring aromaticity dominates within molecule, blocking the macrocycle aromaticity. The comparison of aromatic character of different macrocycles is shown in the Fig 1.7 [38].

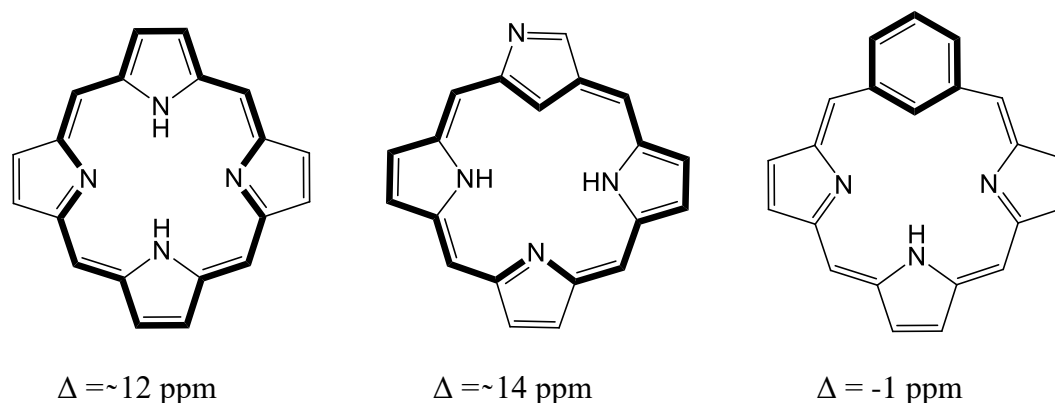


Fig. 1.7 Representation of delocalisation pathway and Δ 's value for porphyrin (18π electrons), N-confused Porphyrin (18π electrons) and in *meta*-benzporphyrin (6π electrons) [38]

1.6 GENERAL SYNTHETIC PROCEDURES FOR PORPHYRINS AND THEIR ANALOGUES

The synthesis of symmetrical tetrapyrrolic porphyrins is now well established and does not involve such great difficulties which otherwise are common in the synthesis of specialized class of porphyrins [39]. Various approaches have been invented to obtain the specially designed moieties which otherwise look difficult to obtain. These special techniques generally involve the use of either Brønsted or Lewis acid catalyst to guide the reaction involving pyrrole and aryl aldehyde(s), followed by oxidation with a quinone type agent to obtain the desired product [8h].

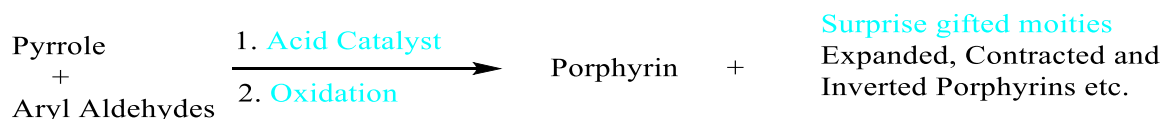


Fig. 1.8 General Condensation procedure for Porphyrin

It is very common that these processes not only give the desired product but other gifted compounds like expanded, contracted, inverted and other categories compounds also. It is thus necessary to optimize the conditions of reactions in a number of ways for obtaining our desired product only. Thus the one pot synthesis of porphyrins pioneered by Rothmund [32] has been optimized in the past, in a number of ways by using various modified catalysts to direct the synthesis towards a particular moiety and to reduce or eradicate the unwanted products [39].

Other important alternatives to these statistical approaches are also used to obtain the porphyrinoid moieties. These alternative methods are largely used in the formation of carba porphyrinoids and their derivatives. These methodologies involve the condensation of predefined moieties like dipyrromethane (2+2 condensation approach) or tripyrromethane (3+1 Condensation approach) moiety with other small molecules. It is possible to obtain a moiety using [2 + 2] MacDonald reaction, which has all four different meso-aryl substituents [40]. The [3 + 1] methodology (Scheme, Routes C and D) is widely used in the synthesis of β -substituted porphyrins including their carba analogs [41].

Variations within the [3 + 1] strategy provide two different routes when applied to heteroporphyrins, including carbaporphyrins. It is necessary to specify two possible categories. The first [3 + 1], Route C will be applied for syntheses where the “3” synthon provides an inner carbon atom. The second [1 + 3], Route D implies a reaction between tripyrrane and carbocycle or heterocycle. The [3 + 1] or [1 + 3] condensation gave a large family of β -substituted carbaporphyrins containing a wide scope of the built-in carbocycles. Besides β -substituted porphyrins, the core modification of tetraaryl analogs was also performed by applying the [3 + 1] condensation [42].

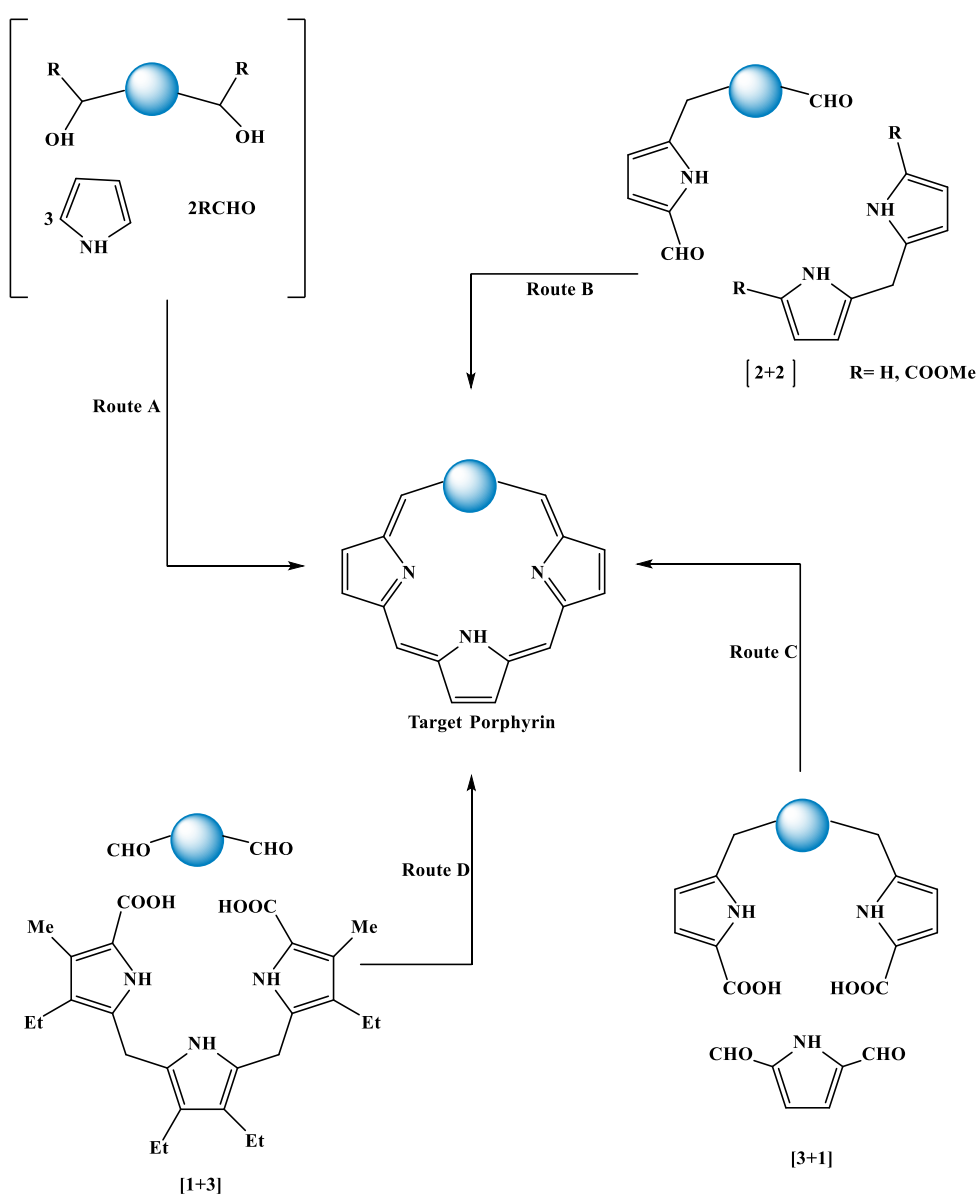


Fig. 1.9 some of the possible approaches for the synthesis of carbocyclic ring moieties

1.7 PHOTO-PHYSICAL PROPERTIES OF PORPHYRINS

Because of their extensive macrocyclic delocalisation porphyrin ring moieties are highly deep in colour. The UV-Vis absorption spectrum of porphyrin consists of two distinct regions namely, violet and visible region. In the violet region, extremely intense absorption band known as Soret band is present at around 400 nm. The number of absorptions known as the Q bands are present in visible region around 500- 650 nm. Soret band has a typical extinction coefficient of approximately $1 \times 10^5 \text{ M}^{-1}\text{cm}^{-1}$ whereas Q bands possess typical extinction coefficient of approximately $1 \times 10^4 \text{ M}^{-1}\text{cm}^{-1}$. The characteristic intense Soret band in the region of $\sim 400 \text{ nm}$ was discovered in haemoglobin by Soret [35a] and this was later observed in porphyrins by Gamgee [35b]. The inner 16-membered ring of the porphyrin is responsible for maintaining the $18\text{-}\pi$ electrons conjugated pathways that generate typical porphyrin-type optical spectrum, Fig. 1.10.

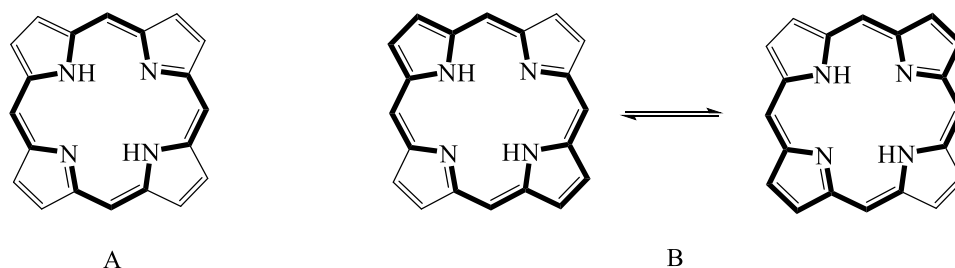


Fig. 1.10 The inner 16 membered ring (A) responsible for maintaining the conjugation for $18\text{-}\pi$ electrons pathways (B) that generate the porphyrin optical spectrum

Further, the ring is susceptible to perturbation through various chemical modifications to the basic structure of porphyrin. The absorption spectra of free-base porphyrins display four lower intensity Q bands between 500-650 nm due to D_{2h} symmetry, whereas metallo porphyrins show only two Q-bands due to D_{4h} symmetry. The Soret and the Q bands both arise from $\pi\text{-}\pi^*$ transitions and can be explained by considering the four frontier orbitals of the Gouterman four orbital model [43]. Typical absorption spectra of meso-tetraphenylporphyrin (TPP) and zinc (II) meso-tetraphenylporphyrin (Zn-TPP) are shown in Fig. 1.11.

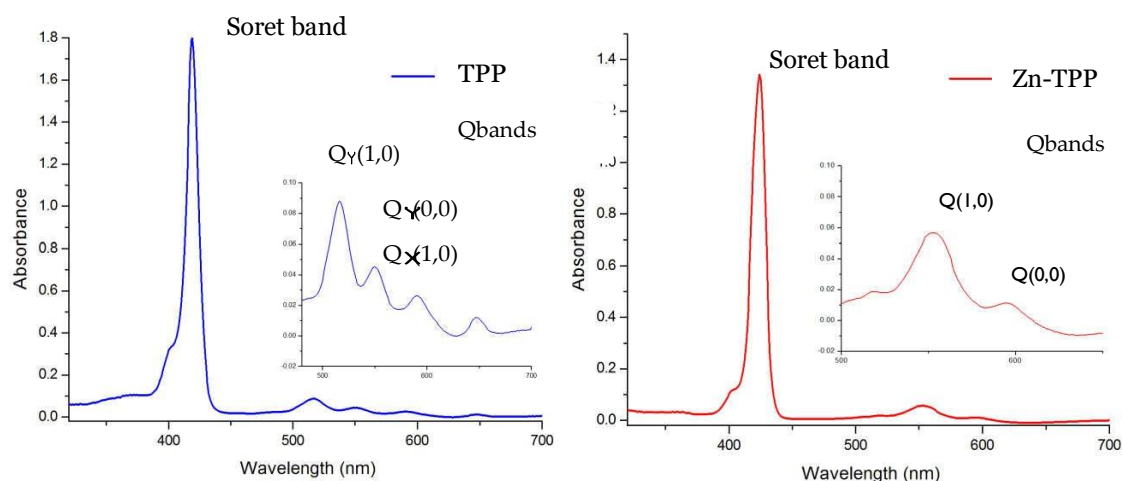


Fig. 1.11 Electronic absorption spectra of TPP and Zn-TPP

1.8 THE GOUTERMAN FOUR ORBITAL MODEL

Gouterman developed the four orbital model which has been used extensively to explain the absorption and emission spectra of metallo-porphyrins [44]. For the metalloporphyrin with D_{4h} symmetry, a 16 membered cyclic polyene model is applied. The highest filled orbitals are singly degenerate and denoted by a_{1u} and a_{2u} , while the lowest empty orbitals to which electron can be promoted are doubly degenerate and denoted by e_g . The excitation of electron from a_{1u} or a_{2u} to e_g results in the transitions seen in the absorption spectra of porphyrins (Fig. 1.12 and 1.13). The four-orbital model has been confirmed satisfactorily by the results of numerous spectroscopic studies. The modifications at the periphery of the porphyrin ring normally result in the change of intensity and wavelength of the absorption bands. Moreover, a disrupted porphyrin macrocycle results in the disappearance of the Soret band [45].

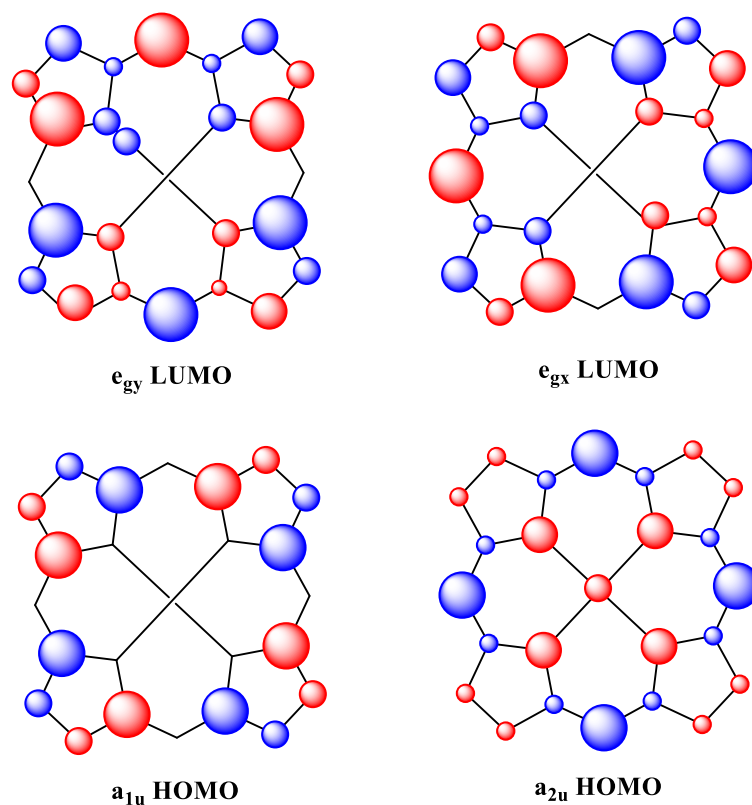


Fig. 1.12 Gouterman four orbital model

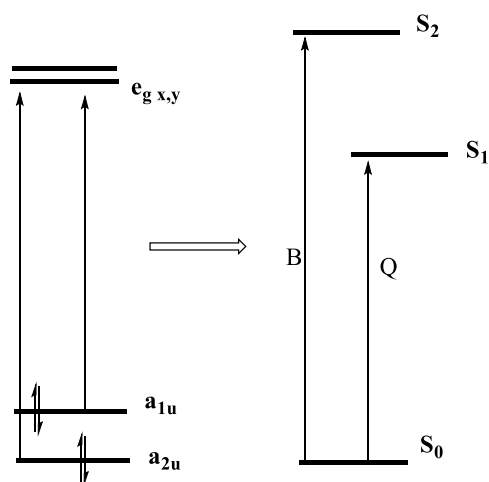


Fig. 1.13 Orbital diagram showing possible transitions for porphyrin macrocycle

1.9 BENZIPORPHYRIN: A CLASS OF CARBAPORPHYRINOIDS

The work involved in this present research is largely on the core modified porphyrins which generally involves replacement of pyrrolic nitrogens by some other elements. If the replacing atom is carbon then the originated class of porphyrins is called carbaporphyrinoids. The presence of -CH moiety in the inner core gives higher possibility for stabilization of rare metal carbon interaction [10]. It is important to notice that in the Carbaporphyrinoids due to the -CH moiety in the inner core, the π electrons delocalization is deeply affected and in some case it ceases completely [8d]. The loss of electronic current can be detected by NMR spectroscopy [8d]. When one of the pyrrole ring in porphyrin macrocycle is replaced by phenylene ring then it creates a subclass called **benziporphyrins**. Benziporphyrins is important to us as it gives a possibility to study the behaviour of aromatic ring in vicinity of metal ions [46].

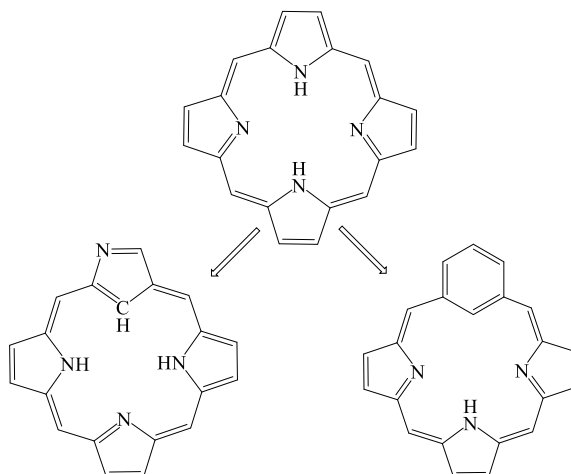


Fig. 1.14 Representation of pathway from porphyrin to carbaporphyrinoids

An important compound in the class of benziporphyrin is *meta*-benziporphyrin, where a *meta*-phenylene ring replaces a pyrrolic moiety of porphyrin. *meta*-benziporphyrin was firstly synthesized by Berlin and Breitmaier in 1994 [8a]. The condensation of isophthalaldehyde with the tripyrrane followed by oxidation with chloranil (tetrachloro-*p*-benzoquinone, TCQ) yielded the benziporphyrin in a 6% overall yield (Fig 1.15).

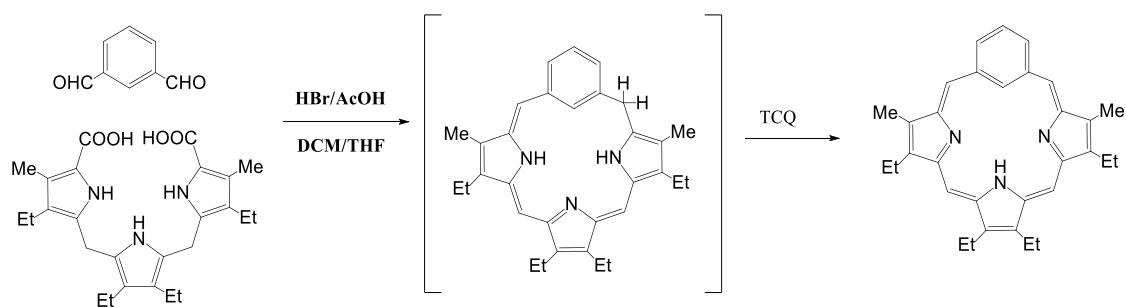


Fig. 1.15 Synthesis of *meta*-benziporphyrin by Berlin and Breitmaier in 1994

meta-benziporphyrin was found to be quite unstable in solution and hence it is difficult to obtain a pure sample. Synthetic analog like meso substituted benziporphyrins were prepared for obtaining a pure sample by Martin Stępień, and Latos-Grażyński [47]. The synthesis involved a condensation of pyrrole, aromatic aldehyde and a precursor (α, α' diol) followed by oxidation with DDQ, and further purification by chromatography, yielded 15% [47] and shown in Fig 1.16.

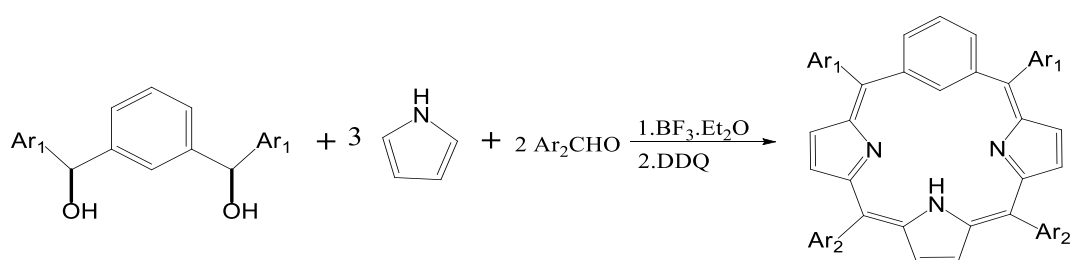


Fig. 1.16 Synthesis of meso substituted *meta*-benziporphyrins

1.10 OXY-BENZIPORPHYRIN AND *PARA*-BENZIPORPHYRIN

Another important compound in the category of Benziporphyrin is Oxybenziporphyrin and shown in Fig. 1.17. First synthesized and reported by Lash [48]. 2-Oxybenziporphyrin was synthesized by T.D. Lash in a modified synthesis from 5-formyl salicylaldehyde and a tripyrrane according to the following scheme.

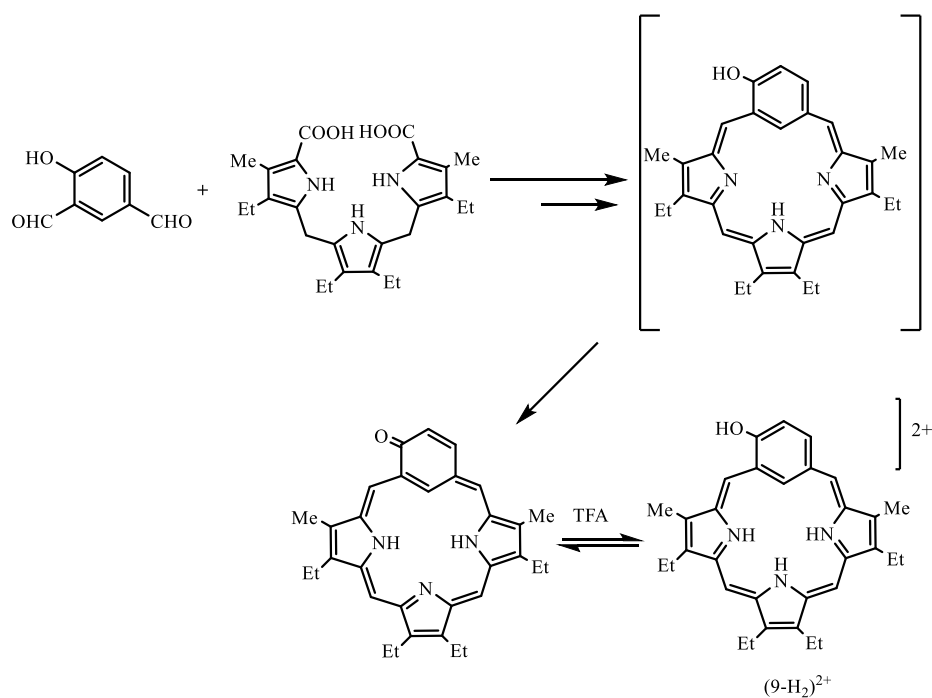


Fig. 1.17 Synthesis of Oxybenziporphyrins

2-oxybenziporphyrin solely exists as semiquinone ring system which is aromatic in nature. However it can be protonated twice to form first monocation and later a dication. It has been observed that protonation leads to drastic decrease in aromaticity of the moiety. Later Chandrasekhar and co-workers also synthesized hetero analogues of Oxybenziporphyrins [49]. Use of hetero atoms substituted tripyrrane moiety results in the synthesis of 24-oxa and 24-thia 2-oxybenziporphyrins (Fig. 1.18).

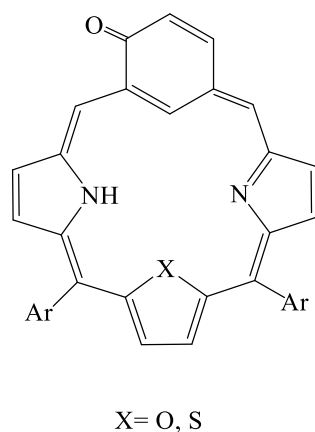


Fig. 1.18 Hetero Oxybenziporphyrins

It is to be noted that in the meta-benziporphodimethene the structural limitation restrict the aromaticity of the molecule and hence the ring current is attenuated. In oxy-

benziporphyrin the semiquinone arrangement reconstruct the ring current in the system. These two classes clearly indicates that the orientation of phenylene ring affects the aromaticity of the molecule drastically. The same was observed when the phenylene ring was incorporated in the system with 1 and 4 position of linkage, resulted in the new class of benziporphyrins, called ***para*-benziporphyrins**. *Para*-benziporphyrin was first reported by Martin Stępień and Lechosław Latos-Grażyński in 2001 in a synthesis similar to the *meta*-benziporphyrin [50]. The α, α' -dihydroxy-1, 3-diisopropylbenzene in the synthesis was replaced by 1, 4 isomer to obtain *para*-benziporphyrin. However the yield was reduced drastically to 1-3% (Fig 1.19).

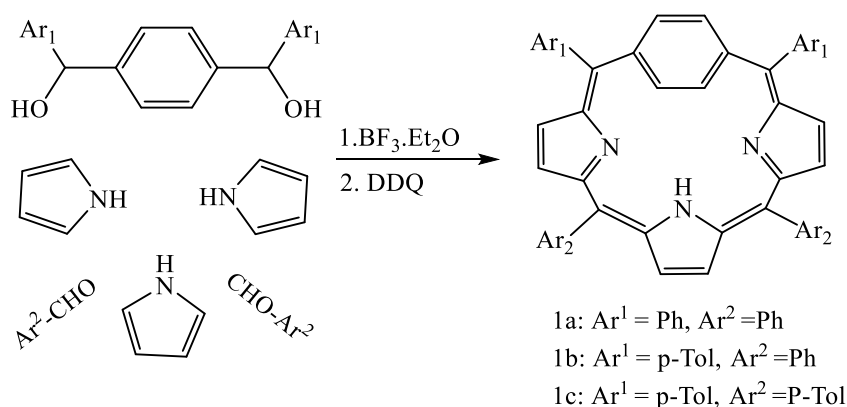


Fig. 1.19 Synthesis scheme for *para* benziporphyrins

Later Hung and co-workers synthesized the hetero analogue by using α, α' -dihydroxy-1, 4-diisopropylbenzene with 16-thiatripyrrane to give a 6% yield [51].

It is worth mentioning here that the *p*-phenylene ring in *para*-benziporphyrin was found out of the plane of three N atoms and is 45° tilted from the plane. A weak conjugation was also indicated by deviation in C-C bonds in *para* phenylene from normal benzene ring. The NMR study reveals that the *para* phenylene ring protons faces different magnetic field at low temperatures while the difference end up at high temperature clearly indicating the rotation of *para* phenylene ring in a see-saw motion at higher temperatures. While at low temperature the outer protons 2 and 3 comes at aromatic region, the inside proton 21 and 22 comes upfield due to inner shielding ring current [50] and shown in Fig. 1.20.

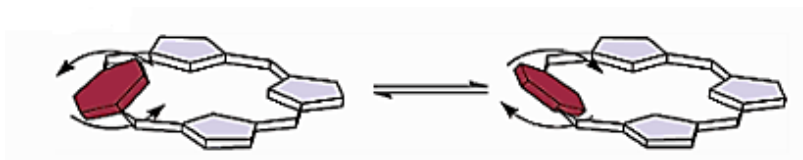


Fig. 1.20 Rotation of *para* benzene in *para*-benziporphyrin moiety

Further molecular and spectral study indicates that *para*-benziporphyrin behaves like extended conjugated macromolecules having aromaticity which differentiate it with *meta*-benziporphyrins. It is also different with oxy-benziporphyrin as that achieves aromaticity because of semiquinone arrangement.

1.11 BENZIPHORINS AND SUBSTITUTED BENZIPORPHODIMETHENES

Phlorins are the reduced form of porphyrin ring system containing a single tetrahedral meso carbon atom.

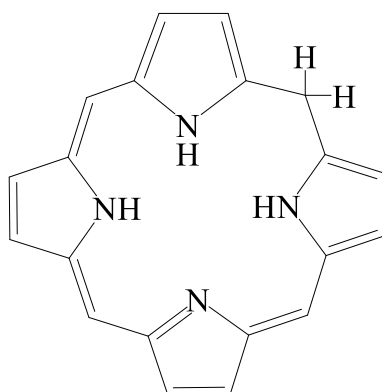


Fig. 1.21 Phlorin

Reduction at meso carbon of a porphyrin molecule generates Phlorins. Since this reduction is achieved by loss of aromaticity hence generally phlorins reverts back to porphyrins. The reversal however can be prevented by the presence of aryl or alkyl substituents. Since *meta*-benziporphyrins don't have stability due to macrocyclic aromaticity and hence their phlorin type derivative are less prone to oxidation. Past researches has revealed that *meta*-benziphlorins can be generated from *meta*-benziporphyrins by addition of water or alcohol molecules. The acid catalyzed reaction

selectively yields 6-hydroxy or 6-alkoxy *meta*-benziphlorins and the scheme is shown in Fig. 1.22.

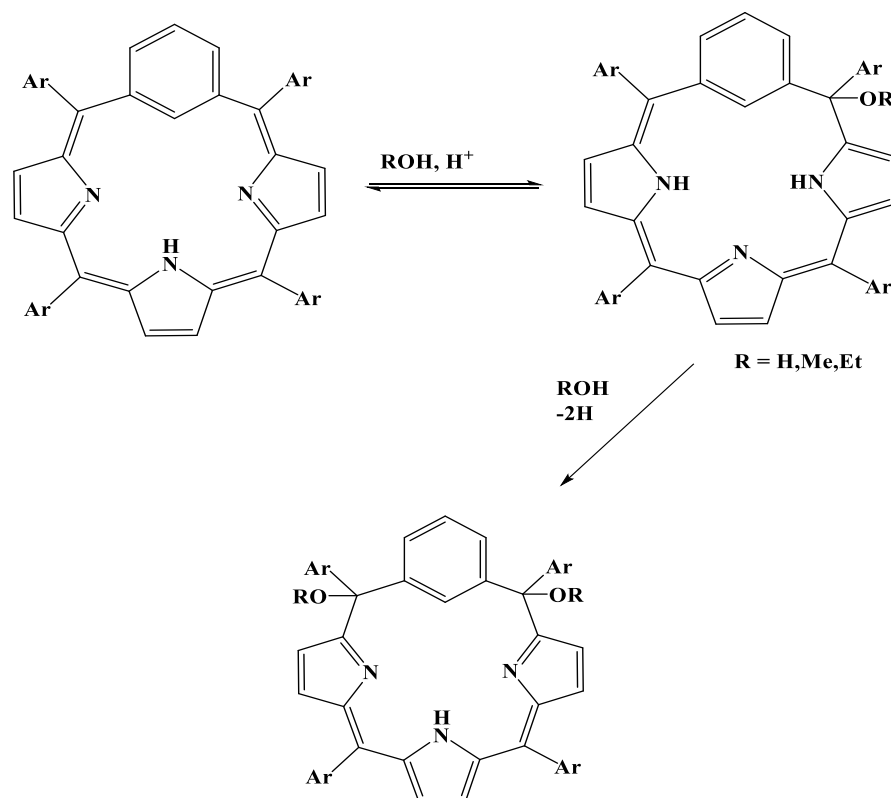


Fig. 1.22 Synthesis of *meta*-benziphlorins from *meta*-benziporphyrin

In this reaction procedure benziphlorins can be synthesized reversibly and hence concentration of nucleophile plays an important role in this reaction. In the presence of oxidants benziphlorins results in the red color compounds [52] which are alkoxy or hydroxyl analogues of benziporphodimethenes [33].

1.12 *meta*-BENZIPORPHODIMETHENES

meta-benziporphodimethene was firstly synthesized by Martin Stępień during his work of Ph.D. thesis [52]. Those synthesized benziporphodimethene were alkoxy and hydroxy analogues and were obtained from *meta*-benziporphyrins by oxidation. *meta*-benziporphodimethenes are actually modified *meta*-benziporphyrins with two tetrahedral meso carbon atoms at 6 and 21 position [33], and shown in Fig. 1.23.

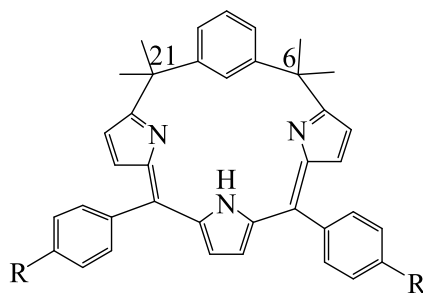


Fig. 1.23 *meta*-benziporphodimethene

meta-benziporphodimethenes can be prepared in good yield by the method adopted by Latos Grażyński and Martin Stępień which involves a mixed condensation of pyrrole, α , α' -dihydroxy-1, 3-diisopropylbenzene and an aromatic aldehyde in a fixed ratio, catalyzed by a lewis acid generally boron-trifluoride [33]. This reaction produces a good yield of approximately 27% and shown in Fig. 1.24.

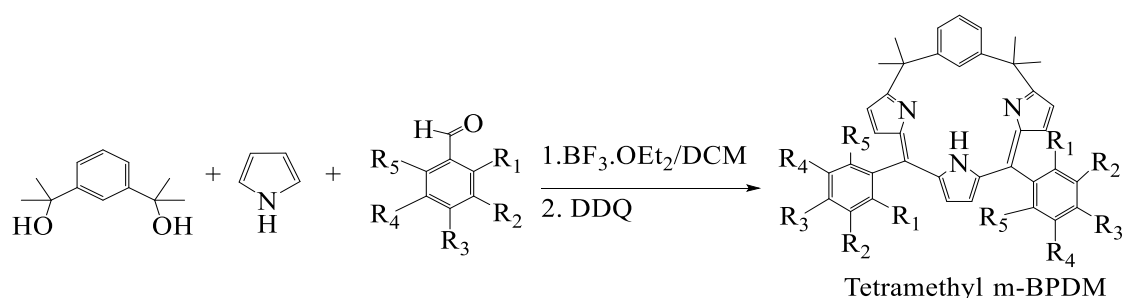


Fig. 1.24 Synthesis of *meta*-benziporphodimethenes

meta-benziporphodimethenes are generally red color compounds. Since they have a discrete conjugated system hence they show a broad UV-Vis spectrum. In *meta*-benziporphodimethenes a high energy Soret band is observed at about 350 nm and lower energy Q band is observed at about 510 and 550 nm approximately.

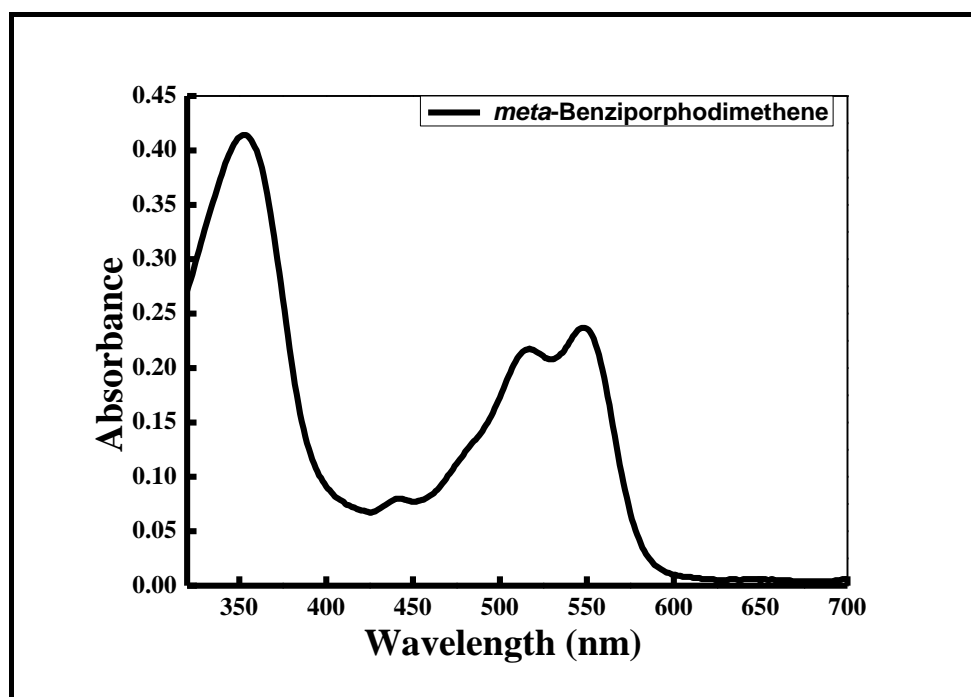


Fig. 1.25 UV Spectra of *meta*-benziporphodimethene

The synthesis of *meta*-benziporphodimethene with the procedure mentioned above also results in the synthesis of isomeric α , β -unsaturated γ -Lactam embedded N-Confused-tetra-methyl *meta*-benziporphodimethenes [53]. The two isomeric macrocycle with the carbonyl group of the lactam ring either close to (O-Up) or away from (O-Down) the neighbouring sp^3 meso carbon has also been synthesized and characterized and shown in Fig. 1.26.

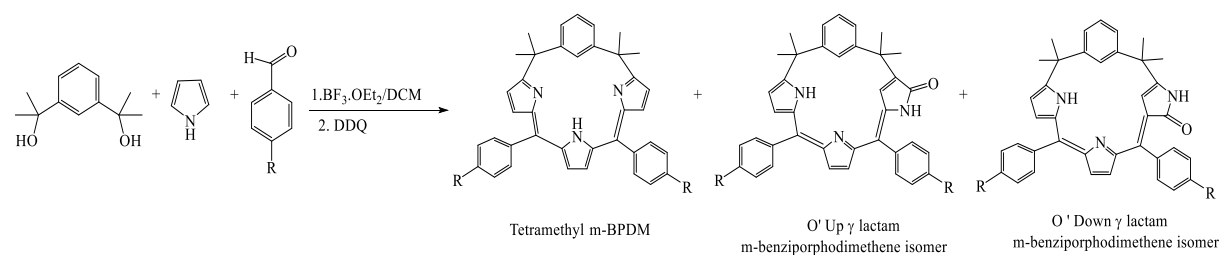


Fig. 1.26 The O' Up and O' Down γ lactam embedded N-confused isomers

X-ray analysis shows that *meta*-benziporphodimethenes are more distorted than the other two isomers. The average deviation of 25 atoms on the macrocycle from a mean tripyrrin

plane for 1 is 1.044 Å while the values for 2 and 3 are 0.680 and 0.630 Å, respectively. The angle between the CN₂ inner-core plane and the macrocyclic-phenylene plane is 70.35° for 2 and 69.76° for 3, but in case of 1, the angle between the phenylene plane and the three pyrrolic nitrogen plane is only 52.39°. Another interesting feature in the crystal structure is that the angle between the vector along two *sp*³ meso carbons and the plane, defined by the mean plane of 17 atoms on a tripyrrin moiety, is 28.51° for 1, which is significantly larger than 15.79° and 14.34° for 2 and 3, respectively. These data are in good agreement with the fact that 2 and 3 are less puckered than 1 with the phenylene rings oriented vertical to the mean plane of the macrocycles [53].

It is interesting to note that the two N-confused isomers exist as dimers through the intermolecular hydrogen bonding of lactam amide bond. The dimerization was confirmed by taking the concentration dependent NMR spectra in CDCl₃. It was observed that with increasing concentration the outer NH proton comes more downfield as the extent of hydrogen bonding increases. The impact was observed more dominant in the O' down isomer than in the O' up isomer. This shows that O' down isomers have more effective intermolecular hydrogen bonding than the O' up isomer.

The DFT calculations show that the O-Up isomer is energetically more stable than the O-Down N-confused isomer by 8.49 Kcal mol⁻¹ and this is due to the fact that the O-Up isomer has a long path of conjugation involving 14 π electrons than 12 π electrons of the O-Down isomer. Similarly when the DFT calculation was performed on the keto and enol form of the O-Up and O-Down N-confused isomers it was found that an increase of 16.63 kcal mol⁻¹ and 13.65 kcal mol⁻¹ in enol form comparing with their corresponding keto tautomer were observed and this confirms that the keto form is more stable than the enol form [53].

1.13 NMR SHIFTS IN *meta*-BENZIPORPHODIMETHENE

meta-benziporphodimethene are non-aromatic as the ring current is attenuated due to tetrahedral meso carbon atoms. The same is observed in the NMR spectra of these compounds as the internal N-H protons come at δ~12.0, which shows the absence of internal shielding by ring current. The methyl peaks of the tetrahedral group appear at ~1.7 ppm. The pyrrolic protons appear at δ ~ 6.0-7.0 ppm. The pyrrolic protons 13 and 14 appear as a singlet and come at ~ 6.0 ppm, the other pyrrolic protons 9,18 and 8,19 come

slightly downfield at around 6.5 ppm and gives a 'ab quartet'. The aromatic protons of meso aryl substituents and of *meta*-phenylene ring appears in between δ 7-8 ppm as multiplet. The C(22)-H comes at around 8.0 ppm and also shows the absence of inner shielding ring current.

1.14 METAL COMPLEXES OF *meta*-BENZIPORPHODIMETHENES

Various metal complexes of *meta*-benziporphodimethenes have been prepared so far, which are quite stable also. The Ni, Zn, Cd, Hg and Ag [46] complexes of *meta*-benziporphodimethenes have been reported so far. The metal complexes of *meta*-benziporphodimethenes with Zinc, Cadmium, Mercury and Nickel were reported by Latos Grażyński and co-workers in 2004 [33]. Later Hung and co-workers also reported the complexes of Zn, Cd, Hg and Ag for agostic metal arene interaction, hydrogen bonding, η^2 and π co-ordination [46]. The general synthesis includes mixing of free base *meta*-benziporphodimethenes with anhydrous metal salt in mixed solvents of acetonitrile with either dichloromethane or chloroform in presence of mild base 2, 6-lutidine. The metal complexes results minutes after mixing at room temperature and is indicated by changing of color of solution from red to greenish blue. Evaporation of solvent in vacuo under reduced pressure yields the metal complexes. The crystals can be obtained by crystallization of metal complexes in Hexane.

Hung and co-workers also reported the di-nuclear and tetra-nuclear complexes of Ag-*meta* benziporphodimethenes [46], using AgNO₃ as the starting metal salt. It is quite interesting that the metallation procedure with water extraction yielded the di-nuclear complex (Ag₂) while without water extraction yielded the tetra-nuclear Complex (Ag₄). It is evident from the experimental and calculation studies that di-nuclear complex (Ag₂) which involves a η^2 - π -co-ordination between pyrrolic segment (C13-C14) and silver metal, acts as scaffold for both the di-nuclear and tetra-nuclear complexes.

1.15 SOME IMPORTANT PROPERTIES OF METALLATED-*meta* BENZIPORPHODIMETHENE COMPLEXES

1. **Weak Metal-Arene Interaction:** One of the most important property of metal tetra methyl-*meta*-benziporphodimethenes complexes is the presence of metal arene interaction in them. *meta*-benziporphodimethenes have the advantage to

activate the C-H bond of *meta* phenylene ring in the vicinity of transition metal atoms and that gave it a new horizon to explore. X-ray structure analysis has confirmed the Weak metal–arene interactions in cadmium and nickel complexes of *meta*-benziporphyrin, with distances shorter than the sum of vander Waals radii [33]. The unusually large intramolecular through-space scalar couplings between the cadmium nucleus and the arene protons in *meta*-benziporphyrin Cd(II) complexes as well as the downfield chemical shifts as a result of spin transfer from nickel center to an Agostic proton in the paramagnetic *meta*-benziporphyrin Ni(II) complexes provide solid supporting evidence for the presence of the metal-arene interaction [33]. Interestingly, the strength of the metal-arene interaction is highly dependent on the conformation of the arene moiety. As in the case of *meta*-Benziporphyrins this kind of interaction not only helps in the activation of phenylene ring but also in the stabilization of metal complexes [46, 33].

- 2. Fluorescence enhancement:** An important property of these compounds is that they are non-fluorescent in free base form but turn on fluorescence upon zinc metallation with no background emission [54]. The most important part of this finding is that *meta*-benziporphodimethenes acts as a specific sensor for zinc ions [55]. Very less fluorescence is observed for cadmium and mercury ions comparatively. Since the fluorescence “switch on” upon zinc metallation and hence this kind of fluorescence comes under the category of “**chelation enhanced fluorescence**” (CHEF). Most CHEF sensors are based on fluorophores, such as fluorescein [56-57], dansyl and anthracene, which emit at wavelength shorter than 600 nm. Sensors that are effective above 600 nm, where background emission is minimal, minimize light induced tissue damage, penetrate better and scatter less in optically diffuse samples. It is interesting to note that these kind of moieties do not form complexes with alkali, alkaline earth and other some transition metals which are physiologically important as shown by hung and co-workers [54]. Hung and coworkers also proved that the stability constant for zinc complexation with *meta*-benziporphodimethene is greater than the cadmium and mercury respectively and hence Zn^{2+} have a tendency to replace Cd^{2+} and Hg^{2+} ions from their corresponding complexes [54].

1.16 FLUORESCENCE PHENOMENA: STRUCTURE CO-RELATION

It is to be noted that *meta*-benziporphodimethene is a selective Zn^{2+} ion sensor and the intensity of fluorescence is comparatively high than in case of cadmium or mercury. The most important reason for this phenomena is planarity of the macrocycle in the bind state. The free base macrocycle exist as highly distorted non-planer molecule, but on metallation it has been observed that the tripyrrin moiety becomes planar. The average deviation of the three nitrogen atoms of the tripyrrin plane get reduced from 0.27 Å to 0.10 Å upon metallation. The metal ions in the complex occupies a tetrahedral coordination which involves three nitrogen of tripyrrin moiety and a chlorine which sits at the axial position. It has also been found that the zinc has the least apical deviation of (0.48-0.50) Å from the tripyrrin plane as compared to that of (0.62-0.67) Å for cadmium and (0.70-0.71) Å for mercury, and the orientation of *meta*-phenylene ring in metal-*meta*-benziporphodimethene changed from 81.4° in Zn -*meta*-benziporphodimethene to 89.3° for Cd and 92.1° for Hg. The data is highly in line with the efficient transfer of electron density from ligand to metal and plots a better resonance tendency in case of zinc as binding metal ion [46].

1.17 APPLICATIONS

Zinc ions in the human body are involved in various biological processes. Zinc in the human body can be found in bound state with protein as structural cofactors [58] and gene expression regulator [59]. Labile pool of zinc ions can also be found in the vesicles of neurons. Besides, Zn^{2+} is also an important regulator of the cellular apoptosis [60], and it is relevant to severe diseases such as Alzheimer's disease [61, 62] and Parkinson's disease [63, 64] while a disorder of zinc metabolism has occurred. Patients with inflammatory diseases and tumors also show abnormal Zn^{2+} concentration in sera and tissues [65]. Since both vital roles and toxic influences of Zn^{2+} are commonly observed, real-time detection of Zn^{2+} may help to unveil its physiological and pathological roles. A small-sized semiconductor optoelectronic device is therefore needed for a real-time and indicator-free detection of Zn^{2+} in liquid environment.

With such commercial application in mind Hung and co-workers have designed an organic hydrogel film with micron-sized pillar array for real-time and indicator free detection of zinc ions in the solution by embedding a fluorescent indicator 11,16-bis(phenyl)-6,6,21,21-tetramethyl-*meta*-benzi-6,21-porphodimethene in a hydrogel

host poly(2-hydroxyethyl methacrylate). The sensing film shows high stability and selectivity to Zn^{2+} ions. The sensitivity of the sensing film was increased by fabricating a micron-sized pillar array on the surface of the sensing film to increase the surface area. For Zn^{2+} concentrations of 10^{-4} & 10^{-3} M, the response time was estimated around 30 and 3 s, respectively [55].

REFERENCES

1. S. D. Straight, G. Kodis, Y. Terazono, M. Hamburger, T. A. Moore, A. L. Moore, D. Gust, *Nature nanotechnology* **2008**, *3*, 280-283.
2. S. D. Starnes, S. Arungundram, C. H. Saunders, *Tetrahedron letters* **2002**, *43*, 7785-7788.
3. V. S. Lin, S. G. DiMagno, M. J. Therien, *Science* **1994**, *264*, 1105-1111.
4. (a) J. Králová, Z. Kejík, T. Bříza, P. Poučková, A. Král, P. Martásek, V. Král, *Journal of Medicinal Chemistry* **2010**, *53*, 128-138. (b). G. Jori, C. Fabris, M. Soncin, S. Ferro, O. Coppellotti, D. Dei, L. Fantetti, G. Chiti, G. Roncucci, *Lasers in Surgery and Medicine* **2006**, *38*, 468-481. (c). T. Ozawa, R. A. Santos, K. R. Lamborn, W. F. Bauer, M. S. Koo, S. B. Kahl, D. F. Deen, *Molecular pharmaceuticals* **2004**, *1*, 368-374.
5. (a) *The Porphyrin Handbook*, K. M. Kadish, K. M. Smith and R. Guilard (Eds.) Academic Press: San Diego, CA, **2000**. (b) *Handbook of Porphyrin Science*, K. M. Kadish, K. M. Smith and R. Guilard (Eds.) World Scientific: London, **2010**.
6. L. R. Milgrom, *The Colors of Life. An introduction to the chemistry of porphyrins and related compounds*; Oxford University Press: Oxford, ed.; **1997**, 1-249.
7. D. Dolphin, *The porphyrins* Academic press, New York. **1978**, vol 1-6.
8. (a) K. Berlin, E. Breitmaier, *Angewandte Chemie International Edition in English* **1994**, *33*, 1246-1247. (b) M. Pawlicki and L. Latos-Grazynski, In *Handbook of Porphyrin Science*, Vol. 2, K. M. Kadish, K. M. Smith and R. Guilard (Eds.) World Scientific: Singapore, **2010**; Chapter 8, pp. 103–192. (c) T. D. Lash, In *Handbook of Porphyrin Science*, Vol. 16, K. M. Kadish, K. M. Smith and R. Guilard (Eds.) World Scientific: Singapore, **2012**; Chapter 74, pp. 1–329. (d) M. Stępień, L. Latos-Grażyński, *Accounts of Chemical Research* **2005**, *38*, 88-98. (e) T. D. Lash *Synlett.* **2000**, 279–295. (f) T. D. Lash, *European Journal of Organic Chemistry* **2007**, *2007*, 5461-5481. (g) T. D. Lash, *Chemistry, an Asian journal* **2014**, *9*, 682-705. (h) A. Kumar, S. Maji, P. Dubey, G. J. Abhilash, S. Pandey, S. Sarkar, *Tetrahedron Letters* **2007**, *48*, 7287-7290. (i) R. K. Sharma, L. K. Gajanan, M. S. Mehata, F. Hussain, A. Kumar, *Spectrochimica Acta Part A: Molecular and Biomolecular Spectroscopy* **2016**, *169*, 58-65.
9. M. Yedukondalu, M. Ravikanth, *Coordination Chemistry Reviews* **2011**, *255*, 547-573.

10. L. Latos-Grażyński, Core Modified Heteroanalogues of Porphyrins and Metalloporphyrins; In *The Porphyrin Handbook*; K. M. Kadish, K.M. Smith, R. Guilard, (Eds), Academic Press: New York, **2000**.
11. I. Gupta, M. Ravikanth, *Coordination Chemistry Reviews* **2006**, *250*, 468-518.
12. P. J. Chmielewski, L. Latos-Grażyński, M. M. Olmstead, A. L. Balch, *Chemistry – A European Journal* **1997**, *3*, 268-278.
13. Z. Gross, I. Saltsman, R. P. Pandian, C. M. Barzilay, *Tetrahedron Letters* **1997**, *38*, 2383-2386. (b) A. Kumar, I. Goldberg, M. Botoshansky, Y. Buchman, Z. Gross, *J. Am. Chem. Soc.* **2010**, *132*, 15233-15245. (c) Z. Gross, N. Galili, I. Saltsman, *Angewandte Chemie International Edition* **1999**, *38*, 1427-1429. (d) Z. Gross, N. Galili, *Angewandte Chemie* **1999**, *38*, 2366-2369. (e) Z. Gross, L. Simkhovich, N. Galili, *Chemical Communications* **1999**, 599-600. (f) L. Simkhovich, A. Mahammed, I. Goldberg, Z. Gross, *Chemistry – A European Journal* **2001**, *7*, 1041-1055. (g) L. Simkhovich, Z. Gross, *Tetrahedron Letters* **2001**, *42*, 8089-8092. (h) A. Mahammed, Z. Gross, *Angewandte Chemie* **2006**, *118*, 6694-6697. (i) I. Aviv, Z. Gross, *Chemical Communications* **2007**, 1987-1999. (j) I. Aviv-Harel, Z. Gross, *Chemistry – A European Journal* **2009**, *15*, 8382-8394. (k) J. Bendix, H. B. Gray, G. Golubkov, Z. Gross, *Chemical Communications* **2000**, 1957-1958. (l) Z. Gross, G. Golubkov, L. Simkhovich, *Angewandte Chemie International Edition* **2000**, *39*, 4045-4047. (m) G. Golubkov, J. Bendix, H. B. Gray, A. Mahammed, I. Goldberg, A. J. DiBilio, Z. Gross, *Angewandte Chemie* **2001**, *113*, 2190-2192.
14. A. Ulman, J. Manassen, *Journal of the American Chemical Society* **1975**, *97*, 6540-6544.
15. L. Latos-Grazynski, J. Lisowski, M. M. Olmstead, A. L. Balch, *Journal of the American Chemical Society* **1987**, *109*, 4428-4429.
16. A. Ulman, J. Manassen, F. Frolow, D. Rabinowich, *Tetrahedron Lett.* **1978**, *19*, 1885.
17. L. Latos-Grażyński, E. Pacholska, P. J. Chmielewski, M. M. Olmstead, A. L. Balch, *Angew. Chem. Int. Ed. Engl.* **1995**, *107*, 2252.
18. A. Ulman, J. Manassen, F. Frolow, D. Rabinowich, *Tetrahedron Lett.* **1978**, *19*, 167.
19. L. Latos-Grażyński, E. Pacholska, P. J. Chmielewski, M. M. Olmstead, A. L. Balch, *Inorg. Chem.* **1996**, *35*, 566.

20. Y. Matano, T. Nakabuchi, T. Miyajima, H. Imahori, *Organometallics* **2006**, *25*, 3105.
21. Y. Matano, T. Nakabuchi, T. Miyajima, H. Imahori, H. Nakano, *Org. Lett.* **2006**, *8*, 5713.
22. Y. Matano, M. Nakashima, T. Nakabuchi, H. Imahori, S. Fujishige, H. Nakano, *Org. Lett.* **2008**, *10*, 553.
23. Y. Matano, H. Imahori, *Acc. Chem. Res.* **2009**, *42*, 1193.
24. (a) P. J. Chmielewski, *Angew. Chem. Int. Ed.* **2004**, *43*, 5655. (b) M. Siczek, P. J. Chmielewski, *Angew. Chem. Int. Ed.* **2007**, *46*, 7432. (c) P. J. Chmielewski, *Angew. Chem. Int. Ed.* **2005**, *44*, 6417. (d) T. Ishizuka, A. Osuka, H. Furuta, *Angewandte Chemie International Edition* **2004**, *43*, 5077-5081. (e) T. Ishizuka, S. Ikeda, M. Toganoh, I. Yoshida, Y. Ishikawa, A. Osuka, H. Furuta, *Tetrahedron* **2008**, *64*, 4037-4050.
25. R. Paollesse, Synthesis and application of corroles. In *The porphyrin handbook*, K. M. Kadish, K. M. Smith and R. Guilard (Eds.), New York: Academic Press, **2000**.
26. J. L. Sessler, A. Gebauer and E. Vogel, Porphyrin isomers. In *The porphyrin handbook*, K. M. Kadish, K. M. Smith and R. Guilard (Eds), New York: Academic Press, **2000**.
27. (a) J. L. Sessler and S. J. Weighorn **1997** Expanded, contracted and isomeric porphyrins (Oxford: *Elsevier*), and references therein; (b) J. L. Sessler, A. Gebauer and S. J. Weighorn, Expanded porphyrins. In *The porphyrin handbook*, K. M. Kadish, K. M. Smith and R. Guilard (Eds.), New York: Academic Press, **2000**.
28. J. Sessler, D. Seidel, *Angew. Chem. Int. Ed.* **2003**.
29. (a) V. J. Bauer, D. L. J. Clive, D. Dolphin, J. B. Paine, F. L. Harris, M. M. King, J. Loder, S. W. C. Wang, R. B. Woodward, *Journal of the American Chemical Society* **1983**, *105*, 6429-6436. (b) M. J. Broadhurst, R. Grigg, A. W. Johnson, *Journal of the Chemical Society, Perkin Transactions 1* **1972**, 2111-2116. (c) J. L. Sessler, J. M. Davis, V. Lynch, *The Journal of organic chemistry* **1998**, *63*, 7062-7065. (d) H. Rexhausen, A. Gossauer, *Journal of the Chemical Society, Chemical Communications* **1983**, 275-275. (e) (i) A. Gossauer, *Bulletin des Sociétés Chimiques Belges* **1983**, *92*, 793-795. (ii) A. Gossauer, *Chimia* **1983**, *37* 341. (f) J. L. Sessler, S. J. Weighorn, Y. Hiseada, V. Lynch, *Chemistry – A European Journal* **1995**, *1*, 56-67. (g) E. Vogel, M. Bröring, J. Fink, D. Rosen, H. Schmickler, J. Lex, K. W. K. Chan, Y.-D. Wu, D. A. Plattner, M. Nendel, K. N.

- Houk, *Angewandte Chemie International Edition in English* **1995**, *34*, 2511-2514.
- (h) M. Bröring, J. Jendryny, L. Zander, H. Schmickler, J. Lex, Y.-D. Wu, M. Nendel, J. Chen, D. A. Plattner, K. N. Houk, E. Vogel, *Angewandte Chemie* **1995**, *107*, 2709-2711. (i) A. Werner dagger, M. Michels, L. Zander, J. Lex, E. Vogel, *Angewandte Chemie (International ed. in English)* **1999**, *38*, 3650-3653. (j) J. L. Sessler, S. J. Weghorn, T. Morishima, M. Rosingana, V. Lynch, V. Lee, *Journal of the American Chemical Society* **1992**, *114*, 8306-8307. (k) J. L. Sessler, T. Morishima, V. Lynch, *Angewandte Chemie International Edition in English* **1991**, *30*, 977-980. (l) D. C. Miller, M. R. Johnson, J. J. Becker, J. A. Ibers, *Journal of Heterocyclic Chemistry* **1993**, *30*, 1485-1490. (m) M. R. Johnson, D. C. Miller, K. Bush, J. J. Becker, J. A. Ibers, *The Journal of organic chemistry* **1992**, *57*, 4414-4417. (n) D. C. Miller, M. R. Johnson, J. A. Ibers, *The Journal of organic chemistry* **1994**, *59*, 2877-2879. (o) J. L. Sessler, D. Seidel, V. Lynch, *Journal of the American Chemical Society* **1999**, *121*, 11257-11258. (p) J. L. Sessler, S. J. Weghorn, V. Lynch, M. R. Johnson, *Angewandte Chemie International Edition in English* **1994**, *33*, 1509-1512. (q) J.-i. Setsune, Y. Katakami, N. Iizuna, *Journal of the American Chemical Society* **1999**, *121*, 8957-8958.
30. H. Furuta, T. Asano, T. Ogawa, *Journal of the American Chemical Society* **1994**, *116*, 767-768.
31. P. J. Chmielewski, L. Latos-Grażyński, K. Rachlewicz, T. Glowiak, *Angewandte Chemie International Edition in English* **1994**, *33*, 779-781.
32. S. Aronoff, M. J. Calvin, *Org. Chem.* **1943**, *6*, 205.
33. M. Stępień, L. Latos-Grażyński, L. Szterenber, J. Panek, Z. Latajka, *Journal of the American Chemical Society* **2004**, *126*, 4566-4580.
34. (a) G. P. Moss, *Pure and Applied Chemistry, Vol. 59*, **1987**, p. 779. (b) G. P. Moss, *European Journal of Biochemistry* **1988**, *178*, 277-328.
35. (a) J. L. Soret, *Compt. Rend.* **1883**, *97*, 1267. (b) A. Z. Gamgee, *Biol. Munich* **1897**, *34*, 505.
36. M. O. Senge, *Chemical Communications* **2006**, 243-256.
37. M. Stępień, L. Latos-Grażyński, Aromaticity and tautomerism in porphyrins and porphyrinoids; In *Aromaticity in Heterocyclic Compounds*; Springer: Berlin/Heidelberg, **2009**; *19*, pp. 83–153.
38. M. Pawlicki, L. Latos-Grażyński, In *Handbook of Porphyrin Science*, World Scientific Publishing Company, **2012**, pp. 103-192.

39. (a) J. S. Lindsey, Synthesis of meso-Substituted Porphyrins; In the Porphyrin Handbook, K. M. Kadish, K. M. Smith, R. Guilard, (Eds), Academic Press: San Diego, CA, **2000**, pp. 45–118. (b) P. Rothmund, *Journal of the American Chemical Society* **1935**, *57*, 2010-2011. (c) P. Rothmund, *Journal of the American Chemical Society* **1936**, *58*, 625-627. (d) A. D. Adler, F. R. Longo, W. Shergalis, *Journal of the American Chemical Society* **1964**, *86*, 3145-3149. (e) J. B. Kim, J. J. Leonard, F. R. Longo, *Journal of the American Chemical Society* **1972**, *94*, 3986-3992. (f) A. D. Adler, F. R. Longo, J. D. Finarelli, J. Goldmacher, J. Assour, L. Korsakoff, *The Journal of organic chemistry* **1967**, *32*, 476-476. (g) J. S. Lindsey, I. C. Schreiman, H. C. Hsu, P. C. Kearney, A. M. Marguerettaz, *The Journal of organic chemistry* **1987**, *52*, 827-836.
40. D. M. Wallace, S. H. Leung, M. O. Senge, K. M. Smith, *The Journal of organic chemistry* **1993**, *58*, 7245-7257.
41. (a) K. M. Smith, Strategies for the Synthesis of Octaalkylporphyrin Systems; In The Porphyrin Handbook; K. M. Kadish, K. M. Smith, R. Guilard, (Eds), Academic Press: San Diego, CA, **2000**; pp. 1–43. (b) T. D. Lash, *Chemistry – A European Journal* **1996**, *2*, 1197-1200.
42. R. Myśliborski, L. Latos-Grażyński, *Eur. J. Org. Chem.* **2005**, 5039.
43. M. J. Gouterman, *Chem. Phys.* **1959**, *30*, 1139.
44. M. Gouterman, G. H. Wagnière, L. C. Snyder, *Journal of Molecular Spectroscopy* **1963**, *11*, 108-127.
45. C. Weiss, *Journal of Molecular Spectroscopy* **1972**, *44*, 37-80.
46. G. F. Chang, C. H. Wang, H. C. Lu, L. S. Kan, I. Chao, W. H. Chen, A. Kumar, L. Lo, M. A. C. Dela Rosa, C. H. Hung, *Chemistry - A European Journal* **2011**, *17*, 11332-11343.
47. M. Stępień, L. Latos-Grażyński, *Chemistry – A European Journal* **2001**, *7*, 5113-5117.
48. T. D. Lash, *Angewandte Chemie International Edition in English* **1995**, *34*, 2533-2535.
49. S. Venkatraman, V. G. Anand, S. K. Pushpan, J. Sankar, T. K. Chandrashekar, *Chemical Communications* **2002**, 462-463.
50. M. Stępień, L. Latos-Grażyński, *Journal of the American Chemical Society* **2002**, *124*, 3838-3839.

51. C.-H. Hung, C.-Y. Lin, P.-Y. Lin, Y.-J. Chen, *Tetrahedron Letters* **2004**, *45*, 129-132.
52. M. Stępień, Ph.D. Thesis, *Uniwersytet Wrocławski*, **2003**.
53. G. F. Chang, A. Kumar, W. M. Ching, H. W. Chu, C. H. Hung, *Chemistry - An Asian Journal* **2009**, *4*, 164-173.
54. C.-H. Hung, G.-F. Chang, A. Kumar, G.-F. Lin, L.-Y. Luo, W.-M. Ching, E. Diau, *Chemical Communications* **2007**, *0*, 978-980.
55. Y.-C. Chao, Y.-S. Huang, H.-P. Wang, S.-M. Fu, C.-H. Huang, Y.-C. Liang, W.-C. Yang, Y.-S. Huang, G.-F. Chang, H.-W. Zan, H.-F. Meng, C.-H. Hung, C.-C. Fu, *Organic Electronics* **2011**, *12*, 1899-1902.
56. P. Chavez-Crooker, N. Garrido, G. J. Ahearn, *Exp. Biol.* **2001**, *204*, 1433–44.
57. W. Breuer, S. Epsztejn, P. Millgram, I. Z. Cabantchik, *Am. J. Physiol.* **1995**, *268*, C1354–C1361.
58. E.H. Cox, G.L. McLendon, *Curr. Opin. Chem. Biol.* **2000**, *4*, 162.
59. G.K. Andrews, *Biometals* **2001**, *14*, 223.
60. A.Q. Truong-Tran, J. Carter, R.E. Ruffin, P.D. Zalewski, *Biometals* **2001**, *14*, 315.
61. M.P. Cuajungco, G.J. Lees, *Brain Res. Rev.* **1997**, *23*, 219.
62. C. Devirgiliis, P.D. Zalewski, G. Perozzi, C. Murgia, *Mutat. Res.* **2007**, *622*, 84.
63. D.T. Dexter, A. Carayon, F. Javoy-Agid, Y. Agid, F.R. Wells, S.E. Daniel, A.J. Lees, P. Jenner, C.D. Marsden, *Brain* **1991**, *114*, 1953.
64. G.A. Qureshi, A.A. Qureshi, S.A. Memon, S.H. Parvez, *J. Neural Transm.* **2006**, *71*, 229.
65. M. Murakami, T. Hirano, *Cancer Sci.* **2008**, *99*, 1515.

SCOPE OF THE PRESENT WORK

There are large numbers of fluorescent molecules known to visualize metal ions in live cells for particular purpose. These known synthetic molecules are having drawbacks of background fluorescence and having lesser excitation and emission wavelength. It has also been known that the initial requirement for the cellular imaging of metal ions in cells: higher excitation wavelength and higher emission wavelength to avoid any photo-damage of tissues and cells. Using these parameters in mind, all the successful molecules known in the literature, varies from different systems like nanoparticles, protein based molecules, dansyl, anthracene, BODIPY and fluorescein etc. are well documented in the literature.

Besides various fluorescent molecules synthesized so far, there has been serious problem persistent to all molecules that they have background fluorescence. Porphyrin and related porphyrinoid molecules has also been used in sensing zinc ions and cellular imaging purpose. Though, porphyrin and their zinc complex have low quantum yield in comparison to other porphyrinoid, but these porphyrinoid systems also have background fluorescence. So, to the best of our knowledge, all previously synthesized sensors suffer from same problem, less excitation and emission wavelength and background fluorescence. It would be beneficial if the synthesis of such type of sensor (with low or zero background emission and high wavelength for absorption and emission) for sensing zinc ions and other metal ions is possible. So, in this direction, Latos-Grażyński and their co-workers synthesized a new class of molecule: *meta*-benziporphodimethenes. Further, Hung and his coworkers explored this new molecule and established it as a non-

fluorescent molecule in its free base form which becomes fluorescent when bind with zinc, cadmium or mercury. Hence these molecules acts as sensing units for zinc, cadmium and mercury by using its fluorescence ‘*turn on*’ properties.

Based on the observations the present work describes:

1. The development in the extension of a series of free base *meta*-benziporphodimethenes and their zinc complex with varied substituents on *meso*-phenyl group. The effect of electron releasing and withdrawing group on *meso*-phenyl group may be compared with the *meta*-benziporphodimethenes having unsubstituted *meso*-phenyl group.
2. These molecules are non-fluorescent in their free base form and becomes highly fluorescent when bind to zinc. Hence, this property could be used in cellular imaging of zinc ions in different cancerous cells.
3. Correlation of energy level of varied *meta*-benziporphodimethenes with zinc metal ions would be interesting to know and could be studied using Density Functional Theory (DFT).

All the complexes synthesized may be characterized using several spectroscopic technique followed by applications in cellular imaging of zinc ions. Some of the representative newly synthesized complex may be subjected to full characterization using 3D X-ray structural crystallography.

EXPERIMENTAL SECTION

3.1 MATERIALS

The materials which have been used for the synthesis and characterization of the compounds involved in this work are *para* chloro benzaldehyde, *para* bromo benzaldehyde, 2, 6 di-chloro benzaldehyde, 2, 6 di-fluoro benzaldehyde, penta-fluoro benzaldehyde, *para* trifluoro-methyl benzaldehyde, *para*-methoxy benzaldehyde, 3, 4, 5 trimethoxy benzaldehyde, BF₃·OEt₂ from Sigma Aldrich, pyrrole from E. Merck, α,α' -dihydroxy-1,3-diisopropylbenzene from TCI, 2, 3-dichloro- 5, 6-dicyano-p-benzoquinone (DDQ), anhydrous zinc chloride from S. D. Fine-Chem Ltd. The solvents used in this work are dichloromethane, acetonitrile, hexane, ethyl acetate, were used after distillation and purification from S.D. Fine-Chem Ltd. Solvents used for crystallization like n-hexane, DCM, ethyl acetate were purchased from E. Merck. Deuterated solvents like CDCl₃, DMSO-d₆ etc. were purchased from Sigma Aldrich and used as supplied. Pyrrole and other liquid aldehydes were purified by distillation prior to the usage.

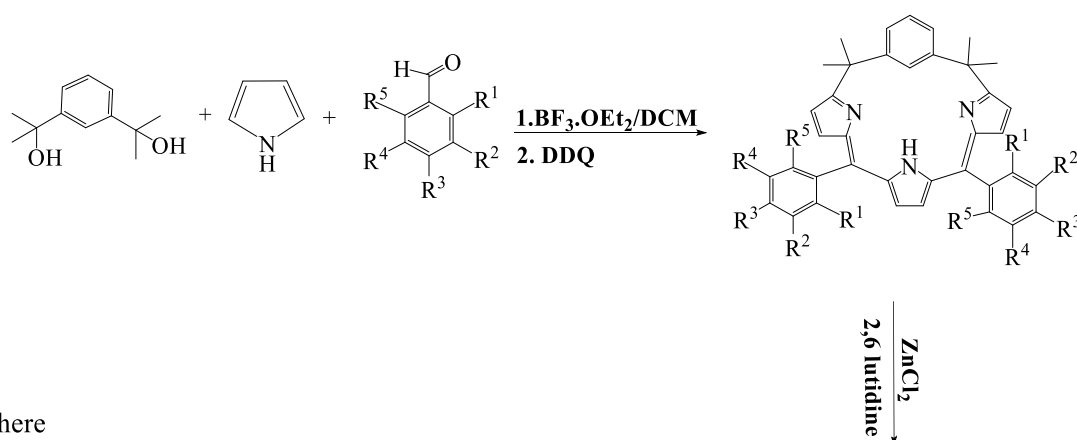
3.2 CHARACTERIZATION AND MEASUREMENTS

Absorption spectra were recorded with Shimadzu UV-1800 at room temperature. Fluorescence spectra were recorded by JobinYvon HoribaFluorolog-3 spectrofluorometer equipped with double-grating at excitation and emission monochromators and an R928P photomultiplier tube (PMT). The excitation source was 450WCWxenon lamp. Fluorescence decay profiles were recorded using time-correlated single photon counting (TCSPC) system (DeltaFlex-01-DD, Horiba JobinYvon IBH Ltd) coupled with Delta Diode Laser. ¹H-NMR (400 MHz) and ¹³C-NMR (101 MHz) spectra were recorded on Bruker and Jeol Delta. Fourier transform infrared (FTIR) spectra were obtained in the wavenumber range of 4000–400 cm⁻¹ by using a Nicolet 380FTIR spectrometer with the KBr pellet technique. NMR spectra were referenced to residual solvent signals. ESI-mass spectra were recorded on

Waters Synapt G2 HDMS. Column chromatography was carried out on Merck silica gel with gravity-feed-column technique. Thin-layer chromatographies were performed on Merck silica gel 60 F254 precoated aluminium sheets.

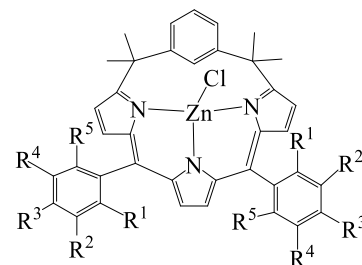
Single crystal structure determination: Intensity data were collected at 273(2) K on Bruker diffractometer (a single wavelength Enhance X-ray source with MoK α radiation, $\lambda = 0.71073$ Å) [1a]. The selected suitable single crystals were mounted using paratone oil on the top of a glass fibre fixed on a goniometer head and immediately transferred to the diffractometer. Pre-experiment, data collection, data reduction and analytical absorption corrections were performed with the Bruker SAINT program [1b]. The crystal structures were solved with SHELXL-97 using direct methods. The structure refinements were performed by full-matrix least-squares on F2 with SHELXL-97 [1c]. All programs used during the crystal structure determination process are included in the WINGX software [1d].

3.3 GENERAL REACTION SCHEME



Where

- 1 R¹=R²=R⁴=R⁵=H, R³=Cl
- 2 R¹=R²=R⁴=R⁵=H, R³=Br
- 3 R¹=R⁵=Cl, R²=R³=R⁴=H
- 4 R¹=R⁵=F, R²=R³=R⁴=H
- 5 R¹=R²=R³=R⁴=R⁵=F,
- 6 R¹=R²=R⁴=R⁵=H, R³=CF₃
- 7 R¹=R²=R⁴=R⁵=H, R³=OCH₃
- 8 R¹=R⁵=H, R²=R³=R⁴=OCH₃



3.4 SYNTHESIS OF COMPOUNDS 1-8 AND Zn²⁺.1-8

Synthesis of 11, 16-Bis(p-chloro phenyl)-6, 6, 21, 21-tetramethyl-meta-benziporphodimethene (1)

A solution of α , α' -dihydroxy-1, 3-diisopropylbenzene (196 mg, 1 mmol), *para* chloro benzaldehyde (281 mg, 2 mmol), and pyrrole (208 μ L, 3 mmol) in dichloromethane (300 mL) was treated with BF₃·OEt₂ (26 μ L, 0.2 mmol) and stirred at room temperature (27°C) for 2 Hours. DDQ (750 mg, 3.3 mmol) was then added into the reaction mixture and the solution was stirred again for 2 hours at room temperature (27°C). The reaction was quenched with trimethylamine (10-15 drops), and the solvent was removed in vacuo. The crude mixture was dissolved in a minimum amount of CH₂Cl₂ and was purified using silica gel column chromatography (450 mL) eluting with a mixture of CH₂Cl₂ and n-hexane to give **1** (17% yield) as a red powder.

Analytical data: λ_{max} (log ϵ): 548 (4.31), 517 (4.27), 353 (4.55). **ESI-MS (m/z):** 600.0937 (M + 1), **¹H-NMR(400 MHz, CDCl₃, 25°C):** 12.32 (br, 1H,NH),7.93 (s, 1H, 22-ArH), 7.24–7.39 (m,11H, (2,3,4-ArH+ meso Ar-H), 6.81(ab quartet ³JH,H = 4.88 Hz, HH, 8,9,18,19-Pyrr H), 6.15 (s,2H, 13,14-Pyrr H), 1.72 (s,12H, CH₃). **¹³C-NMR (101 MHz, CDCl₃, 20 °C):** 181.79,153.72, 152.44, 151.77, 147.41, 143.63, 138.84, 138.58, 138.22, 136.53,133.59, 131.79, 128.68, 127.38, 125.24, 123.15, 121.27, 42.10, 29.06. **IR (KBr, 25 °C):** 3290.6 (N-H Stretch), 2929.5 (C-H Stretch, *sp*³Hybridised), 1691.9 (C-N Stretch), 1582.7, 1502.9 (C-C Stretch Aromatic), 1383.1 (C-H Bending, *sp*³Hybridised out of plane), 799.9, 756.9 (C-H Bending, Aromatic, out of plane), 717.0 (C-Cl Stretch).

Synthesis of 11, 16-Bis(p-bromo phenyl)-6, 6, 21, 21-tetramethyl-meta-benziporphodimethene (2)

A solution of α , α' -dihydroxy-1, 3-diisopropylbenzene (196 mg, 1 mmol), *para* bromo benzaldehyde (374 mg, 2 mmol), and pyrrole (208 μ L, 3 mmol) in dichloromethane (300 mL) was treated with BF₃·OEt₂ (26 μ L, 0.2 mmol) and stirred at room temperature (27°C) for 2 Hours. DDQ (750 mg, 3.3 mmol) was then added into the reaction mixture and the solution was stirred again for 2 hours at room temperature (27°C). The reaction was quenched with trimethylamine (10-15 drops), and the solvent was removed in vacuo. The crude mixture was dissolved in a minimum amount of CH₂Cl₂ and was purified using

silica gel column chromatography (450 mL) eluting with a mixture of CH₂Cl₂ and n-hexane to give **2** (14% yield) as a red powder.

Analytical data: λ_{\max} (log ϵ): 542 (4.078), 513 (4.05), 351 (4.344). **ESI-Mass (m/z):** 690.0589 (M + 1). **¹H-NMR(400 MHz, CDCl₃, 25 °C):** 12.32 (br, 1H, NH), 7.94 (s, 1H, 22-ArH), 7.31–7.57 (m, 11H, (2,3,4-ArH+ meso Ar-H), 6.83 (ab quartet ³J_{H,H} = 5.90 Hz, HH, 8,9,18,19-Pyrr H), 6.16 (s, 2H, 13,14-Pyrr H), 1.74 (s, 12H, CH₃). **¹³C-NMR (101 MHz, CDCl₃, 20 °C):** 182.68, 152.00, 147.06, 138.57, 137.10, 136.45, 133.29, 131.02, 128.52, 127.11, 125.60, 123.56, 123.29, 121.24, 42.25, 28.98. **IR (KBr, 25 °C):** 3281.3 (N-H Stretch), 2924.1 (C-H Stretch, *sp*³ Hybridised), 1586.6, 1484.4 (C-C Stretch Aromatic), 1382.8 (C-H Bending, *sp*³ Hybridised out of plane), 798.1, 735.7, 703.8 (C-H Bending, Aromatic, out of plane).

Synthesis of 11, 16-Bis(2, 6 dichloro phenyl)-6, 6, 21, 21-tetramethyl-meta-benziporphodimethene (3)

A solution of α , α' -dihydroxy-1, 3-diisopropylbenzene (196 mg, 1 mmol), 2, 6 di-chloro benzaldehyde (350 mg, 2 mmol), and pyrrole (208 μ L, 3 mmol) in dichloromethane (300 mL) was treated with BF₃·OEt₂ (26 μ L, 0.2 mmol) and stirred at room temperature (27 °C) for 2 Hours. DDQ (750 mg, 3.3 mmol) was then added into the reaction mixture and the solution was stirred again for 2 hours at room temperature (27 °C). The reaction was quenched with trimethylamine (10-15 drops), and the solvent was removed in vacuo. The crude mixture was dissolved in a minimum amount of CH₂Cl₂ and was purified using silica gel column chromatography (450 mL) eluting with a mixture of CH₂Cl₂ and n-hexane to give **3** (17% yield) as a red powder.

Analytical data: λ_{\max} (log ϵ): 538 (4.22), 508 (4.19), 321 (4.32). **ESI-Mass (m/z):** 670.0478 (M + 1). **¹H-NMR(400 MHz, CDCl₃, 25 °C):** 12.16 (br, 1H, NH), 8.06 (s, 1H, 22-ArH), 7.28–7.41 (m, 9H, (2,3,4-ArH+ meso Ar-H), 6.82 (doublet ²J_{H,H} = 4.59 Hz, HH, 9,18-Pyrr H), 6.56 (doublet ²J_{H,H} = 4.59 Hz, HH, 8,19-Pyrr H), 5.86 (s, 2H, 13,14-Pyrr H), 1.81 (s, 12H, CH₃). **¹³C-NMR (101 MHz, CDCl₃, 20 °C):** 184.33, 162.24, 159.69, 152.99, 146.25, 144.66, 137.77, 135.65, 130.61, 127.94, 127.08, 125.92, 123.59, 123.15, 120.16, 118.37, 111.48, 111.24, 42.50, 29.82, 28.73. **IR (in KBr, 25 °C):** 3300.4 (N-H Stretch), 2967.7 (C-H Stretch, *sp*³ Hybridised), 1678.9 (C-N Stretch), 1591.0,

1480.9 (C-C Stretch Aromatic), 1381.7 (C-H Bending, sp^3 Hybridised out of plane), 828.6, 796.8 (C-H Bending, Aromatic, out of plane), 709.0 (C-Cl Stretch).

Synthesis of 11, 16-Bis(2, 6 difluoro phenyl)-6, 6, 21, 21-tetramethyl-meta-benziporphodimethene (4)

A solution of α , α' -dihydroxy-1, 3-diisopropylbenzene (196 mg, 1 mmol), 2, 6 di-fluoro benzaldehyde (216 μ L, 2 mmol), and pyrrole (208 μ L, 3 mmol) in dichloromethane (300 mL) was treated with $\text{BF}_3 \cdot \text{OEt}_2$ (26 μ L, 0.2 mmol) and stirred at room temperature (27°C) for 2 Hours. DDQ (750 mg, 3.3 mmol) was then added into the reaction mixture and the solution was stirred again for 2 hours at room temperature (27°C). The reaction was quenched with trimethylamine (10-15 drops), and the solvent was removed in vacuo. The crude mixture was dissolved in a minimum amount of CH_2Cl_2 and was purified using silica gel column chromatography (450 mL) eluting with a mixture of CH_2Cl_2 and n-hexane to give **4** (17% yield) as a red powder.

Analytical data: λ_{max} (log ϵ): 533 (4.24), 507 (4.213), 320 (4.372). **ESI-Mass (m/z):** 604.1306 (M+1). **$^1\text{H-NMR}$ (300 MHz, CDCl_3 , 25°C):** 12.18 (br, 1H, NH), 7.97 (s, 1H, 22-ArH), 7.35–7.45 (m, 3H, (2,3,4-ArH)), 6.91–7.05 (m, 6H, ArH), 6.83 (doublet $^2\text{J}_{\text{H,H}} = 4.40$ Hz, HH, 9.18-Pyrr H), 6.70 (doublet $^2\text{J}_{\text{H,H}} = 4.22$ Hz, HH, 8,19-Pyrr H), 6.00 (s, 2H, 13,14- Pyrr H), 1.79 (s, 12H, CH_3). **$^{13}\text{C-NMR}$ (101 MHz, CDCl_3 , 20 °C):** 184.35, 162.17, 159.75, 153.00, 146.25, 144.65, 137.78, 135.66, 130.63, 127.95, 127.51, 127.08, 125.94, 123.61, 123.16, 120.18, 118.40, 111.50, 111.26, 42.51, 29.83, 28.74. **IR (in KBr, 25 °C):** 3282.8 (N-H Stretch), 2924.0 (C-H Stretch, sp^3 Hybridised), 1621.6 (C-N Stretch), 1589.3 (C-C Stretch Aromatic), 1381.0 (C-H Bending, sp^3 Hybridised out of plane), 783.6, 753.9, 706.8 (C-H Bending, Aromatic, out of plane), 1000.3 (C-F Stretch).

Synthesis of 11, 16-Bis(penta fluoro phenyl)-6, 6, 21, 21-tetramethyl-meta-benziporphodimethene (5)

A solution of α , α' -dihydroxy-1, 3-diisopropylbenzene (196 mg, 1 mmol), penta fluoro benzaldehyde (247 μ L, 2 mmol), and pyrrole (208 μ L, 3 mmol) in dichloromethane (300 mL) was treated with $\text{BF}_3 \cdot \text{OEt}_2$ (26 μ L, 0.2 mmol) and stirred at room temperature (27°C) for 2 Hours. DDQ (750 mg, 3.3 mmol) was then added into the reaction mixture and the

solution was stirred again for 2 hours at room temperature (27°C). The reaction was quenched with trimethylamine (10-15 drops), and the solvent was removed in vacuo. The crude mixture was dissolved in a minimum amount of CH₂Cl₂ and was purified using silica gel column chromatography (450 mL) eluting with a mixture of CH₂Cl₂ and n-hexane to give **5** (16% yield) as a red powder.

Analytical data: λ_{\max} (log ϵ): 531 (4.287), 508 (4.254), 319 (4.418). **ESI-Mass (m/z):** 712.1006 (M + 1). **¹H-NMR(400 MHz, CDCl₃, 25°C):** 12.08 (br, 1H, NH), 7.89 (s, 1H, 22-ArH), 7.25–7.34 (m, 3H, (2,3,4-ArH), 6.90 (doublet ²J_{H,H}=4.58 Hz, HH, 9,18-Pyrr H), 6.65 (doublet ²J_{H,H}=4.58 Hz, HH, 8,19-Pyrr H), 5.98 (s, 2H, 13,14-Pyrr H), 1.78 (s, 12H, CH₃). **¹³C-NMR (101 MHz, CDCl₃, 20 °C):** 185.93, 153.54, 145.91, 137.11, 135.14, 128.11, 127.31, 126.82, 123.74, 119.90, 119.37, 115.97, 42.64, 28.51. **IR (in KBr, 25 °C):** 3300.0 (N-H Stretch), 2967.2 (C-H Stretch, *sp*³Hybridised), 1651.5 (C-N Stretch), 1594.3, 1494.8 (C-C Stretch Aromatic), 1384.9 (C-H Bending, *sp*³Hybridised out of plane), 799.4, 755.0, 706.3 (C-H Bending, Aromatic, out of plane), 1053.1 (C-F Stretch).

Synthesis of 11, 16-Bis(4-trifluoromethyl-phenyl)-6, 6, 21, 21-tetramethyl-meta-benziporphodimethene (6)

A solution of α , α' -dihydroxy-1, 3-diisopropylbenzene (196 mg, 1 mmol), para trifluoromethyl benzaldehyde (348 mg, 2 mmol), and pyrrole (208 μ L, 3 mmol) in dichloromethane (300 mL) was treated with BF₃·OEt₂ (26 μ L, 0.2 mmol) and stirred at room temperature (27°C) for 2 Hours. DDQ (750 mg, 3.3 mmol) was then added into the reaction mixture and the solution was stirred again for 2 hours at room temperature (27°C). The reaction was quenched with trimethylamine (10-15 drops), and the solvent was removed in vacuo. The crude mixture was dissolved in a minimum amount of CH₂Cl₂ and was purified using silica gel column chromatography (450 mL) eluting with a mixture of CH₂Cl₂ and n-hexane to give **6** (17% yield) as a red powder.

Analytical data: λ_{\max} (log ϵ): 539 (4.23), 509 (4.22), 342 (4.414). **ESI-Mass (m/z):** 668.1482 (M + 1). **¹H-NMR(400 MHz, CDCl₃, 25°C):** 12.0 (br, 1H, NH), 7.92 (s, 1H, 22-ArH), 7.68 (d, 4H-ArH), 7.56 (d, 4H-ArH), 7.29 (m, 3H-ArH), 6.85 (doublet ²J_{H,H}=4.58 Hz, HH, 9,18-Pyrr H), 6.75 (doublet ²J_{H,H}=4.58 Hz, HH, 8,19-Pyrr H), 6.07 (s, 2H, 13,14-Pyrr H), 1.75 (s, 12H, CH₃). **¹³C-NMR (101 MHz, CDCl₃, 20°C):** 183.38, 152.24, 146.85,

141.83, 138.51, 136.44, 135.82, 131.86, 128.48, 126.97, 125.94, 124.73, 123.40, 121.28, 42.36, 28.91. **IR (in KBr, 25°C):** 3278.2 (N-H Stretch), 2968.9 (C-H Stretch, sp^3 Hybridised), 1692.9 (C=N Stretch), 1587.5, 1472.2 (C=C Stretch Aromatic), 1382.5 (C-H Bending, sp^3 Hybridised out of plane), 747.4, 707.1 (=C-H Bending, Aromatic, out of plane), 1322.2 (C-F Stretch).

Synthesis of 11, 16-Bis(4-methoxy-phenyl)-6, 6, 21, 21-tetramethyl-meta-benziporphodimethene (7)

A solution of α , α' -dihydroxy-1, 3-diisopropylbenzene (196 mg, 1 mmol), *para*-methoxy benzaldehyde (242 μ L, 2 mmol), and pyrrole (208 μ L, 3 mmol) in dichloromethane (300 mL) was treated with $BF_3 \cdot OEt_2$ (26 μ L, 0.2 mmol) and stirred at room temperature (27°C) for 2 Hours. DDQ (750 mg, 3.3 mmol) was then added into the reaction mixture and the solution was stirred again for 2 hours at room temperature (27°C). The reaction was quenched with trimethylamine (10-15 drops), and the solvent was removed in vacuo. The crude mixture was dissolved in a minimum amount of CH_2Cl_2 and was purified using silica gel column chromatography (450 mL) eluting with a mixture of CH_2Cl_2 and n-hexane to give **7** (16% yield) as a red powder.

Analytical data: λ_{max} (log ϵ): 545 (4.31), 513 (4.27), 378 (4.55). **1H -NMR(400 MHz, $CDCl_3$, 25°C):** 12.38 (br, 1H, NH), 7.93 (s, 1H, 22-Ar-H), 7.44 (d, 4 Ar-H $^2J_{H,H}=8.4$ Hz), 7.27-7.32 (m, 3H 2,3,4 Ar-H), 6.95 (d, 4 Ar-H $^2J_{H,H}=8.4$ Hz), 6.88 (doublet $^2J_{H,H}=4.58$ Hz, HH, 9,18-Pyrr H), 6.77 (doublet $^2J_{H,H}=4.58$ Hz, HH, 8,19-Pyrr H), 6.30 (broad s, 2H, 13,14-Pyrr H), 3.87 (s, 6H, OMe), 1.69 (s, 12H, CH_3). **IR (in KBr, 25°C):** 3337.4 (N-H Stretch), 2926.4 (C-H Stretch, sp^3 Hybridised), 1745.0 (C=N Stretch), 1601.2, 1508.2 (C=C Stretch Aromatic), 1384.5 (C-H Bending, sp^3 Hybridised out of plane), 797.4, 739.7, 711.8 (=C-H Bending, Aromatic, out of plane), 1252.7, 1040.1 (C-O Stretch).

Synthesis of 11, 16-Bis(3, 4, 5-trimethoxy-phenyl)-6, 6, 21, 21-tetramethyl-meta-benziporphodimethene (8)

A solution of α , α' -dihydroxy-1, 3-diisopropylbenzene (196 mg, 1 mmol), 3, 4, 5 trimethoxy benzaldehyde (392 mg, 2 mmol), and pyrrole (208 μ L, 3 mmol) in dichloromethane (300 mL) was treated with $BF_3 \cdot OEt_2$ (26 μ L, 0.2 mmol) and stirred at

room temperature (27°C) for 2 Hours. DDQ (750 mg, 3.3 mmol) was then added into the reaction mixture and the solution was stirred again for 2 hours at room temperature (27°C). The reaction was quenched with trimethylamine (10-15 drops), and the solvent was removed in vacuo. The crude mixture was dissolved in a minimum amount of CH₂Cl₂ and was purified using silica gel column chromatography (450 mL) eluting with a mixture of CH₂Cl₂ and n-hexane to give **8** (17% yield) as a red powder.

Analytical data: λ_{\max} (log ϵ): 546 (4.31), 513 (4.27), 376 (4.55). **¹H-NMR(400 MHz, CDCl₃, 25°C):** 12.33 (br, 1H, NH), 7.92 (s, 1H, 22-ArH), 7.30 (q, J=5.34 Hz 3H 2,3,4 Ar-H), 6.95 (d, ²J_{H,H}=3.81HzHH, 9,18-Pyrr H), 6.80 (d, ²J_{H,H}=4.58HzHH, 8,19-Pyrr H), 6.74 (s, 4Ar-H (AA'BB')) 6.35 (s, 2H, 13,14-Pyrr H), 3.92 (s, 6H, para OMe-H's), 3.83 (s, 12H, meta OMe-H's), 1.70 (s, 12H, CH₃). **¹³C-NMR (101 MHz, CDCl₃, 20°C):** 152.45, 147.34, 139.37, 136.53, 133.43, 128.75, 127.29, 125.11, 123.25, 109.62, 61.11, 56.34, 42.07, 29.78, 28.98. **IR in (KBr, 25° C):** 3300.0 (N-H Stretch), 2923.5 (C-H Stretch, *sp*³Hybridised), 1683.4 (C=N Stretch), 1577.2, 1504.1 (C=C Stretch Aromatic), 1344.3 (C-H Bending, *sp*³Hybridised out of plane), 795.6, 759.6, 717.1 (=C-H Bending, Aromatic, out of plane), 1236.7 (C-O Stretch).

Synthesis of Zn²⁺.1

1 (10 mg) was dissolved in 25 mL CH₂Cl₂/CH₃CN (1:2) solution. To this solution anhydrous zinc chloride (51.3 mg, 0.376 mmol) which was pre-dissolved in minimum amount of CH₃CN was added, later that 1 drop of 2, 6-lutidine was also added into the solution. After two minutes of stirring, the solvent was removed under reduced pressure. The residue was dissolved in CH₂Cl₂ and excess zinc salt was extracted using distilled water. The organic layer was collected and solvent was removed in *vacuo* and crystallized in n-hexane to afford bluish green product **Zn²⁺.1** (yield 98%).

Analytical data: λ_{\max} (log ϵ): 639 (4.477), 594 (4.216), 351 (4.499). **IR (in KBr, 25° C):** 2975.5 (C-H Stretch, *sp*³ Hybridised), 1672.9 (C=N Stretch), 1545.8, 1491.2 (C=C Stretch Aromatic), 1360.4 (C-H Bending, *sp*³ Hybridised, out of plane), 964.1, 804.6 (=C-H Bending, Aromatic, out of plane), 713.5 (C-Cl Stretch).

Synthesis of Zn²⁺.2

2 (10 mg) was dissolved in 25 mL CH₂Cl₂/CH₃CN (1:2) solution. To this solution anhydrous zinc chloride (51.3 mg, 0.376 mmol) which was pre-dissolved in minimum amount of CH₃CN was added, later that 1 drop of **2**, 6-lutidine was also added into the solution. After two minutes of stirring, the solvent was removed under reduced pressure. The residue was dissolved in CH₂Cl₂ and excess zinc salt was extracted using distilled water. The organic layer was collected and solvent was removed in *vacuo* and crystallized in n-hexane to afford bluish green product **Zn²⁺.2** (yield 98%).

Analytical data: λ_{\max} (log ϵ):638 (4.45), 594 (4.19), 350 (4.48). **IR (in KBr, 25° C):** 2969.3 (C-H Stretch, *sp*³*Hybridised*), 1712.0 (C=N Stretch), 1547.9, 1489.4 (C=C Stretch Aromatic), 1360.6 (C-H Bending, *sp*³*Hybridised*, out of plane), 967.3, 802.2 (=C-H Bending, Aromatic, out of plane), 465.9 (C-Br Stretch).

Synthesis of Zn²⁺.3

3 (10 mg) was dissolved in 25 mL CH₂Cl₂/CH₃CN (1:2) solution. To this solution anhydrous zinc chloride (51.3 mg, 0.376 mmol) which was pre-dissolved in minimum amount of CH₃CN was added, later that 1 drop of **2**, 6-lutidine was also added into the solution. After two minutes of stirring, the solvent was removed under reduced pressure. The residue was dissolved in CH₂Cl₂ and excess zinc salt was extracted using distilled water. The organic layer was collected and solvent was removed in *vacuo* and crystallized in n-hexane to afford bluish green product **Zn²⁺.3** (yield 97%).

Analytical data: λ_{\max} (log ϵ):649 (4.517), 602 (4.26), 348 (4.608). **IR (in KBr, 25° C):** 2880.9(C-H Stretch, *sp*³*Hybridised*), 1675.2 (C=N Stretch), 1555.1, 1488.8 (C=C Stretch Aromatic), 1321.5 (C-H Bending, *sp*³*Hybridised*, out of plane), 906.3, 835.5, 797.6 (=C-H Bending, Aromatic, out of plane), 718.7 (C-Cl Stretch).

Synthesis of Zn²⁺.4

4 (10 mg) was dissolved in 25 mL CH₂Cl₂/CH₃CN (1:2) solution. To this solution anhydrous zinc chloride (51.3 mg, 0.376 mmol) which was pre-dissolved in minimum amount of CH₃CN was added, later that 1 drop of 2, 6-lutidine was also added into the solution. After two minutes of stirring, the solvent was removed under reduced pressure. The residue was dissolved in CH₂Cl₂ and excess zinc salt was extracted using distilled water. The organic layer was collected and solvent was removed in *vacuo* and crystallized in n-hexane to afford bluish green product Zn²⁺.4 (yield 98%).

Analytical data: λ_{\max} (log ϵ):642 (4.36), 598 (4.122), 346 (4.458). **ESI-Mass (m/z):** 666.0491 (M - Cl). **IR (in KBr, 25° C):** 2881.2(C-H Stretch, *sp*³Hybridised), 1622.1 (C=N Stretch), 1556.9, 1496.0(C=C Stretch Aromatic), 1362.4 (C-H Bending, *sp*³Hybridised, out of plane), 835.3, 787.5, 717.3 (=C-H Bending, Aromatic, out of plane), 1072.7 (C-F Stretch).

Synthesis of Zn²⁺.5

5 (10 mg) was dissolved in 25 mL CH₂Cl₂/CH₃CN (1:2) solution. To this solution anhydrous zinc chloride (51.3 mg, 0.376 mmol) which was pre-dissolved in minimum amount of CH₃CN was added, later that 1 drop of 2, 6-lutidine was also added into the solution. After two minutes of stirring, the solvent was removed under reduced pressure. The residue was dissolved in CH₂Cl₂ and excess zinc salt was extracted using distilled water. The organic layer was collected and solvent was removed in *vacuo* and crystallized in n-hexane to afford bluish green product Zn²⁺.5 (yield 97%).

Analytical data: λ_{\max} (log ϵ):642 (4.346), 600 (4.108), 346 (4.436). **IR (in KBr, 25° C):** 2923.8 (C-H Stretch, *sp*³Hybridised), 1652.2 (C=N Stretch), 1561.7, 1495.4(C=C Stretch Aromatic), 1362.7 (C-H Bending, *sp*³Hybridised, out of plane), 931.8, 908.1, 832.8 (=C-H Bending, Aromatic, out of plane), 1074.5 (C-F Stretch).

Synthesis of Zn²⁺.6

6 (10 mg) was dissolved in 25 mL CH₂Cl₂/CH₃CN (1:2) solution. To this solution anhydrous zinc chloride (51.3 mg, 0.376 mmol) which was pre-dissolved in minimum amount of CH₃CN was added, later that 1 drop of 2, 6-lutidine was also added into the solution. After two minutes of stirring, the solvent was removed under reduced pressure. The residue was dissolved in CH₂Cl₂ and excess zinc salt was extracted using distilled water. The organic layer was collected and solvent was removed in *vacuo* and crystallized in n-hexane to afford bluish green product **Zn²⁺.6** (yield 98%).

Analytical data: λ_{\max} (log ϵ):641 (4.50), 594 (4.24), 347 (4.57). **IR (in KBr, 25° C):** 2966.1 (C-H Stretch, *sp*³*Hybridised*), 1550.3, 1484.9 (C=C Stretch Aromatic), 1362.7 (C-H Bending, *sp*³*Hybridised*, out of plane), 801.9, 708.1 (=C-H Bending, Aromatic, out of plane), 1322.5(C-F Stretch).

Synthesis of Zn²⁺.7

7 (10 mg) was dissolved in 25 mL CH₂Cl₂/CH₃CN (1:2) solution. To this solution anhydrous zinc chloride (51.3 mg, 0.376 mmol) which was pre-dissolved in minimum amount of CH₃CN was added, later that 1 drop of 2, 6-lutidine was also added into the solution. After two minutes of stirring, the solvent was removed under reduced pressure. The residue was dissolved in CH₂Cl₂ and excess zinc salt was extracted using distilled water. The organic layer was collected and solvent was removed in *vacuo* and crystallized in n-hexane to afford bluish green product **Zn²⁺.7** (yield 98%).

Analytical data: λ_{\max} (log ϵ):643 (4.48), 592 (4.24), 343 (4.47). **IR (in KBr, 25° C):** 2882.8 (C-H Stretch, *sp*³*Hybridised*), 1658.1 (C=N Stretch), 1603.6, 1509.1(C=C Stretch Aromatic), 1360.2 (C-H Bending, *sp*³*Hybridised*, out of plane), 815.1, 717.3 (=C-H Bending, Aromatic, out of plane), 1254.4, 1033.7(C-O Stretch).

Synthesis of Zn²⁺.8

8 (10 mg) was dissolved in 25 mL CH₂Cl₂/CH₃CN (1:2) solution. To this solution anhydrous zinc chloride (51.3 mg, 0.376 mmol) which was pre-dissolved in minimum

amount of CH₃CN was added, later that 1 drop of 2, 6-lutidine was also added into the solution. After two minutes of stirring, the solvent was removed under reduced pressure. The residue was dissolved in CH₂Cl₂ and excess zinc salt was extracted using distilled water. The organic layer was collected and solvent was removed in *vacuo* and crystallized in n-hexane to afford bluish green product **Zn²⁺.8** (Yield 98%).

Analytical data: λ_{\max} (**log ϵ**):642 (4.38), 598 (4.12), 346 (4.46). **IR (in KBr, 25° C):** 2880.3(C-H Stretch, *sp³Hybridised*), 1708.9 (C=N Stretch), 1544.0, 1501.4 (C=C Stretch Aromatic), 1341.0 (C-H Bending, *sp³Hybridised*, out of plane), 934.9, 811.6, 724.8 (=C-H Bending, Aromatic, out of plane), 1232.3 (C-O Stretch).

3.5 PHOTO LUMINESCENCE OF ZINC COMPLEXES OF BPDM COMPOUNDS

Photo luminescence of all Zinc complexes of meta-BPDM compounds were recorded using JobinYvon Horiba Fluorolog-3 spectrofluorometer equipped with double-grating at excitation and emission monochromators and an R928P photomultiplier tube (PMT). The excitation source was a 450 Watt CW xenon lamp. λ_{exi} for fluorescence spectra was 564 nm and λ_{emi} was observed from 672-680 nm.

3.6 TIME RESOLVED PHOTO LUMINESCENCE OF ZINC COMPLEXES OF *meta*-BPDM COMPOUNDS.

Time resolved photo luminescence of all Zinc complexes of meta-benziporphodimethenes compounds were recorded using time-correlated single photon counting (TCSPC) system (DeltaFlex-01-DD, Horiba JobinYvon IBH Ltd) coupled with Delta Diode Laser. λ_{exi} for time resolved fluorescent decay was 450 nm and λ_{emi} was observed 680 nm. Quantum yield of all *meta*-BPDM zinc complexes were calculated using Strickler and Berg equation.

3.7 CELL IMAGING WITH *meta*-BPDM COMPOUNDS IN BREAST CARCINOMA CELLS.

CELL CULTURE

Human breast cancer cell line was procured from National Center for Cell Science, Pune, India. Monolayer culture of MDA-MB-468 and MDA-MB-231 cell was maintained in Dulbecco's modified Eagle's medium containing 10% fetal bovine serum, 1% antibiotic-antimycotic in a humidified incubator at 37 °C with 5% carbon dioxide and 95% atmospheric air. For imaging and cytotoxicity studies cells were harvested by trypsinization and plated in appropriate well plates.

IMAGING

Actively dividing cells were plated over coverslip in a twenty four well plate (2×10^5 cells per well) and incubated overnight to adhere. Stock (1 mM) solutions of various receptors, (compound **1**, **4**, **7**, **8** for MDA-MB-468 and **4** for MDA-MB-231) were prepared in 1% aqueous dimethyl sulfoxide (DMSO). Cells were washed with phosphate buffers (pH 7.4). The washed cells were treated with Zn^{2+} ions ($ZnCl_2$) for 30 minutes. After incubation, the cells were again washed with phosphate buffer and then incubated with solution of various receptors, (compound **1**, **4**, **7**, **8** for MDA-MB-468 and **4** for MDA-MB-231) for 30 min. Control cells were incubated with DMEM and receptors without Zn^{2+} . Finally, again cells were washed with phosphate buffer saline (pH 7.4) to avoid any residual receptors as well as Zn^{2+} ions in the media and coverslip were mounted on grease-free microscopic slide. Cells were observed under fluorescence microscope. Brightfield and fluorescence images were examined using a Zeiss microscope (Carl Zeiss, Germany) aided with epifluorescence and AxioCam camera system coupled with Axio Vision software (Carl Zeiss, Germany) at 100 \times magnification.

CYTOTOXICITY

Cells in log phase were harvested, seeded in 96 well plate (1×10^4 cells/well) and allowed to adhere overnight. Stock solutions (1 mM) of (compound **1**, **4**, **7**, **8** for MDA-MB-468 and **4** for MDA-MB-231) were prepared as described above. Solution of various

compounds **1**, **4**, **7**, **8** was added to the wells at a final concentration of (10, 20, 30, 50, 75, and 100 μM). Control cells were incubated with DMEM and receptors without Zn^{2+} . After 12 h of incubation at 37°C 20 μl of MTT (3-(4, 5-Dimethylthiazol-2-yl)-2, 5-Diphenyltetrazolium Bromide) (5 mg/ml) was added and allowed for reduction reaction for 4 hr. Formazan crystal formed by cellular reduction of MTT was dissolved by addition of 200 μl of DMSO and incubation for 6 hr. Solution was stirred for 5 sec to mix it properly and absorbance was taken at 570 nm in BioRadiMark microplate reader [2]. Percent cell viability was calculated and presented as the mean \pm standard deviation (SD). Values were evaluated by one-way analysis of variation (ANOVA) followed by Dunnett's test for comparison of individual treated groups to control one.

$$\text{Percent cell viability} = 1 - \frac{\text{Absorbance of treated group}}{\text{Absorbance of control group}} \times 100$$

3.8 DENSITY FUNCTIONAL THEORY CALCULATION

Density functional theory calculation (DFT) were performed using the Gaussian 09W program [3]. Geometry optimizations were carried out within unconstrained C1 symmetry. Initial structures were obtained from the crystal structures of free receptor and modified accordingly using GaussView 5.0.9 program. Becke's three parameters exchange functional with the gradient corrected correlation formula of Lee, Yang, and Parr [DFTB3LYP] was used with the 6-31g** basis set to optimize the geometry [4]. Harmonic vibrational frequencies were calculated using analytical second derivatives for all structures. Calculated vibrational frequencies show that the obtained geometries represent true minima since no imaginary frequencies were found. In all calculation, convergence was reached when the relative change in the density matrix between subsequent iteration was less than 1×10^{-8} .

REFERENCES

1. (a) Bruker CCD System **2003**. (b) R. C. Clark, J.S. Reid, **1995**, *A51*, 887-897 (c) G. M. Sheldrick, *Acta Cryst.* **2008**, *A64*, 112-122 (d) L. J. Farrugia, *J. Appl. Cryst.* **2012**, *45*, 849-854.
2. M. Y. Lee, M. H. Liao, Y. N. Tsai, K. H. Chiu, H. C. Wen, *Journal of agricultural and food chemistry*, **2011**, *59*(6), 2347-2355.
3. Gaussian 09W, Revision D.01, M. J. Frisch, G. W. Trucks, H. B. Schlegel, G. E. Scuseria, M. A. Robb, J. R. Cheeseman, J. A. Montgomery, Jr., T. Vreven, K. N. Kudin, J. C. Burant, J. M. Millam, S. S. Iyengar, J. Tomasi, V. Barone, B. Mennucci, M. Cossi, G. Scalmani, N. Rega, G. A. Petersson, H. Nakatsuji, M. Hada, M. Ehara, K. Toyota, R. Fukuda, J. Hasegawa, M. Ishida, T. Nakajima, Y. Honda, O. Kitao, H. Nakai, M. Klene, X. Li, J. E. Knox, H. P. Hratchian, J. B. Cross, V. Bakken, C. Adamo, J. Jaramillo, R. Gomperts, R. E. Stratmann, O. Yazyev, A. J. Austin, R. Cammi, C. Pomelli, J. W. Ochterski, P. Y. Ayala, K. Morokuma, G. A. Voth, P. Salvador, J. J. Dannenberg, V. G. Zakrzewski, S. Dapprich, A. D. Daniels, M. C. Strain, O. Farkas, D. K. Malick, A. D. Rabuck, K. Raghavachari, J. B. Foresman, J. V. Ortiz, Q. Cui, A. G. Baboul, S. Clifford, J. Cioslowski, B. B. Stefanov, G. Liu, A. Liashenko, P. Piskorz, I. Komaromi, R. L. Martin, D. J. Fox, T. Keith, M. A. Al-Laham, C. Y. Peng, A. Nanayakkara, M. Challacombe, P. M. W. Gill, B. Johnson, W. Chen, M. W. Wong, C. Gonzalez and J. A. Pople, Gaussian, Inc., Wallingford CT, **2013**.
4. (a) A. D. Becke, *Physical Review A* **1988**, *38*, 3098-3100. (b) A. D. Becke, *The Journal of Chemical Physics* **1993**, *98*, 1372-1377. (c) A. D. Becke, *The Journal of Chemical Physics* **1993**, *98*, 5648-5652. (d) C. Lee, W. Yang, R. G. Parr, *Physical Review B* **1988**, *37*, 785-789.

RESULTS AND DISCUSSION

4.1 SPECTROSCOPIC RESULTS

4.1.1 ELECTRONIC SPECTROSCOPY

The UV-visible spectra of the synthesized compounds and complexes were recorded in acetonitrile. The concentration of $\sim 10^{-5}$ M was taken to record the spectrum in the range of 300-800 nm. The typical *meta*-benziporphodimethenes spectra and for their zinc complexes have been represented in Fig 4.1 to 4.18. The *meta*-benziporphodimethenes is a member of benzicarbaporphyrinoid system and one of the pyrrole ring in porphyrin molecule is replaced by a carbocyclic ring system (in present case the carbocyclic ring is phenylene) and the mode of attachment to this ring changed from sp^2 to sp^3 carbon atoms. Thus *meta*-benziporphodimethenes constitute a discrete conjugated system where discontinuation of the conjugated system is due to the presence of sp^3 hybridized carbon atoms. Their UV-Vis spectrum is broad in nature due to presence of sp^3 - sp^2 mixed *meso*-carbon atoms non-conjugated system. The ground state absorption spectra characteristics of free base *meta*-benziporphodimethenes and their zinc complexes are tabulated in Table 4.1. The Soret like high energy band was observed around 342-378 nm for *para* and *ortho*-substituted *meso*-phenyl groups in free base *meta*-benziporphodimethenes, **1-8**. The *para*-substituted electron releasing group reduce the Soret like band energy and obtained at 378 and 376 nm, for **7** and **8**, respectively. *Ortho*-halogenations significantly enhance the Soret like band energy and appeared at 321, 320, and 319 nm for **3**, **4**, and **5**, respectively. The zinc complexes of *meta*-benziporphodimethenes Soret like high energy band are in the range of 343-353 nm. The Q bands are shifted towards low energy after metallation with zinc. Stokes shift of 80 nm and 100 nm were observed in Q (1-0) and Q (0-0), respectively. The significant red shift of Q bands is due to strong interaction of *d*-orbital of zinc (II) with the macrocycle observed in ground state absorption spectra of zinc complexes of *meta*-benziporphodimethenes with respect to free base *meta*-benziporphodimethenes [**1**]. Though, the Gouterman four-orbital model is given for porphyrin and other

porphyrinoids having complete conjugated systems [2] but if we assign the bands based on four-orbital model, the highest energy band, Soret like, is S_0-S_2 transition while the low energy bands, Q-bands, are S_0-S_1 transition. The introduction of halogen atoms at *para* positions of the *meso*-phenyl substituents shows bathochromic shift of 1-3 nm with respect to **R** and $Zn^{2+} \cdot R$ [3]. *Ortho*-halogenation does not follow the trend and large blue shift was observed when halogenations shift from *para* to *ortho* positions. A large value of blue shift, 28-30 nm, was measured after the replacement of halogen from *para* to *ortho* position in free base *meta*-benzporphodimethenes compared to unsubstituted form, **R**. Addition to support this we also expect there is change in geometry from perturbed to lesser perturbed geometry once metallated with zinc [3].

Table 4.1 Absorption spectra of *meta*-benzporphodimethenes and their zinc complexes obtained in degassed acetonitrile. (the values of **R** and $Zn^{2+} \cdot R$ were obtained from ref. [3] to discuss the effect of substituent on *meso*-phenyl group; **R** is with unsubstituted *meso*-phenyl)

Compound	λ_{max} in nm		
	Soret like or B (0-0)	Q(1-0)	Q(0-0)
R	349	514	542
$Zn^{2+} \cdot R$	350	593	639
1	353	517	548
$Zn^{2+} \cdot 1$	351	594	639
2	351	513	542
$Zn^{2+} \cdot 2$	350	594	638
3	321	508	538
$Zn^{2+} \cdot 3$	348	602	649
4	320	507	533
$Zn^{2+} \cdot 4$	346	598	642
5	319	508	531
$Zn^{2+} \cdot 5$	346	600	642
6	342	509	539
$Zn^{2+} \cdot 6$	347	594	641
7	378	513	545
$Zn^{2+} \cdot 7$	343	592	643
8	376	513	546
$Zn^{2+} \cdot 8$	346	598	642

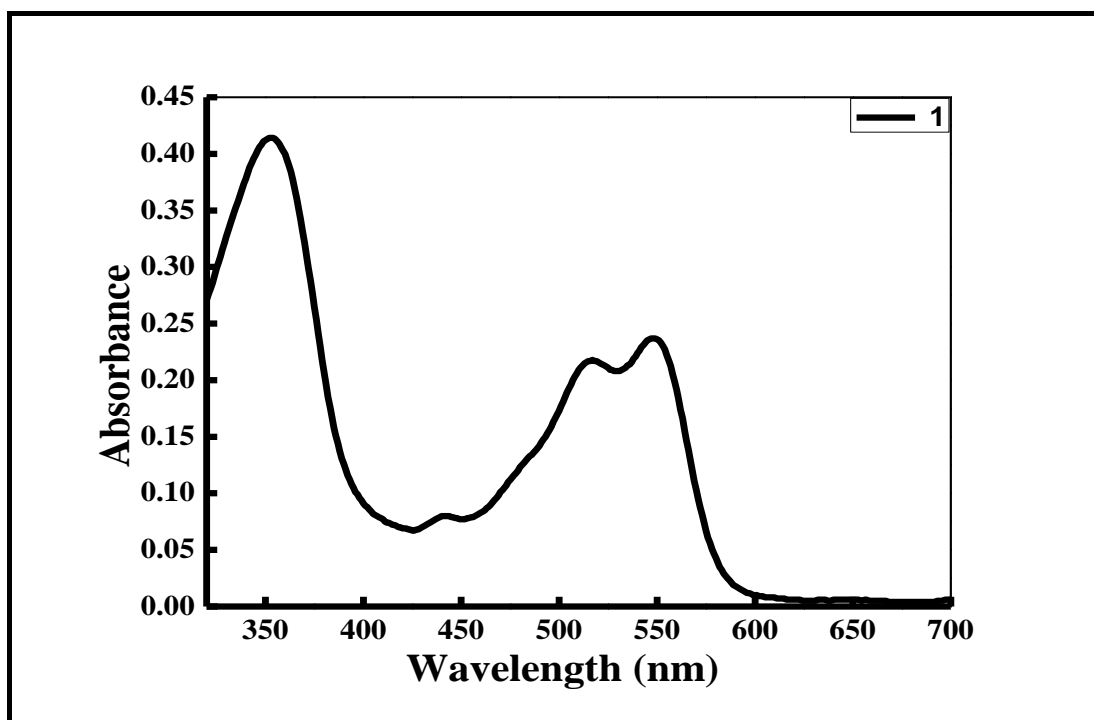


Fig. 4.1 Electronic spectra of compound 1

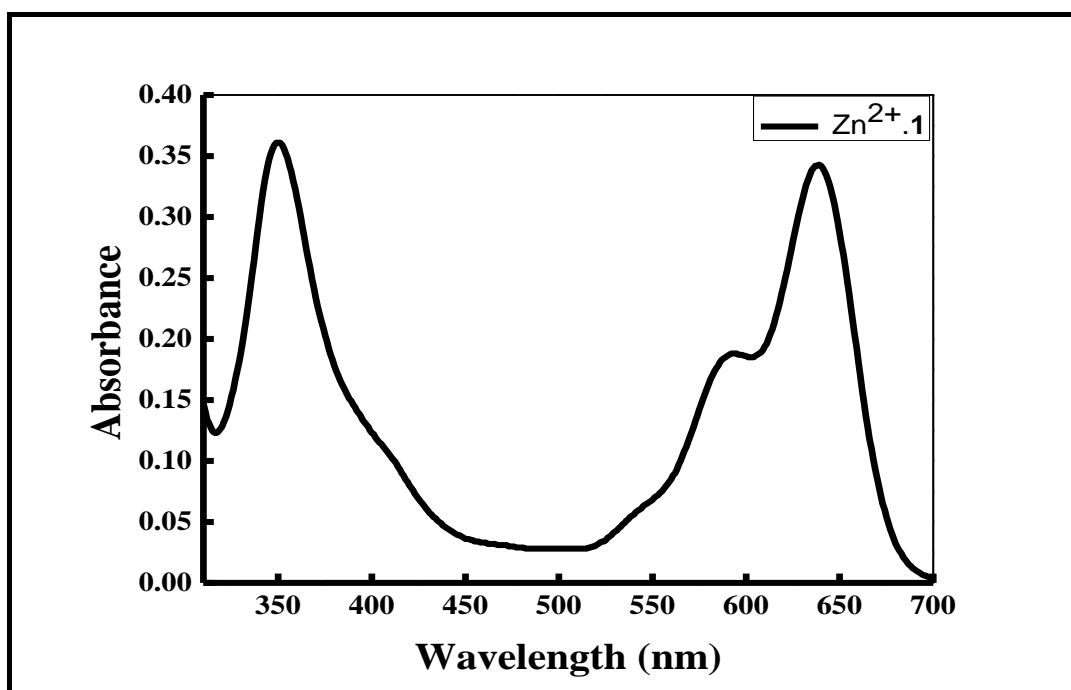


Fig. 4.2 Electronic spectra of compound Zn²⁺.1

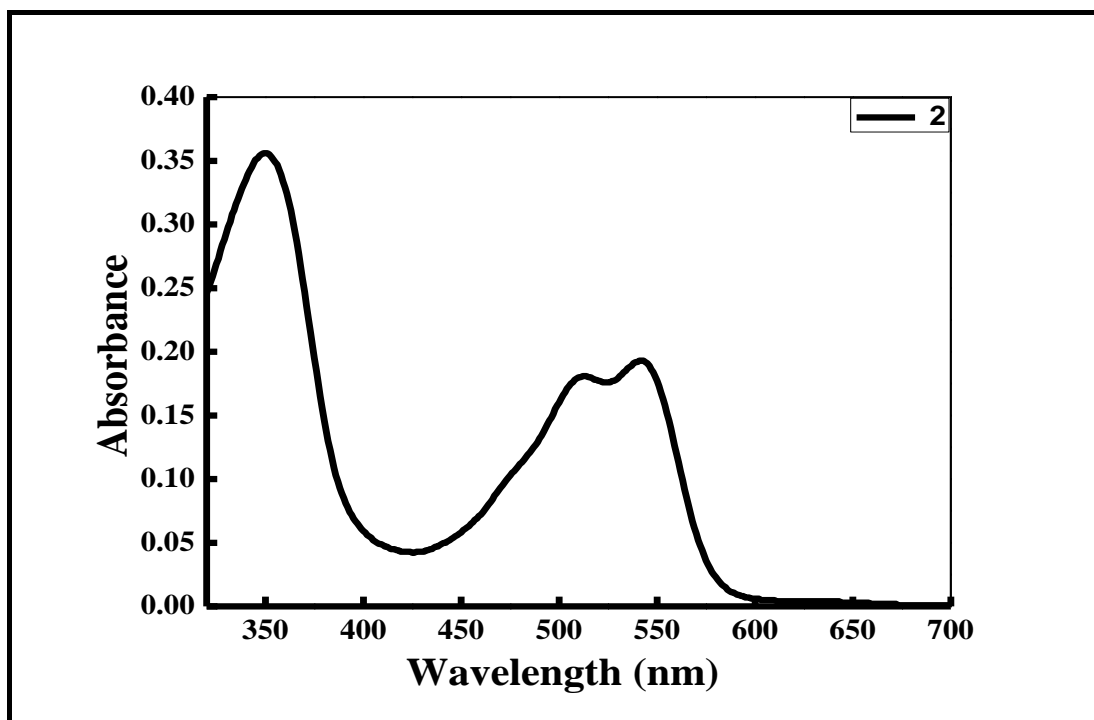


Fig. 4.3 Electronic spectra of compound 2.

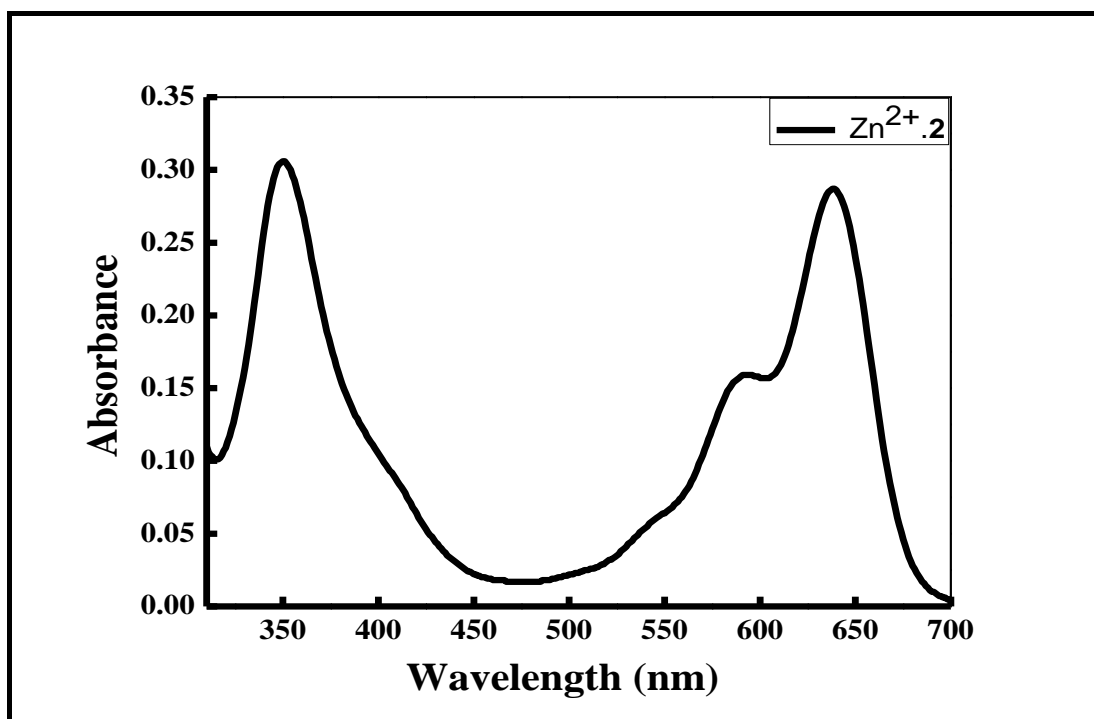


Fig. 4.4 Electronic spectra of compound Zn²⁺.2

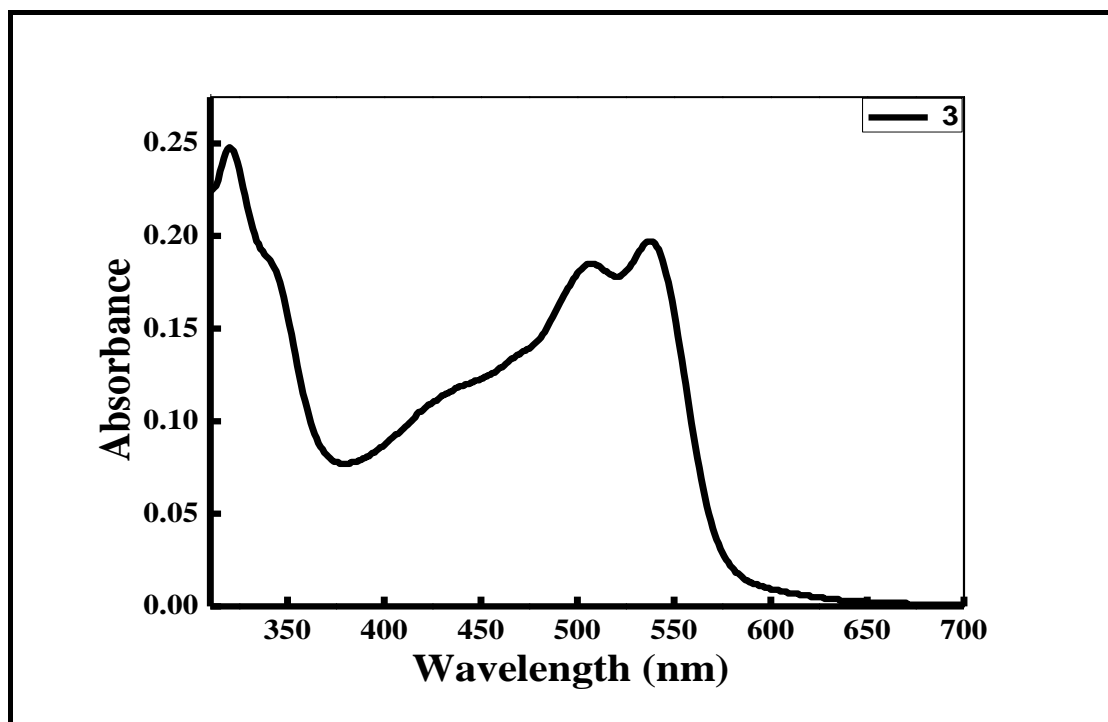


Fig. 4.5 Electronic spectra of compound 3

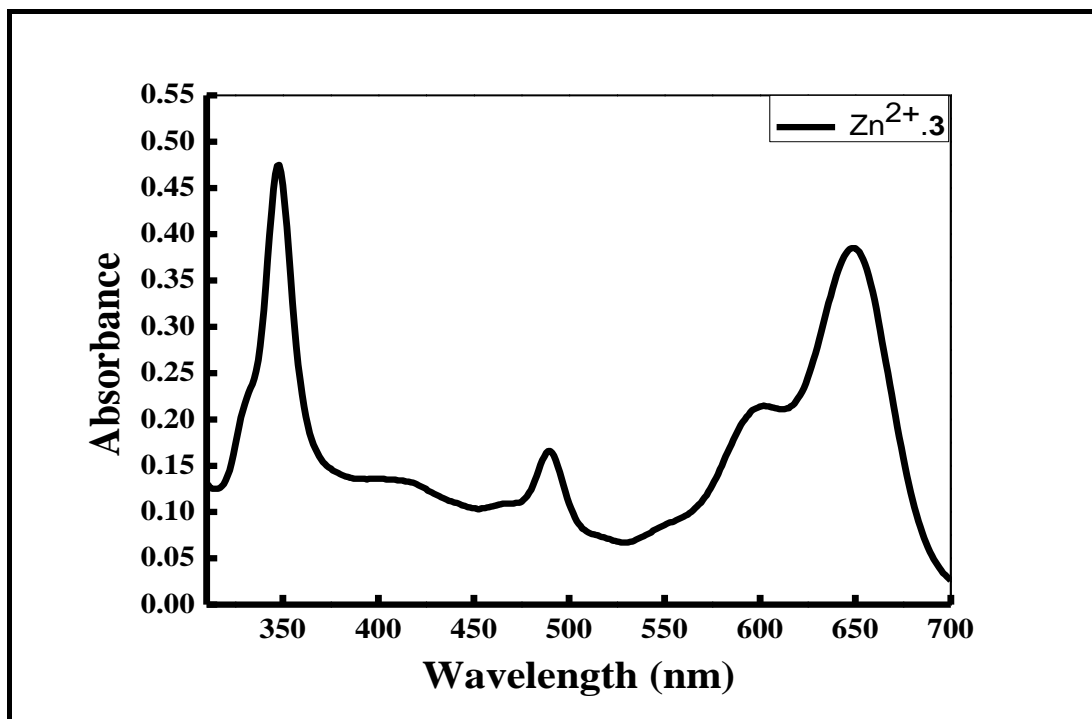


Fig. 4.6 Electronic spectra of compound Zn²⁺.3

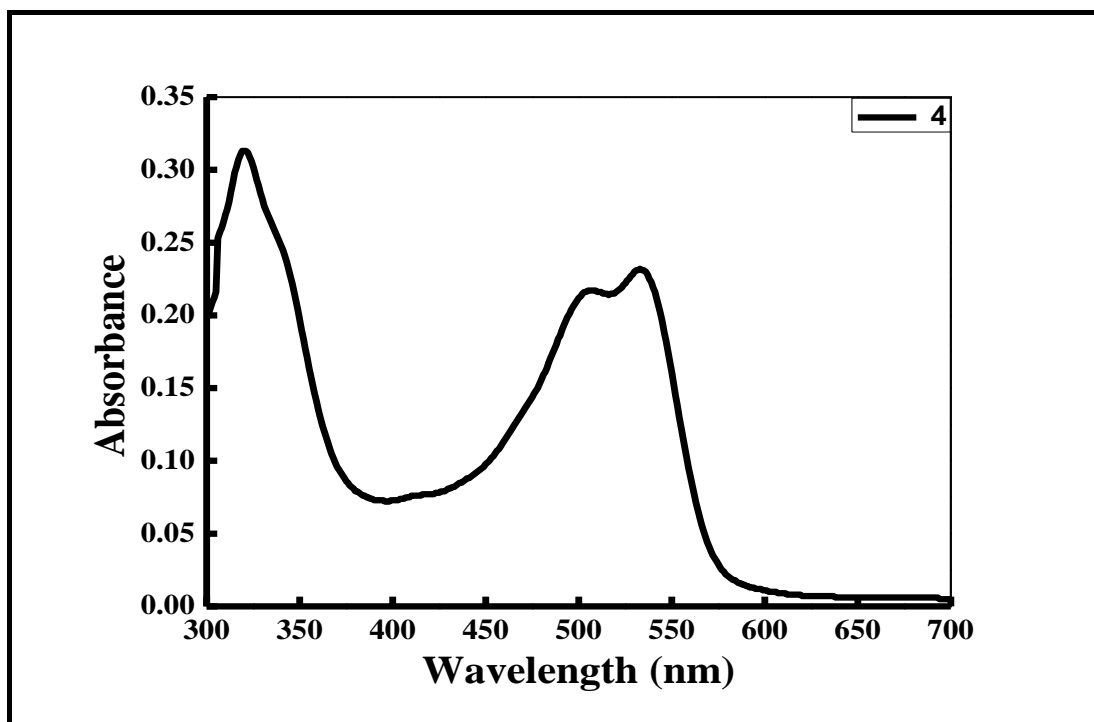


Fig. 4.7 Electronic spectra of compound 4

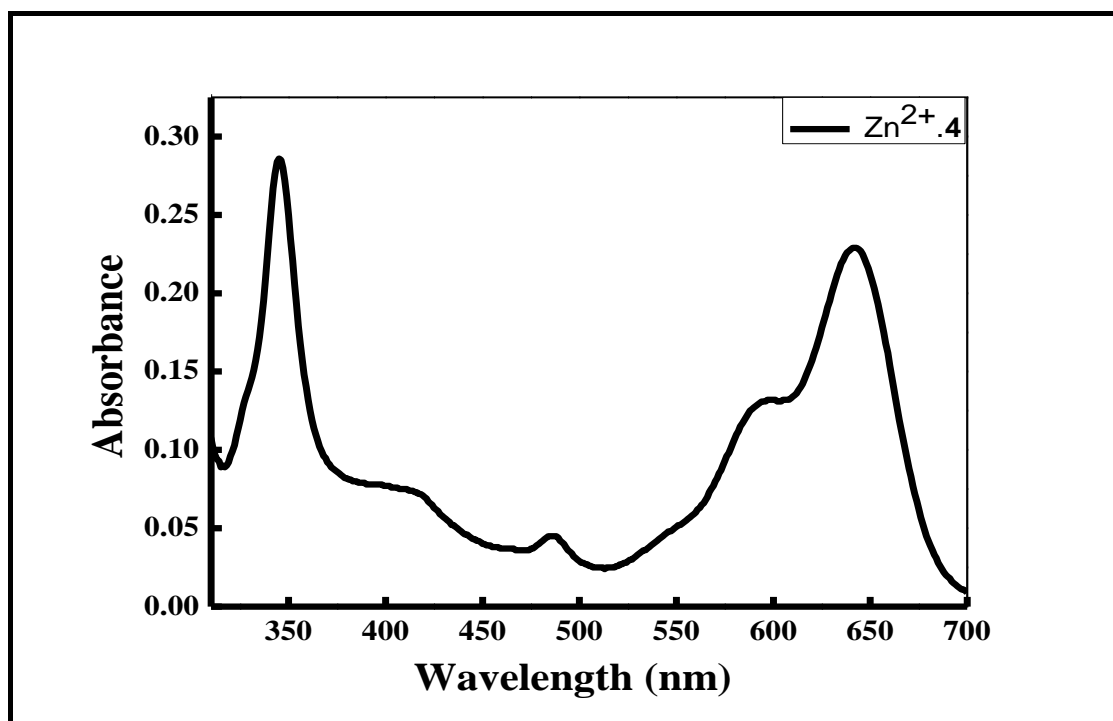


Fig. 4.8 Electronic spectra of compound Zn²⁺.4

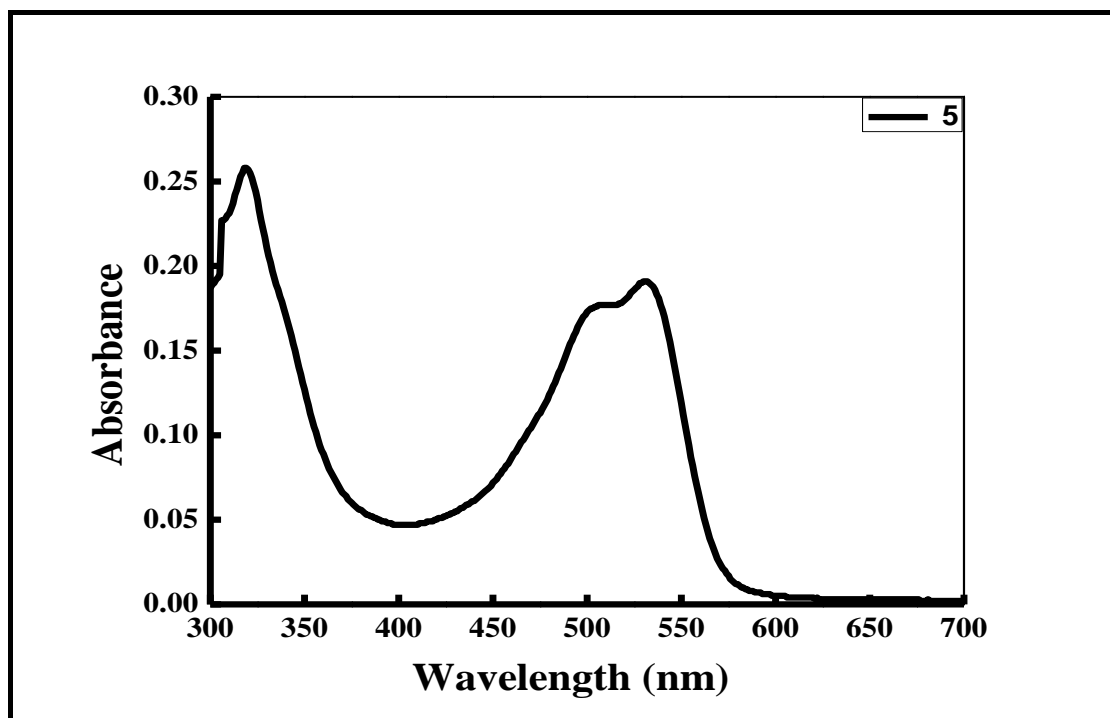


Fig. 4.9 Electronic spectra of compound 5

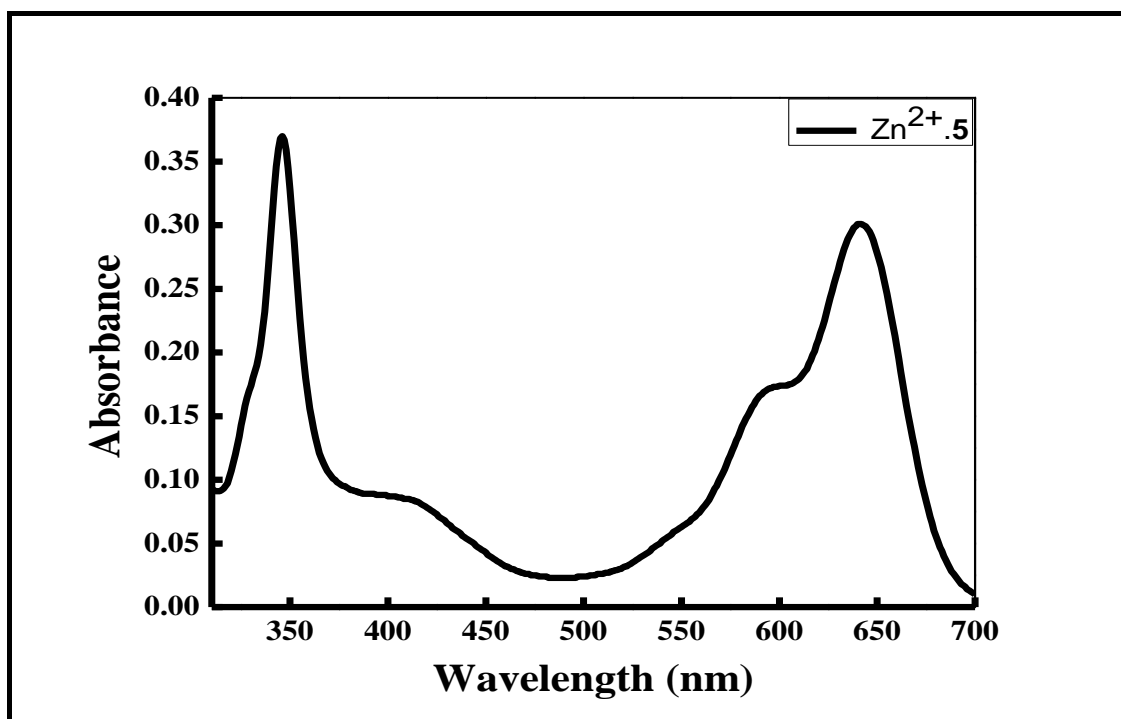


Fig. 4.10 Electronic spectra of compound Zn²⁺.5

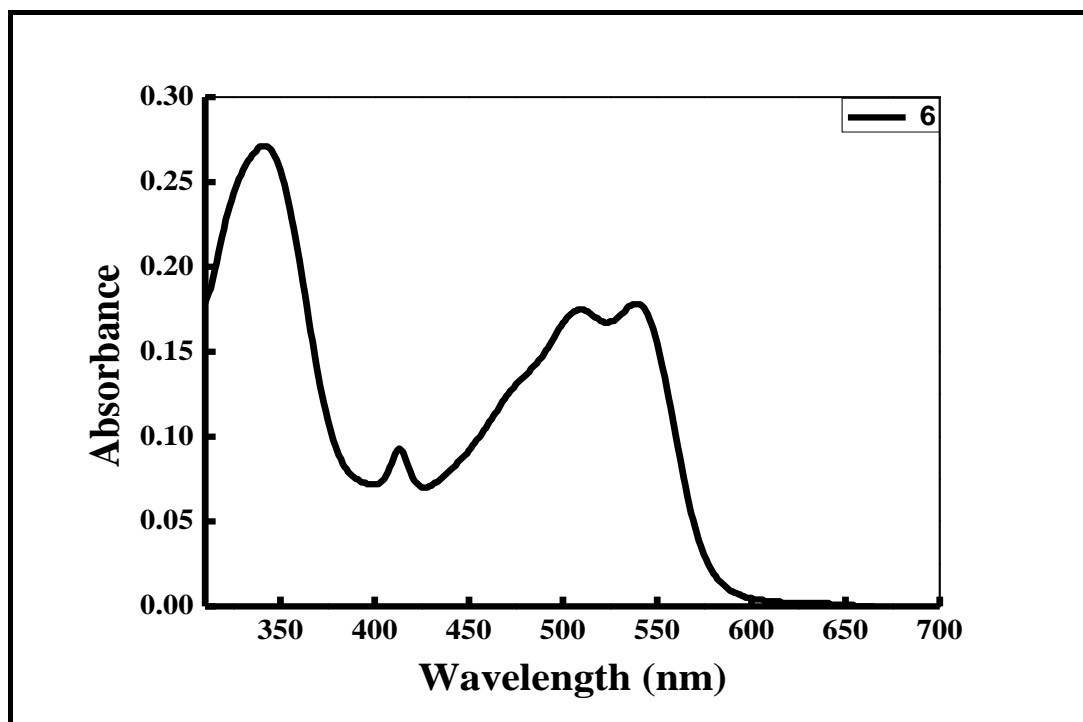


Fig. 4.11 Electronic spectra of compound 6

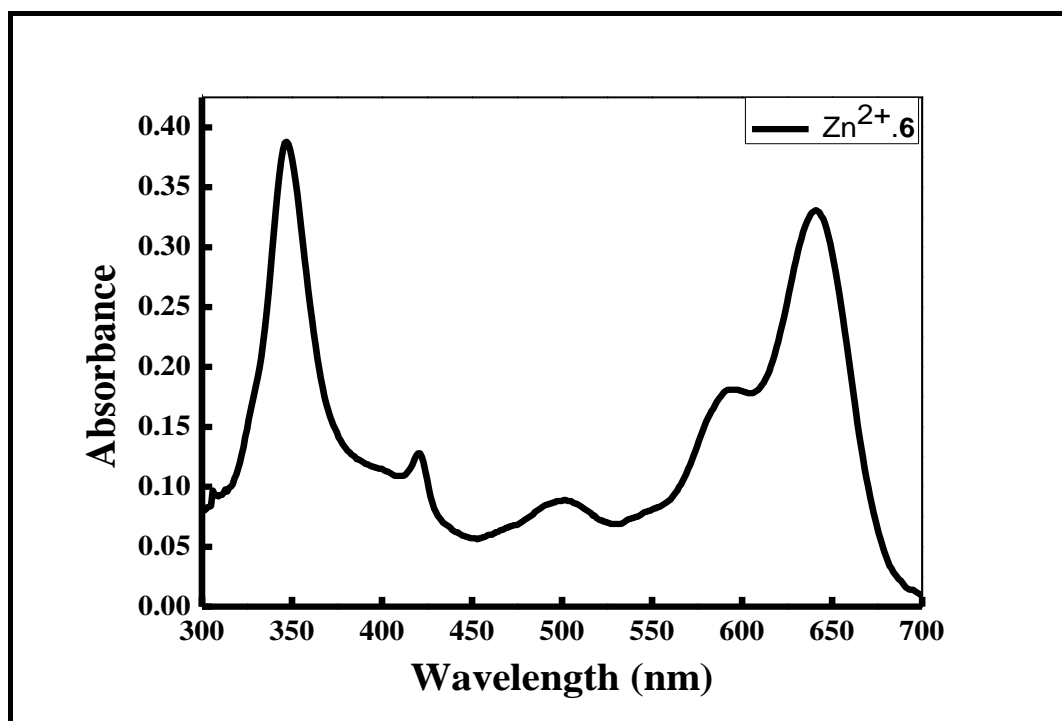


Fig. 4.12 Electronic spectra of compound Zn²⁺.6

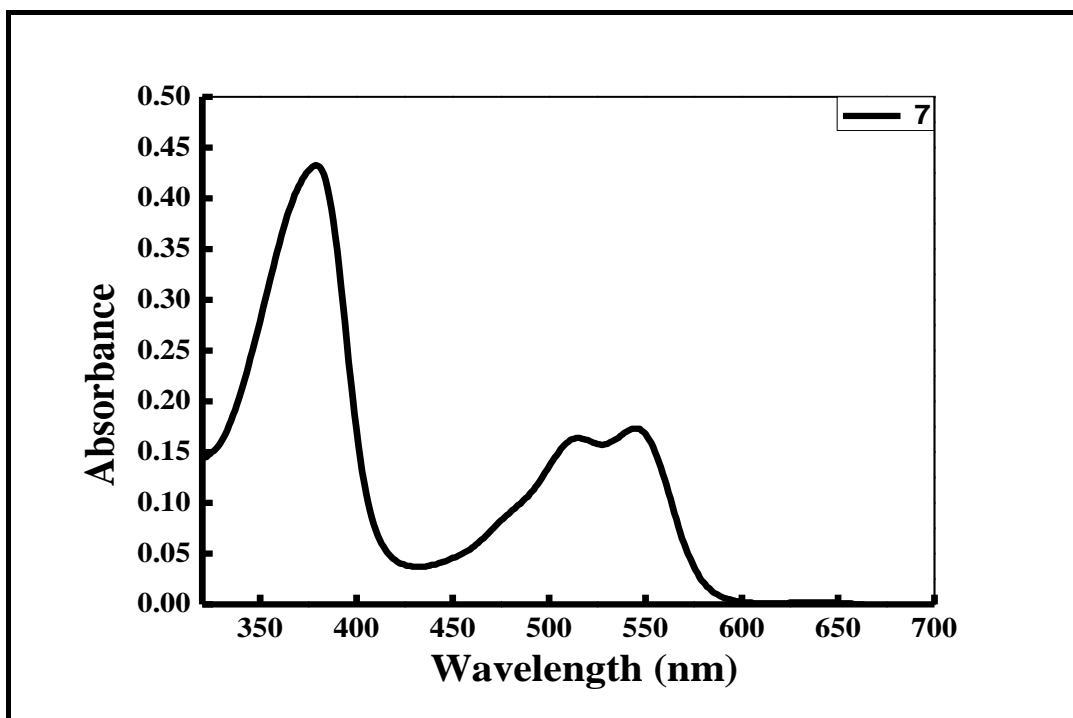


Fig. 4.13 Electronic spectra of compound 7

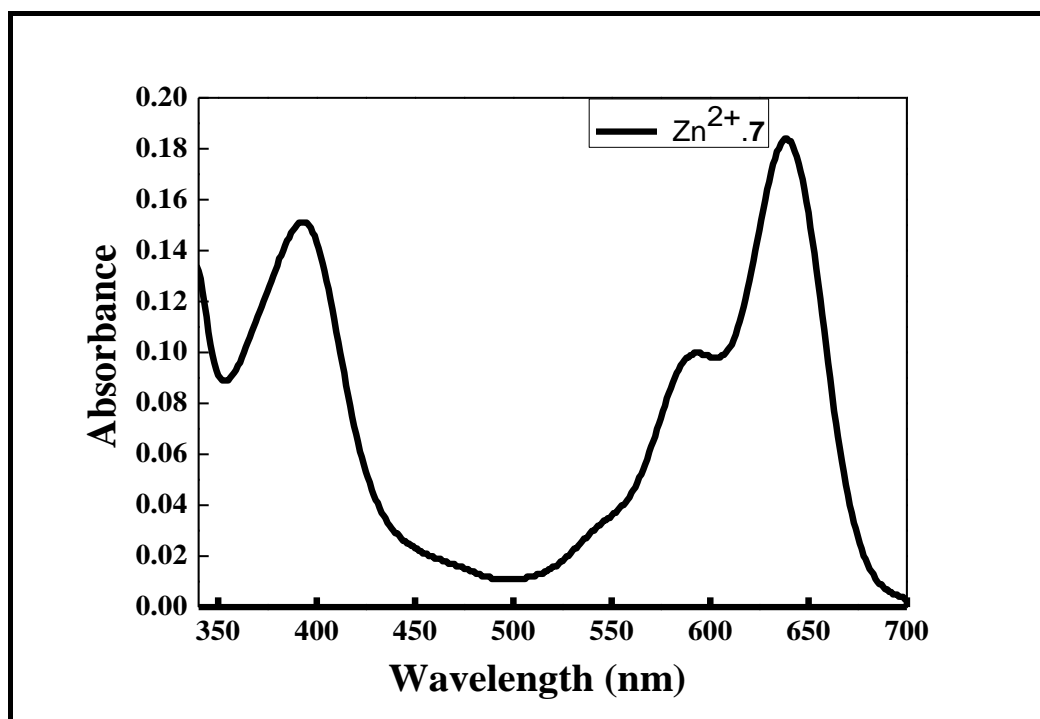


Fig. 4.14 Electronic spectra of compound Zn²⁺.7

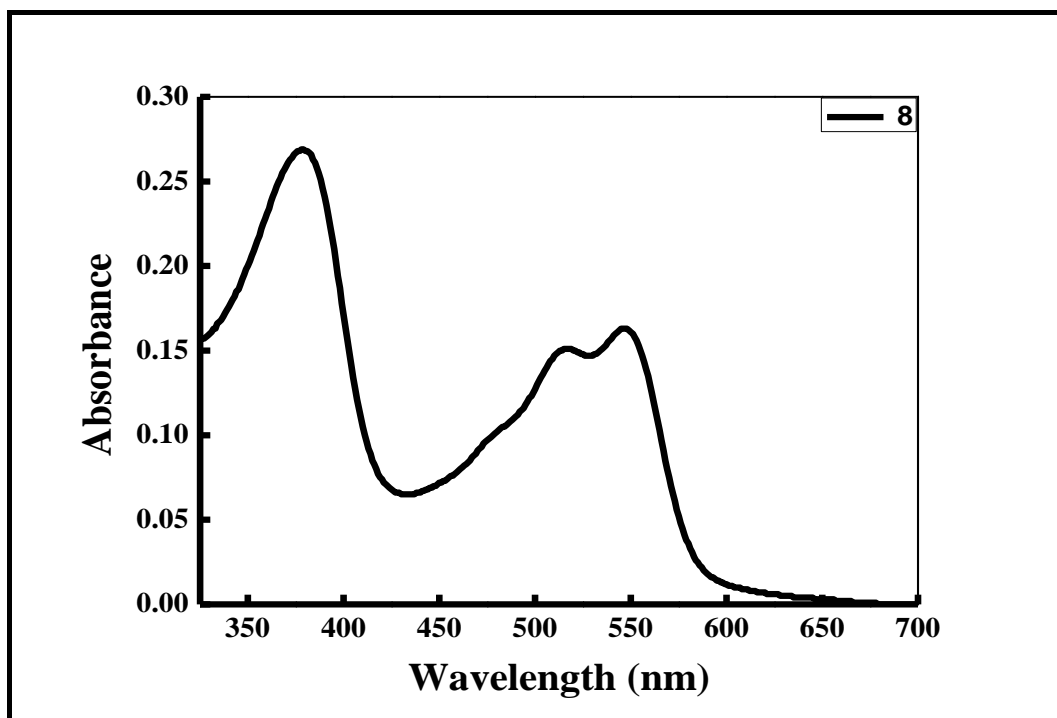


Fig. 4.15 Electronic spectra of compound 8

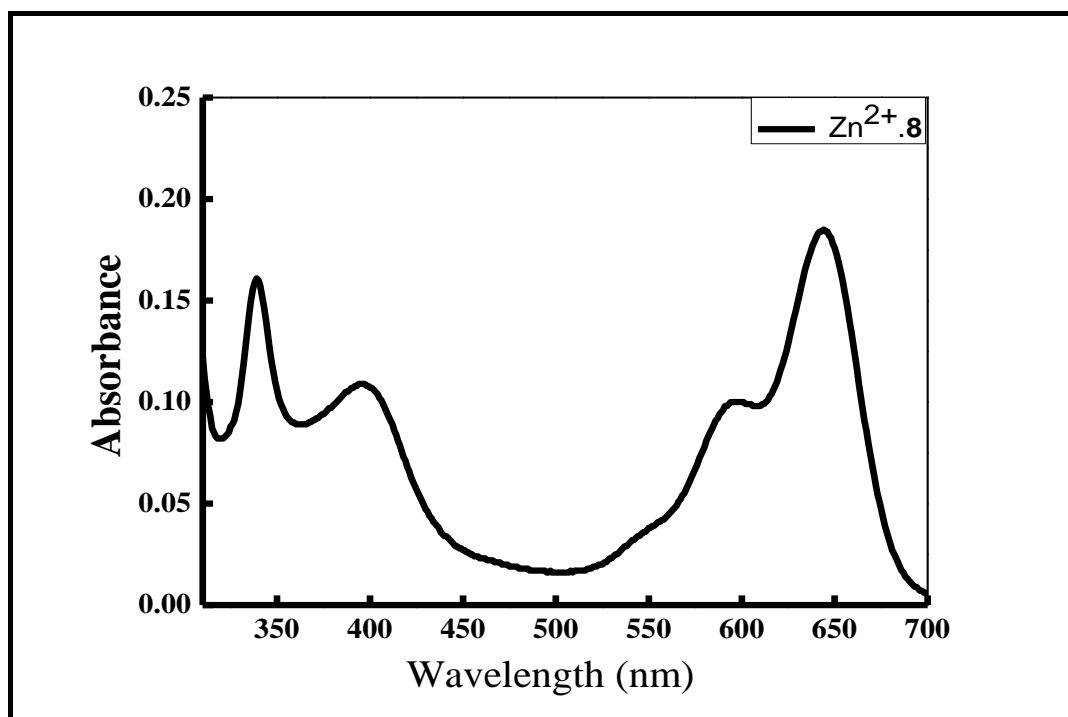


Fig. 4.16 Electronic spectra of compound Zn²⁺.8

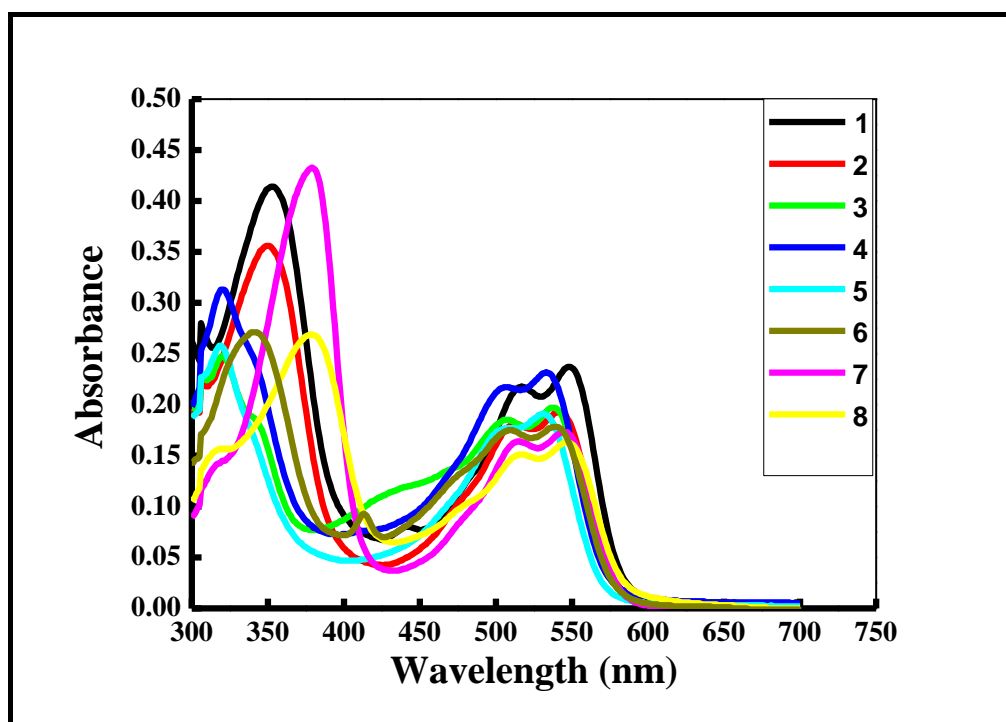


Fig. 4.17 Combined electronic spectra for compounds 1-8

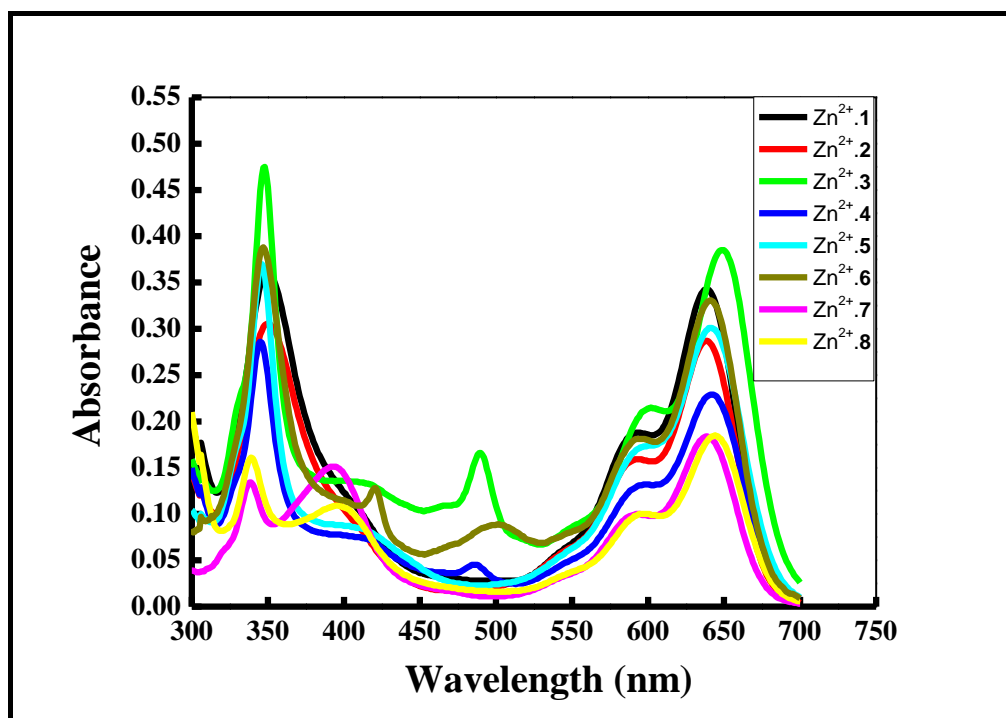


Fig. 4.18 Combined electronic spectra for complexes Zn²⁺.1-8

4.1.2 NUCLEAR MAGNETIC RESONANCE (NMR) SPECTROSCOPY

First NMR investigation of porphyrin ring systems were reported by Becker and Bradley in 1959 [4]. In the porphyrin ring system the protons gets divided into 2 types, the inner or shielded protons and secondly the outer or de-shielded protons because of the porphyrin ring current as it is a conjugated system. However in the case of *meta*-benziporphodimethenes which is a discrete conjugated system in which the ring current get attenuated at the sp^3 *meso* carbon atoms. There is no ring current in the molecule and hence none of the proton of the ring get shielded. All of the protons of *meta*-benziporphodimethenes appeared at the normal values.

^1H NMR spectra of free base, **1-8**, in CDCl_3 showed a symmetrical pattern with a singlet in between 1.70-1.81 ppm integrated into twelve hydrogens which corresponds to four methyl groups on two sp^3 hybridized *meso* carbons. In compound **7** a singlet appeared at 3.87 ppm while in the case of **8** having two types of $-\text{OCH}_3$ groups, a singlet at 3.92 ppm and 3.83 ppm integrated into six and twelve hydrogens, corresponding to *ortho* and *meta* groups, respectively. The NMR signals for hydrogen on C(22) appeared in the range of 7.92-8.06 ppm for compounds **1-8** and inner core NH proton resonated at 12.0-12.38 ppm as broad signal in compounds, **1-8**.

^{13}C NMR spectra pattern were also observed as expected. The sp^3 hybridised *meso* carbons appear at around 40 ppm whereas the methyl carbons appears at around 29 ppm. The aromatic carbons of *meso* phenyl rings and the benzene of the ring system appear in between 125-145 ppm. Carbon atoms of pyrrolic fragments which are present at α positions and are directly linked to sp^3 hybridized *meso* carbons appear downfield at around 165-185 ppm while the other α carbons of pyrrolic fragments appear at around 145-150 ppm. The β carbons of pyrrolic fragments appear at around 120-135 ppm.

The ^1H NMR and ^{13}C NMR data of various synthesized free base *meta*-benziporphodimethenes are tabulated in Table 4.2 and Table 4.3. ^1H NMR and ^{13}C NMR spectra of synthesized free base *meta*-benziporphodimethenes have been shown in Fig. 4.19 to 4.33.

Table 4.2 ¹H NMR spectral data for compounds **1-8**

Compound	N-H	22C's H	Aromatic Protons	9,18 Pyr. H	8,19 Pyr. H	13,14Pyr. H	-OCH ₃ H's	CH ₃ H's
1	12.32 (br, s)	7.93(s)	7.24-7.39(m)	6.81(ab quartet)	6.81(ab quartet)	6.15(s)	---	1.72(s)
2	12.32 (br, s)	7.94(s)	7.31-7.57(m)	6.83(ab quartet)	6.83(ab quartet)	6.16(s)	---	1.74(s)
3	12.16 (br, s)	8.06(s)	7.28-7.41(m)	6.82(d) J=4.59Hz	6.56(d) J=4.59Hz	5.86(s)	---	1.81(s)
4	12.18 (br, s)	7.97(s)	6.91-7.45(m)	6.83(d) J=4.40Hz	6.70(d) J=4.22Hz	6.00(s)	---	1.79(s)
5	12.08 (br, s)	7.89(s)	7.25-7.34(m)	6.90(d) J=4.58Hz	6.65(d) J=4.58Hz	5.98(s)	---	1.78(s)
6	12.00 (br, s)	7.92(s)	7.68(d,4H-ArH), 7.56(d,4H-ArH), 7.29(m,3H-ArH)	6.85(d) J=4.58Hz	6.75(d) J=4.58Hz	6.07(s)	---	1.75(s)
7	12.38 (br, s)	7.93(s)	7.44(d, 4 Ar-H J=8.4 Hz), 7.27-7.32(m, 3H,2,3,4 Ar-H), 6.95(d, 4 Ar-H J=8.4 Hz)	6.88(d) J=4.58Hz	6.77(d) J=4.58Hz	6.30(s)	3.87(s)	1.69(s)
8	12.33 (br, s)	7.92(s)	7.30(q, J=5.34 Hz 3H 2,3,4 Ar-H) + 6.74(s, 4Ar-H (AA'BB'))	6.95(d) J=3.81 Hz	6.80(d) J=4.58Hz	6.35(s)	3.92(s,6H, para OMe- H's) + 3.83(s,12H, meta OMe- H's)	1.70(s)

Table 4.3 ^{13}C NMR spectral data for compounds **1-8**.

Table for ^{13}C -NMR DATA	
δ value for ^{13}C -NMR Peaks (101 MHz, CDCl_3 , 20°C)	
Compound	Peak values
1	181.79, 153.72, 152.44, 151.77, 147.41, 143.63, 138.84, 138.58, 138.22, 136.53, 133.59, 131.79, 128.68, 127.38, 125.24, 123.15, 121.27, 42.10, 29.06.
2	182.68, 152.00, 147.06, 138.57, 137.10, 136.45, 133.29, 131.02, 128.52, 127.11, 125.60, 123.56, 123.29, 121.24, 42.25, 28.98
3	184.33, 162.24, 159.69, 152.99, 146.25, 144.66, 137.77, 135.65, 130.61, 127.94, 127.08, 125.92, 123.59, 123.15, 120.16, 118.37, 111.48, 111.24, 42.50, 29.82, 28.73.
4	184.35, 162.17, 159.75, 153.00, 146.25, 144.65, 137.78, 135.66, 130.63, 127.95, 127.51, 127.08, 125.94, 123.61, 123.16, 120.18, 118.40, 111.50, 111.26, 42.51, 29.83, 28.74.
5	185.93, 153.54, 145.91, 137.11, 135.14, 128.11, 127.31, 126.82, 123.74, 119.90, 119.37, 115.97, 42.64, 28.51.
6	183.38, 152.24, 146.85, 141.83, 138.51, 136.44, 135.82, 131.86, 128.48, 126.97, 125.94, 124.73, 123.40, 121.28, 42.36, 28.91.
8	152.45, 147.34, 139.37, 136.53, 133.43, 128.75, 127.29, 125.11, 123.25, 109.62, 61.11, 56.34, 42.07, 29.78, 28.98.

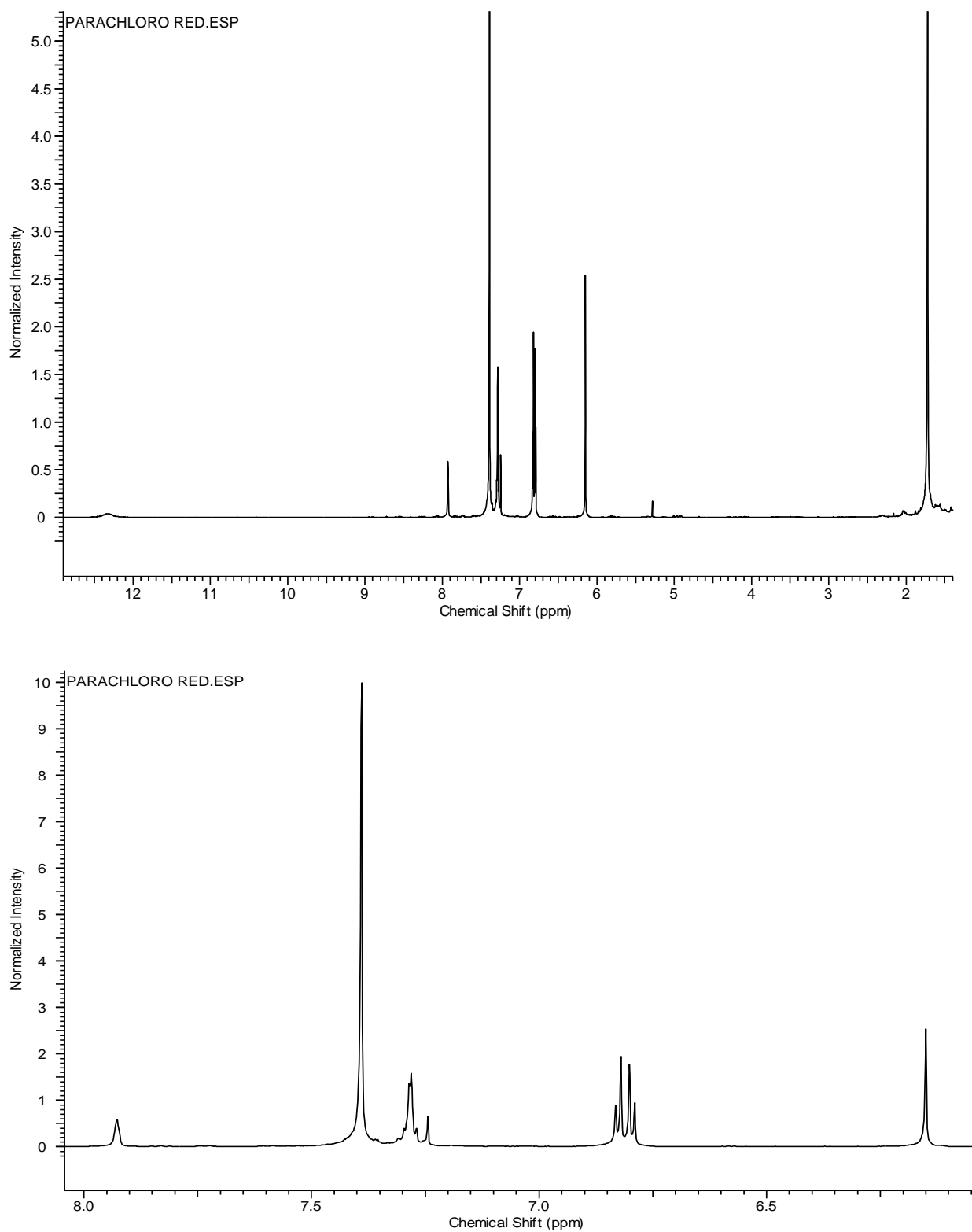


Fig. 4.19 ¹H-NMR spectra of compound **1**

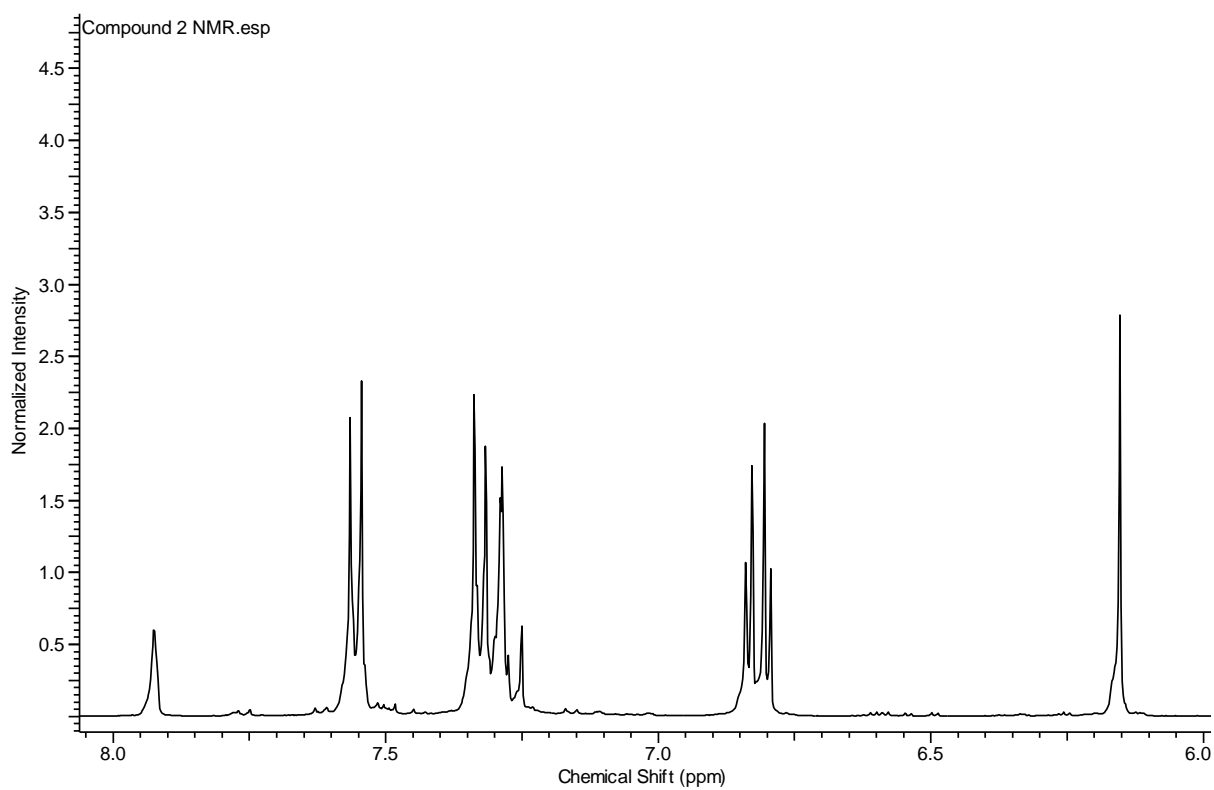
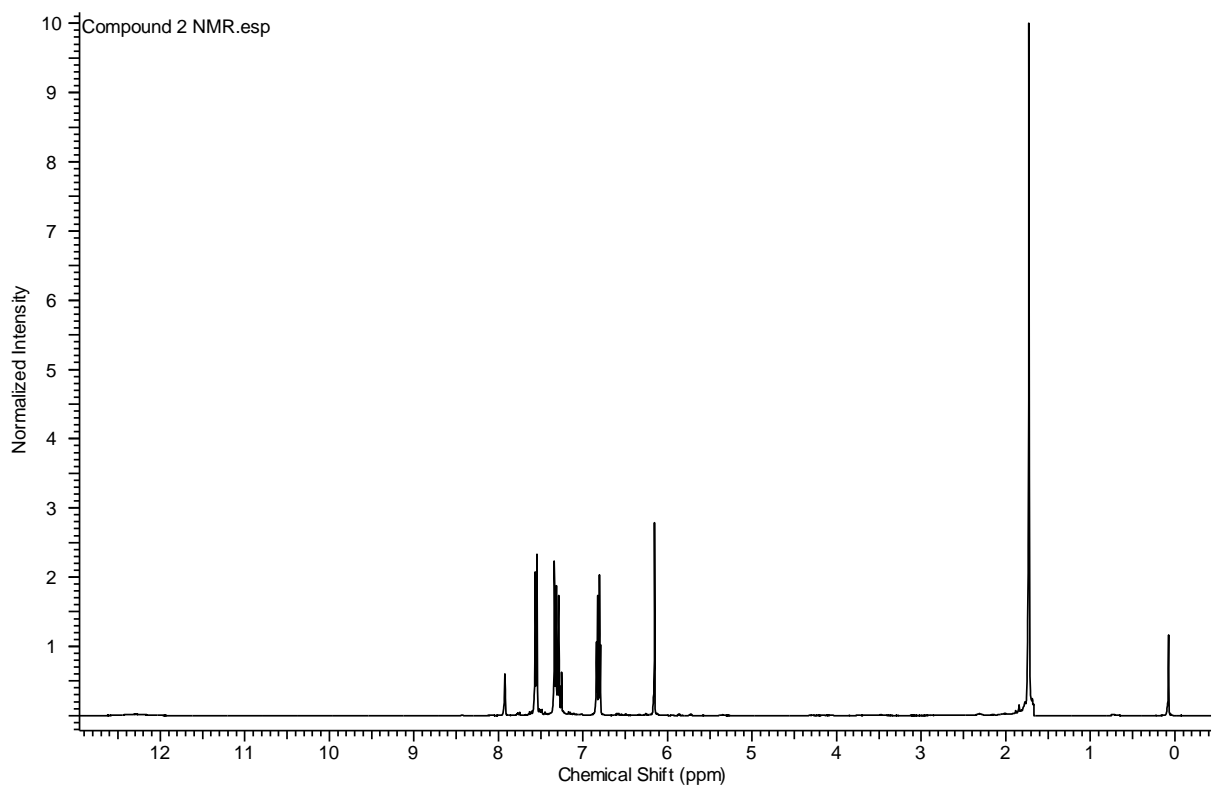


Fig. 4.20 ¹H-NMR spectra of compound 2

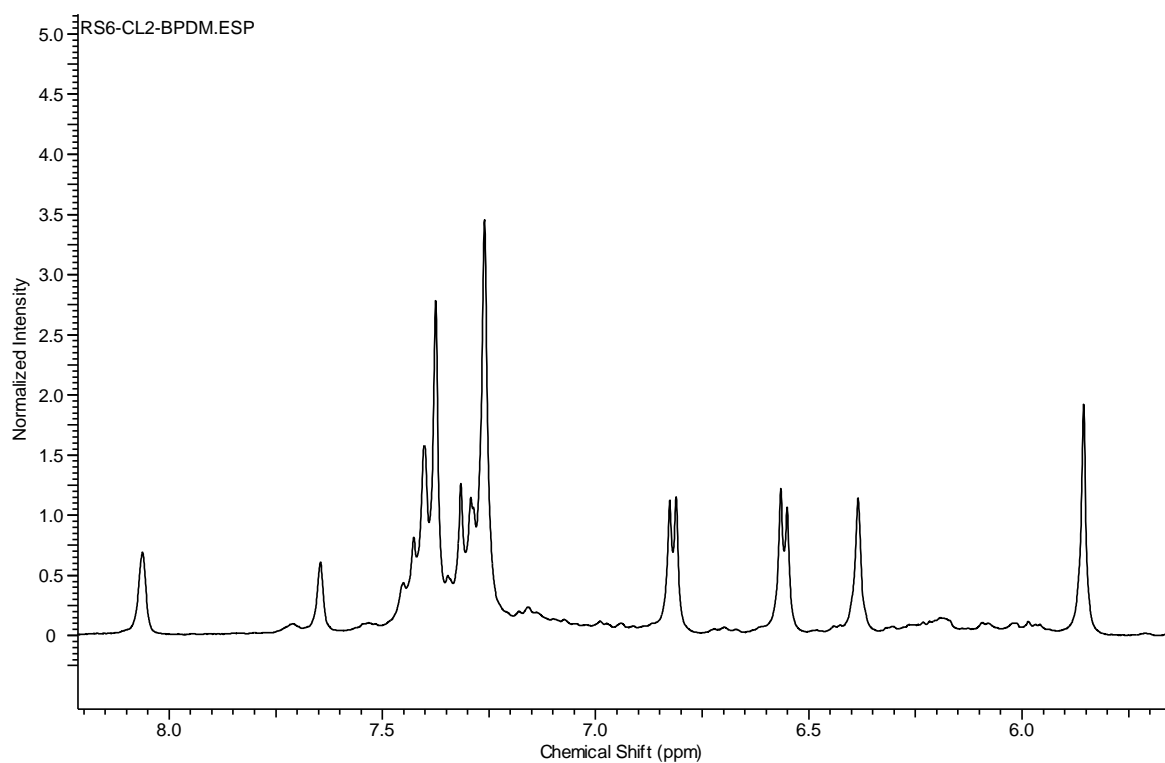
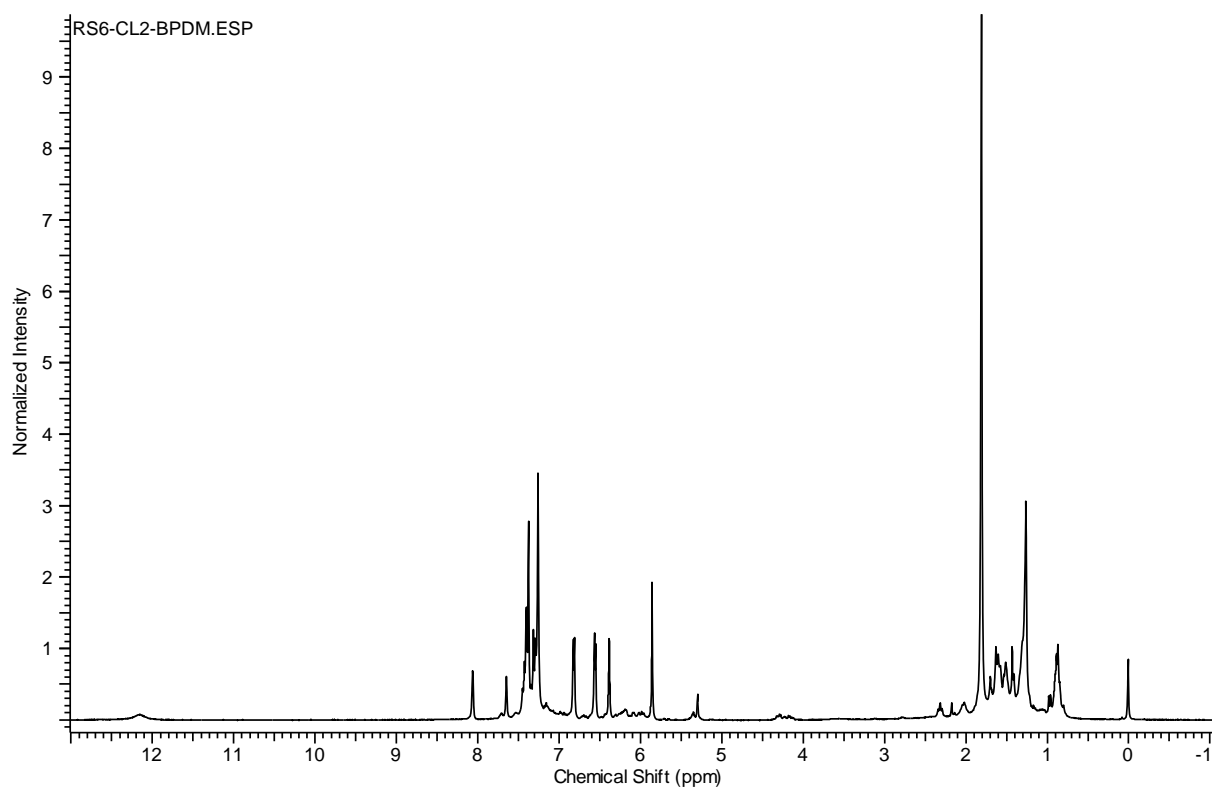


Fig. 4.21 ¹H-NMR spectra of compound **3**

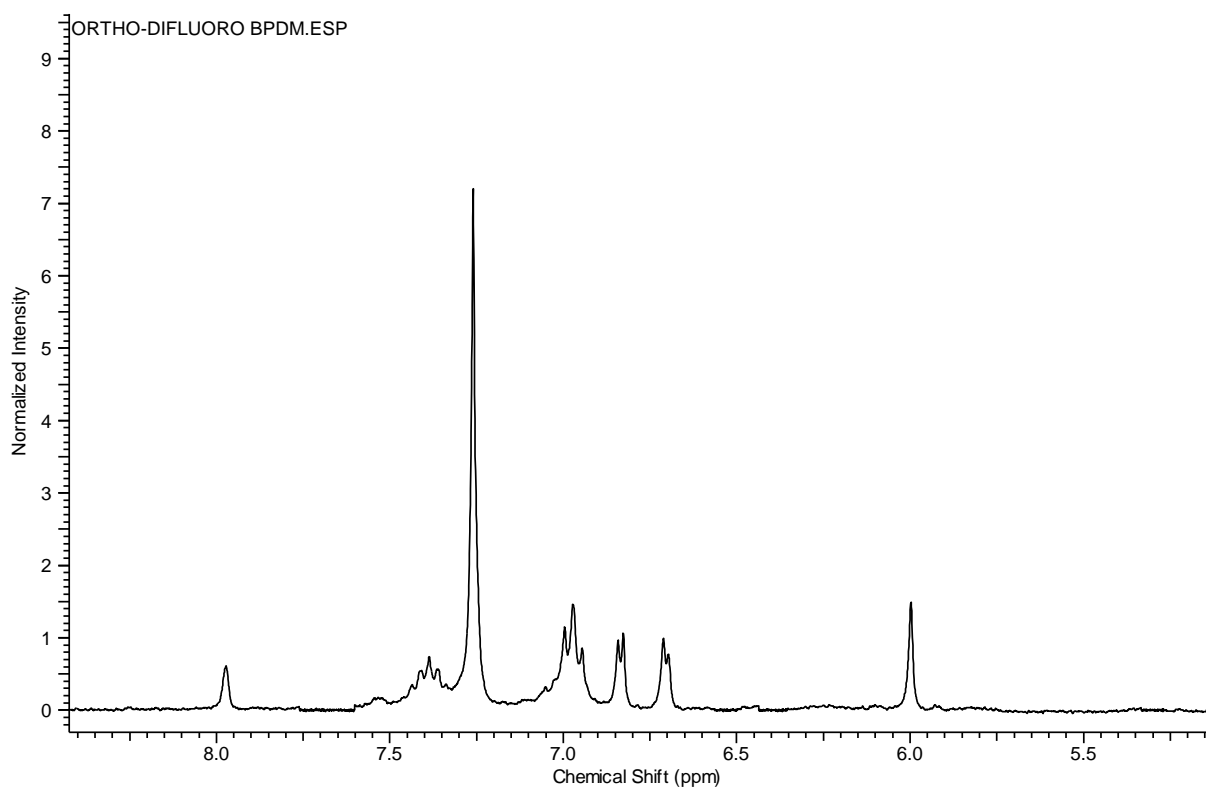
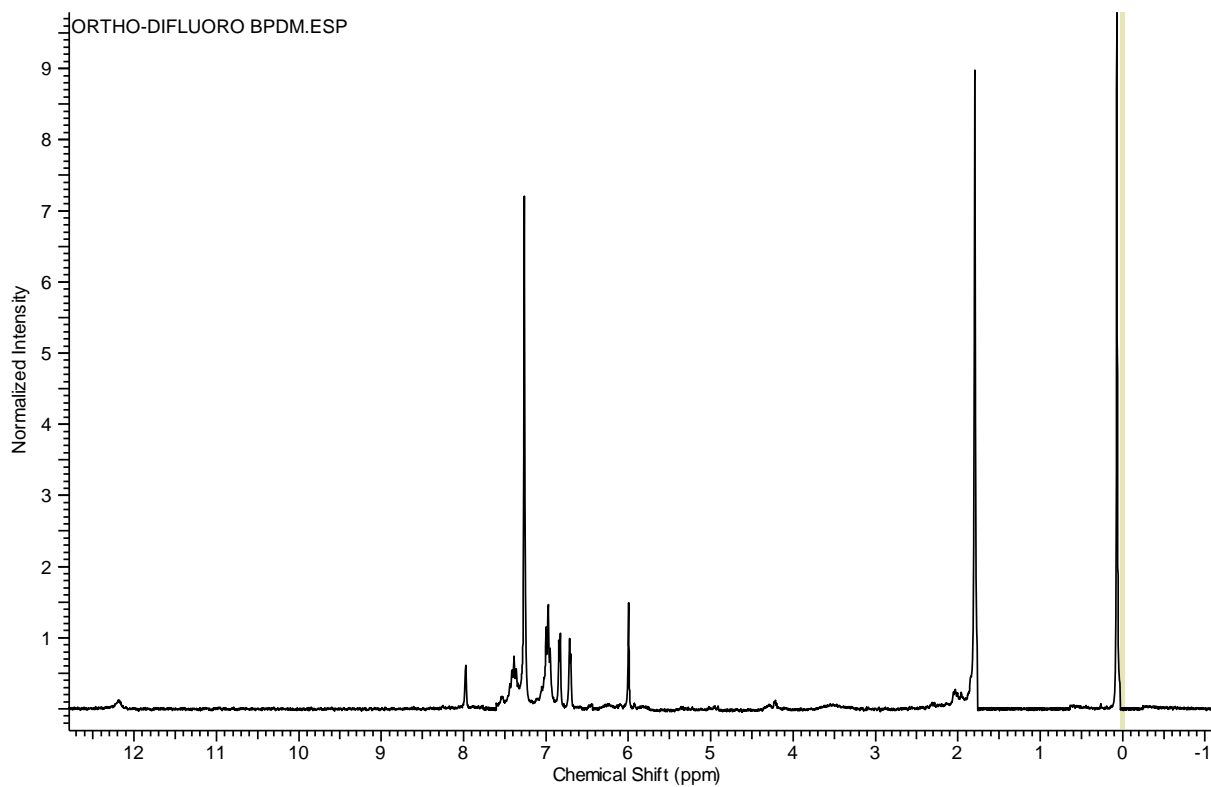


Fig. 4.22 ¹H-NMR spectra of compound **4**

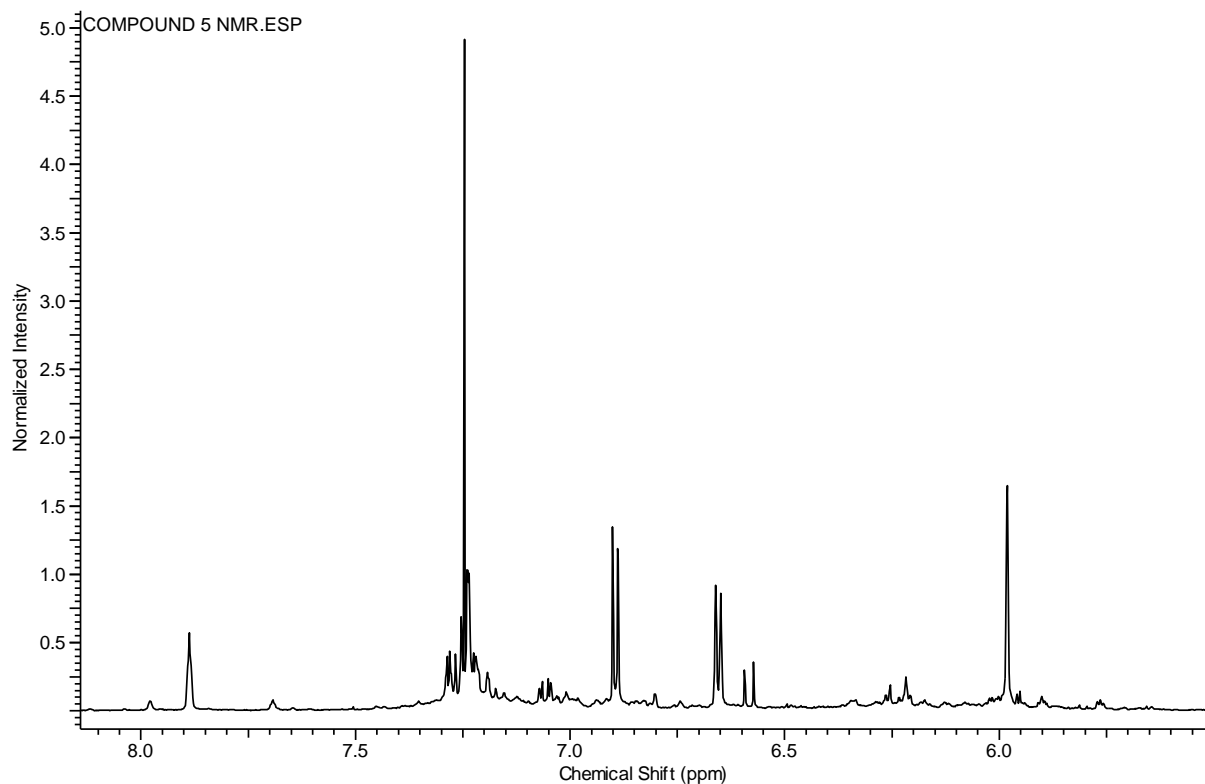
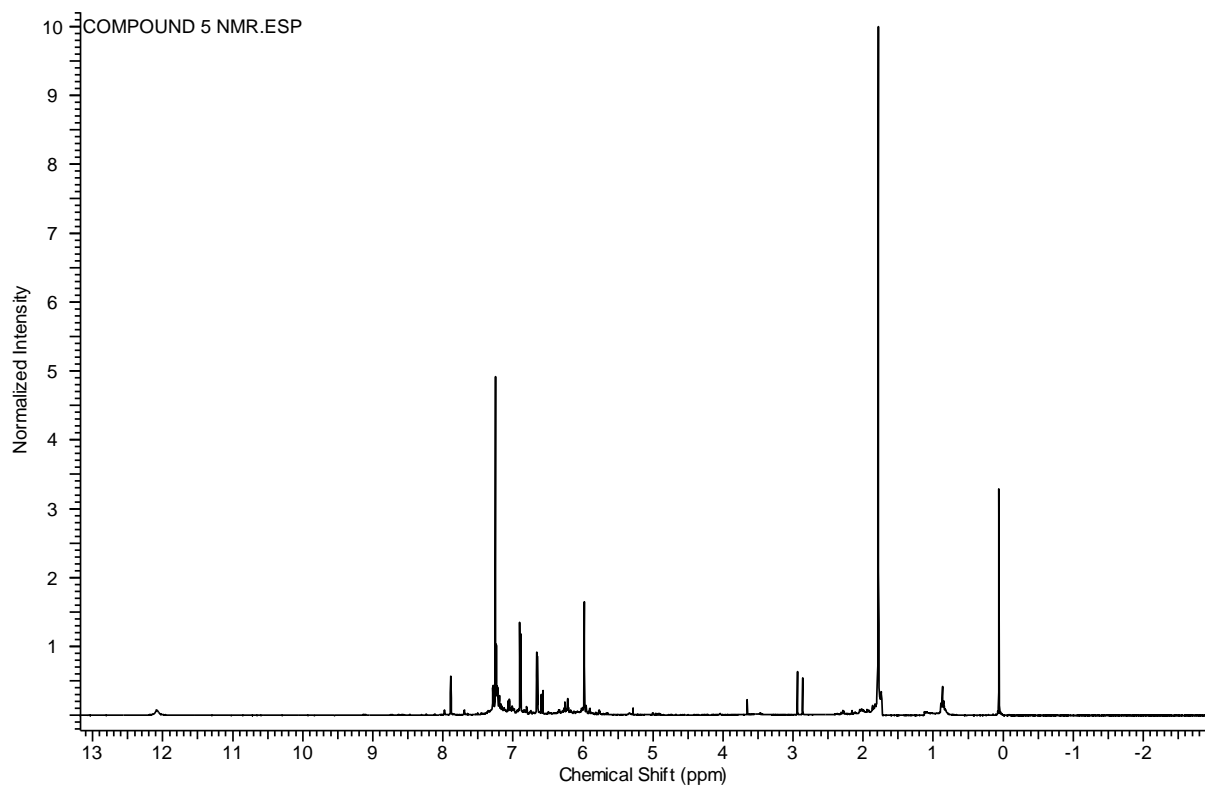


Fig. 4.23 ¹H-NMR spectra of compound 5

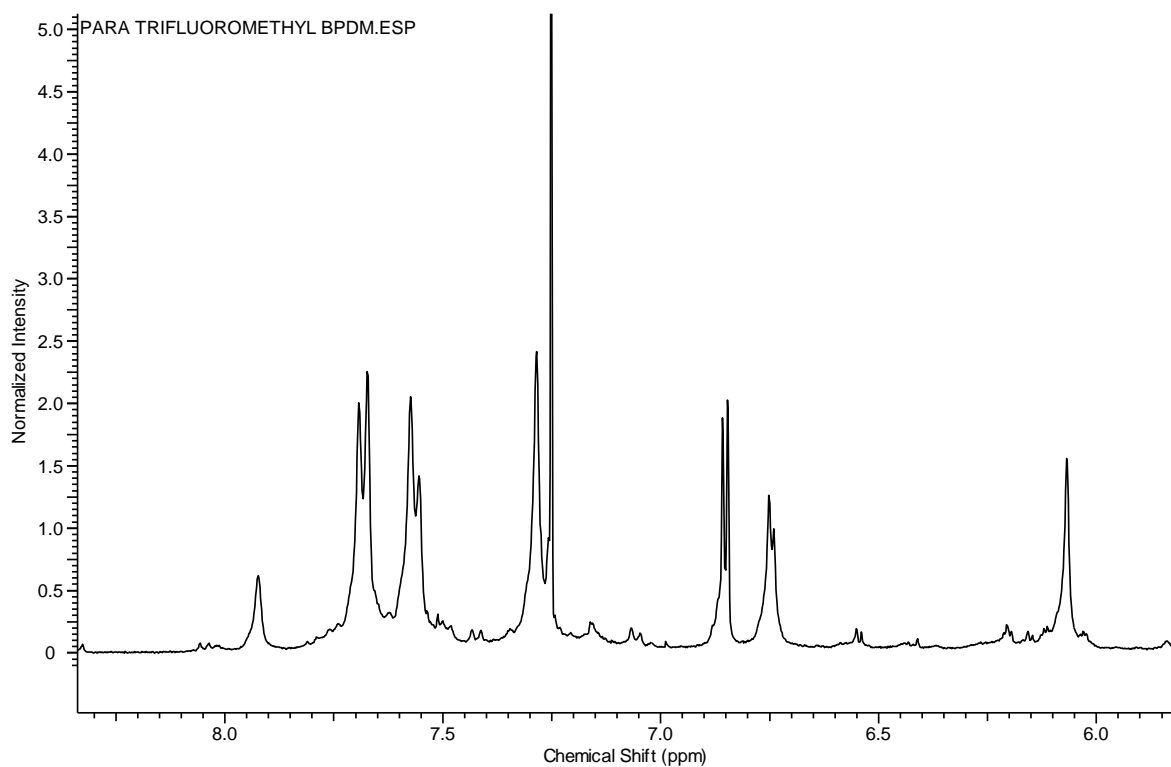
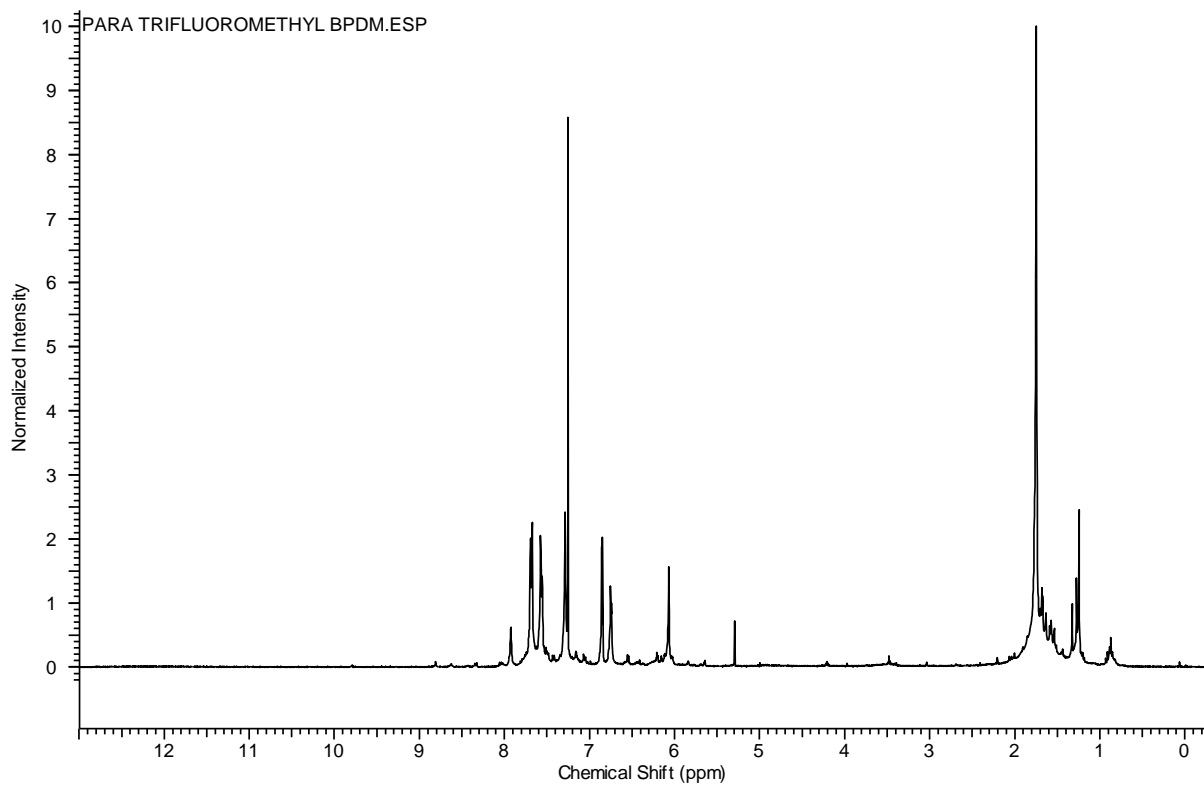


Fig. 4.24 ¹H-NMR spectra of compound **6**.

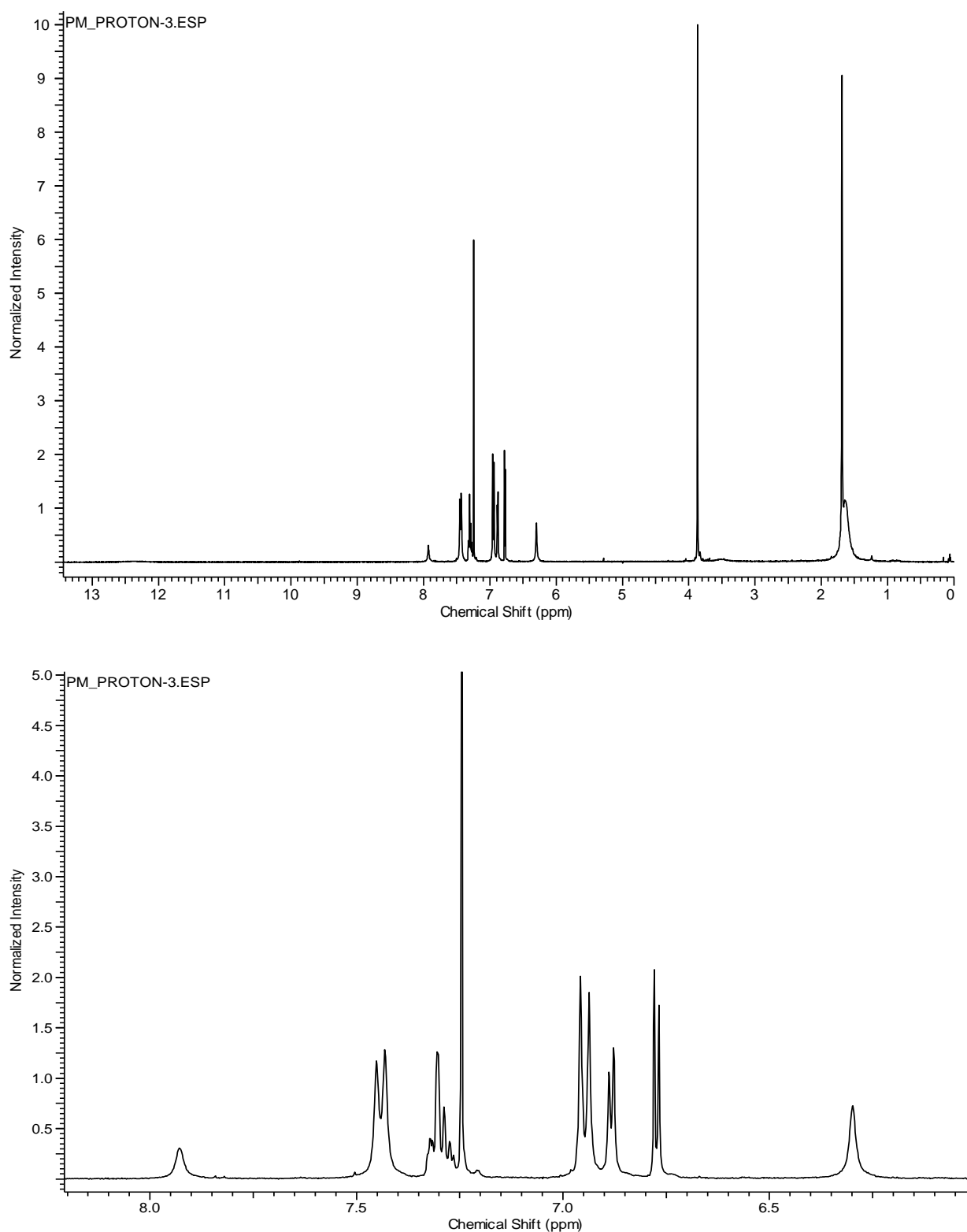


Fig. 4.25 $^1\text{H-NMR}$ spectra of compound 7

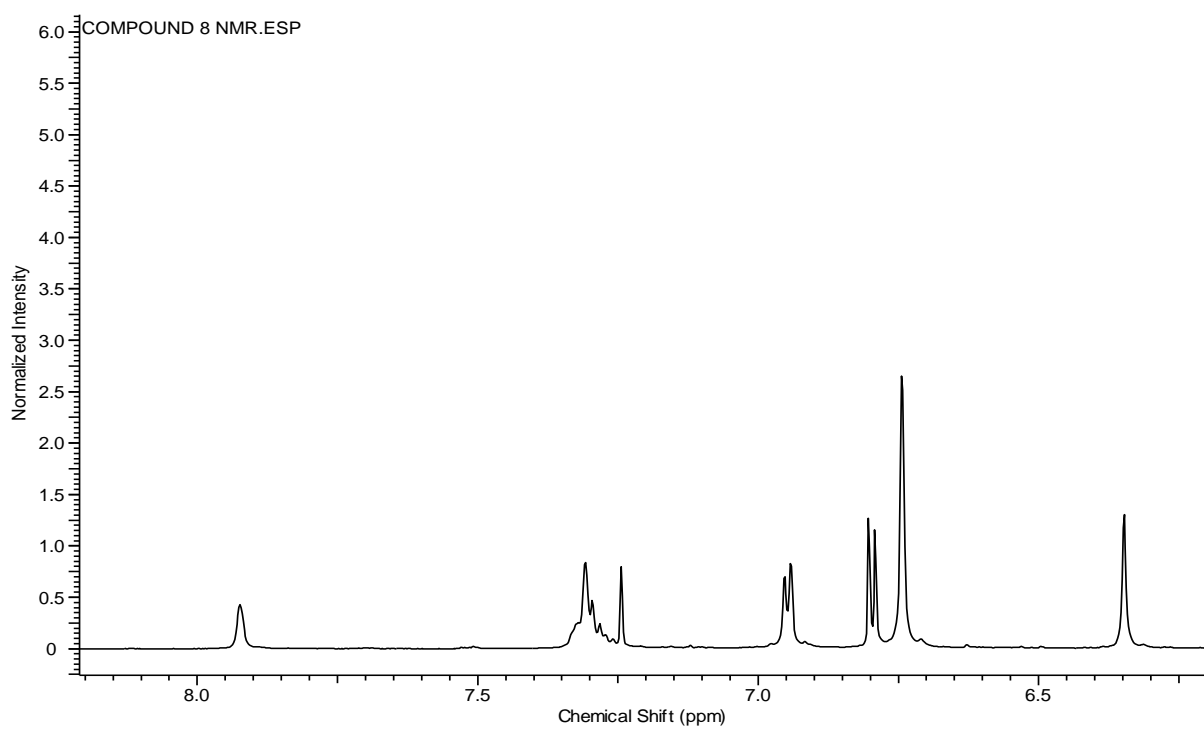
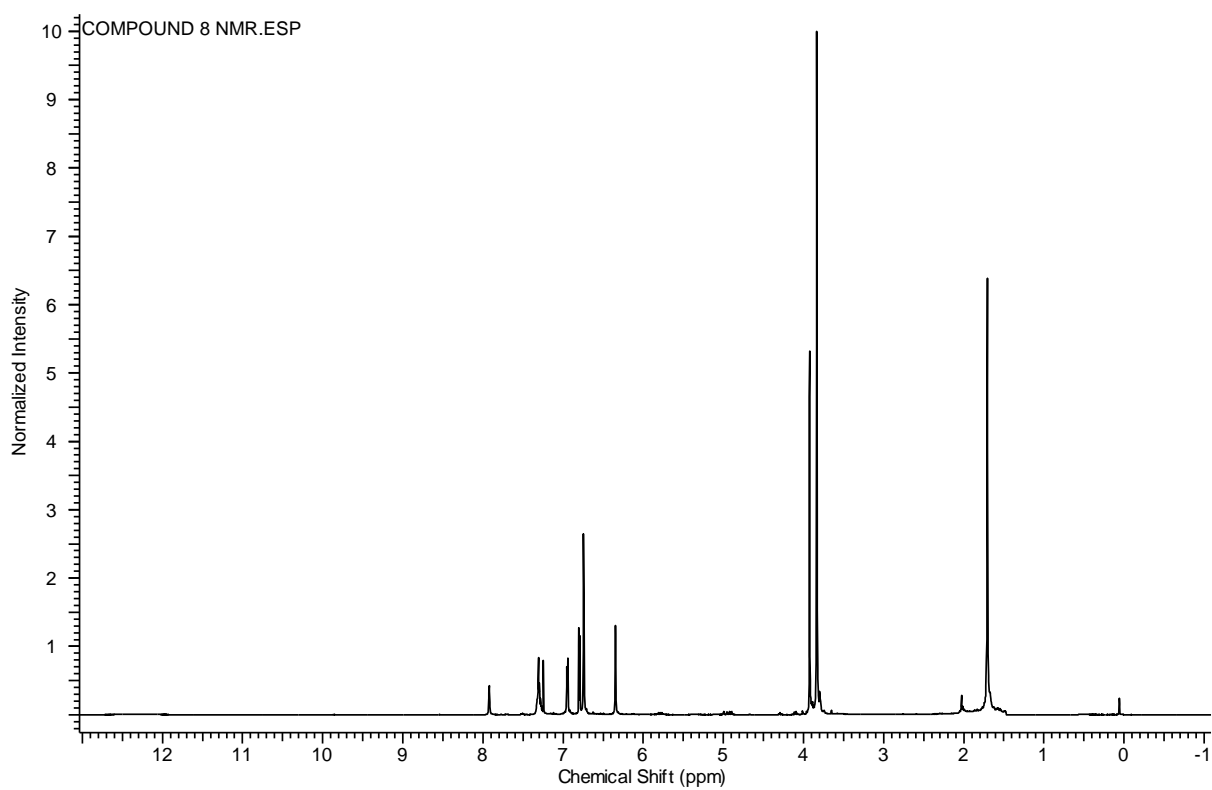


Fig. 4.26 ¹H-NMR spectra of compound **8**

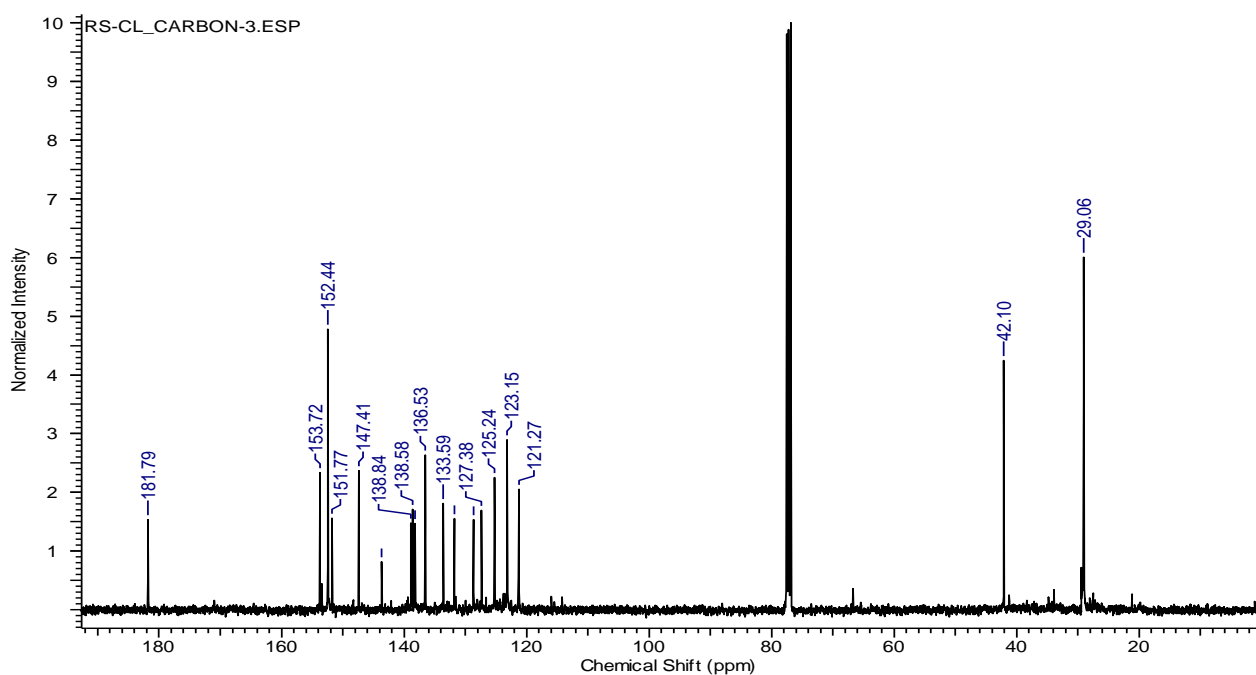


Fig. 4.27 ¹³C-NMR spectra of compound 1

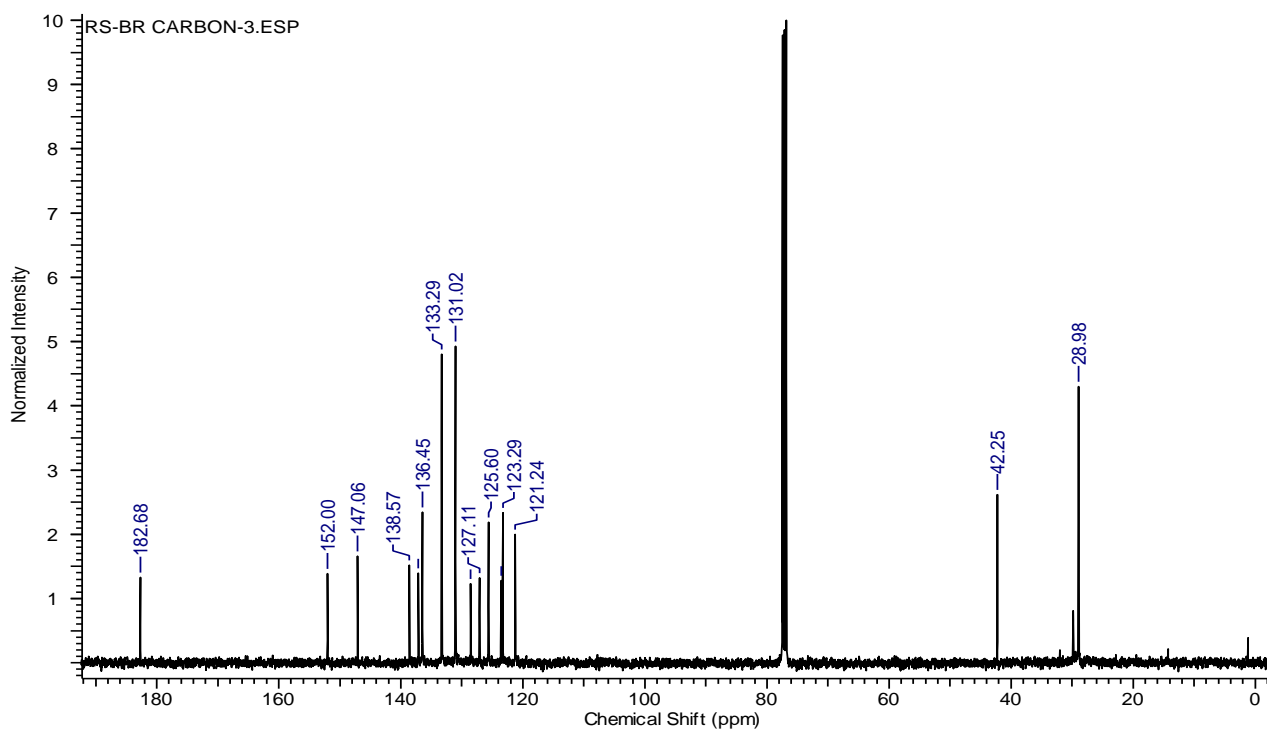


Fig. 4.28 ¹³C-NMR spectra of compound 2

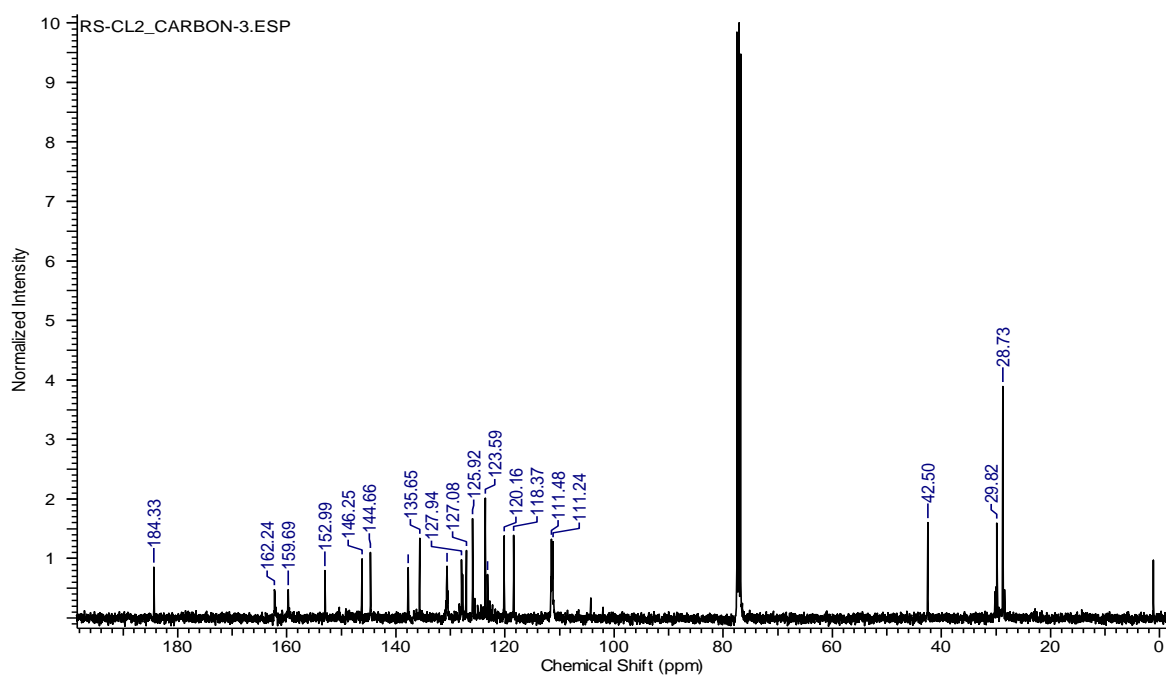


Fig. 4.29 ¹³C-NMR spectra of compound 3

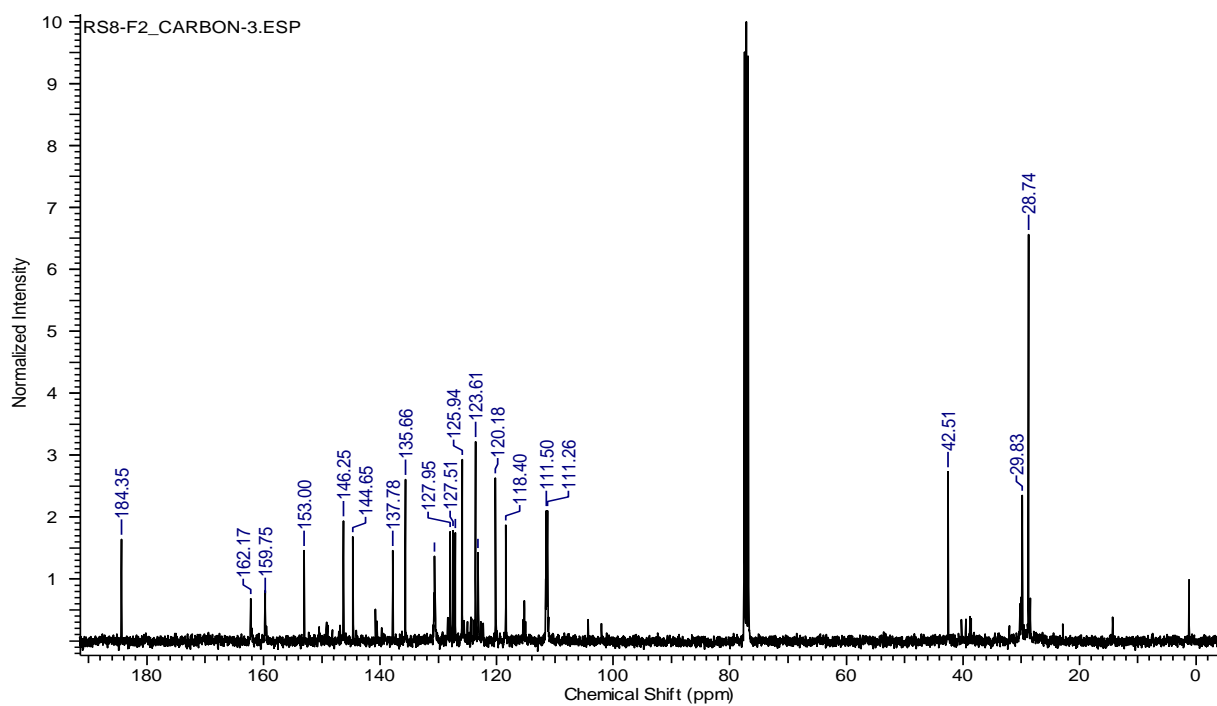


Fig. 4.30 ¹³C-NMR spectra of compound 4

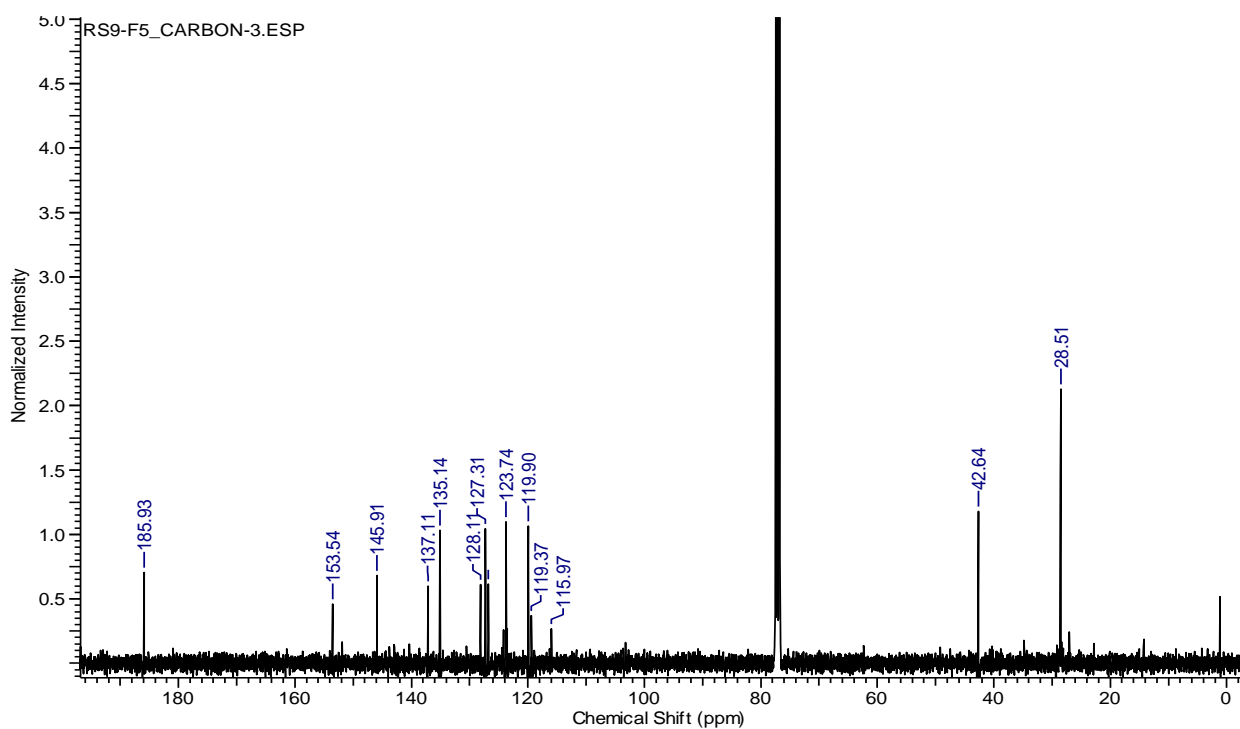


Fig. 4.31 ^{13}C -NMR spectra of compound 5

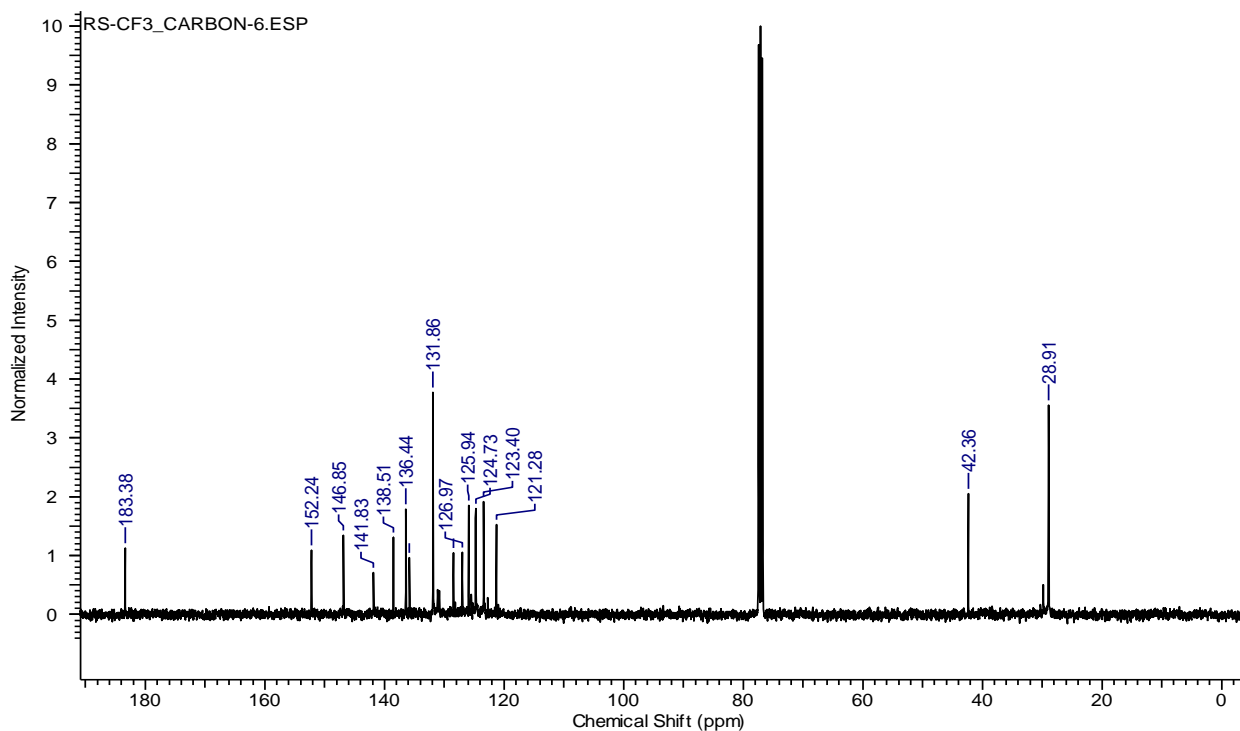


Fig. 4.32 ^{13}C -NMR spectra of compound 6

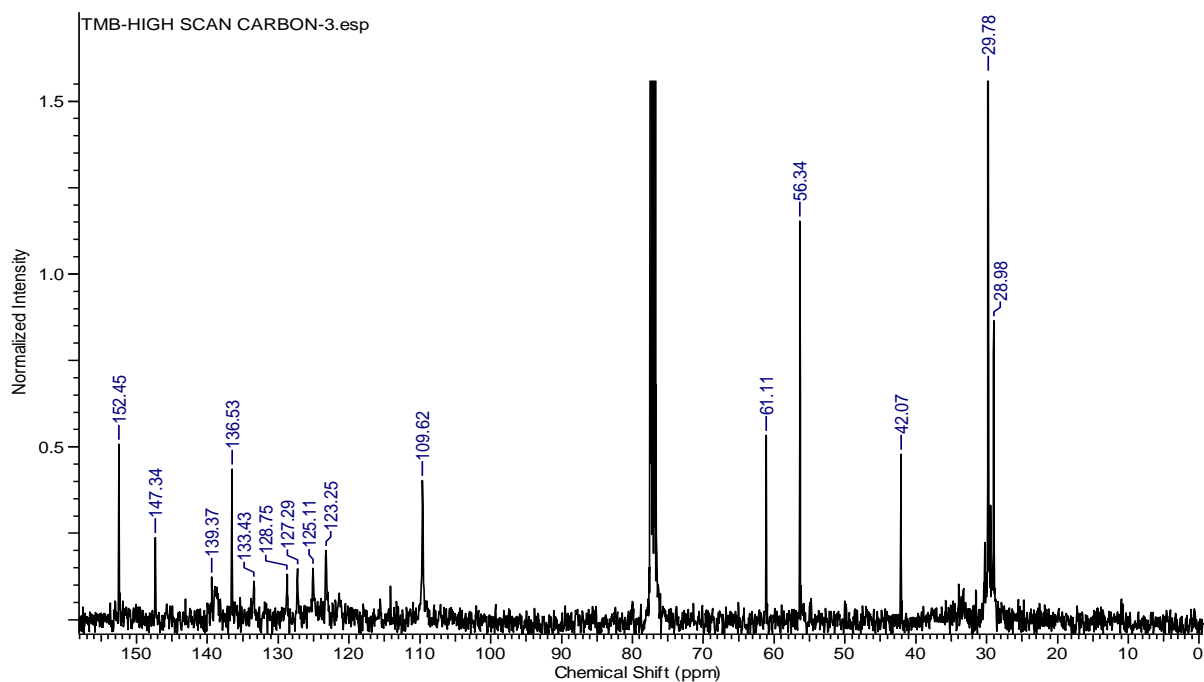


Fig. 4.33 ^{13}C -NMR spectra of compound **8**

4.1.3 FTIR SPECTRAL ANALYSIS

The infra-red spectra shows ν (cm^{-1}) for $-\text{NH}$ in free base in the range of $3200\text{--}3300$ cm^{-1} and were absent in case of their corresponding metal complexes. The sp^3 hybridized $-\text{CH}$ stretching frequencies were also observed in all the complexes in the range of $2800\text{--}3000$ cm^{-1} as expected. The obtained infra-red stretching frequencies are comparable to porphyrins and other porphyrinoid macrocycle [5]. The stretching frequencies of various bonds are tabulated in Table 4.4 and Table 4.5 and shown in Figure 4.34-4.49.

Table 4.4 FTIR data for free base *meta*-BPDM Compounds.

FTIR data table for free base *meta*-BPDM's compounds (values in cm^{-1}):

S. No	Compound Name	N-H Stretch	C-H Stretch (sp ³ -Hyb.)	C=N Stretch	C=C Stretch (Aro)	C-H Bending (sp ³ -Hyb) out of plane	=C-H Bending (Aro) out of plane	C-X Stretch (X may be a heteroatom)
1.	1	3290	2929	1691	1582, 1502	1383	799, 756	717 (X= Cl)
2.	2	3281	2924	---	1586, 1484	1382	798, 735, 703	---
3.	3	3300	2967	1678	1591, 1480	1381	828, 796	709 (X= Cl)
4.	4	3282	2924	1621	1589	1381	783, 753, 706	1000 (X= F)
5.	5	3300	2967	1651	1594, 1494	1384	799, 755, 706	1053 (X= F)
6.	6	3278	2968	1692	1587, 1472	1382	747, 707	1322 (X= F) (sp ³ Hyb.)
7.	7	3337	2926	1745	1601, 1508	1384	797, 739, 711	1252, 1040 (C-O Stretch)
8.	8	3300	2923	1683	1577, 1504	1344	795, 759, 717	1236 (C-O Stretch)

Table 4.5 FTIR data for zinc complexes of *meta*-BPDM Compounds.

FTIR data table for zinc complex of *meta*-BPDM's compounds (values in cm^{-1}):

S.No	Compound Name	C-H Stretch (sp ³ -Hyb.)	C=N Stretch	C=C Stretch (Aro)	C-H Bending (sp ³ -Hyb) out of plane	=C-H Bending (Aro) out of plane	C-X Stretch (X may be a heteroatom)
1.	Zn ²⁺ .1	2975	1672	1545, 1491	1360	964, 804	713 (X=Cl)
2.	Zn ²⁺ .2	2969	1712	1547, 1489	1360	967, 802	465 (X=Br)
3.	Zn ²⁺ .3	2880	1675	1555, 1488	1321	906, 835, 797	718 (X=Cl)
4.	Zn ²⁺ .4	2881	1622	1556, 1496	1362	835, 787, 717	1072 (X=F)
5.	Zn ²⁺ .5	2923	1652	1561, 1495	1362	931, 908, 832	1074 (X=F)
6.	Zn ²⁺ .6	2966	---	1550, 1484	1362	801, 708	1322 (X=F) (sp ³ Hyb.)
7.	Zn ²⁺ .7	2882	1658	1603, 1509	1360	815, 717	1254, 1033 (C-O stretch)
8.	Zn ²⁺ .8	2880	1708	1544, 1501	1341	934, 811, 724	1232 (C-O stretch)

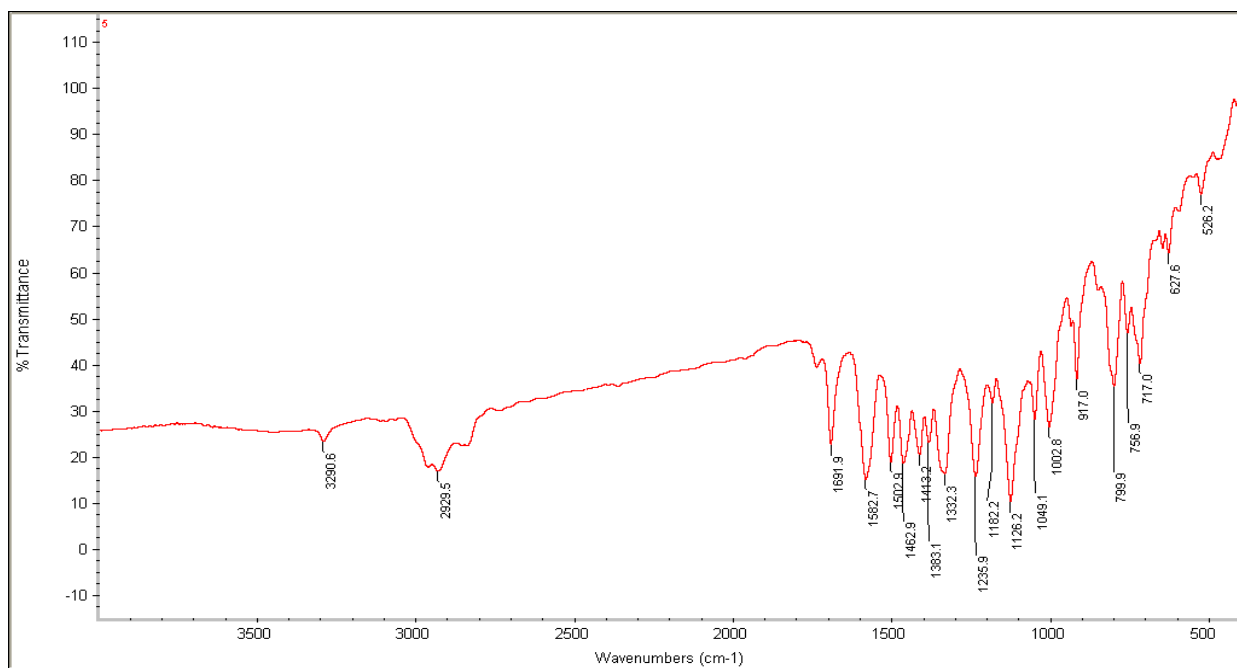


Fig. 4.34 FTIR spectra of compound 1

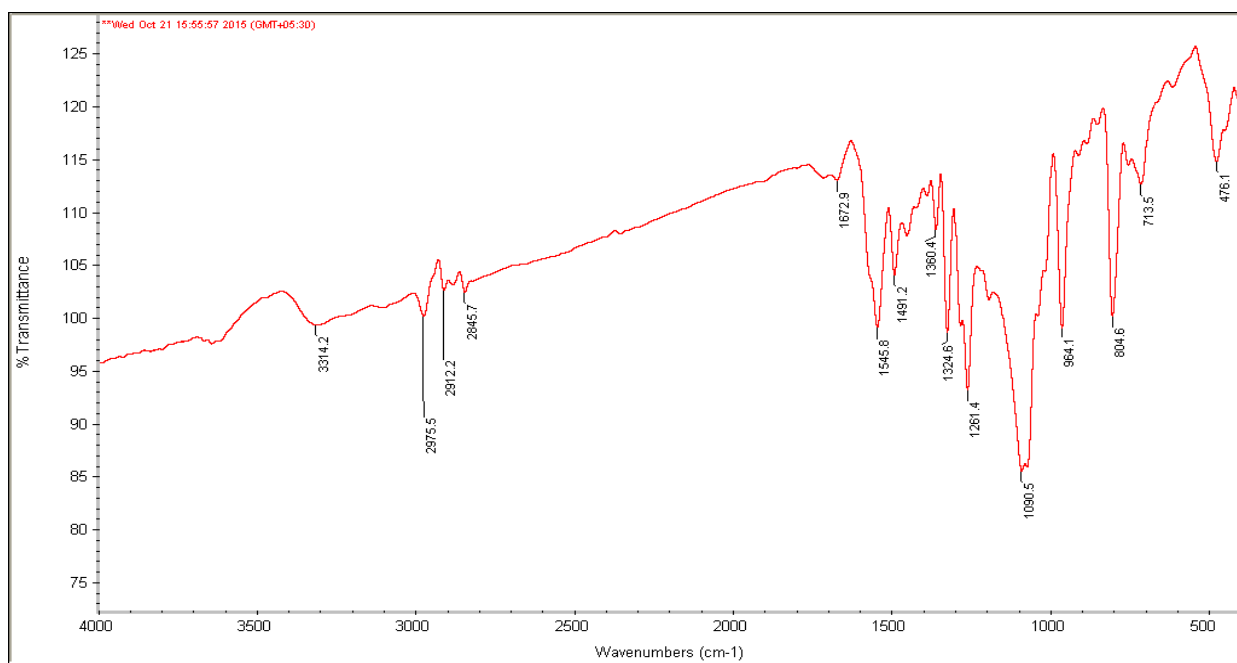


Fig. 4.35 FTIR spectra of Compound Zn²⁺.1

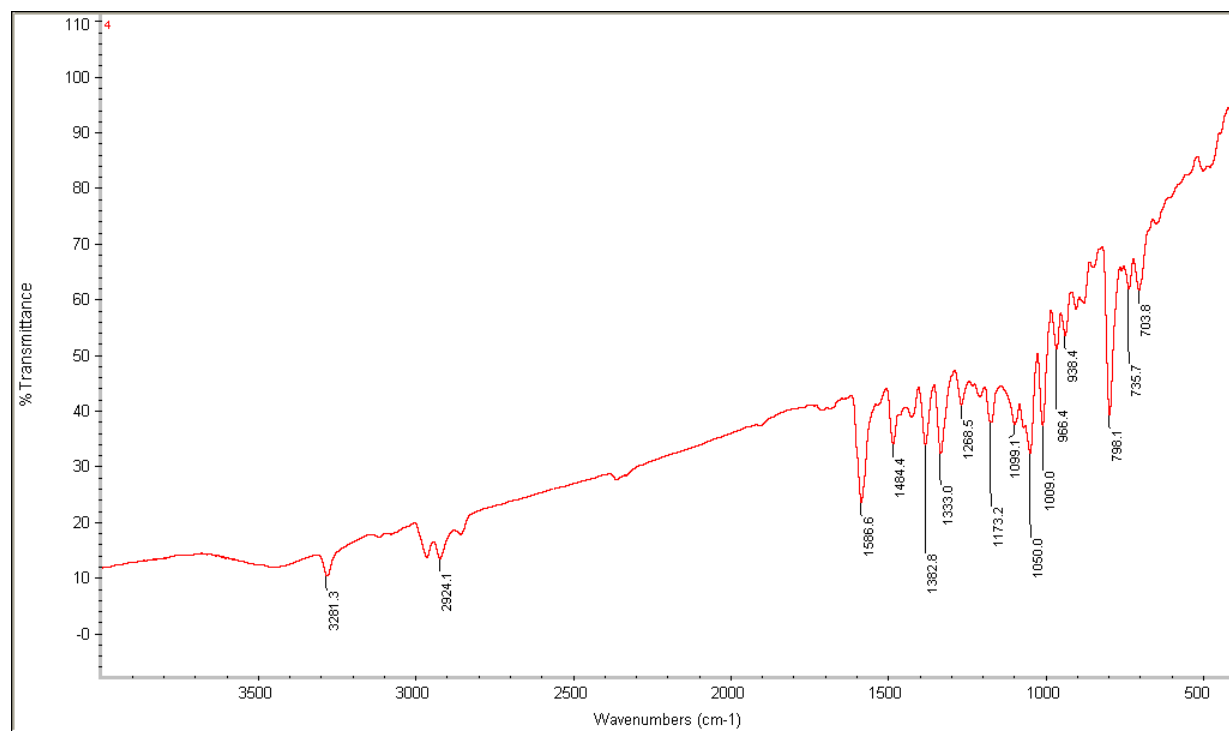


Fig. 4.36 FTIR spectra of Compound 2

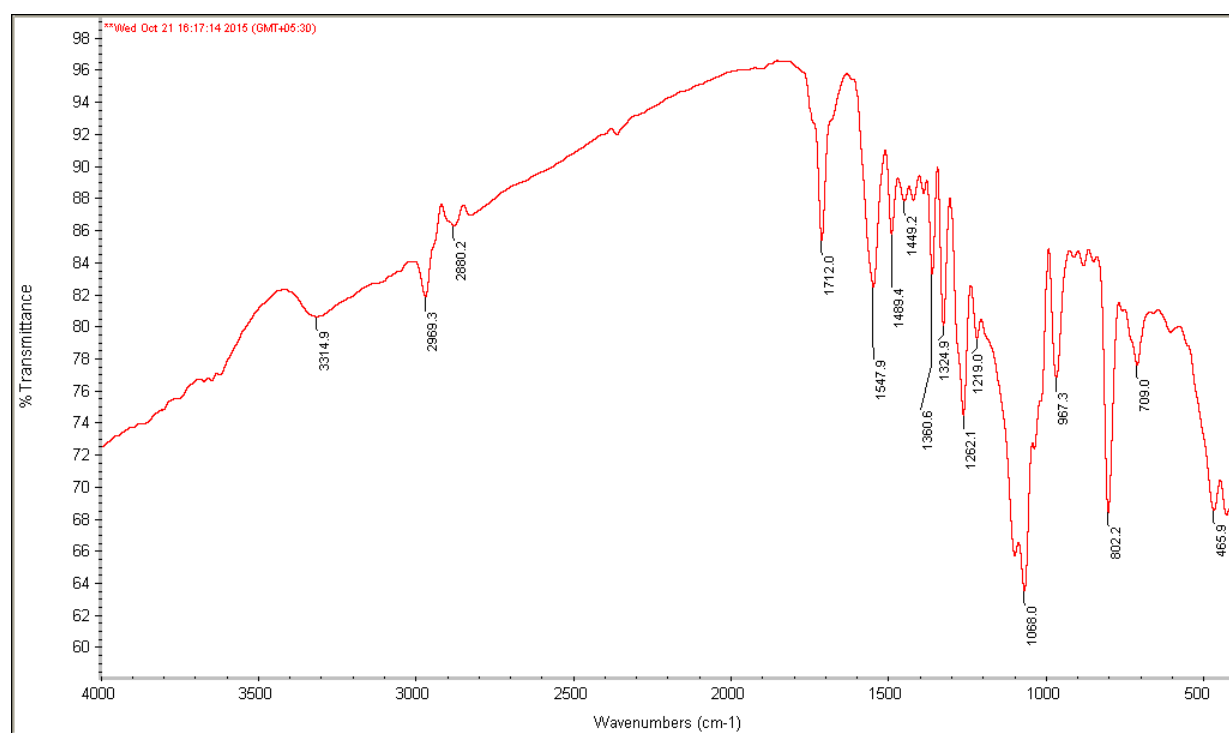


Fig. 4.37 FTIR spectra of Compound $Zn^{2+}.2$

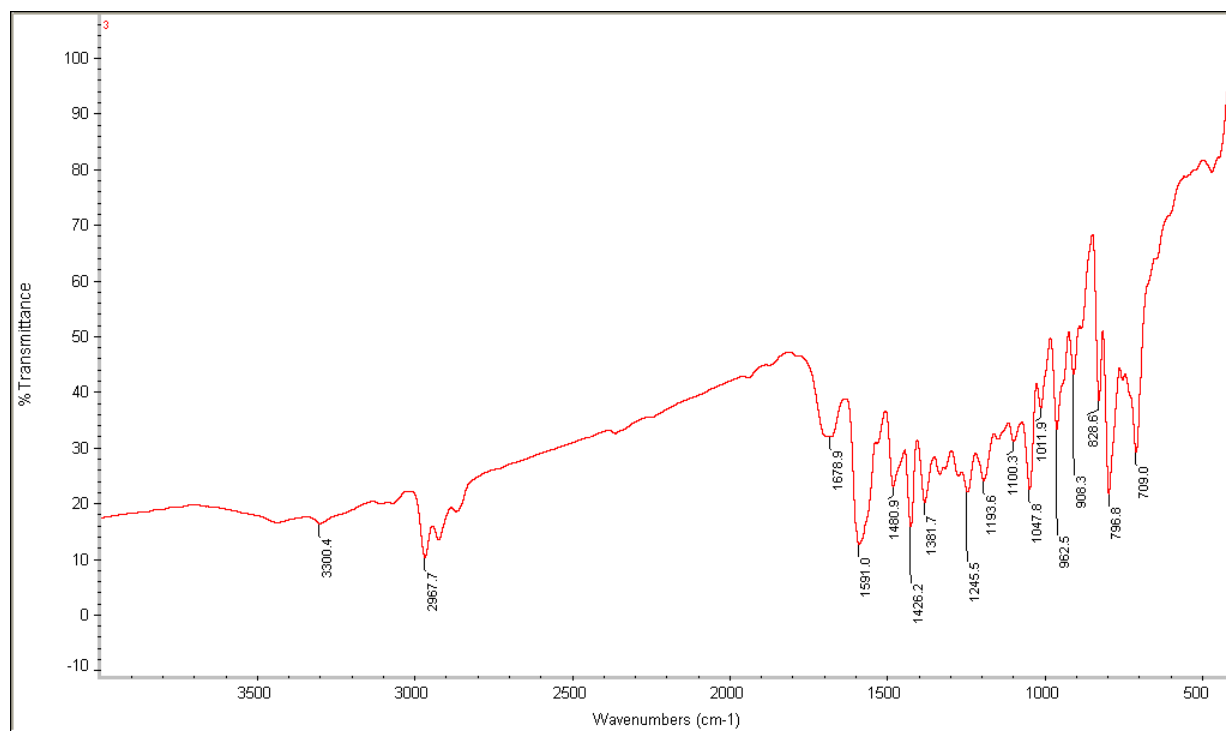


Fig. 4.38 FTIR spectra of Compound 3

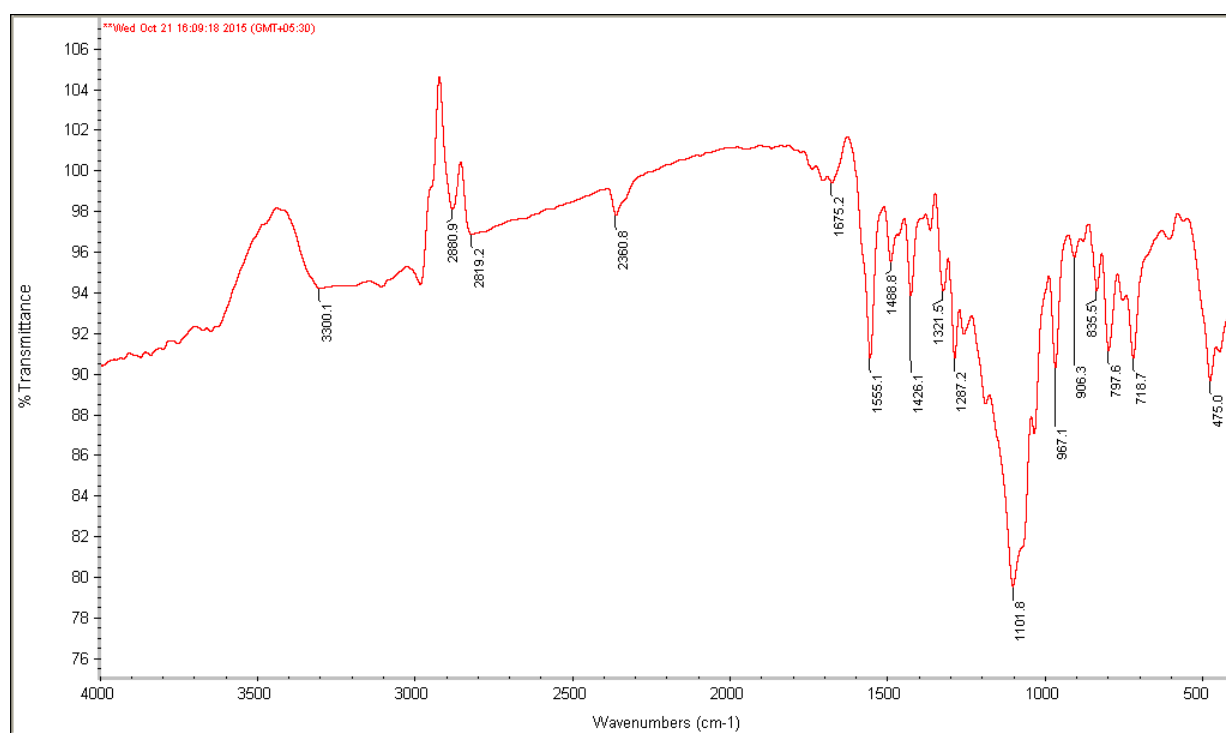


Fig. 4.39 FTIR spectra of Compound Zn²⁺.3

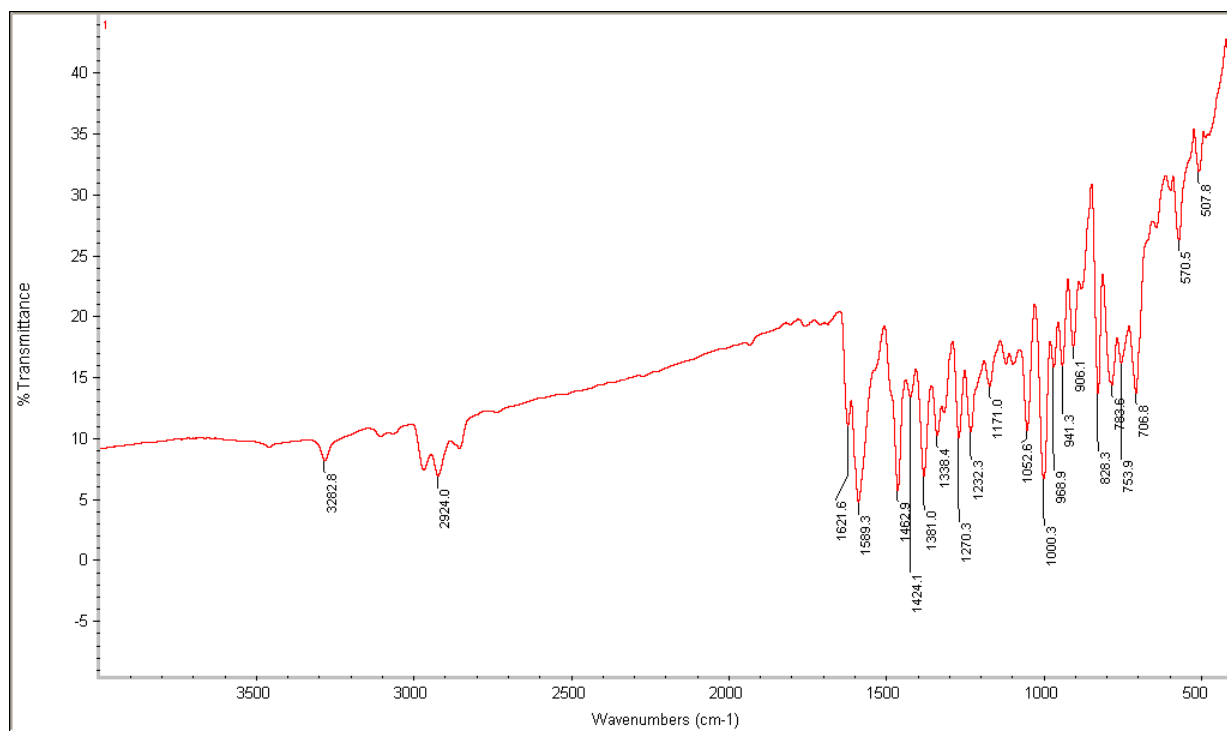


Fig. 4.40 FTIR spectra of Compound 4

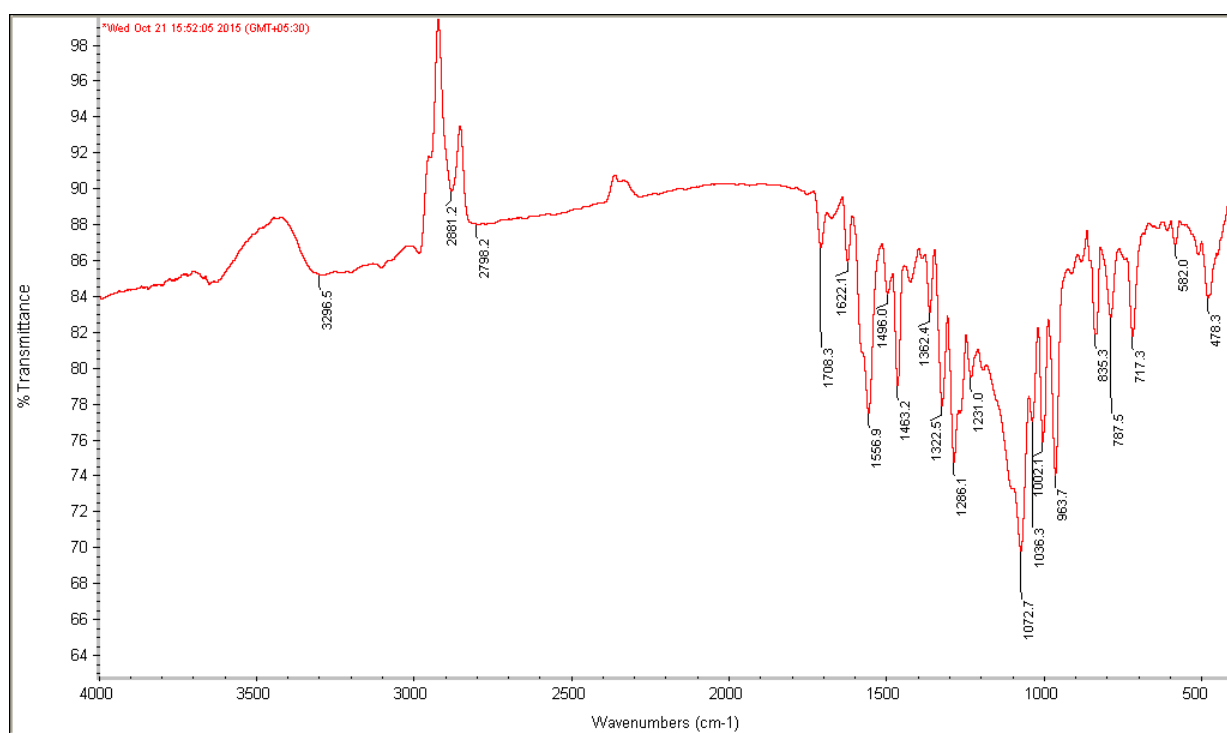


Fig. 4.41 FTIR spectra of Compound $Zn^{2+}.4$

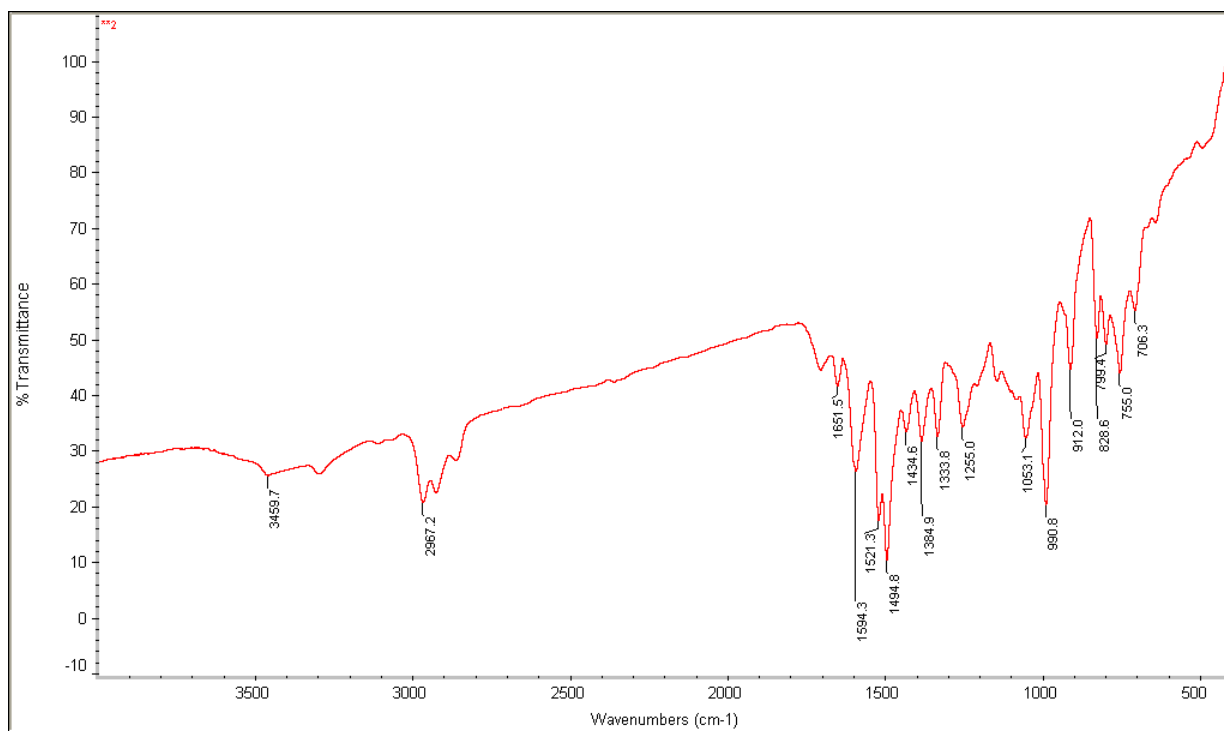


Fig. 4.42 FTIR spectra of Compound 5

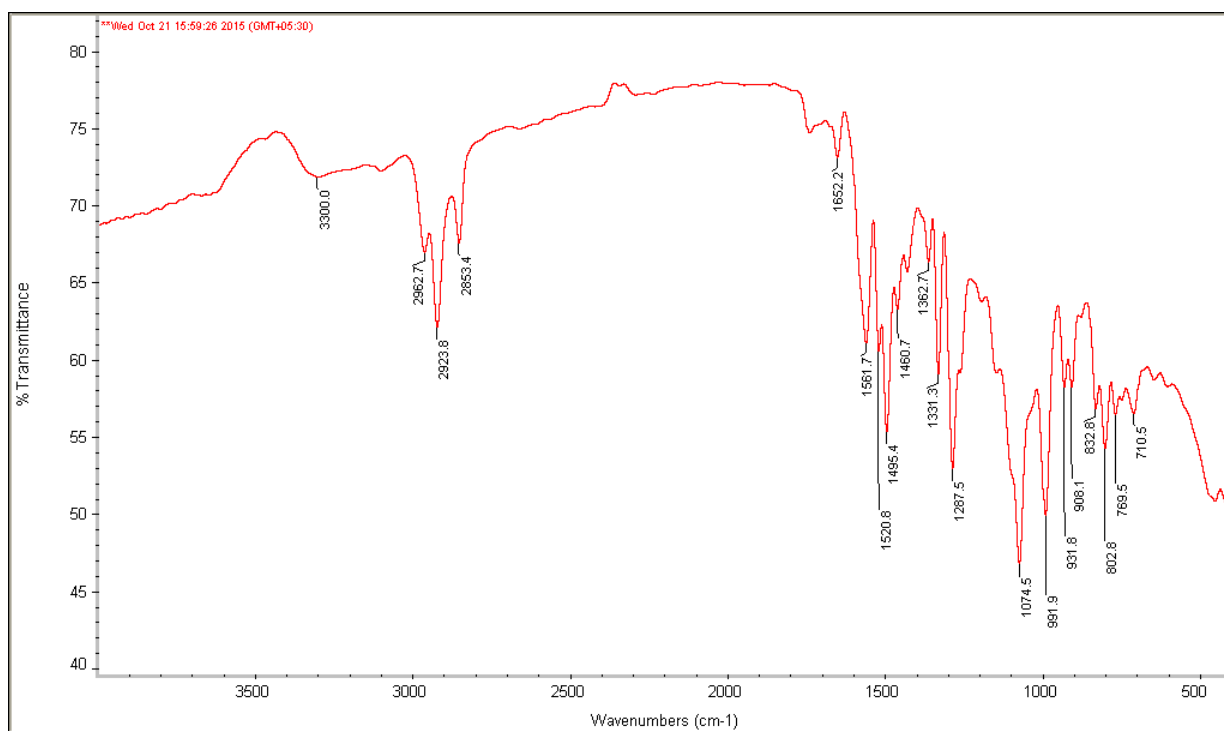


Fig. 4.43 FTIR spectra of Compound Zn²⁺.5

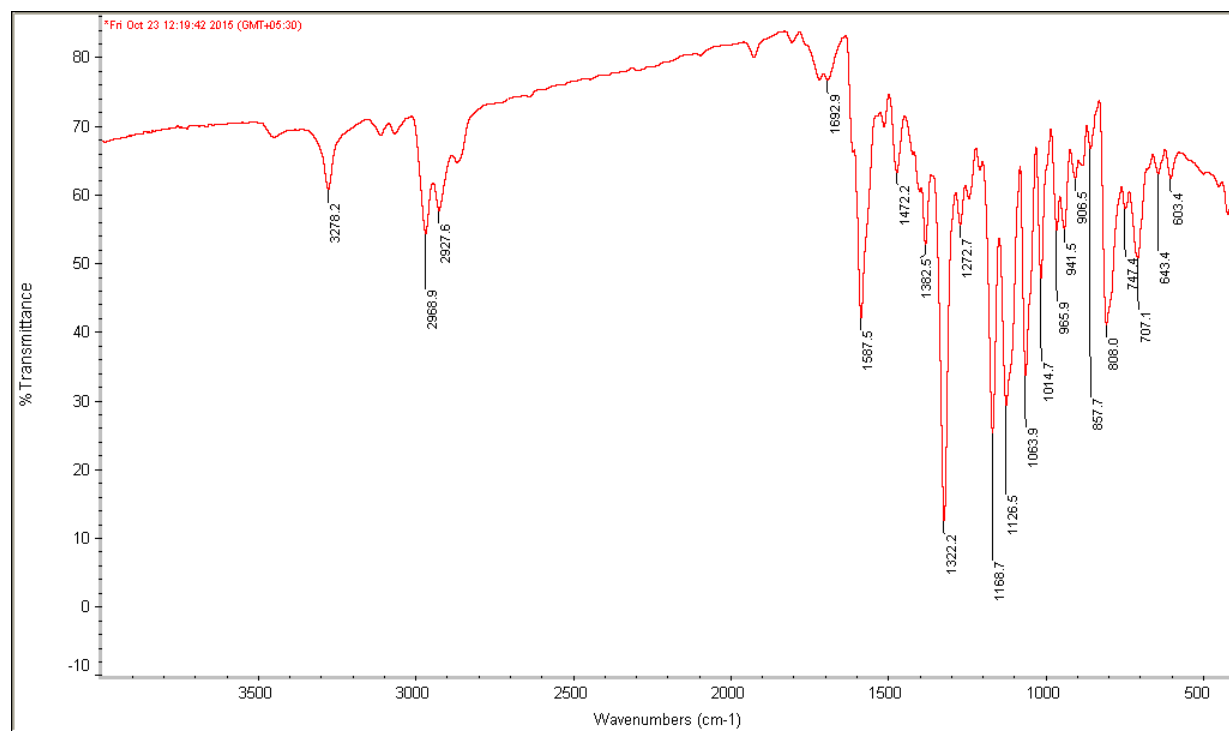


Fig. 4.44 FTIR spectra of Compound 6



Fig. 4.45 FTIR spectra of Compound Zn²⁺.6

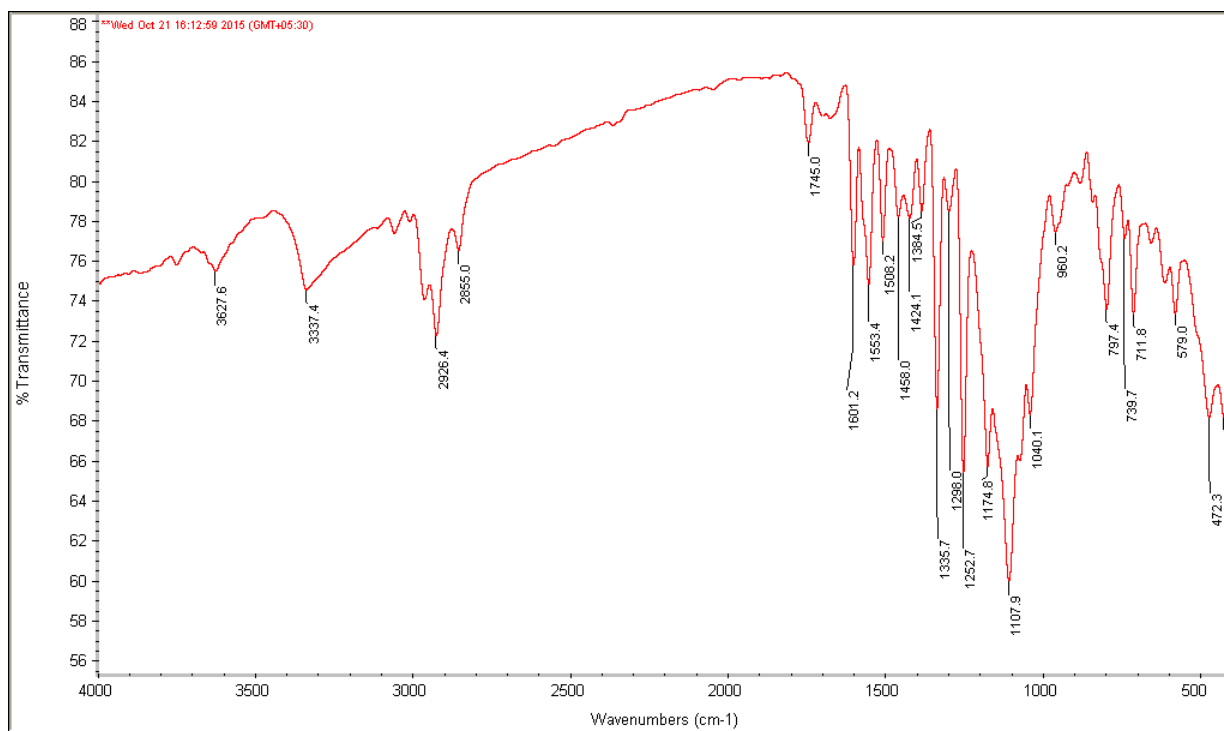


Fig. 4.46 FTIR spectra of Compound 7

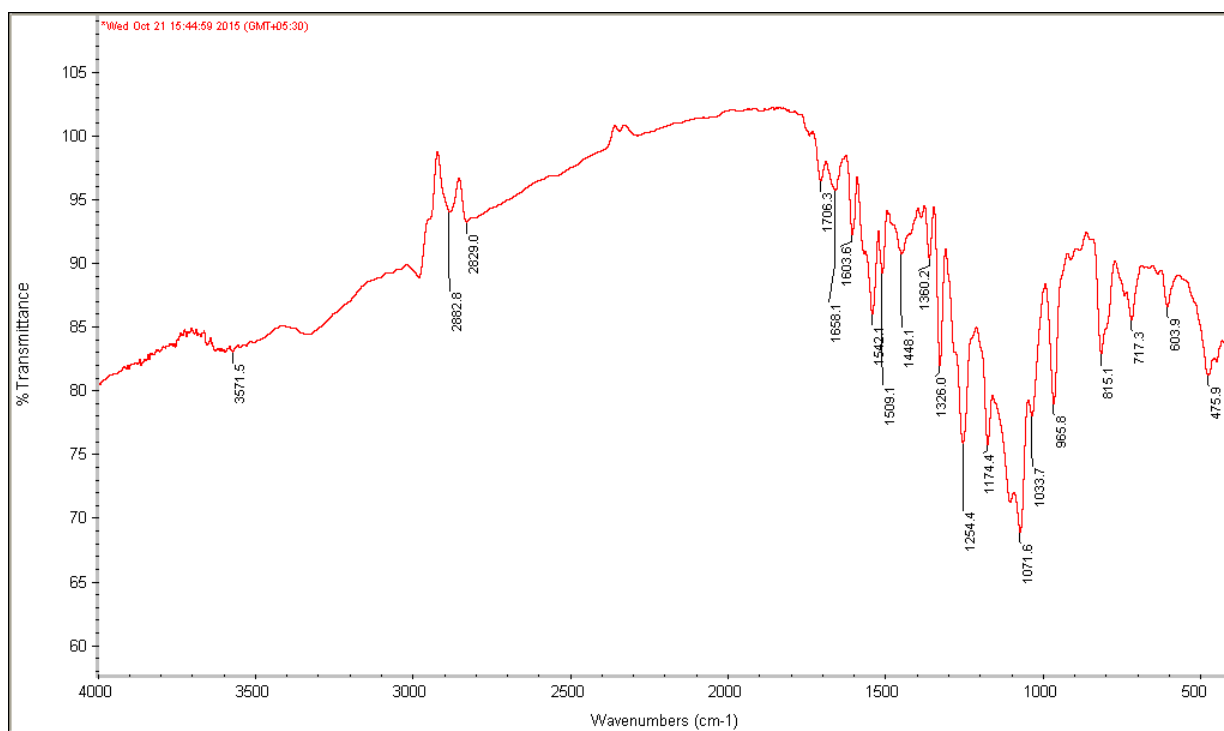


Fig. 4.47 FTIR spectra of Compound Zn²⁺.7

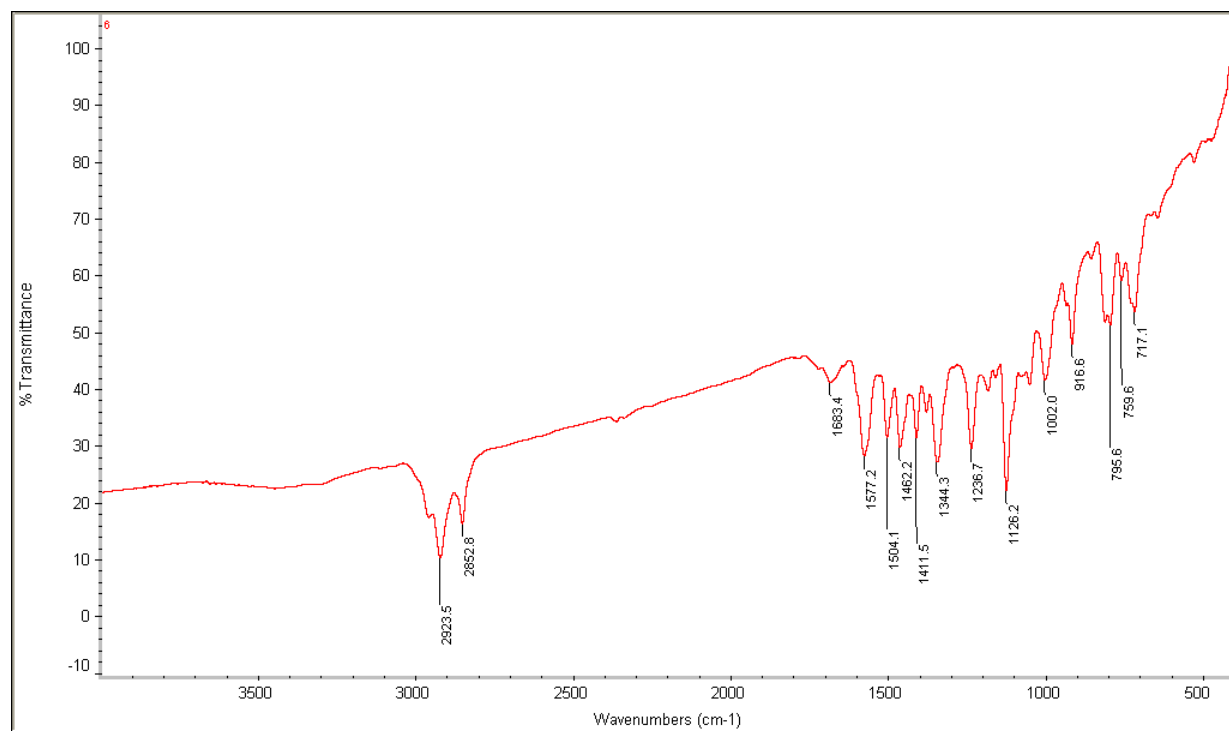


Fig. 4.48 FTIR spectra of Compound 8

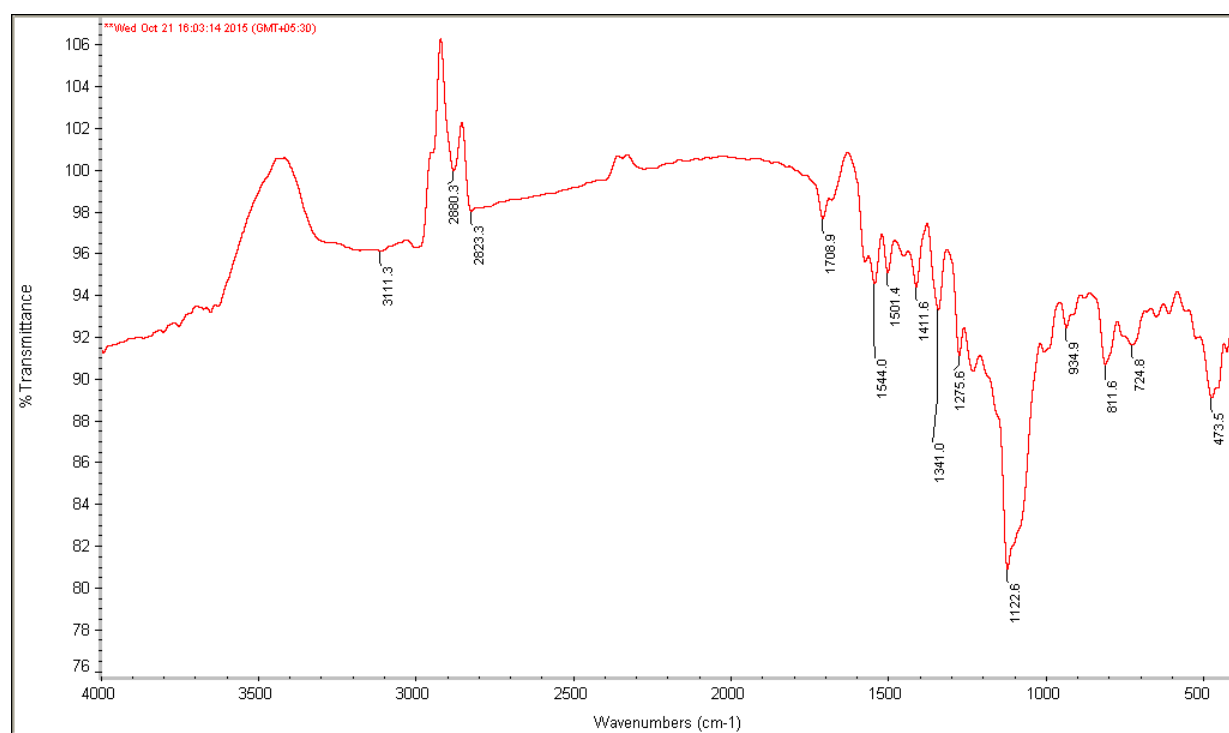


Fig. 4.49 FTIR spectra of Compound Zn²⁺.8

4.1.4 ESI MASS SPECTROSCOPY

The mass of the synthesized compounds and complexes were determined by using ESI mass spectroscopy. The compound, **1-8**, forms 1:1 complex with Zn²⁺ ions [**6**, **7**]. The ESI-Mass spectrum gave a peak of m/z at $[M+1]^+$ for free base and $[M - Cl]^+$ for its corresponding metal complexes. The mass spectrum also confirms the formation of various *meso*-substituted *meta*-benziporphodimethenes and their corresponding metal complexes. Mass spectra of few of the compounds are presented in Fig. 4.50-4.56. The molecular ion peaks of representative compounds are tabulated in Table 4.6.

Table 4.6 ESI-mass value for *meta*-benziporphodimethenes and zinc complex.

Compound	ESI mass (m/z)
1	600.0937
2	690.0589
3	670.0478
4	604.1306
5	712.1006
6	668.1482
Zn ²⁺ . 4	666.0491

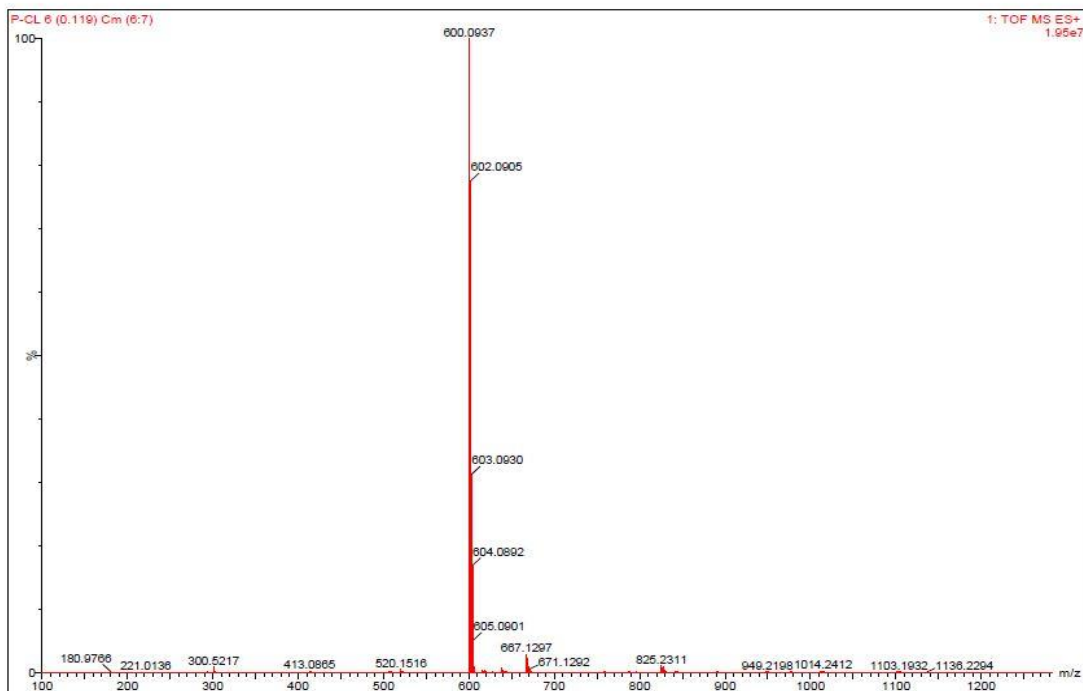


Fig. 4.50 ESI mass spectra of compound 1

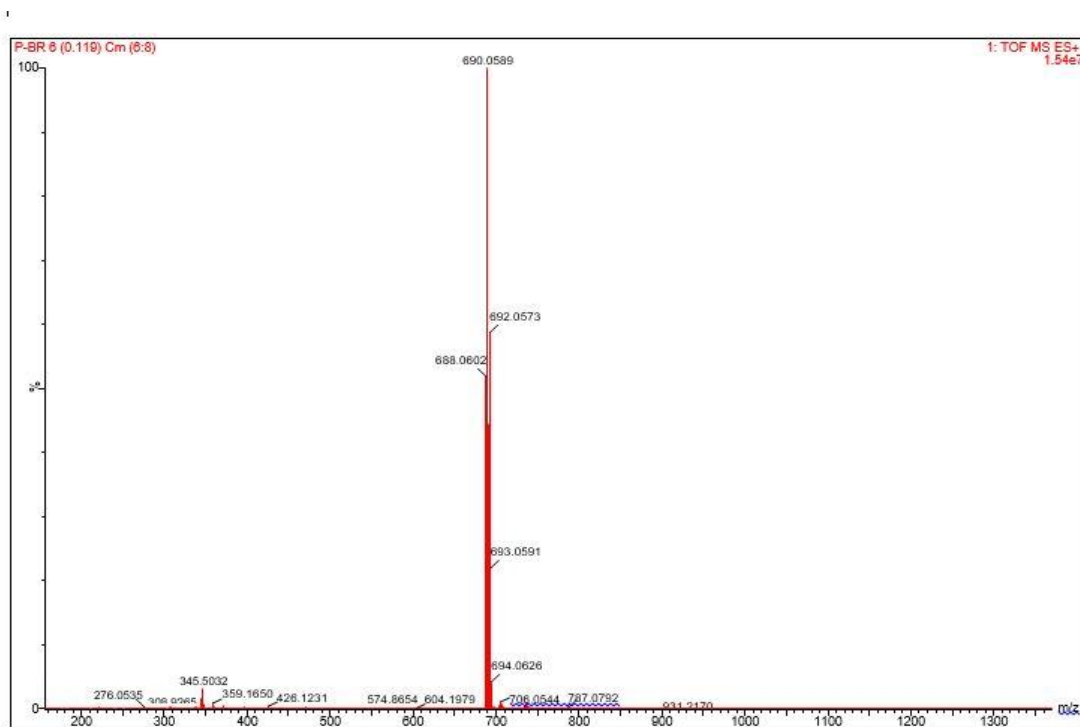


Fig. 4.51 ESI mass spectra of compound 2

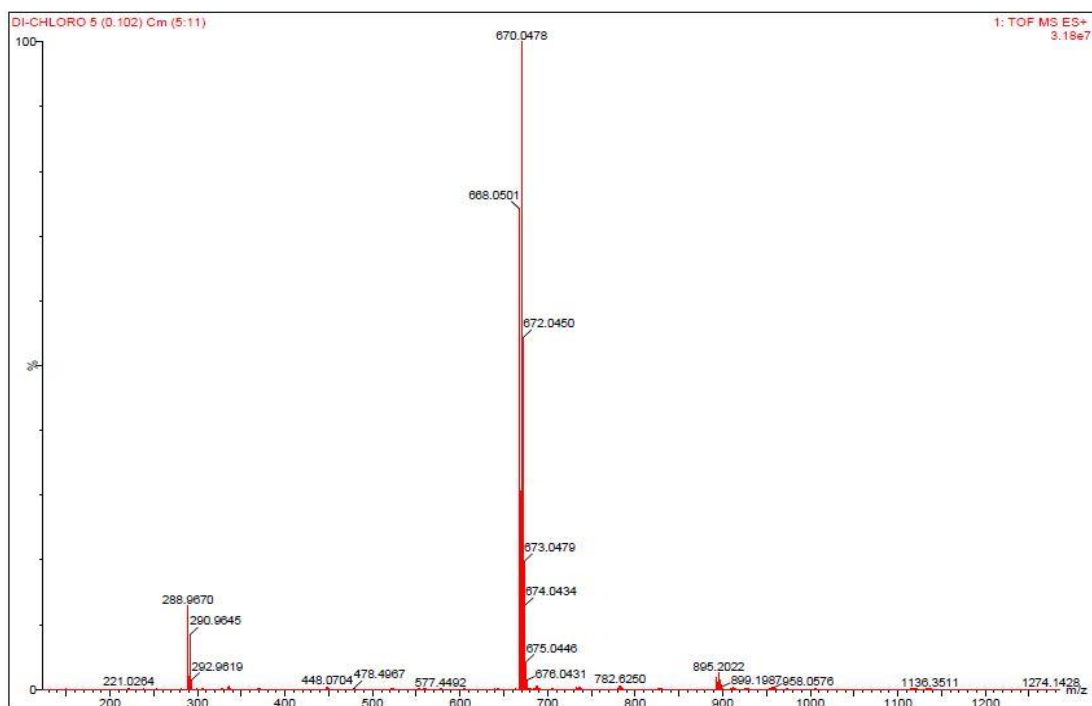


Fig. 4.52 ESI mass spectra of compound 3

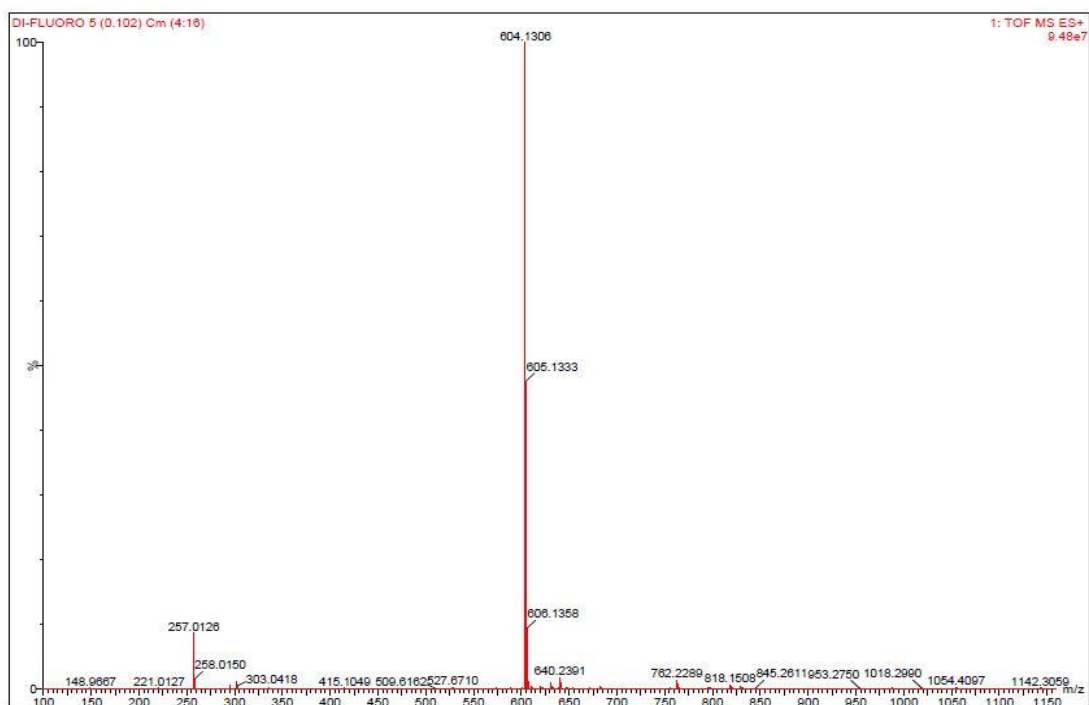


Fig. 4.53 ESI mass spectra of compound 4

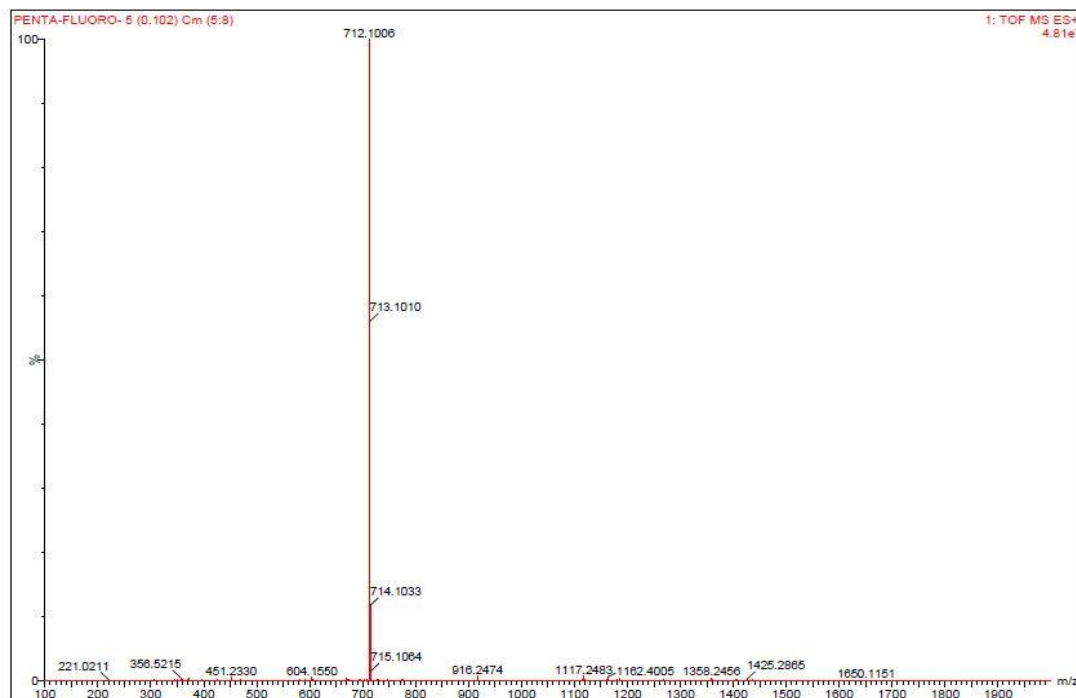


Fig. 4.54 ESI mass spectra of compound 5

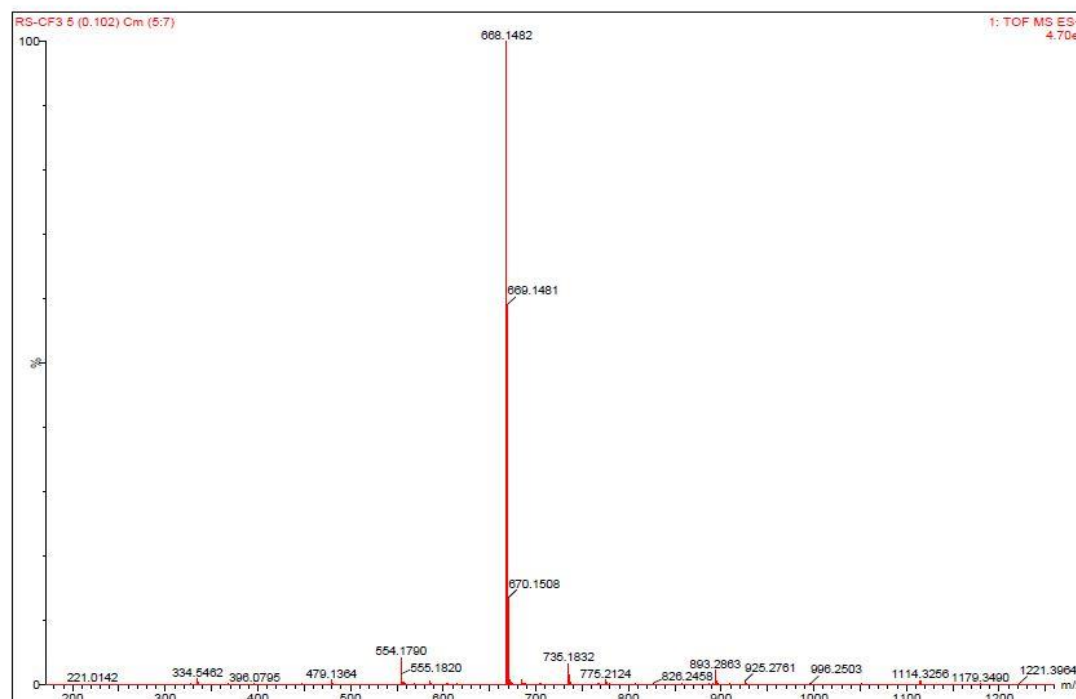


Fig. 4.55 ESI mass spectra of compound 6

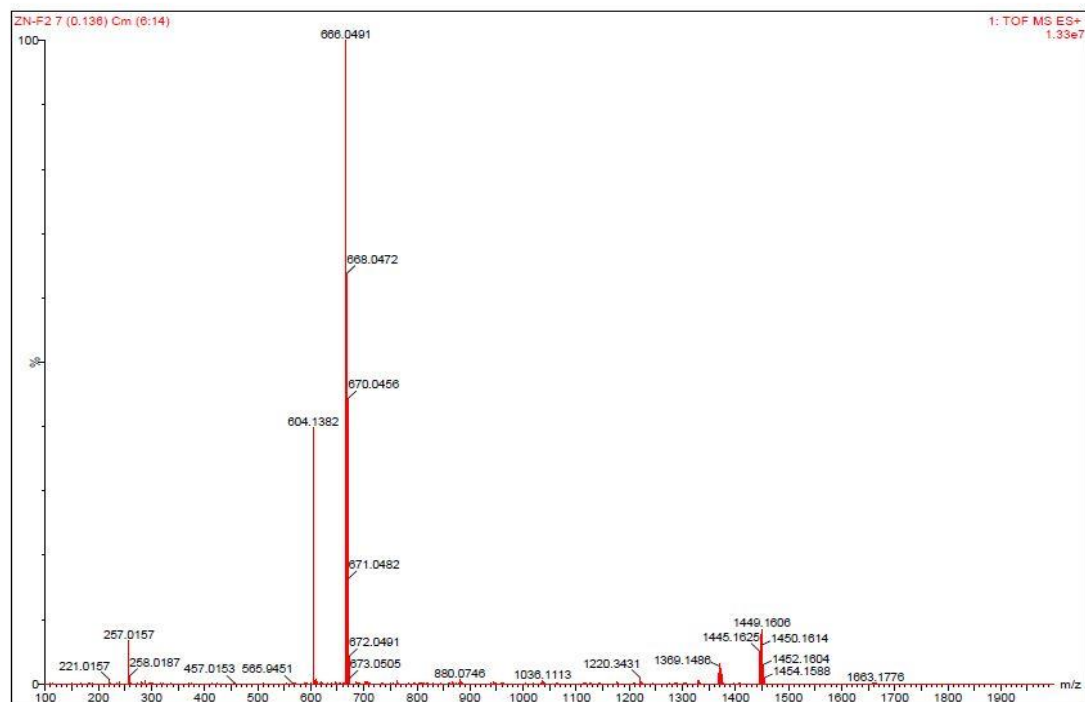


Fig. 4.56 ESI mass spectra of complex Zn²⁺.4

4.2 SINGLE CRYSTAL XRD ANALYSIS

Suitable diffraction quality single crystals were obtained from the crystallization procedures by layering n-hexane on ethyl acetate or by diffusion method using ethyl acetate and n-hexane. Intensity data were collected at 273(2) K on Bruker diffractometer (a single wavelength Enhance X-ray source with MoK_α radiation, ($\lambda = 0.71073 \text{ \AA}$) [8a]. The selected suitable single crystals were mounted using paratone oil on the top of a glass fiber fixed on a goniometer head and immediately transferred to the diffractometer. Pre-experiment, data collection, data reduction and analytical absorption corrections [8b] were performed with the Bruker SAINT program. The crystal structures were solved with SHELXL-97 [8c] using direct methods. The structure refinements were performed by full-matrix least-squares on F^2 with SHELXL-97. All programs used during the crystal structure determination process are included in the WINGX software [8d].

4.2.1 11, 16-Bis(3, 4, 5-trimethoxy-phenyl)-6, 6, 21, 21-tetramethyl-*meta*-benziporphodimethene (8)

The diffraction quality single crystals of 11,16-Bis(3,4,5-trimethoxy-phenyl)-6,6,21,21-tetramethyl-*meta*-benziporphodimethene were grown by direct solvent diffusion of n-hexane in a saturated solution of compound (8) in ethyl acetate in a long cylindrical tube standing on several days at room temperature. The chemical formula and ring labelling system is shown in Fig. 4.57. Crystal data for compound 8: $C_{44}H_{45}N_3O_6$, Mw, 711.84; system, monoclinic; space group, P-1; unit cell dimensions, $a = 8.7020(4)\text{\AA}$; $b = 14.8084(6)\text{\AA}$; $c = 15.7963(7)\text{\AA}$; $\alpha = 76.9060(10)^\circ$; $\beta = 88.9270(10)^\circ$; $\gamma = 76.9610(10)^\circ$; $V = 1951.82(15)\text{\AA}^3$; $Z = 2$; $T = 298\text{ K}$; R_{int} , 0.0746; $R_{(all)}$, 0.1046; $Gof = 0.958$; $\Delta\rho_{max} = 1.418\text{ e \AA}^{-3}$; $\Delta\rho_{min} = -1.905\text{ e \AA}^{-3}$. The resolution obtained for the structure of the compounds was limited by the poor quality of the available crystals. The solvent molecule was badly disordered and could not be modelled. All hydrogen atoms were calculated after each cycle of refinement using a riding model, with $C-H = 0.93\text{ \AA} + U_{iso}(H) = 1.2U_{eq}(C)$ for aromatic H atoms, with $C-H = 0.97\text{ \AA} + U_{iso}(H) = 1.2U_{eq}(C)$ for methylene H atoms.

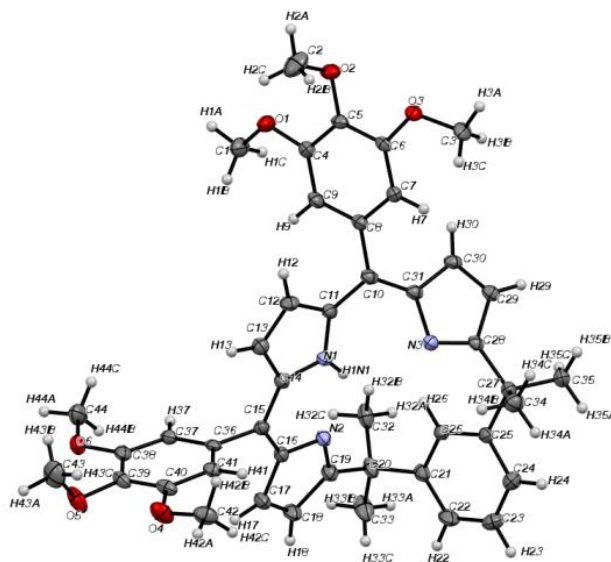


Fig. 4.57 X-ray structure of free base *meta*-benziporphodimethene, 8.

Crystal structure of free base *meta*-benziporphodimethene, 8, was determined by single crystal X-ray diffraction analyses. The geometry of 8 was found lesser distorted than

earlier reported structures of *meta*-benziporphodimethenes [6b, 9]. The average deviation of atoms which constitute the macrocycle was measured to be 0.646 Å which is sufficiently lesser as compared to 1.044 Å for free base *meta*-benziporphodimethenes earlier reported by Hung and co-workers [6b, 9]. The angle between the phenylene ring plane and three pyrrolic nitrogens of macrocycle is 46.63° which is remarkably lesser. Important and interesting observation in the crystal structure is that the angle between the plane formed by 17 tripyrrin atoms and the vector along the two sp^3 meso carbons is only 15.45°. These observation confirms that obtained structure of compound 8 is lesser puckered than the earlier reported structures of *meta*-benziporphodimethenes [6, 9]. These finding may be attributed to substituents on the sp^3 meso carbons of free base *meta*-benziporphodimethenes. The anisotropic parameters for all atoms are listed in Table 4.7. The bond lengths and bond angles are summarized in Table 4.8. A crystallographic data are tabulated in the Table 4.9.

Table 4.7 Atomic co-ordinates and equivalent isotropic displacements parameters for Compound 8. $U(eq)$ is defined as one third of the trace of the orthogonalized U^{ij} tensor.

Atomic parameters				
Atom	x/a	y/b	z/c	U [Å ²]
C1	0.3599(7)	0.6931(5)	0.6709(4)	
H1A	0.4555	0.7176	0.6625	0.049
H1B	0.3818	0.6261	0.6768	0.049
H1C	0.3112	0.7071	0.7225	0.049
C2	0.1118(9)	0.8234(6)	0.4084(4)	
H2A	0.1316	0.8809	0.3712	0.064
H2B	0.0465	0.7946	0.378	0.064
H2C	0.2089	0.7813	0.4249	0.064
C3	-0.4113(7)	0.7947(4)	0.4890(4)	
H3A	-0.4709	0.8414	0.4438	0.044
H3B	-0.4496	0.8031	0.5446	0.044
H3C	-0.4213	0.7331	0.4826	0.044
C4	0.1157(6)	0.7066(4)	0.6003(4)	
C5	0.0023(7)	0.7639(4)	0.5418(4)	
C6	-0.1488(6)	0.7433(4)	0.5429(3)	
C7	-0.1844(6)	0.6647(4)	0.6003(3)	
H7	-0.2851	0.6515	0.6018	0.021
C8	-0.0672(6)	0.6053(4)	0.6563(3)	
C9	0.0818(7)	0.6262(4)	0.6562(4)	
H9	0.1589	0.5864	0.6935	0.028

C10	-0.1041(6)	0.5181(4)	0.7145(4)	
C11	-0.0030(6)	0.4311(4)	0.7092(4)	
C12	0.0958(7)	0.4122(4)	0.6422(4)	
H12	0.1078	0.4541	0.5899	0.027
C13	0.1730(7)	0.3194(4)	0.6676(4)	
H13	0.2446	0.2879	0.6351	0.027
C14	0.1238(6)	0.2821(4)	0.7508(3)	
C15	0.1857(6)	0.1949(4)	0.8095(4)	
C16	0.1493(6)	0.1725(4)	0.8957(4)	
C17	0.2095(7)	0.0871(4)	0.9587(4)	
H17	0.2792	0.0355	0.9488	0.031
C18	0.1444(7)	0.0972(4)	1.0348(4)	
H18	0.1611	0.0539	1.0879	0.033
C19	0.0436(7)	0.1881(4)	1.0179(4)	
C20	-0.0517(7)	0.2323(4)	1.0845(4)	
C21	-0.2243(7)	0.2427(4)	1.0606(4)	
C22	-0.3157(8)	0.1791(4)	1.1018(4)	
H22	-0.274	0.13	1.1477	0.04
C23	-0.4699(8)	0.1886(5)	1.0748(4)	
H23	-0.5302	0.1451	1.1028	0.043
C24	-0.5349(7)	0.2607(4)	1.0078(4)	
H24	-0.6381	0.2654	0.9904	0.033
C25	-0.4466(6)	0.3269(4)	0.9659(4)	
C26	-0.2925(6)	0.3157(4)	0.9924(4)	
H26	-0.2317	0.3586	0.9637	0.024
C27	-0.5234(6)	0.4094(4)	0.8928(4)	
C28	-0.4114(6)	0.4738(4)	0.8516(3)	
C29	-0.4323(7)	0.5757(4)	0.8428(3)	
H29	-0.5084	0.6126	0.8683	0.024
C30	-0.3197(6)	0.6051(4)	0.7904(3)	
H30	-0.3034	0.6668	0.7715	0.024
C31	-0.2282(6)	0.5222(4)	0.7689(4)	
C32	-0.0032(7)	0.3289(4)	1.0823(4)	
H32A	-0.0626	0.3582	1.1238	0.044
H32B	-0.0231	0.3688	1.0252	0.044
H32C	0.106	0.3195	1.0967	0.044
C33	-0.0111(8)	0.1705(5)	1.1765(4)	
H33A	-0.0713	0.1987	1.2183	0.06
H33B	0.0981	0.1654	1.1888	0.06
H33C	-0.0348	0.1089	1.1795	0.06
C34	-0.5832(7)	0.3712(4)	0.8201(4)	
H34A	-0.655	0.33	0.8433	0.042

H34B	-0.4968	0.3371	0.7952	0.042
H34C	-0.6353	0.4227	0.776	0.042
C35	-0.6655(7)	0.4660(4)	0.9287(4)	
H35A	-0.7352	0.4245	0.9547	0.039
H35B	-0.719	0.5138	0.8821	0.039
H35C	-0.6307	0.495	0.9717	0.039
C36	0.3101(6)	0.1293(4)	0.7764(3)	
C37	0.4638(6)	0.1282(4)	0.7987(3)	
H37	0.487	0.1676	0.8331	0.023
C38	0.5834(7)	0.0681(4)	0.7694(4)	
C39	0.5480(7)	0.0063(4)	0.7216(4)	
C40	0.3924(7)	0.0085(4)	0.6982(4)	
C41	0.2745(7)	0.0714(4)	0.7250(3)	
H41	0.1714	0.0745	0.7083	0.023
C42	0.2148(8)	- 0.0432(4)	0.6151(4)	
H42A	0.2125	-0.0898	0.5818	0.048
H42B	0.1849	0.0184	0.5783	0.048
H42C	0.1433	-0.052	0.6621	0.048
C43	0.7103(9)	- 0.0403(5)	0.6118(5)	
H43A	0.7934	-0.0891	0.6032	0.065
H43B	0.745	0.0193	0.5972	0.065
H43C	0.6224	-0.0385	0.5753	0.065
C44	0.7766(7)	0.1326(5)	0.8295(5)	
H44A	0.8878	0.1238	0.8371	0.056
H44B	0.7286	0.1245	0.8853	0.056
H44C	0.7391	0.195	0.7958	0.056
N1	0.0143(5)	0.3513(3)	0.7731(3)	
N2	0.0462(5)	0.2331(3)	0.9364(3)	
N3	-0.2896(5)	0.4429(3)	0.8102(3)	
O1	0.2570(5)	0.7355(3)	0.5974(3)	
O2	0.0347(5)	0.8434(3)	0.4848(3)	
O3	-0.2512(4)	0.8046(3)	0.4831(2)	
O4	0.3697(5)	- 0.0526(3)	0.6494(3)	
O5	0.6661(5)	- 0.0590(3)	0.6999(3)	
O6	0.7384(4)	0.0652(3)	0.7853(3)	
H1N1	-0.029(9)	0.343(5)	0.826(5)	0.05(2)

Table 4.8 Bond distance (Å) and bond angles (deg) for compound **8**.

Selected geometric information			
Atoms 1,2	d 1,2 [Å]	Atoms 1,2	d 1,2 [Å]
C1—O1	1.433(7)	C23—H23	0.93
C1—H1A	0.96	C24—C25	1.392(8)
C1—H1B	0.96	C24—H24	0.93
C1—H1C	0.96	C25—C26	1.384(8)
C2—O2	1.434(8)	C25—C27	1.542(8)
C2—H2A	0.96	C26—H26	0.93
C2—H2B	0.96	C27—C28	1.518(8)
C2—H2C	0.96	C27—C34	1.526(8)
C3—O3	1.426(7)	C27—C35	1.543(8)
C3—H3A	0.96	C28—N3	1.304(7)
C3—H3B	0.96	C28—C29	1.462(8)
C3—H3C	0.96	C29—C30	1.337(8)
C4—O1	1.367(7)	C29—H29	0.93
C4—C9	1.386(8)	C30—C31	1.446(8)
C4—C5	1.392(8)	C30—H30	0.93
C5—O2	1.378(7)	C31—N3	1.396(7)
C5—C6	1.400(8)	C32—H32A	0.96
C6—O3	1.368(6)	C32—H32B	0.96
C6—C7	1.381(8)	C32—H32C	0.96
C7—C8	1.402(7)	C33—H33A	0.96
C7—H7	0.93	C33—H33B	0.96
C8—C9	1.384(8)	C33—H33C	0.96
C8—C10	1.486(8)	C34—H34A	0.96
C9—H9	0.93	C34—H34B	0.96
C10—C31	1.370(8)	C34—H34C	0.96
C10—C11	1.447(7)	C35—H35A	0.96
C11—N1	1.358(7)	C35—H35B	0.96
C11—C12	1.398(8)	C35—H35C	0.96
C12—C13	1.392(8)	C36—C41	1.382(8)
C12—H12	0.93	C36—C37	1.386(8)
C13—C14	1.396(8)	C37—C38	1.391(8)
C13—H13	0.93	C37—H37	0.93
C14—N1	1.375(7)	C38—O6	1.368(7)
C14—C15	1.432(8)	C38—C39	1.386(8)
C15—C16	1.371(8)	C39—O5	1.378(7)
C15—C36	1.494(7)	C39—C40	1.403(9)
C16—N2	1.408(7)	C40—O4	1.356(7)

C16—C17	1.444(8)	C40—C41	1.389(8)
C17—C18	1.346(8)	C41—H41	0.93
C17—H17	0.93	C42—O4	1.435(8)
C18—C19	1.445(8)	C42—H42A	0.96
C18—H18	0.93	C42—H42B	0.96
C19—N2	1.311(7)	C42—H42C	0.96
C19—C20	1.521(8)	C43—O5	1.416(8)
C20—C21	1.528(8)	C43—H43A	0.96
C20—C33	1.542(8)	C43—H43B	0.96
C20—C32	1.554(9)	C43—H43C	0.96
C21—C22	1.381(9)	C44—O6	1.427(8)
C21—C26	1.398(8)	C44—H44A	0.96
C22—C23	1.39(1)	C44—H44B	0.96
C22—H22	0.93	C44—H44C	0.96
C23—C24	1.371(9)	N1—H1N1	0.91(8)
Atoms 1,2,3			
O1—C1—H1A	109.5	C28—C27—C34	106.6(5)
O1—C1—H1B	109.5	C28—C27—C25	113.1(4)
H1A—C1—H1B	109.5	C34—C27—C25	109.7(5)
O1—C1—H1C	109.5	C28—C27—C35	110.3(4)
H1A—C1—H1C	109.5	C34—C27—C35	107.5(5)
H1B—C1—H1C	109.5	C25—C27—C35	109.5(5)
O2—C2—H2A	109.5	N3—C28—C29	111.8(5)
O2—C2—H2B	109.5	N3—C28—C27	121.1(5)
H2A—C2—H2B	109.5	C29—C28—C27	126.7(5)
O2—C2—H2C	109.5	C30—C29—C28	106.1(5)
H2A—C2—H2C	109.5	C30—C29—H29	126.9
H2B—C2—H2C	109.5	C28—C29—H29	126.9
O3—C3—H3A	109.5	C29—C30—C31	106.7(5)
O3—C3—H3B	109.5	C29—C30—H30	126.7
H3A—C3—H3B	109.5	C31—C30—H30	126.7
O3—C3—H3C	109.5	C10—C31—N3	123.0(5)
H3A—C3—H3C	109.5	C10—C31—C30	127.6(5)
H3B—C3—H3C	109.5	N3—C31—C30	109.3(5)
O1—C4—C9	124.4(5)	C20—C32—H32A	109.5
O1—C4—C5	115.5(5)	C20—C32—H32B	109.5
C9—C4—C5	120.1(5)	H32A—C32—H32B	109.5
O2—C5—C4	120.9(5)	C20—C32—H32C	109.5
O2—C5—C6	119.2(5)	H32A—C32—H32C	109.5
C4—C5—C6	119.8(5)	H32B—C32—H32C	109.5
O3—C6—C7	124.8(5)	C20—C33—H33A	109.5

O3—C6—C5	115.0(5)	C20—C33—H33B	109.5
C7—C6—C5	120.2(5)	H33A—C33—H33B	109.5
C6—C7—C8	119.4(5)	C20—C33—H33C	109.5
C6—C7—H7	120.3	H33A—C33—H33C	109.5
C8—C7—H7	120.3	H33B—C33—H33C	109.5
C9—C8—C7	120.6(5)	C27—C34—H34A	109.5
C9—C8—C10	120.3(5)	C27—C34—H34B	109.5
C7—C8—C10	119.1(5)	H34A—C34—H34B	109.5
C8—C9—C4	119.8(5)	C27—C34—H34C	109.5
C8—C9—H9	120.1	H34A—C34—H34C	109.5
C4—C9—H9	120.1	H34B—C34—H34C	109.5
C31—C10—C11	123.2(5)	C27—C35—H35A	109.5
C31—C10—C8	120.6(5)	C27—C35—H35B	109.5
C11—C10—C8	116.2(5)	H35A—C35—H35B	109.5
N1—C11—C12	107.1(5)	C27—C35—H35C	109.5
N1—C11—C10	124.1(5)	H35A—C35—H35C	109.5
C12—C11—C10	128.8(5)	H35B—C35—H35C	109.5
C13—C12—C11	107.9(5)	C41—C36—C37	120.5(5)
C13—C12—H12	126.1	C41—C36—C15	121.5(5)
C11—C12—H12	126.1	C37—C36—C15	117.9(5)
C12—C13—C14	107.7(5)	C36—C37—C38	119.8(5)
C12—C13—H13	126.2	C36—C37—H37	120.1
C14—C13—H13	126.2	C38—C37—H37	120.1
N1—C14—C13	106.8(5)	O6—C38—C39	116.5(5)
N1—C14—C15	123.9(5)	O6—C38—C37	123.6(5)
C13—C14—C15	128.7(5)	C39—C38—C37	119.9(5)
C16—C15—C14	124.1(5)	O5—C39—C38	119.4(5)
C16—C15—C36	118.3(5)	O5—C39—C40	120.5(5)
C14—C15—C36	117.3(5)	C38—C39—C40	120.0(5)
C15—C16—N2	123.5(5)	O4—C40—C41	124.7(5)
C15—C16—C17	127.0(5)	O4—C40—C39	115.8(5)
N2—C16—C17	109.5(5)	C41—C40—C39	119.5(5)
C18—C17—C16	106.1(5)	C36—C41—C40	120.1(5)
C18—C17—H17	126.9	C36—C41—H41	120
C16—C17—H17	126.9	C40—C41—H41	120
C17—C18—C19	106.8(5)	O4—C42—H42A	109.5
C17—C18—H18	126.6	O4—C42—H42B	109.5
C19—C18—H18	126.6	H42A—C42—H42B	109.5
N2—C19—C18	112.1(5)	O4—C42—H42C	109.5
N2—C19—C20	121.5(5)	H42A—C42—H42C	109.5
C18—C19—C20	126.3(5)	H42B—C42—H42C	109.5
C19—C20—C21	107.9(5)	O5—C43—H43A	109.5

C19—C20—C33	109.7(5)	O5—C43—H43B	109.5
C21—C20—C33	112.1(5)	H43A—C43—H43B	109.5
C19—C20—C32	108.2(5)	O5—C43—H43C	109.5
C21—C20—C32	112.0(5)	H43A—C43—H43C	109.5
C33—C20—C32	107.0(5)	H43B—C43—H43C	109.5
C22—C21—C26	117.9(6)	O6—C44—H44A	109.5
C22—C21—C20	122.0(5)	O6—C44—H44B	109.5
C26—C21—C20	120.0(5)	H44A—C44—H44B	109.5
C21—C22—C23	120.0(6)	O6—C44—H44C	109.5
C21—C22—H22	120	H44A—C44—H44C	109.5
C23—C22—H22	120	H44B—C44—H44C	109.5
C24—C23—C22	121.3(6)	C11—N1—C14	110.5(5)
C24—C23—H23	119.3	C11—N1—H1N1	128.(5)
C22—C23—H23	119.3	C14—N1—H1N1	121.(5)
C23—C24—C25	120.0(6)	C19—N2—C16	105.5(4)
C23—C24—H24	120	C28—N3—C31	106.0(4)
C25—C24—H24	120	C4—O1—C1	115.9(4)
C26—C25—C24	118.1(5)	C5—O2—C2	113.0(5)
C26—C25—C27	122.7(5)	C6—O3—C3	117.4(4)
C24—C25—C27	119.3(5)	C40—O4—C42	116.8(5)
C25—C26—C21	122.7(5)	C39—O5—C43	115.6(5)
C25—C26—H26	118.7	C38—O6—C44	116.9(4)
C21—C26—H26	118.7		

Table 4.9 Summary of X-ray crystallographic data for compound **8**

Formula sum	C ₄₀ H ₄₀ N ₁₀ O ₁₀
Formula weight	820.82 g/mol
Crystal system	Triclinic
Space-group	P -1 (2)
Cell parameters	a=8.7020(4) Å b=14.8084(6) Å c=15.7963(7) Å α=76.91(0)° β=88.93(0)° γ=79.96(0)°
Cell ratio	a/b=0.5876 b/c=0.9375 c/a=1.8152
Cell volume	1951.82(60) Å ³
Z	2

Calc. density	1.39657 g/cm ³
R(All)	0.1599
Pearson code	aP196
Formula type	N ₃ O ₆ P ₄₄ Q ₄₅
Wyckoff sequence	i98

4.3 DENSITY FUNCTIONAL THEORY (DFT) CALCULATION STUDY

4.3.1 COMPUTATIONAL DETAILS

The DFT calculation for *meta*-benziporphodimethene (**4**) and its zinc complex (Zn²⁺.**4**), energy and the population analysis of the molecular orbital were calculated out by gas-phase single point density functional theoretical (DFT) calculations which were performed using the *Gaussian 09W, revision D.01* package on an HP PC platform [10]. Becke's three parameters exchange functional with the gradient corrected correlation formula of Lee, Yang, and Parr [DFTB3LYP] was used with the 6-31g** basis set to optimize the geometry [11]. Harmonic vibrational frequencies were calculated using analytical second derivatives for all structures. Molecular orbitals were visualized using 'Gauss view'.

4.3.2 DFT CALCULATION RESULTS

It has been well documented in the literature the use of DFT calculation to calculate the electronic structure of porphyrinoid molecules to gain information on their energetic, conformational behaviour, tautomerism, stability of structure and aromaticity [12]. In the present work, we have demonstrated our one of the synthesized compound and its zinc complex to emphasize on the structural behaviour. Also, it is desirable to know the effect of metallation on the geometries of receptor to address the nearly non-fluorescent nature of free receptors. Figure 4.58 shows the optimized geometries of free *meta*-benziporphodimethene, **4**, and its metal complex, Zn²⁺.**4**. Free *meta*-benziporphodimethene, **4**, structure is more perturbed than its zinc complex. Comparison of various parameter values have been given in Table 4.10. The angle between the phenylene plane and the plane of the three pyrrolic nitrogen's (C6-

N_3) is markedly dependent on the orientation of the substituents at sp^3 meso carbons, which in turn, affects the M---C and M---H distances in the conformation core (Table 4.10). The C_6-N_3 angle obtained for the $Zn^{2+}.\mathbf{R}$ and $Zn^{2+}.\mathbf{4}$ are in such a way that the phenylene rings remain to be perpendicular to the N_3 plane. The C(22)-H(22) bond distance are 1.0501 Å and 1.0795 Å for $Zn^{2+}.\mathbf{R}$ and $Zn^{2+}.\mathbf{4}$, respectively. The metal ion lies above the three pyrrolic nitrogen's plane (N_3) in both the complexes $Zn^{2+}.\mathbf{R}$ and $Zn^{2+}.\mathbf{4}$. The angle between the 17 tripyrrin atoms plane and plane of the pyrrole with N(3) and N(1) are almost same in the case of **4** while a difference of almost 12° was measured in the case of **R**. Another notable difference of almost 10° was observed in the angle between 17 tripyrrin atoms and phenylene ring atoms of **R** and **4**. Due to non-conjugated π -system of receptor the HOMO and LUMO of receptor, **4** and its zinc complex are mainly localized on tripyrrin moiety. A slight delocalization of electron density was seen on metal in HOMO-1 of $Zn^{2+}.\mathbf{4}$ and are shown in Figure 4.59.

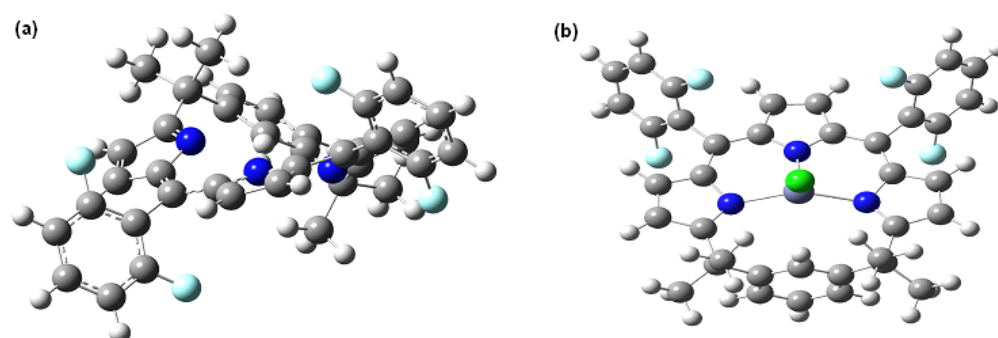
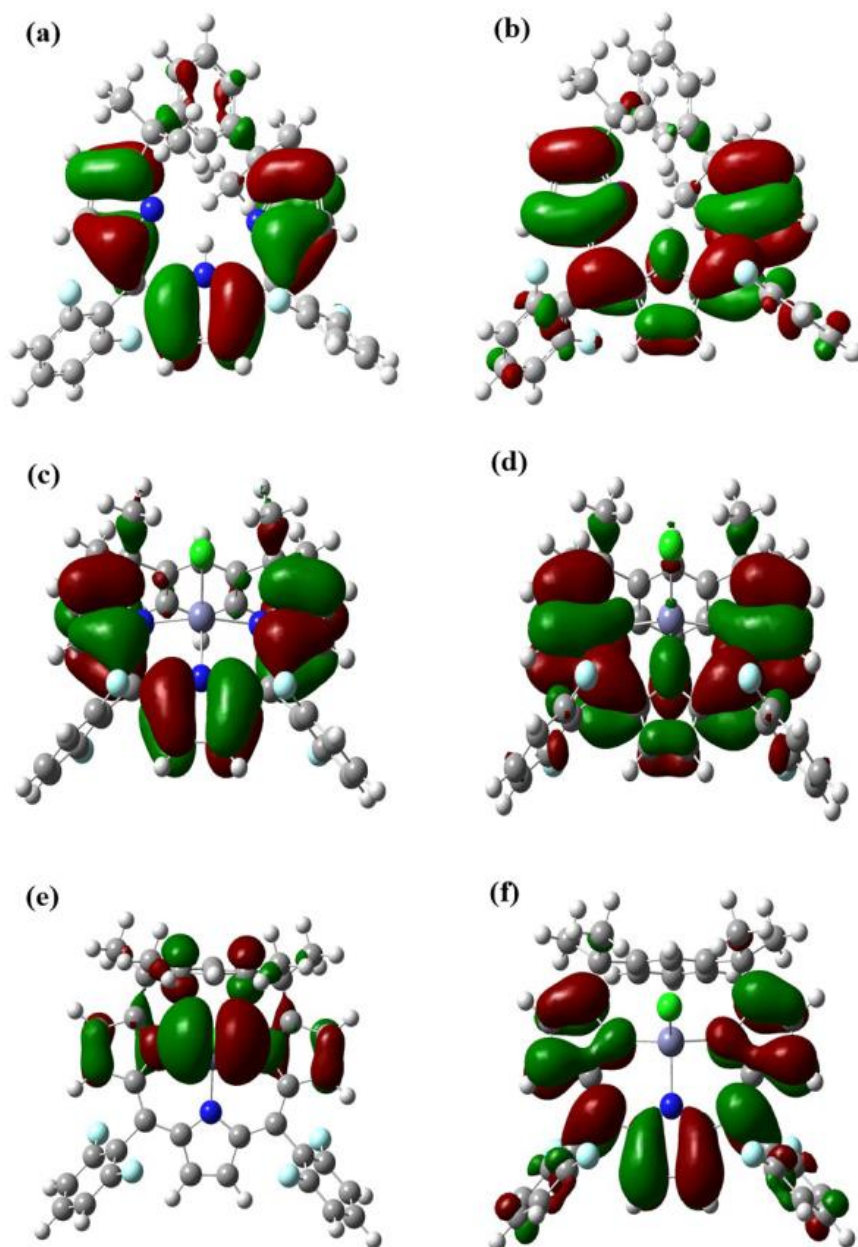


Fig. 4.58 B3LYP/6-31g** DFT optimized structure of receptor **4** and $Zn^{2+}.\mathbf{4}$.

Table 4.10 Comparison of Selected bond lengths [\AA] and angles [$^\circ$] of **R** and $\text{Zn}^{2+}\cdot\mathbf{R}$ with receptor, **4** and its $\text{Zn}^{2+}\cdot\mathbf{4}$. values for **R** and $\text{Zn}^{2+}\cdot\mathbf{R}$ were taken from ref. [6] where a = angle between the 17-tripyrin atoms and pyrrole with N(3); b = angle between the 17-tripyrin atoms and pyrrole with N(1); c = angle between the 17-tripyrin atoms and phenylene ring (C_6). (R = unsubstituted *meta*-benziporphodimethenes).

	$\text{Zn}^{2+}\cdot\mathbf{R}$	$\text{Zn}^{2+}\cdot\mathbf{4}$	R	4
M-N ₃	0.51	0.5585		
M-N(1)	2.121	2.1443		
M-N(2)	1.995	1.9902		
M-N(3)	2.129	2.1444		
M-Cl	2.243	2.2657		
M..C(22)	2.823	2.9201		
M...H(22)	3.04	2.8285		
C(22)-H(22)	1.05	1.0799		
C_6/N_3	81.4	86.541	19.233	18.347
A		71.921	65.387	65.250
B		65.883	52.826	64.993
C	77.780	89.091	36.131	46.752
N(1)-N(3)			2.8453	2.7893
N(1)-N(2)			2.7360	2.7899
N(2)-N(3)			3.9997	4.0013

Fig. 4.59 Molecular orbital diagram of receptor, **4** and its zinc complex. (a) HOMO of receptor, **4**. (b) LUMO of receptor, **4**. (c) HOMO of Zn^{2+} .**4**. (d) LUMO of Zn^{2+} .**4**. (e) HOMO-1 of Zn^{2+} .**4**. (f) LUMO-1 of Zn^{2+} .**4**.



4.4 FLUORESCENCE STUDY

meta-benziporphodimethenes free base compounds are non-fluorescent molecules however when complexed with zinc (Zn^{2+}), cadmium (Cd^{2+}) or mercury (Hg^{2+}), they turn on fluorescence. These *meta*-benziporphodimethenes are CHEF based sensors (The coordination of metal ion with fluorophore increases the fluorescence intensity of chromophore, called chelation-enhanced fluorescence, CHEF). Mostly sensors like fluorescein [13, 14], dansyl [15-18], anthracene [19, 20], and BODIPY [21] shows CHEF. These CHEF based sensors emit lower than 600 nm and constitute background fluorescence. Still, there is a crunch and need of development of sensors emitting above 600 nm or even low and zero background fluorescence, high penetration and lesser scattering in optically diffuse samples which in turn may induce lesser tissue damage [22-24].

4.4.1 PHOTOLUMINESCENCE (PL) AND TIME RESOLVED PHOTOLUMINESCENCE (TRPL) SPECTRAL ANALYSIS

meta-benziporphodimethene are such promising molecules which are CHEF based sensors having zero background emission and shows turn on fluorescence when bind with Zn^{2+} metal ions. The Photoluminescence and Time resolved photoluminescence spectra of all *meta*-benziporphodimethene zinc complexes (Zn^{2+} .1-8) were recorded in degassed acetonitrile while maintaining 10 μ M concentration. The Photoluminescence spectra of all zinc complexes (Zn^{2+} .1-8) are recorded at $\lambda_{exi}= 564$ nm which is the isobestic point in the titration analysis of free base BPDM with $ZnCl_2$ solution. Photoluminescence and Time resolved photoluminescence spectra of all *meta*-benziporphodimethene zinc complexes (Zn^{2+} .1-8) are represented in Fig. 4.60-4.76.

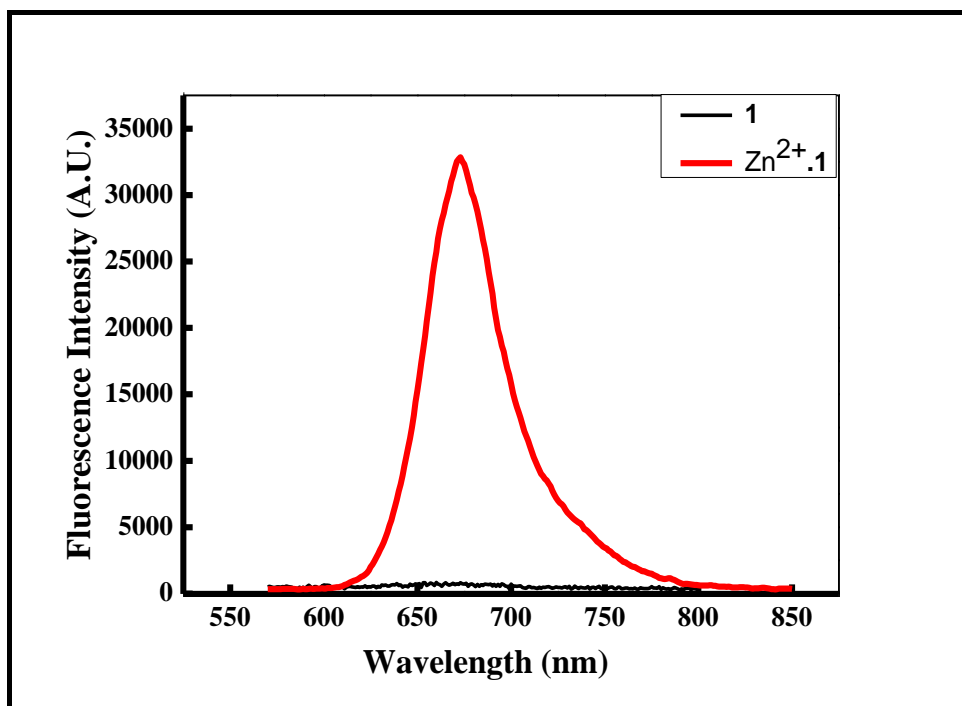


Fig 4.60 Photoluminescence of complex Zn²⁺.1

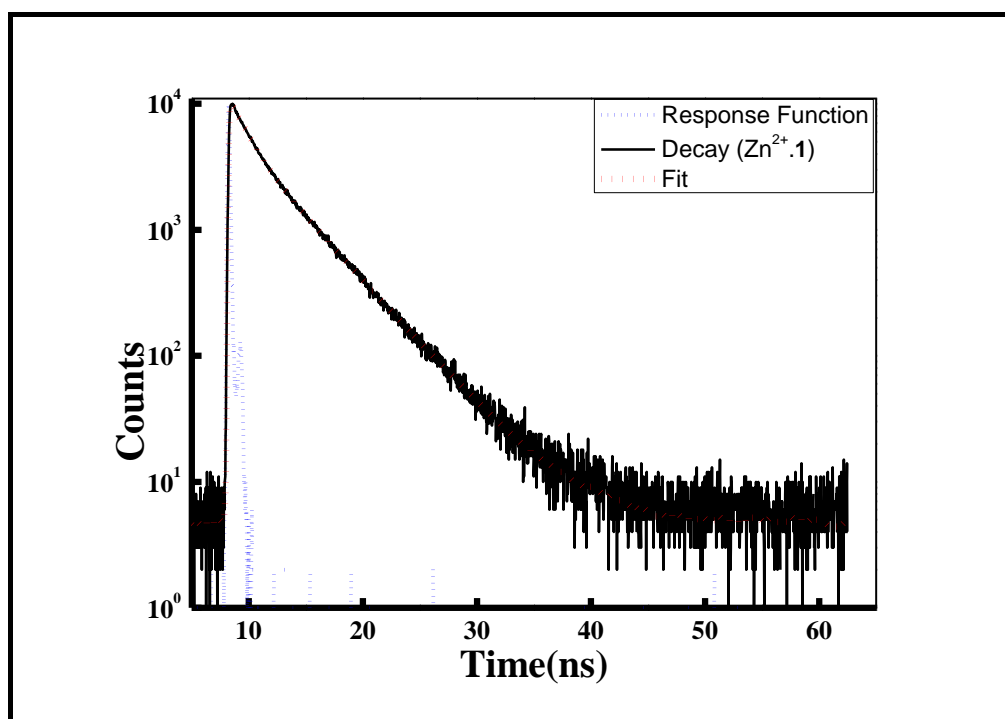


Fig 4.61 Time resolved photoluminescence of complex Zn²⁺.1

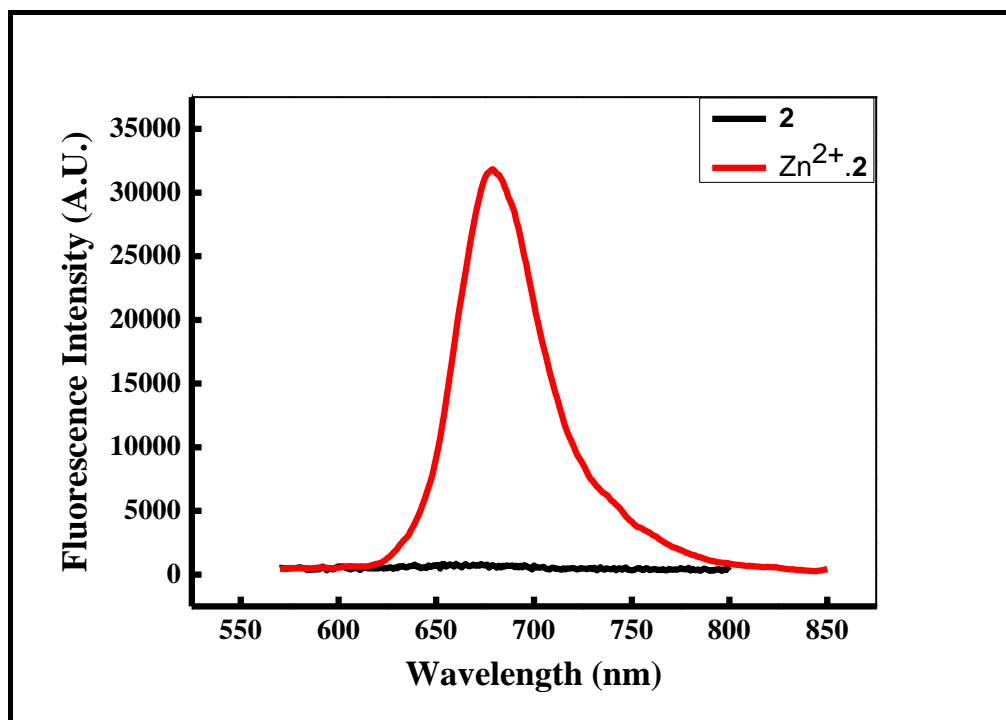


Fig 4.62 Photoluminescence of complex Zn²⁺.2

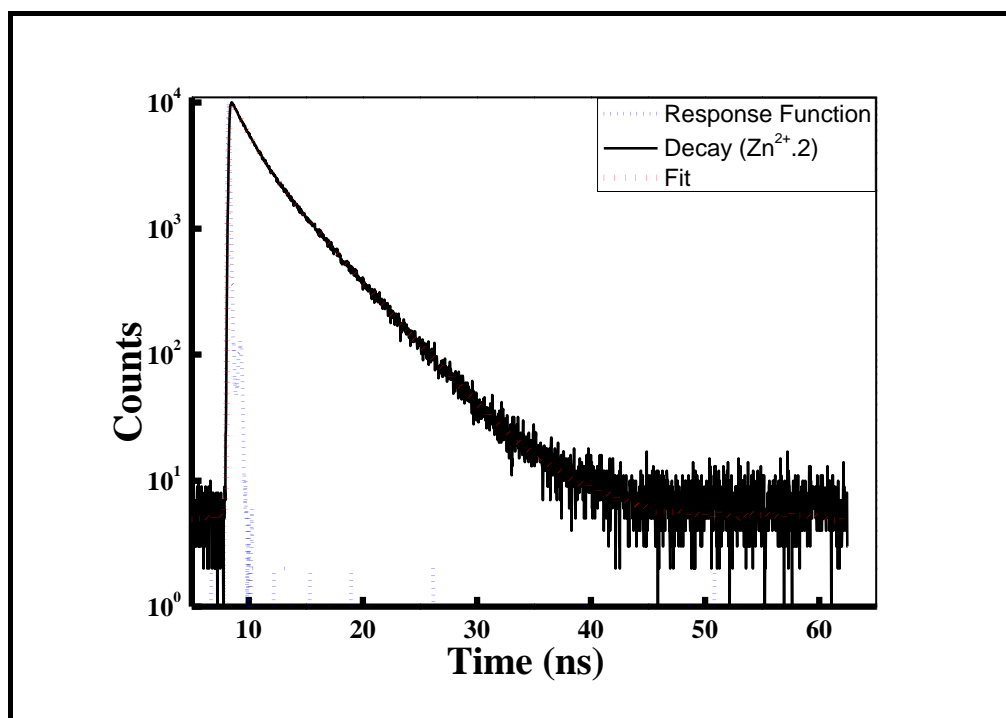


Fig 4.63 Time resolved photoluminescence of complex Zn²⁺.2

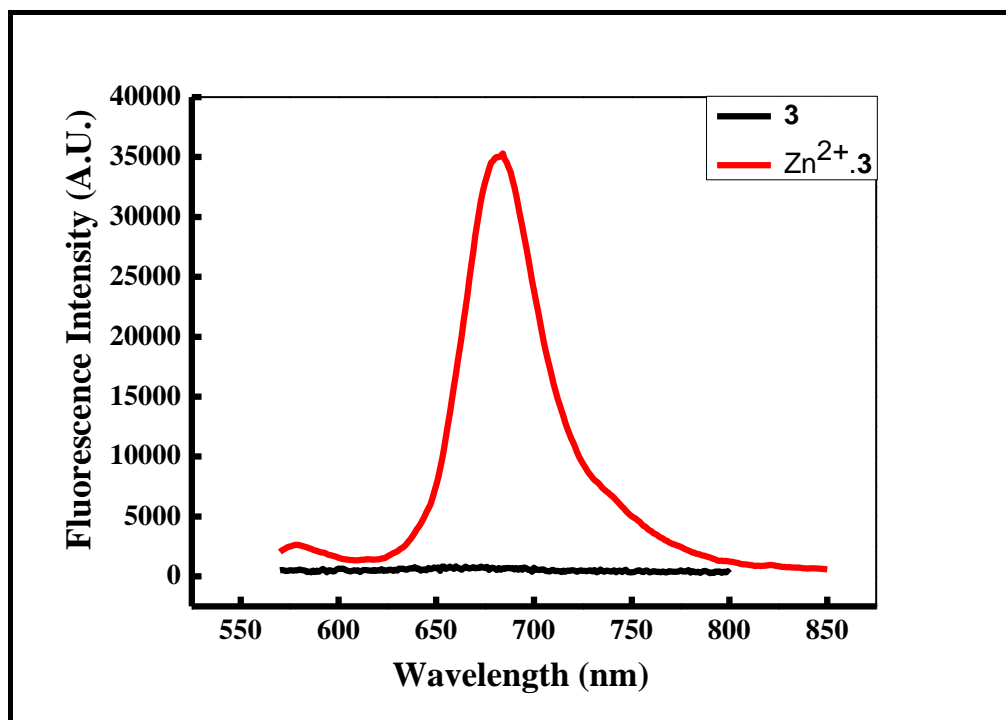


Fig 4.64 Photoluminescence of complex $Zn^{2+}.3$

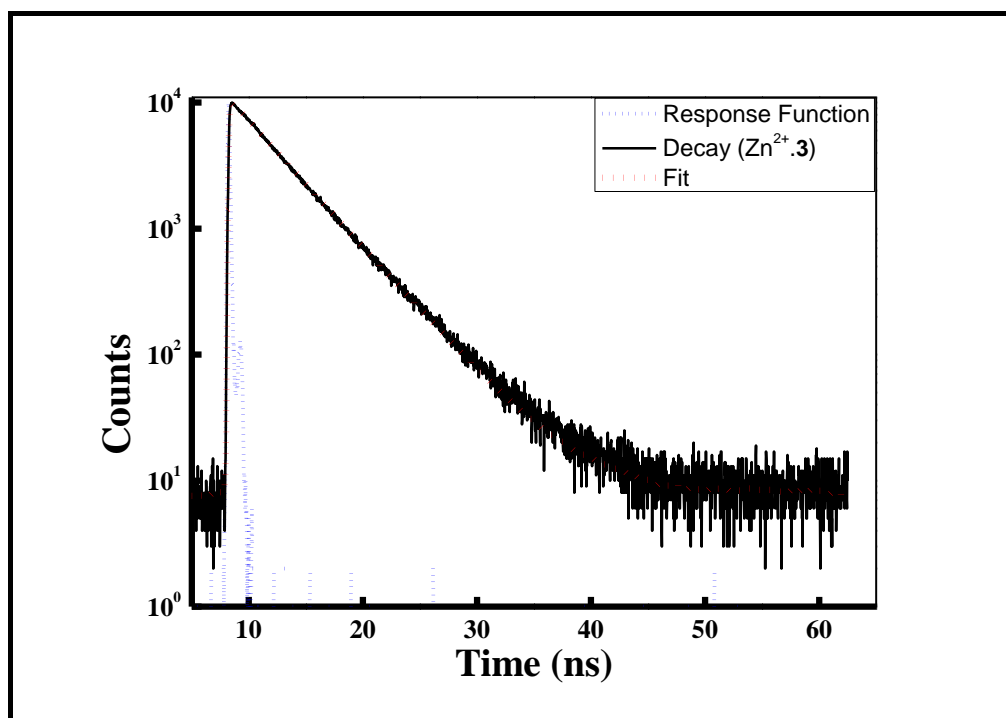


Fig 4.65 Time resolved photoluminescence of complex $Zn^{2+}.3$

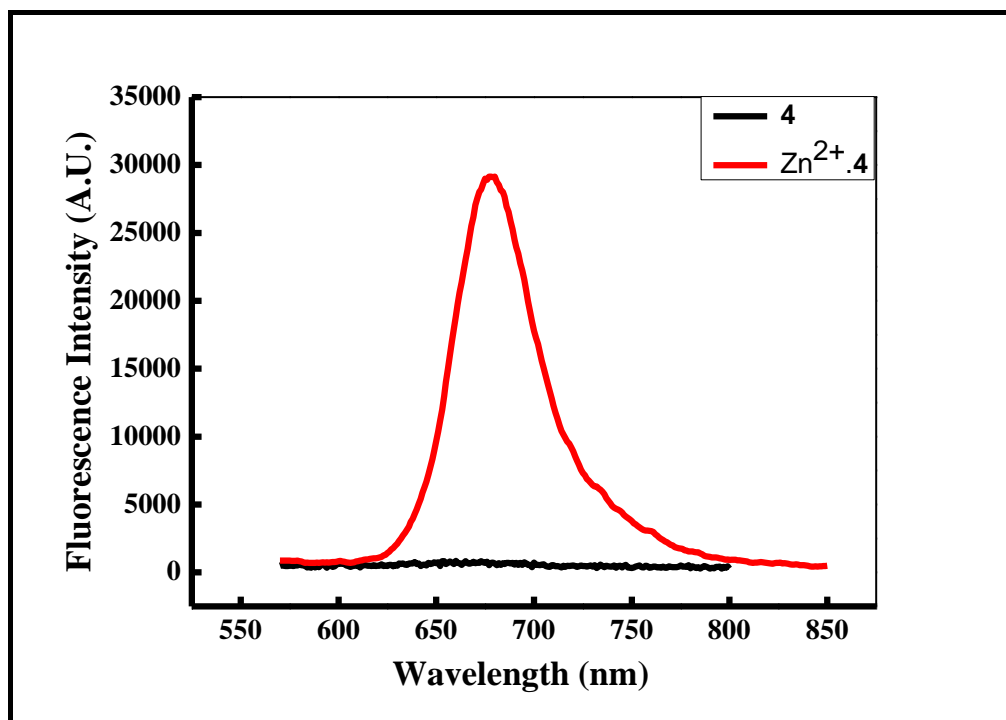


Fig 4.66 Photoluminescence of complex Zn²⁺.4

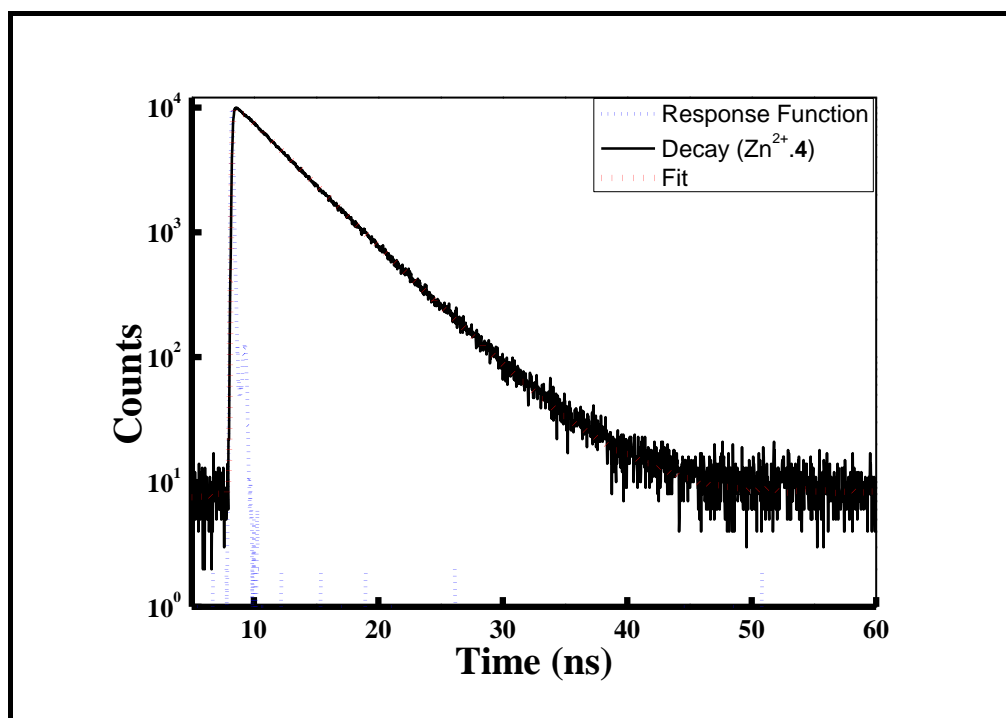


Fig 4.67 Time resolved photoluminescence of complex Zn²⁺.4

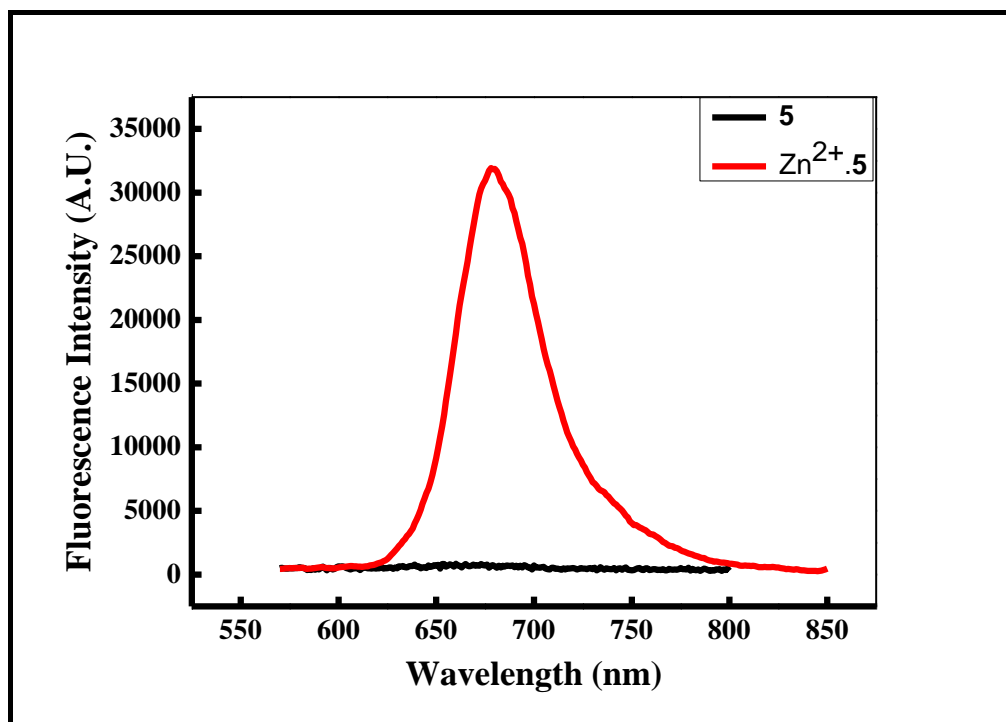


Fig 4.68 Photoluminescence of complex Zn²⁺.5

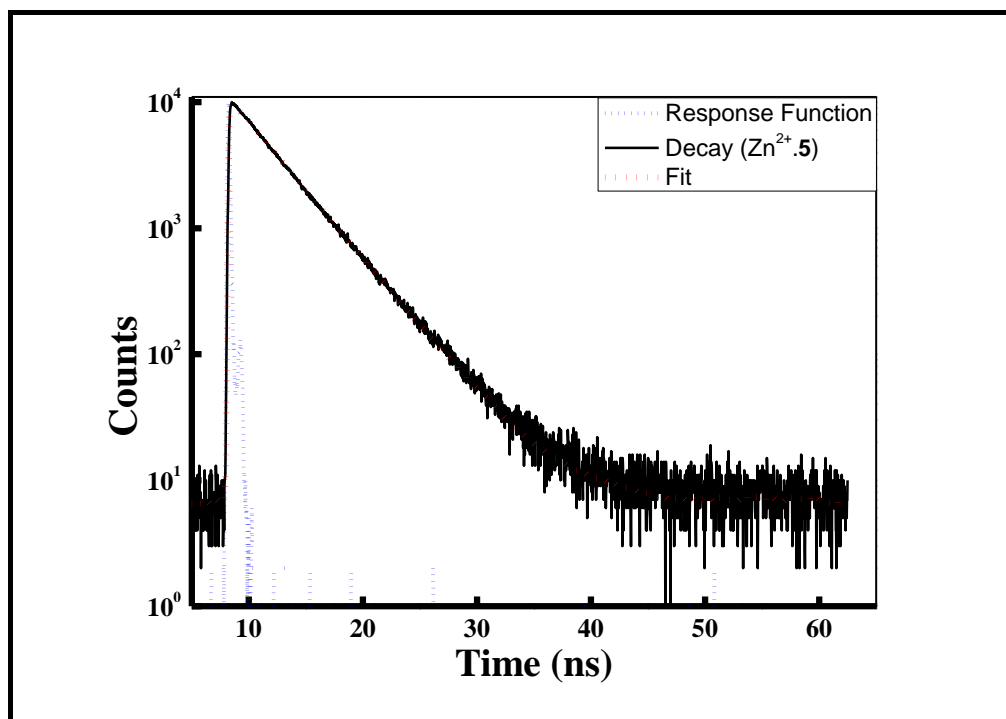


Fig 4.69 Time resolved photoluminescence of complex Zn²⁺.5

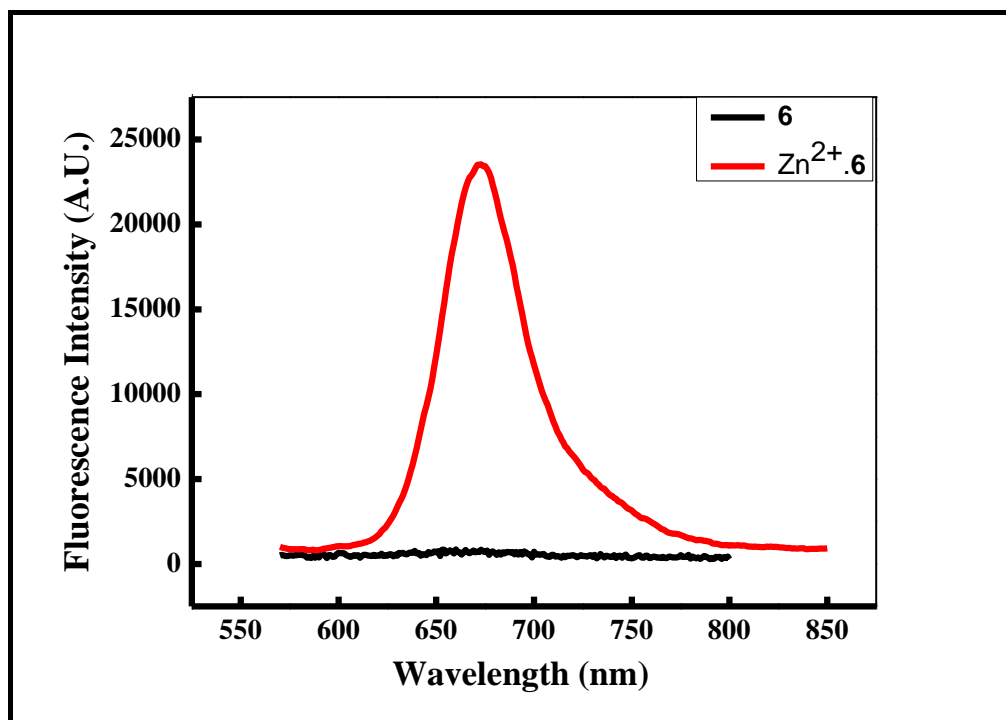


Fig 4.70 Photoluminescence of complex $Zn^{2+}.6$

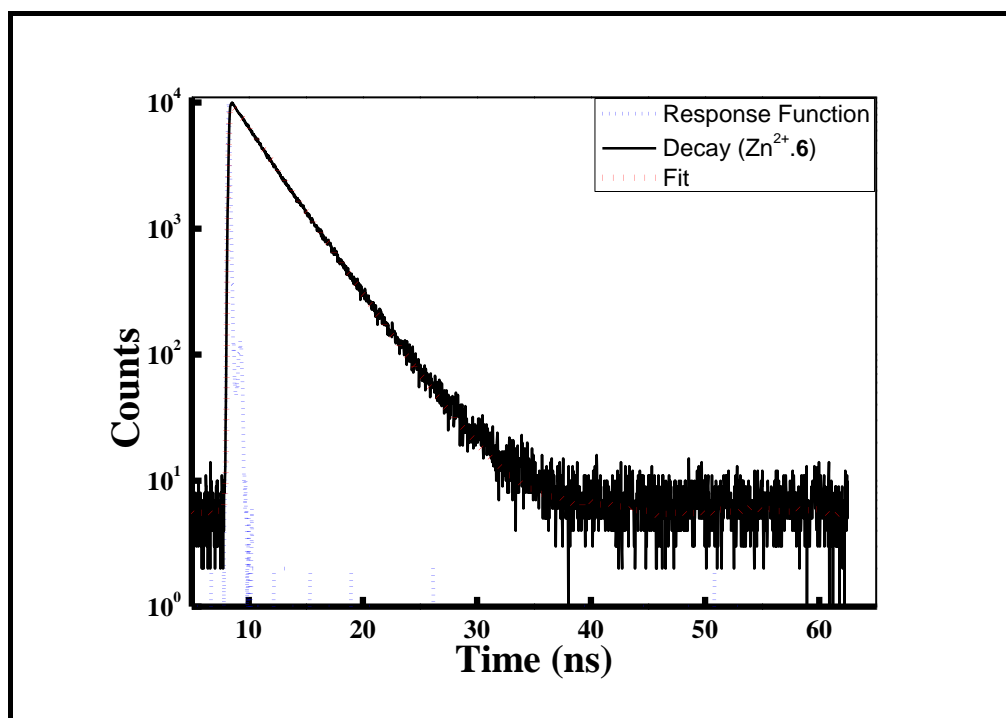


Fig 4.71 Time resolved photoluminescence of complex $Zn^{2+}.6$

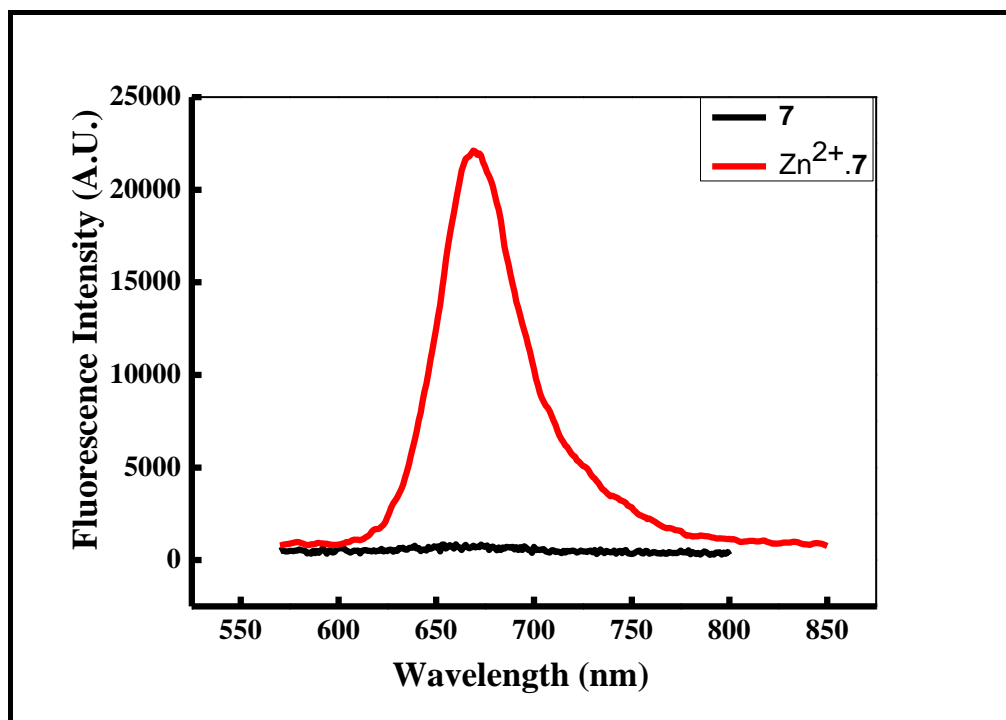


Fig 4.72 Photoluminescence of complex Zn²⁺.7

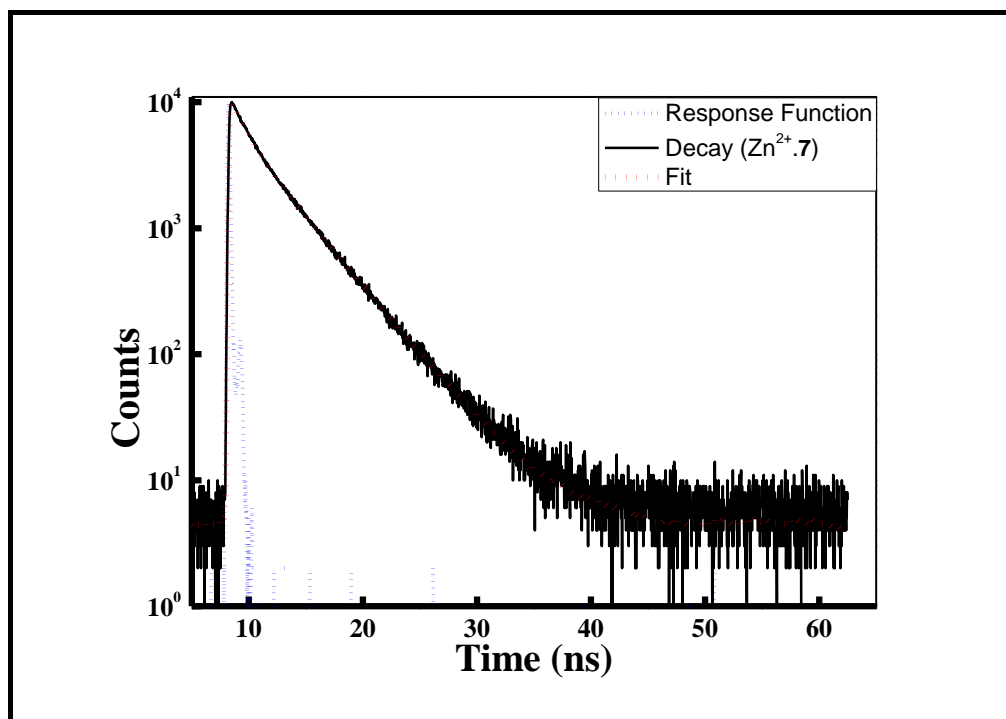


Fig 4.73 Time resolved photoluminescence of complex Zn²⁺.7

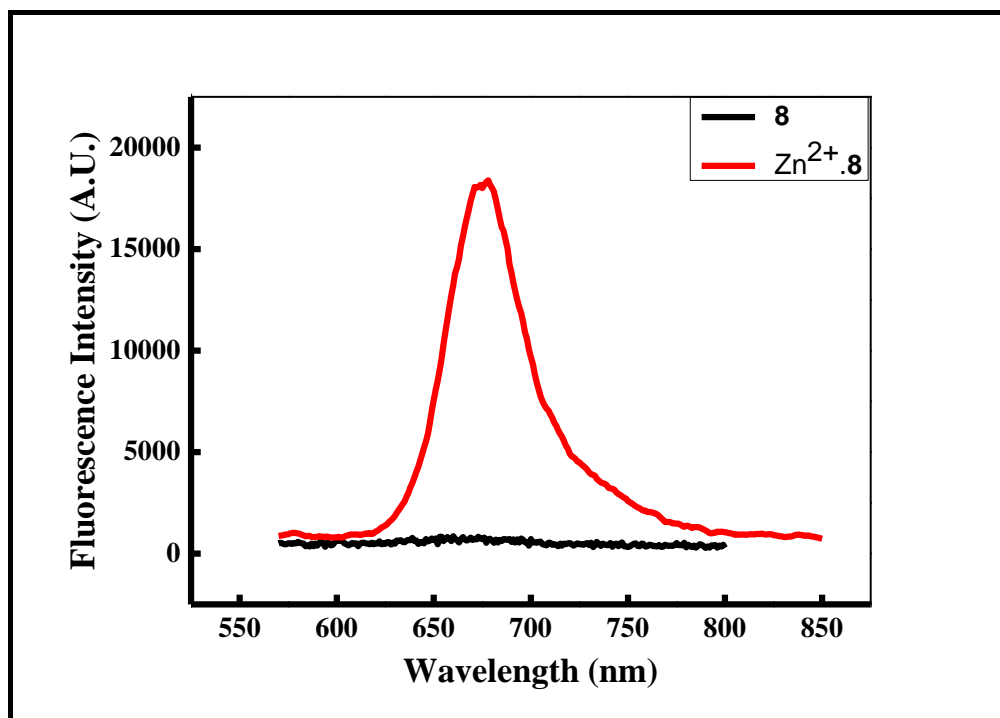


Fig 4.74 Photoluminescence of complex Zn²⁺.8

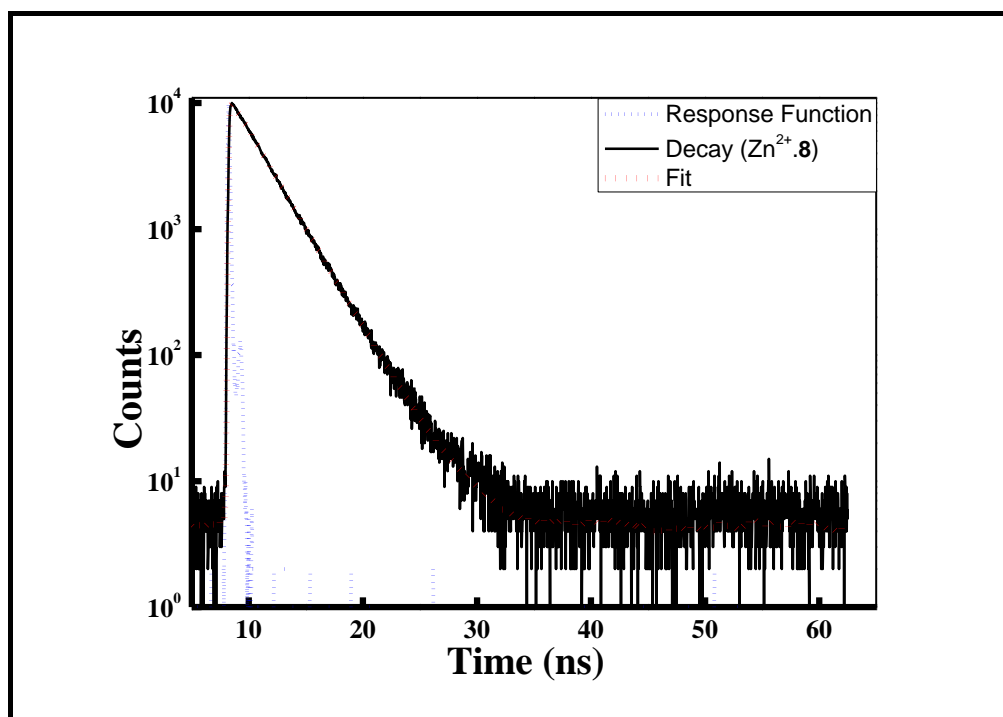


Fig 4.75 Time resolved photoluminescence of complex Zn²⁺.8

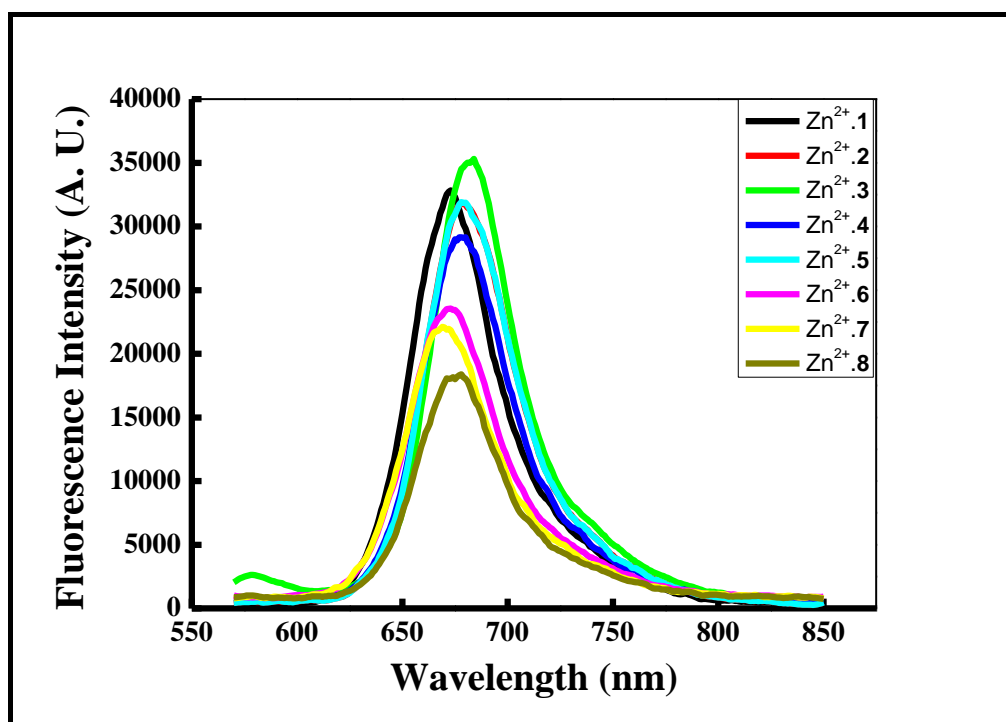


Fig. 4.76 Combined photoluminescence for complexes Zn²⁺.1-8

4.4.2 QUANTUM YIELD ANALYSIS

The fluorescence quantum yield (QY) for Zn²⁺.1-Zn²⁺.8 were calculated in degassed toluene at room temperature from the ratio of τ_s/τ_r , where τ_s is fluorescence lifetime obtained from fluorescence decay curves recorded with time-correlated single photon counting system combined with Delta diode laser and the radiative life time, τ_r is calculated using Strickler-Berg relation [25].

$$1/\tau_r = 2.880 \times 10^{-9} n^2 \langle \tilde{\nu}_f^{-3} \rangle_{Av}^{-1} \cdot (g_1/g_2) \int \epsilon d \ln \tilde{\nu}$$

Where g_1 and g_2 : degeneracies of the 1, 2 states, n is refractive index of the medium and

$$\frac{\int I(\tilde{\nu}) d\tilde{\nu}}{\int \tilde{\nu}^{-3} I(\tilde{\nu}) d\tilde{\nu}} = \langle \tilde{\nu}_f^{-3} \rangle_{Av}^{-1}$$

The calculated fluorescence QY were comparable to the value obtained for 5, 10, 15, 20-tetraphenylporphyrin free base and its zinc complex, 0.11 and 0.033, respectively. The emission spectra of all the zinc complexes are nearly same and are in good agreement with previously reported analogue zinc porphyrin derivatives [26]. The fluorescence

quantum yields, ϕ , calculated for compounds Zn^{2+} .1- Zn^{2+} .8 are shown in Table 4.11. The lowest values were obtained for compound Zn^{2+} .6, Zn^{2+} .7 and Zn^{2+} .8. It was observed that fluorescence quantum yield are comparatively on higher side when substituents on *meso*-phenyl are electron withdrawing than electron releasing groups. The observation is opposite to previously reported zinc porphyrin derivatives [1, 26]. We believe this may be due to the presence of sp^3 - sp^2 *meso*-carbons which distinguish these macrocycles from tetraphenylporphyrin and other related porphyrinoids [26]. The fluorescence quantum yield of Zn^{2+} .7 and Zn^{2+} .8 are 0.17 and 0.14, respectively which clearly depicts the effect of electron releasing substituents on *meso*-phenyl. The Zn^{2+} .8 contains three -OMe groups while only one -OMe group on Zn^{2+} .7. The presence of halogen on the *meso*-phenyl groups dramatically affect the magnitude of derived fluorescence emission quantum yields. *Para*-halogenation quenches the fluorescence emission in both free base (non-fluorescent) and their zinc derivatives progressively as the atomic number of the attached halogen increases [1, 2, 26]. The interaction of halo-substituent to the π -system of the macrocycle has significant effect on the quantum yields. It was also observed that the lowest value for Zn^{2+} .6 (0.13) indicate that electronegative *para*-substituent effect the fluorescence quantum yield when halo-substituent are on *meso*-phenyl group. Contrastingly, *ortho*-chlorination has significant effect and having the highest value of quantum yield (Zn^{2+} .3, 0.37). A similar increase in the quantum yield of zinc porphyrin derivatives has been previously reported, but not justified, in the literature [26-27]. *Ortho*-chlorination facilitate smooth interaction between the halo-substituent and the π -system of the macrocycle by locking the position of *meta*-benziporphodimethenes and the *meso*-phenyl group in a perpendicular arrangement and inhibit the indirect conjugation between the induced electron withdrawing halogens and the macrocycle [28]. The strong electronic communication between the π -system of macrocycle and the *ortho*-chlorine overcomes the obvious steric effect of halogens and has been well documented in the literature [27, 29, 30]. The observed fluorescence quantum yield is consistent with the principles of heavy atom effect of halo-substituent in the case of Zn^{2+} .1 and Zn^{2+} .2 as the halo-substituent on *para*-position. The fluorescence quantum yields are not consistent with the principles of heavy atom effect as the position of halo-substituent changes from *ortho* to *para* position (Zn^{2+} .4 (0.28), Zn^{2+} .5 (0.25) and Zn^{2+} .6 (0.13). The observed quantum yields attribute that endocyclic and exocyclic heavy atom effect in the case zinc derivatives oppose each other [31]. *Para*-halogenations seems to withdraw electron density from the macrocycle weakening the electrostatic interaction between the

macrocycle and the central metal atom, zinc, and subsequently weakening the endocyclic heavy atom effect. The high quantum yield of *ortho*-chlorinated zinc derivatives (Zn^{2+} .**3**, 0.37) supports additionally the above effect. The observed findings are in good agreement with the reported experimental findings. The placement of the chloro-substituent at *ortho*-position facilitates the $2p$ -Cl orbital with the π -orbital of the *meso*-carbon. The high electronegative atom strongly interact with the macrocycle and significantly reduce the electronegativity of the macrocycle and interaction with the central metal atom, zinc, which results in the reduction of endocyclic heavy atom effect [31-32].

Table 4.11 Fluorescence quantum yields of zinc complexes of *meta*-benziporphodimethenes obtained in degassed toluene calculated using Strickler-Berg relation. (where R= unsubstituted *meta*-benziporphodimethene [**6a**]).

Compound	τ_s	τ_r	$\phi = \tau_s / \tau_r$
Zn^{2+} .R			0.34
Zn^{2+} . 1	3.69	11.88	0.31
Zn^{2+} . 2	3.53	12.83	0.28
Zn^{2+} . 3	4.31	11.63	0.37
Zn^{2+} . 4	4.41	15.59	0.28
Zn^{2+} . 5	3.98	16.09	0.25
Zn^{2+} . 6	3.26	24.91	0.13
Zn^{2+} . 7	3.44	20.52	0.17
Zn^{2+} . 8	2.77	20.20	0.14

4.5 CELL IMAGING STUDIES

Zinc is an essential element for growth and development of both plant and animals [33, 34]. Zinc is implicated in a variety of biological processes which include enzyme regulation, cell signalling, DNA synthesis, gene expression, neurotransmission, cell growth and apoptosis, etc. [33, 35-43]. The concentration of Zn^{2+} in different biological cells ranges from 1 nM to about 1 mM. However, because of its closed-shell electronic configuration Zn^{2+} shows neither any type of magnetic signals nor the convenient spectroscopic signature. Therefore, imaging of labile or free intracellular Zn^{2+} using a fluorescence microscopy technique is an important area of research [34]. Large number of fluorescent probes have been developed so far and used in biological imaging but almost all suffer from high background fluorescence and low CHEF. Still, there is a crunch and need of development of sensors emitting above 600 nm or even low and zero background fluorescence, high penetration and lesser scattering in optically diffuse samples which in turn may induce lesser tissue damage [44-46].

meta-benziporphodimethene, has no background emission and upon binding with Zn^{2+} shows tremendous increase in fluorescence intensity and represented turn-on probe for Zn^{2+} sensor [6]. These moieties are specific Zn^{2+} sensors in presence of a number of alkali, alkaline earth and various transition metals [6]. In this thesis work we have shown the biological implication of this fascinating fluorescent molecules, which do not have any background emission to avoid any tissue damage, the cell imaging of breast carcinoma (MDAMB-468) cells for the detection of Zn^{2+} .

4.5.1 CELL IMAGING STUDIES FOR ZINC: COMPARATIVE ANALYSIS

Though several reports have been documented in the literature for cellular imaging of Zn^{2+} ion in cells. The detection and imaging of zinc secretion from pancreatic β -cells using FluoZin-3, is tetraanionic probe based on tetraethylenediamine, was used by Kennedy et al. [47]. The molecule was excited at 488 nm and emission was recorded at 515 nm. The probe had several advantage like lesser signal to noise ratio, lesser background fluorescence and fluorescence enhancement was > 100 fold than 3-5 fold enhancement of 8-aminoquinoaniline based fluorophore [35]. An another fluorophore near-infrared probe was also used to probe zinc in macrophage cells and shows better absorption 730 nm and emission at 783 nm in absence of zinc ($\phi = 0.02$) and 731 nm

and 780 nm in presence of zinc ($\phi = 0.41$) with background fluorescence [48]. Recently, 2-(N, N-Dimethyl amino) naphthalene based probe was used for imaging of zinc ion in HeLa cells and *Arabidopsis* [49]. The fluorescence emission of this probe was recorded at 500 nm (excitation at 370 nm) with a fluorescence enhancement of 10-fold ($\phi = 0.089$) upon the addition of 10 equiv. of zinc ions. Ali et al. Have shown the use of 8-aminoquinoline derivative based fluorophore to sense zinc ion and cell imaging. The addition of zinc ions enhanced the fluorescence (excitation at 430 nm; emission at 539 nm; $\phi = 0.163$) and 3-4 times higher than in absence of zinc ions (0.043) [50]. Later on benzothiazole derivative was used for live cell imaging in Hela cells. The emission spectrum was obtained with excitation at 323 nm and maximum intensity of fluorescence emission was recorded at 385 nm [51]. Ghosh et al. Used cystamine based cell permeable zinc ion specific molecular bio-imaging materials in plant and animals. The probe showed strong blue fluorescence at 448 nm when excited at 370 nm with background fluorescence. The quantum yield value of 0.33 was recorded after the binding of zinc with ligand. The MTT assay showed ligand do not have detrimental effect on cell viability and permeates the membrane without any harm to the cells [52]. Kim et al. have investigated two-photon probe based on modified benzothiazole derivatives for imaging zinc ions in Golgi-localized [53]. The probe had low cytotoxicity and high photostability. The probes exhibited absorption maxima at 389 nm and 384 nm and emission maxima at 497 nm ($\phi = 0.02$) and 518 nm ($\phi = 0.08$) in zinc unbound state and shows almost 3-fold and 100-fold enhancement in fluorescence intensities upon binding with zinc ($\phi = 1.00$ and 0.93) [53]. To the best of our knowledge and literature survey, almost all the probes used for bio-imaging zinc ion in cells had background fluorescence and lower absorption, excitation and emission wavelength which can cause photo-toxicity and artefactual generation of active oxygen species [53]. Though Kim et al. have synthesized a molecule which had higher excitation and emission wavelength but suffers from background fluorescence [53]. In the present work, the cellular imaging of zinc ion in the breast carcinoma (MDA-MB-468& MDA-MB-231) cells using our recently synthesized receptors [7] which had low energy absorption maxima 594 nm and high emission wavelength at 680 nm has been shown. So, it was very interesting to explore simple porphyrin analogue as zinc ion sensor and cellular imaging of zinc ions in cells and with no background fluorescence which other sensors had deficiency, and long wavelength both in excitation and emission.

4.5.2 CELL IMAGING EXPERIMENT AND CYTOTOXICITY STUDIES

CELL CULTURE

Human breast cancer cell line was procured from National Center for Cell Science, Pune, India. Monolayer culture of MDA-MB-468 & MDA-MB-231 cell was maintained in Dulbecco's modified Eagle's medium containing 10% fetal bovine serum, 1% antibiotic-antimycotic in a humidified incubator at 37 °C with 5% carbon dioxide and 95% atmospheric air. For imaging and cytotoxicity studies cells were harvested by trypsinization and plated in appropriate well plates.

IMAGING

Actively dividing cells were plated over coverslip in a twenty four well plate (2×10^5 cells per well) and incubated overnight to adhere. Stock (1 mM) solutions of various receptors, (Compounds **1**, **4**, **7**, **8** for MDA-MB-468 & compound **4** for MDA-MB-231) were prepared in 1% aqueous dimethyl sulfoxide (DMSO). Initially the cells were washed with phosphate buffers (pH 7.4). The washed cells were treated with Zn^{2+} ions ($ZnCl_2$) for 30 min. After incubation, the cells were again washed with phosphate buffer and then incubated with solution of various receptors, (Compounds **1**, **4**, **7**, **8** for MDA-MB-468 & compound **4** for MDA-MB-231) for 30 minutes. Control cells were incubated with DMEM and receptors without Zn^{2+} . Finally, again cells were washed with phosphate buffer saline (pH 7.4) to avoid any residual receptors as well as Zn^{2+} ions in the media and coverslip were mounted on grease-free microscopic slide. Cells were observed under fluorescence microscope. Brightfield and fluorescence images were examined using a Zeiss microscope (Carl Zeiss, Germany) aided with epifluorescence and Axio cam camera system coupled with Axio Vision software (Carl Zeiss, Germany) at 100 \times magnification.

CYTOTOXICITY

Cells in log phase were harvested, seeded in 96 well plate (1×10^4 cells/well) and allowed to adhere overnight. Stock solutions (1 mM) of (Compounds **1**, **4**, **7**, **8** for MDA-MB-468 & compound **4** for MDA-MB-231) were prepared as described above.

Solution of (Compounds **1**, **4**, **7**, **8** for MDA-MB-468 & compound **4** for MDA-MB-231) were added to the wells at a final concentration of (10, 20, 30, 50, 100 μM). Control cells were incubated with DMEM and receptors without Zn^{2+} . After 12 hr of incubation at 37°C 20 μL of MTT (3-(4, 5-Dimethylthiazol-2-yl)-2, 5-Diphenyltetrazolium Bromide) (5mg/ml) was added and allowed for reduction reaction for 4 hr. Formazan crystal formed by cellular reduction of MTT was dissolved by addition of 200 μL of DMSO and incubation for 6hr. Solution was stirred for 5 sec to mix it properly and absorbance was taken at 570 nm in BioRadiMark microplate reader [54]. Percent cell viability was calculated and presented as the mean \pm standard deviation (SD). Values were evaluated by one-way analysis of variation (ANOVA) followed by Dunnett's test for comparison of individual treated groups to control one.

$$\text{Percent cell viability} = 1 - \frac{\text{Absorbance of treated group}}{\text{Absorbance of control group}} \times 100$$

4.5.3 CELL IMAGING RESULTS

The cell imaging result indicates that Compounds **1**, **4**, **7** and **8** are able to internalize successfully in MDA-MB-468 cells and also compound **4** in MDA-MB-231 cells and fluorescence when complex with Zn^{2+} ion inside the cell, thus it could be used fluorescent sensor for intracellular Zn^{2+} ions and presented in Figure 4.77(a) and 4.77(b). To ensure the effect of electron releasing and electron withdrawing group on *meso*-phenyl moiety on internalization of receptors, we have use different receptors containing different *meso*-substituents. The electron withdrawing and releasing group does remarkable effect on QY of Zn^{2+} .**1**, Zn^{2+} .**4**, Zn^{2+} .**7**, and Zn^{2+} .**8**. It is clearly visible from Figure 4.77(a) and 4.77(b) that all the receptors internalize in the cells successfully. Further, to check the interference of other physiologically important metals ion like Na^{+} , Mg^{2+} and Ca^{2+} whose concentration is very high in cells do not enhance the fluorescence intensity and inactive towards receptors. But Cd^{2+} and Hg^{2+} turn-on fluorescence intensity to lesser extent in comparison to Zn^{2+} . Therefore, Cd^{2+} and Hg^{2+} can cause interference in imaging of Zn^{2+} . Also, it is mentioned here that Cd^{2+} and Hg^{2+} are not the essential elements for life and will come through absorption from the environment or exposure to these elements. Therefore, Cd^{2+} and Hg^{2+} are

either rarely present or very low concentration in healthy cells so these ions should not interfere with probing and bio-imaging of Zn^{2+} ion in cells and is well documented in the available literature [6, 55].

To ensure if Compounds **1**, **4**, **7**, **8** cause any cytotoxicity, MTT assay was performed in breast carcinoma (MDA-MB-468 & MDA-MB-231) cells treated with different concentrations of Compounds **1**, **4**, **7**, **8** for MDAMB-468 & compound **4** for MDA-MB-231 for 12 hr. Control cells were treated with DMEM only.

As shown in Figure 4.78(a), there is no significant toxicity from 0 to 75 μM concentration of **4** in MDA-MB-231 cells. Cells treated with 100 μM of **4** displayed significant ($p < 0.05$) cytotoxicity as compared to control. The result supports that up to 50 μM concentration of Compounds **4** can be used as Zn^{2+} sensor without caring about cytotoxicity for at least 12 hr.

Figure 4.78(b) also shows that there is no significant toxicity from 0 to 150 μM concentration of compounds **1**, **4**, and **8** respectively in MDA-MB-468 cells. Only compound **7** shows significant ($p < 0.05$) cytotoxicity for concentration 100 and 150 μM respectively marked with (*).

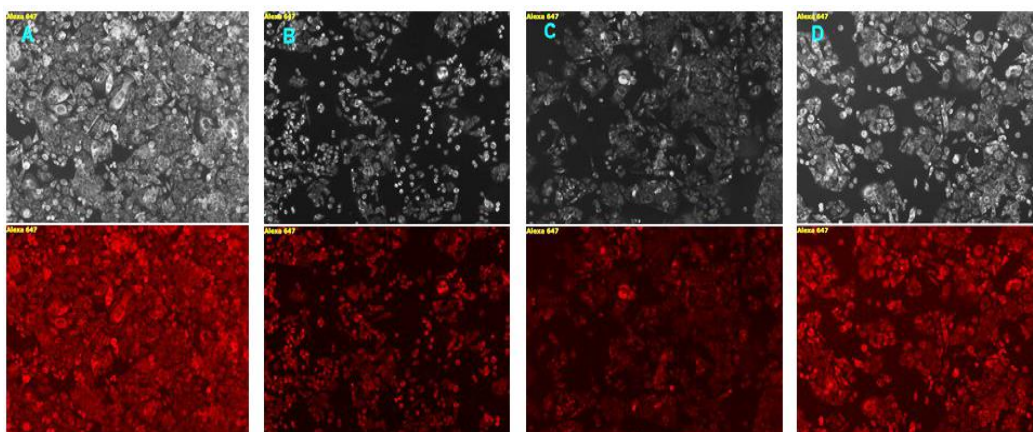


Fig. 4.77(a) MDA-MB-468 cells incubated with compounds **1**, **4**, **7**, **8** and Zn^{2+} ions for 30 min and respective bright field marked with A-D as well as fluorescence images (just down to its respective bright field image) were captured at 10 \times objective lens magnification. (A = **1**, B = **4**, C = **7**, D = **8**).

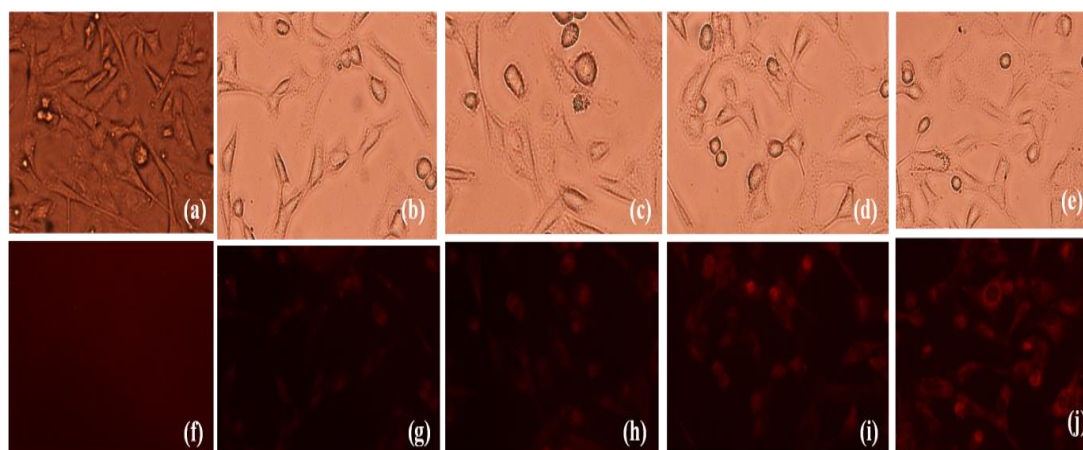


Fig. 4.77(b) MDA-MB-231 cells incubated with Zn^{2+} ions followed by different concentration (control, 10, 20, 30 and 50 μM) of **4** for 30 min and respective bright field (a, b, c, d, e) as well as fluorescence (f, g, h, i, j) images were captured at 40 \times objective lens magnification.

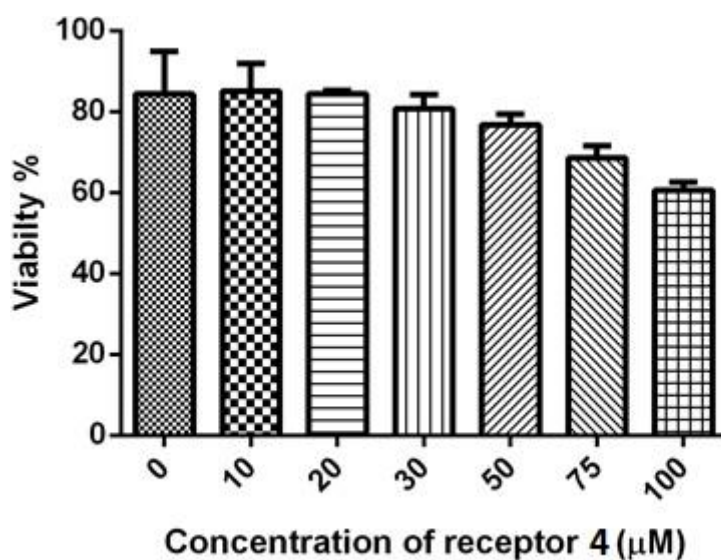


Fig. 4.78(a) MDA-MB-231 cells were incubated with different concentration (control, 10, 20, 30, 50, 75 and 100 μM) of **4**. MTT assay was performed for cytotoxicity. Only 100 μM concentration of **4** was significantly ($p < 0.05$) toxic for the cell.

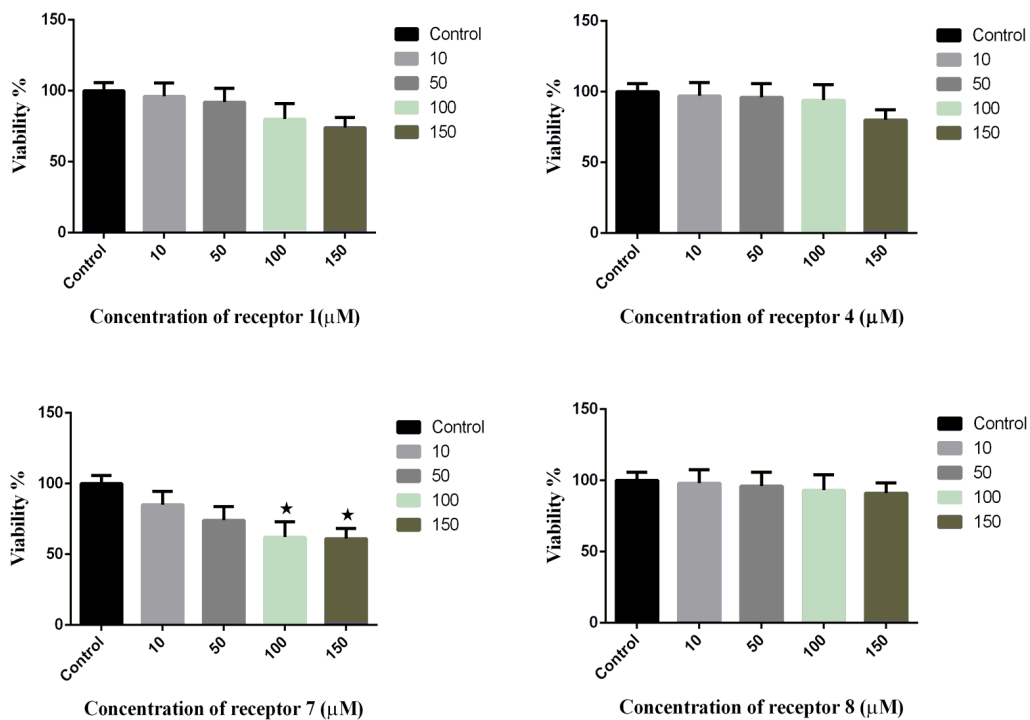


Fig. 4.78(b) MDA-MB-468 cells were incubated with different concentration (control, 10, 50, 100 and 150 μM) of **1**, **4**, **7** and **8** respectively. MTT assay was performed for cytotoxicity. Only 100 μM and 150 μM concentration of **7** were found significantly ($p < 0.05$) toxic for the cell.

The cell imaging results shows that these molecules can internalize successfully. The effect of electron releasing and withdrawing group on internalization have been shown and do not impact on internalization. Therefore, these molecules can be used for sensing intracellular zinc ions. However, these compounds can respond to Cd^{2+} and Hg^{2+} ions but these ions are rarely present in healthy cells so will not cause any interference in imaging of Zn^{2+} ions in healthy cells. MTT assay confirms that these compounds are lesser cytotoxic for longer time period as performed in breast carcinoma MDA-MB-468 and MDA-MB-231 cells treated with different concentration of compounds.

REFERENCES

1. F. Nifiatis, J. C. Athas, D. K. Gunaratne, Y. Gurung, K. Monette, and P. Shivokevich, *The Open Spectroscopy Journal*, **2011**, *5*, 1-12.
2. M. Gouterman, *Journal of Molecular Spectroscopy*, **1961**, *6*, 138-163.
3. C.-H. Hung, G.-F. Chang, A. Kumar, G.-F. Lin, L.-Y. Luo, W.-M. Ching and E. Wei-GuangDiau, *Chem. Commun. (Camb)*, **2008**, 978–980.
4. E. D. Becker, R. B. Bradley, *J. Chem. Phys.* **1959**, *31*, 1413.
5. P. Şen, C. Hirel, C. Andraud, C. Aronica, Y. Bretonnière, A. Mohammed, H. Ågren, B. Minaev, V. Minaeva, G. Baryshnikov, H.-H. Lee, J. Duboisset, M. Lindgren, *Materials*, **2010**, *3*, 4446.
6. (a) C. H. Hung, G. F. Chang, A. Kumar, G. F. Lin, L. Y. Luo, W. M. Ching, E. Wei-GuangDiau, *Chem. Commun. (Camb)*. **2008**, 978–980. (b) G. F. Chang, A. Kumar, W.M. Ching, H. W. Chu, C. H. Hung, *Chem. - An Asian J.* **2009**, *4*, 164–173. (c) G. F.Chang, C. H. Wang, H. C. Lu, L. S. Kan, I. Chao, W. H. Chen, A. Kumar, L. Lo, M.A. C. Dela Rosa, C. H. Hung, *Chem. - A Eur. J.* **2011**, *17*, 11332–11343. (d) Y. C. Chao, Y. S. Huang, H. P. Wang, S. M. Fu, C. H. Huang, Y. C. Liang, W. C. Yang, Y.S. Huang, G. F. Chang, H. W. Zan, et al., *Org. Electron. physics, Mater. Appl.* **2011**,*12*, 1899–1902.
7. R. K. Sharma, L. K. Gajanan, M. S. Mehata, F. Hussain, A. Kumar, *Spectrochimica Acta Part A: Molecular and Biomolecular Spectroscopy*, **2016**, *169*, 58-65.
8. (a) Bruker CCD System **2003**. (b) R. C. Clark, J.S. Reid, **1995**, *A51*, 887-897 (c) G. M. Sheldrick, *ActaCryst.* **2008**, *A64*, 112-122 (d) L. J. Farrugia, *J. Appl. Cryst.* **2012**, *45*, 849-854.
9. M. Stępień, L. Latos-Grażyński, L. Szterenberga, J. Panek and Z. Latajka, *J. Am. Chem. Soc.*, **2004**, *126*, 4566–4580.
10. Gaussian 09W, Revision D.01, M. J. Frisch, G. W. Trucks, H. B. Schlegel, G. E. Scuseria, M. A. Robb, J. R. Cheeseman, J. A. Montgomery, Jr., T. Vreven, K. N. Kudin, J. C. Burant, J. M. Millam, S. S. Iyengar, J. Tomasi, V. Barone, B.

- Mennucci, M. Cossi, G. Scalmani, N. Rega, G. A. Petersson, H. Nakatsuji, M. Hada, M. Ehara, K. Toyota, R. Fukuda, J. Hasegawa, M. Ishida, T. Nakajima, Y. Honda, O. Kitao, H. Nakai, M. Klene, X. Li, J. E. Knox, H. P. Hratchian, J. B. Cross, V. Bakken, C. Adamo, J. Jaramillo, R. Gomperts, R. E. Stratmann, O. Yazyev, A. J. Austin, R. Cammi, C. Pomelli, J. W. Ochterski, P. Y. Ayala, K. Morokuma, G. A. Voth, P. Salvador, J. J. Dannenberg, V. G. Zakrzewski, S. Dapprich, A. D. Daniels, M. C. Strain, O. Farkas, D. K. Malick, A. D. Rabuck, K. Raghavachari, J. B. Foresman, J. V. Ortiz, Q. Cui, A. G. Baboul, S. Clifford, J. Cioslowski, B. B. Stefanov, G. Liu, A. Liashenko, P. Piskorz, I. Komaromi, R. L. Martin, D. J. Fox, T. Keith, M. A. Al-Laham, C. Y. Peng, A. Nanayakkara, M. Challacombe, P. M. W. Gill, B. Johnson, W. Chen, M. W. Wong, C. Gonzalez and J. A. Pople, Gaussian, Inc., Wallingford CT, **2013**.
11. (a) A. D. Becke, *Physical Review A* **1988**, 38, 3098-3100. (b) A. D. Becke, *The Journal of Chemical Physics* **1993**, 98, 1372-1377. (c) A. D. Becke, *The Journal of Chemical Physics* **1993**, 98, 5648-5652. (d) C. Lee, W. Yang, R. G. Parr, *Physical Review B* **1988**, 37, 785-789.
12. A. Ghosh in *The Porphyrin Handbook*, Vol. 7 (Eds.: K. M. Kadish, K. M. Smith, R. Guilard), Academic Press, New York, **2000**, pp. 1–31.
13. W. Breuer, S. Epsztejn, P. Millgram and I. Z. Cabantchik, *Am. J. Physiol.*, **1995**, 268, C1354–C1361.
14. R. Corradini, A. Dossena, G. Galaverna, R. Marchelli, A. Panagia and G. Sartor, *J. Org. Chem.*, **1997**, 62, 6283–6289.
15. Y. Zheng, K. M. Gattás-Asfura, V. Konka and R. M. Leblanc, *Chem. Commun. (Camb)*, **2002**, 2350–2351.
16. A. Torrado, G. K. Walkup and B. Imperiali, *J. Am. Chem. Soc.*, **1998**, 120, 609–610.
17. W.-Y. Lin and H. E. Van Wart, *J. Inorg. Biochem.*, **1988**, 32, 21–38.
18. J. Rosenthal and S. J. Lippard, *J. Am. Chem. Soc.*, **2010**, 132, 5536–7. (b) M. H. Lim, B. A. Wong, W. H. Pitcock, D. Mokshagundam, M. H. Baik and S. J. Lippard, *J. Am. Chem. Soc.*, **2006**, 128, 14364–14373.

19. L. Fabbriizzi, M. Licchelli, P. Pallavicini, A. Perotti, A. Taglietti and D. Sacchi, *Chem. - A Eur. J.*, **1996**, *2*, 75–82.
20. F. Pina, M. A. Bernardo and E. García-España, *Eur. J. Inorg. Chem.*, **2000**, 2000, 2143–2157.
21. V. Dujols, F. Ford and A. W. Czarnik, *J. Am. Chem. Soc.*, **1997**, *119*, 7386–7387.
22. T. Gunnlaugsson, J. P. Leonard, K. Sénéchal and A. J. Harte, *Chem. Commun. (Camb)*, **2004**, 782–3.
23. G. Klein, D. Kaufmann, S. Schürch and J.-L. Reymond, *Chem. Commun.*, **2001**, 561–562.
24. A. Takeda and H. Tamano, *Brain Res. Rev.*, **2009**, *62*, 33–44.
25. S. J. Strickler, R. A. Berg, *J. Chem. Phys.* **1962**, *37*, 814–822.
26. (a) D. J. Quimby and F. R. Longo, *Journal of the American Chemical Society*, **1975**, *97*, 5111-5116. (b) T. Ding, E. Alemán, D. Modarelli, and C. Ziegler, *J Phys Chem A*, **2005**, *109*, 7411–7. (c) N. Kobayashi, H. Ogata, N. Nonaka, *Chem. Eur. Journal*, **2003**, *9*, 5123- 5134.
27. S. I. Yang, J. Seth, J.-P. Strachan, S. Gentemann, D. Kim, D. Holten, J. S. Lindsey, D. F. Bocian, *Journal of Porphyrins and Phthalocyanines*, **1999**, *3*, 117-147.
28. J. P. Strachan, S. Gentemann, J. Seth, *Journal of the American Chemical Society*, **1997**, *119*, 11191-11201. (b) A Osuka, N Tanabe, and S Kawabata, *Journal of Organic Chemistry*, **1995**, *60*, 7177-7185.
29. (a) A. Ghosh, *Journal of the American Chemical Society*, **1995**, *117*, 4691-9 (b) T. Vangberg and A. Ghosh, *Journal of the American Chemical Society*, **1998**, *120*, 6227-6230.
30. W. A. Kalsbeck, J. Seth, and D. F. Bocian, *Inorganic Chemistry*, **1996**, *35*, 7935-7937.
31. D. S .McClure, *Journal of Chemical Physics*, **1949**, *17*, 905-13.

32. (a) K. N. Solov'ev and E. A. Borisevich, *Phys Usp* **2005**, *48*, 231-53. (b) K. N. Solov'ev, M. P. Tsvirko, A. T. Gradyushko and D. T. Kozhich, *Opt. Spectrosc. (USSR)*, **1972**, *33*, 480.
33. J. J. Frau ́sto da Silva and R. J. P. Williams, *The Biological Chemistry of the Elements*, Clarendon Press: Oxford, **1991**, p. 302.
34. R. S. MacDonald, *The Journal of Nutrition*, **2000**, *130*(5), 1500S-1508S.
35. P. D. Zalewski, I. J. Forbes, C. Giannakis, *Biochem. Int.* **1991**, *24*, 1093–1101.
36. S. J. Martin, G. Mazdai, J. J. Strain, T. G. Cotter, B. M. Hannigan, *Clin. Exp. Immunol.*, **2008**, *83*, 338–343.
37. D. E. Epner, H. R. Herschman, *J. Cell. Physiol.* **1991**, *148*, 68–74.
38. R. J. Cousins and L. M. Lee-Ambrose, *J. Nutr.*, **1992**, *122*, 56–64.
39. X. Xie, T. G. Smart, *Nature*, **1991**, *349*, 521–524.
40. C. J. Frederickson, *Int. Rev. Neurobiol.* **1989**, *31*, 145–238.
41. L. M. Canzoniero, S. L. Sensi, D. W. Choi, *Neurobiol. Dis.* **1997**, *4*, 275–279.
42. D. W. Choi, J. Y. Koh, *Annu. Rev. Neurosci.* **1998**, *21*, 347–375.
43. F. Grummt, C. Weinmann-Dorsch, J. Schneider-Schaulies, A. Lux, *Exp. Cell Res.* **1986**, *163*, 191–200.
44. T. Gunnlaugsson, J. P. Leonard, K. S n chal and A. J. Harte, *Chem. Commun. (Camb)*, **2004**, 782–3.
45. G. Klein, D. Kaufmann, S. Sch rch and J.-L. Reymond, *Chem. Commun.*, **2001**, 561–562.
46. A. Takeda and H. Tamano, *Brain Res. Rev.*, **2009**, *62*, 33–44.
47. K. R. Gee, Z.-L. Zhou, W.-J. Qian and R. Kennedy, *J. Am. Chem. Soc.*, **2002**, *124*, 776–778.
48. B. Tang, H. Huang, K. Xu, L. Tong, G. Yang, X. Liu and L. An, *Chem. Commun. (Camb)*, **2006**, 3609–11.

49. J. H. Lee, J. H. Lee, S. H. Jung, T. K. Hyun, M. Feng, J.-Y. Kim, J.-H. Lee, H. Lee, J.S. Kim, C. Kang, K.-Y. Kwon, J. H. Jung, *Chemical Communications* **2015**, *51*, 7463-7465.
50. R. Alam, T. Mistri, A. Katarkar, K. Chaudhuri, S. K. Mandal, A. R. Khuda-Bukhsh, K. K. Das, M. Ali, *The Analyst* **2014**, *139*, 4022-4030.
51. N. Khairnar, K. Tayade, S. K. Sahoo, B. Bondhopadhyay, A. Basu, J. Singh, N. Singh, V. Gite, A. Kuwar, *Dalton Transactions* **2015**, *44*, 2097-2102.
52. S. Sinha, G. Dey, S. Kumar, J. Mathew, T. Mukherjee, S. Mukherjee, S. Ghosh, *ACS Applied Materials & Interfaces* **2013**, *5*, 11730-11740. (b) N. Y. Baek, C. H. Heo, C. S. Lim, G. Masana, B. R. Cho, H. M. Kim, *Chem. Commun.* **2012**, *48*, 4546-4547.
53. (a) H. Singh, H. W. Lee, C. H. Heo, J. W. Byun, A. R. Sarkar, H. M. Kim, *Chemical Communications* **2015**, *51*, 12099-12102. (b) M. J. Jou, S. B. Jou, M. J. Gou, H. Y. Wu and T. I. Peng, *Ann. N. Y. Acad. Sci.*, **2004**, 1011, 45. (c) F. Helmchen and W. Denk, *Nat. Methods*, **2005**, *2*, 932.
54. M. Y. Lee, M. H. Liao, Y. N. Tsai, K. H. Chiu, H. C. Wen, *Journal of agricultural and food chemistry*, **2011**, *59*(6), 2347-2355.
55. A. B. Pradhan, S. K. Mandal, S. Banerjee, A. Mukherjee, S. Das, A. R. KhudaBukhsh, A. Saha, *Polyhedron* **2015**, *94*, 75-82.

CONCLUSION AND FUTURE SCOPE

An attempt has been made in the work described here:

1. We have successfully extended the series of fascinating molecule *meta*-benziporphodimethenes with varied electron releasing and electron withdrawing group on *meso*-phenyl group. The fluorescence quantum yield of their zinc complex has been calculated using Strickler-Berg relation. The electron releasing group reduces the fluorescence quantum yield while electron withdrawing group enhance the fluorescence quantum yield. The calculated quantum yields are comparable to the earlier reported unsubstituted *meso*-phenyl *meta*-benziporphodimethenes zinc complex. The effects of ortho substituent on *meso*-phenyl group have been studied and enhance the fluorescence quantum yield to a great extent.
2. We have successfully explored newly synthesized a very simple new porphyrin analogue *meta*-benziporphodimethenes derivatives for imaging zinc ions in MD-AMB-468 and MD-AMB-231 breast cancer cells. The results show that these molecules can internalize successfully. The effects of electron releasing and withdrawing group on internalization has been shown and do not impact on internalization. Therefore, these molecules can be used for sensing intracellular zinc ions. However, receptors can respond to Cd²⁺ and Hg²⁺ ions but these ions are rarely present in healthy cells so will not cause any interference in imaging of Zn²⁺ ions in healthy cells. MTT assay confirms that receptors **1**, **4**, **7** and **8** are lesser cytotoxic for longer time period as performed in breast carcinoma (MD-AMB-468 and MD-AMB-231) cells treated with different concentration of receptors.

3. In the series of newly synthesized complexes, the intrinsic difference in the structure based on substitution has been correlated with the Density Functional Theory (DFT). DFT studies suggested the symmetrical geometry of Zn^{2+} .⁴ and the values are comparable to the earlier reports.
4. Quantification of Zn^{2+} ions in cells and bio-imaging studies of receptors in different cells are the current foci of ongoing research in our laboratory.

LIST OF PUBLICATION

1. R. K. Sharma, L. K. Gajanan, M. S. Mehata, F. Hussain, A. Kumar, *Spectrochimica Acta Part A: Molecular and Biomolecular Spectroscopy* **2016**, *169*, 58-65.
2. R. K. Sharma, A. Maurya, P. Rajamani, M. S. Mehata, A. Kumar, *ChemistrySelect* **2016**, *1*, 3502-3509.

ABOUT THE AUTHOR



Name: Ravi Kumar Sharma

Father's Name: R. K. Sharma

Nationality: Indian

The author did his graduation and post-graduation studies from S. G. T. B. KHALSA COLLEGE, University of Delhi. He completed his Doctor of Philosophy degree, from Delhi Technological University. His research work is mainly based on “*meta*-benziporphodimethenes” derivatives and their use in zinc sensing for in vivo analysis.